# Delft University of Technology

Phosphorus recovery from iron-coagulated sewage sludge

Prot, T.J.F.

**Important note**
To cite this publication, please use the final published version (if applicable).
Please check the document version above.

**Phosphorus recovery from iron-coagulated sewage sludge**

Dissertation

for the purpose of obtaining the degree of doctor

at Delft University of Technology

by the authority of the Rector Magnificus, Prof. dr. ir. T.H.J.J. van der Hagen

chair of the Board for Doctorates

to be defended publicly on

Wednesday 10th of November at 15:00

By

Thomas Jean-Louis Françoise PROT

Master of Science in Chemical Engineering

Ecole Nationale Supérieure de Chimie de Mulhouse, France

Born in Strasbourg, France

This dissertation has been approved by the promotor.


Composition of the doctoral committee:

Rector Magnificus,                          chairperson

Prof.dr.ir. M.C.M. van Loosdrecht          Delft University of Technology, promotor

Dr. P.K. Wilfert                            Delft University of Technology, co-promotor



Independent members:

Prof.dr.ir. J. van Lier                     Delft University of Technology

Prof.dr.ir. A. Soares                       Cranfield University

Prof.dr. M. Sperandio                       INSA Toulouse

Dr.ir. I. Pikaar                            The University of Queensland

Prof.dr.ir. L. van der Wielen              Delft University of Technology, reserve member


Other member:

Ir. Leon Korving      Wetsus European centre of excellence for sustainable water technology

*"Master has given Dobby a Ph.D. degree. Dobby is free."*

*Dobby*

*For everybody that contributes to make my life joyful.*

# Popular summary of this thesis

Fertilizers are vital for our society since we use them to grow plants. These plants can produce fruits and vegetables that we can consume or use as feedstock for the animals, ending up in our plates. In short, we need fertilizers to make our food, and we are using an increasing quantity of it with the growing population. Phosphorus is an essential constituent of fertilizers and a critical element for every living organism since it is present in DNA and bones. The current approach is to mine phosphate rock to make fertilizer. This strategy is the only option we have so far to produce phosphorus in large quantities, but it is polluting, and the resources are not endless. In our society, we are trying to replace fossil energies with renewable energy. However, this cannot be done for phosphorus; nothing can substitute it. Therefore, we need to find alternatives to obtain phosphorus without further damaging the planet.

After eating, the phosphorus ends up in our excreta and goes to municipal wastewater treatment plants (WWTPs). There, iron salts can be added to the wastewater to bind phosphorus strongly. All the solids, including the phosphate bound to the iron, are separated from the cleaned water and collected as sludge (a mud-like slurry). If you let the sludge age a couple of days under anaerobic conditions, the iron phosphate mineral called vivianite will form because of the reduction of the iron (chemical process when a molecule/atom gains electrons). In a WWTP, the sludge is often kept for 20-30 days at 37°C in a big tank called a digester. In the digester, organic matter is broken down by bacteria to produce methane, which can be used as energy. Because of the absence of oxygen and the long storage time of the sludge, a digester is an excellent place for vivianite to form. By looking at digested sludge (containing iron) under the microscope, you can see some shiny blue particles standing out from the brown/black background: these are vivianite crystals. My predecessor Philipp Wilfert showed that more than 80% of the phosphorus present in sludge could be present as vivianite if enough iron were present. Therefore, focusing on vivianite recovery is a promising option to recover the phosphorus from sludge.

Vivianite is only found as tiny crystals (20-200μm), making it complicated to harvest with conventional gravity-based techniques like hydrocyclones. Therefore, I studied the crystallization of vivianite during my Ph.D. to understand how to grow bigger and easier to separate particles. It turned out that it was a very challenging project and that it might be hard to grow big particles of vivianite under the conditions of pH and concentrations occurring in WWTPs. Fortunately, the gravity-based techniques were not the only option to separate vivianite since this mineral has paramagnetic properties, meaning that strong magnets attract it. The first part of my project was to show that vivianite could indeed be extracted from sludge with a simple magnetic separator. Two axes of research were interesting to pursue. Firstly, it was vital to ensure that enough phosphorus was present as vivianite in sludge since only the phosphorus in vivianite can be recovered with the magnetic approach. Secondly, the system had to be demonstrated on a bigger scale and optimized.

One of our partners, "Waterschap Brabantse Delta", increased the iron dosing at one of their WWTP (Nieuwveer) while the magnetic recovery of vivianite was piloted there. It allowed us to kill two birds with one stone: study the production of vivianite by increased iron dosing and improving the technology. During his Ph.D., Philipp showed that the higher the Fe/P ratio in

sludge, the more phosphorus would be present as vivianite. However, his study was performed on different WWTPs without changes in their iron dosing while we could follow "live" what happened after iron addition in Nieuwveer. During the increased iron dosing, all the additional iron added was transformed into vivianite, which was great news. In addition, a higher iron dosing decreased the concentration of phosphorus in the effluent and the concentration of $H_2S$ in the biogas. The study also showed that a higher iron dosing was not hampering the normal functioning of the WWTP. Comparing our results to previous studies showed that before vivianite can form, iron reacts with sulphide in a ratio of 1:1. It indicated that to maximize the phosphorus quantity present as vivianite, a Fe/P ratio of 1.5 (vivianite is composed of three iron and two phosphates; 3/2=1.5) was not enough; 1.5-2 might be necessary if there is much sulphide.

In parallel to this study, Wokke and his team piloted a magnetic separator (mining industry technology) at the same WWTP. The pilot could handle 1m³/h of digested sludge, which is the equivalent of the sludge produced by 20 000 people (twice the population of my valley in France). It showed that the separation of the vivianite was better than with the simple lab-scale separator, mainly due to the pulsation of the slurry and the use of magnetized steel-rods matrices. By circulating the sludge three times in the separator, around 80% of the vivianite could be recovered. Overall, more than 60% of the phosphorus present in the influent wastewater could be recovered as vivianite, which is better than the 10-30% typically achieved by struvite recovery (another phosphorus mineral recovery approach). In addition, this recovery percentage satisfied the threshold (>50%) of future German legislation that is the strictest at the moment.

In the Netherlands, only 75% of the sludge is digested, which means that it is important to study the vivianite recovery from non-digested sludge as well. At this point of the project, we knew that vivianite was formed after 20-30 days under anaerobic conditions in the digester. Together with Wout Pannekoek from "Waterschapsbedrijf Limburg", we found out that the iron present in freshly formed sludge was reduced very quickly when stored under anaerobic conditions: all the iron was entirely reduced after 2-3 days. This is interesting because vivianite can only form from the reduced form of iron ($Fe^{2+}$). In fact, most of the vivianite that would form after the typical retention time of a digester (20-30 days) was already formed after 2-3 days. In other words, if there is sufficient iron in a sludge, a few days of oxygen-free storage is enough to form a significant amount of vivianite. It means that a digester is not necessary to recover phosphorus with the vivianite formation approach.

As explained before, there is plenty of phosphorus in human excreta, but there is four times more in Europe in animal manure (animal excreta). If we could recover the phosphorus present in sludge and manure, we would no longer need to export phosphorus. In manure, phosphate is present mainly as magnesium ammonia phosphate (struvite) and calcium phosphate but they are difficult to separate from the manure. Vivianite is a thermodynamically stable phosphorus mineral in reduced environments (like sludge and manure). If iron is added to manure, vivianite can be expected to form preferentially to other phosphate minerals. Therefore, we developed a project with Chris Schott in which we studied the formation of vivianite in pig manure after iron addition. It turns out that most of the phosphorus could be transformed to

vivianite when a Fe/P ratio of 4-5 was used. This ratio is much higher than the one necessary in sludge (~2), and we believe that it because iron binds to organic matter before forming vivianite. After showing that vivianite formed, we could extract it from the pig manure with the same lab-scale device used with digested sludge. The project was exciting since it showed that vivianite might also be used to recover phosphorus from manure. However, the iron quantity to use needs to be optimized to make the process economically feasible. This will be an interesting research axis for an upcoming Ph.D. project.

The most original part of my Ph.D. was not about recovering vivianite but understanding why it sometimes forms at unwanted places at WWTPs. After talking to several water authorities, we realized that many of them were suffering from vivianite scaling, which is forming a hard layer of vivianite in the walls of pipe or equipment. It can lead to operational problems and oblige WWTPs to change their pipe or remove it manually, representing a substantial cost. After collecting data on these WWTPs, we realized that vivianite could form at different places: pipes carrying undigested sludge, centrifuges, and heat exchangers. Interestingly, the vivianite formation mechanisms seemed to differ in these three places: iron reduction, pH increase due to $CO_2$ stripping, and temperature dependence of vivianite solubility. We could propose prevention/mitigation strategies for the WWTP to remediate these issues. This project taught us two things. Firstly, you can dose a lot of iron and not have problems with vivianite scaling if you dose iron wisely. Secondly, vivianite scaling has not widely been reported in the literature because people focus on struvite scaling. However, vivianite scaling is more common than people think.

This thesis showed that vivianite is a key player in anaerobic environments containing iron and phosphorus. Magnetic extraction is a good option to recover vivianite, which shows that interdisciplinary collaboration (wastewater treatment + mineral processing in this case) can lead to great scientific breakthroughs. This approach is promising and getting closer to the market, which is very exciting. After its separation, the valorization of the vivianite is a crucial point that will need to be investigated to make the technology viable. This project brought answers to several questions and helped us understand better the mysteries surrounding vivianite. Overall, it raised even more questions (that future PhDs will address) which is, in the end, what research is all about.

## Populaire samenvatting van dit proefschrift

Meststoffen zijn van vitaal belang voor onze samenleving aangezien wij ze gebruiken om planten te laten groeien. Deze planten kunnen fruit en groenten voortbrengen die wij kunnen consumeren of gebruiken als veevoer voor melk en vleesproductie die ook weer op ons bord belanden. Kortom, we hebben meststoffen nodig om ons voedsel te maken, en we gebruiken er steeds meer van met de groeiende wereldbevolking. Fosfor is een essentieel bestanddeel van meststoffen en een kritiek element voor elk levend organisme, aangezien het aanwezig is in ons DNA, onze botten en de stoffen die verantwoordelijk zijn voor onze energiehuishouding (ATP). De huidige aanpak bestaat erin fosfaatgesteente te ontginnen om er kunstmest van te maken. Deze strategie is tot dusver de enige mogelijkheid om fosfor in grote hoeveelheden te produceren, maar zij is vervuilend en de hulpbronnen zijn niet onuitputtelijk. In onze samenleving proberen we fossiele energiebronnen te vervangen door hernieuwbare energiebronnen. Dit is echter niet mogelijk voor fosfor: niets kan het vervangen. Daarom moeten we alternatieven vinden om fosfor te verkrijgen zonder de planeet nog meer schade toe te brengen.

Na het eten komt het fosfor in onze uitwerpselen terecht en gaat het naar communale afvalwaterzuiveringsinstallaties (RWZI's). Daar kunnen ijzerzouten aan het afvalwater worden toegevoegd om fosfor sterk te binden. Alle vaste stoffen, inclusief het aan het ijzer gebonden fosfaat, worden van het gezuiverde water gescheiden en verzameld als slib (een modderige slurry). Als men het slib een paar dagen laat rijpen, vormt zich het ijzerfosfaatmineraal vivianiet door de reductie van het ijzer (chemisch proces waarbij een molecule/atoom elektronen krijgt). In een zuiveringsinstallatie wordt het slib vaak 20-30 dagen bij 37°C bewaard in een grote tank die een gistingstank wordt genoemd. In de gistingstank wordt organisch materiaal door bacteriën afgebroken tot methaan, dat als energiedrager kan worden gebruikt. Door de afwezigheid van zuurstof en de lange opslagtijd van het slib is een gistingstank een uitstekende plaats voor de vorming van vivianiet. Als je uitgegist slib (dat ijzer bevat) onder de microscoop bekijkt, zie je enkele glanzende blauwe deeltjes afsteken tegen de bruinzwarte achtergrond: dit is vivianiet. Mijn voorganger Philipp Wilfert toonde aan dat meer dan 80% van de fosfor in slib aanwezig kan zijn in de vorm van vivianiet als er voldoende ijzer aanwezig is. Daarom is aandacht voor de terugwinning van vivianiet een veelbelovende optie om de fosfor uit slib terug te winnen.

Vivianiet komt enkel voor als kleine kristallen (20-200μm), waardoor het moeilijk te oogsten is met conventionele op zwaartekracht gebaseerde technieken zoals hydrocyclonen. Daarom heb ik tijdens mijn Ph.D. de kristallisatie van vivianiet bestudeerd om te begrijpen hoe grotere en gemakkelijker te scheiden deeltjes kunnen worden gekweekt. Het bleek een zeer uitdagend project te zijn en het zou wel eens moeilijk kunnen zijn om grote vivianietdeeltjes te kweken onder de omstandigheden van pH en concentraties die voorkomen in afvalwaterzuiveringsinstallaties. Gelukkig waren de op zwaartekracht gebaseerde technieken niet de enige optie om vivianiet te scheiden, aangezien dit mineraal paramagnetische eigenschappen heeft, wat betekent dat sterke magneten het aantrekken. Het eerste deel van mijn project bestond erin aan te tonen dat vivianiet inderdaad uit slib kon worden gehaald met een eenvoudige magnetische scheider. Twee onderzoekslijnen waren interessant om na te

streven. Ten eerste was het van vitaal belang ervoor te zorgen dat er voldoende fosfor in de vorm van vivianiet in het slib aanwezig was, aangezien alleen het fosfor in vivianiet met de magnetische aanpak kan worden teruggewonnen. Ten tweede moest het systeem op grotere schaal worden gedemonstreerd en geoptimaliseerd.

Een van onze partners, "waterschap Brabantse Delta", verhoogde de ijzerdosering op één van hun zuiveringsinstallaties (Nieuwveer) terwijl de magnetische terugwinning van vivianiet daar op pilotschaal werd getest. Zo konden we twee vliegen in één klap slaan: de productie van vivianiet bestuderen door een verhoogde ijzerdosering en de technologie verbeteren. Tijdens zijn Ph.D. toonde Philipp aan dat hoe hoger de Fe/P-verhouding in slib, hoe meer fosfor er als vivianiet aanwezig zou zijn. Zijn studie werd echter uitgevoerd op verschillende RWZI's zonder veranderingen in hun ijzerdosering, terwijl wij in Nieuwveer "live" konden volgen wat er gebeurde na toevoeging van ijzer. Tijdens de verhoogde ijzerdosering werd al het extra toegevoegde ijzer omgezet in vivianiet, wat goed nieuws was. Bovendien verminderde een hogere ijzerdosering de concentratie fosfor in het effluent en de concentratie H2S in het biogas. De studie toonde ook aan dat een hogere ijzerdosering de normale werking van de RWZI niet in de weg stond. Vergelijking van onze resultaten met eerdere studies toonde aan dat voordat vivianiet kan worden gevormd, ijzer reageert met sulfide in een verhouding van 1:1. Hieruit bleek dat om de hoeveelheid fosfor aanwezig als vivianiet te maximaliseren, een Fe/P-verhouding van 1,5 (vivianiet is samengesteld uit drie ijzer- en twee fosfaatverbindingen; 3/2=1,5) niet voldoende was; 1,5-2 zou nodig kunnen zijn als er veel sulfide is.

Parallel aan dit onderzoek voerden Wokke en zijn team een pilot uit met een magneetseparator (mijnbouwtechnologie) op dezelfde AWZI. De proefinstallatie kon 1m3/u uitgegist slib verwerken, wat overeenkomt met het slib dat wordt geproduceerd door 20 000 mensen (tweemaal de bevolking van mijn vallei in Frankrijk). Hieruit bleek dat de afscheiding van het vivianiet beter was dan met de eenvoudige scheider op laboratoriumschaal, voornamelijk dankzij de pulsatie van het slib en het gebruik van matrices met gemagnetiseerde stalen staven. Door het slib driemaal in de separator te laten circuleren, kon ongeveer 80% van het vivianiet worden teruggewonnen. In totaal kan meer dan 60% van de fosfor in het instromende afvalwater worden teruggewonnen in de vorm van vivianiet, wat beter is dan de 10-30% die wordt bereikt met struvietterugwinning (een andere methode voor de terugwinning van fosformineralen). Bovendien voldeed dit terugwinningspercentage aan de drempelwaarde (>50%) van de toekomstige Duitse wetgeving, die op dit moment het strengst is.

In Nederland wordt slechts 75% van het slib vergist, wat betekent dat het belangrijk is ook de terugwinning van vivianiet uit niet-gegist slib te bestuderen. Op dit punt van het project wisten we dat vivianiet gevormd werd na 20-30 dagen onder anaerobe omstandigheden in de vergister. Samen met Wout Pannekoek van het Waterschapsbedrijf Limburg ontdekten we dat het ijzer in het vers gevormde slib zeer snel werd gereduceerd wanneer het onder anaerobe omstandigheden werd opgeslagen: na 2-3 dagen was al het ijzer volledig gereduceerd. Dit is interessant omdat vivianiet zich alleen kan vormen uit de gereduceerde vorm van ijzer (Fe2+). In feite was het grootste deel van het vivianiet dat zich zou vormen na de typische verblijftijd van een vergister (20-30 dagen) al gevormd na 2-3 dagen. Met andere woorden, als er

voldoende ijzer in een slib zit, is een paar dagen zuurstofvrije opslag voldoende om een aanzienlijke hoeveelheid vivianiet te vormen. Dit betekent dat een vergister niet nodig is om fosfor terug te winnen met de vivianietvormingsaanpak.

Zoals eerder uitgelegd, zit er veel fosfor in menselijke uitwerpselen, maar zit er in Europa vier keer zoveel fosfor in dierlijke mest (dierlijke excreta). Als we het fosfor dat aanwezig is in slib en mest zouden kunnen terugwinnen, zouden we geen fosfor meer hoeven te exporteren. In mest is fosfaat vooral aanwezig als magnesiumammoniumfosfaat (struviet) en calciumfosfaat dat echter moeilijk af te scheiden is uit de mest. Vivianiet is een thermodynamisch stabiel fosformineraal in gereduceerde milieus (zoals slib en mest). Als ijzer wordt toegevoegd aan mest, kan worden verwacht dat vivianiet zich bij voorkeur zal vormen boven andere fosfaatmineralen. Daarom ontwikkelden we samen met Chris Schott een project waarin we de vorming van vivianiet in varkensmest na toevoeging van ijzer bestudeerden. Het blijkt dat het grootste deel van de fosfor kan worden omgezet in vivianiet wanneer een Fe/P-verhouding van 4-5 wordt gebruikt. Deze verhouding is veel hoger dan de verhouding die nodig is in slib (~2), en wij denken dat dit komt doordat ijzer zich bindt aan organisch materiaal alvorens vivianiet te vormen. Nadat we hadden aangetoond dat vivianiet zich vormde, konden we het op laboratoriumschaal uit de varkensmest extraheren met hetzelfde apparaat dat we voor uitgegist slib gebruikten. Het project was spannend omdat het aantoonde dat vivianiet ook zou kunnen worden gebruikt om fosfor uit mest terug te winnen. De te gebruiken hoeveelheid ijzer moet echter worden verminderd om het proces economisch haalbaar te maken. Dit zal een interessante onderzoekslijn zijn voor een toekomstig Ph.D.-project.

Het meest originele deel van mijn Ph.D. ging niet over het terugwinnen van vivianiet, maar over het begrijpen waarom het zich soms op ongewenste plaatsen in RWZI's vormt. Na gesprekken met verschillende waterschappen realiseerden we ons dat veel van hen last hadden van vivianiet afzettingen: de vorming van een harde laag vivianiet in de wanden van pijp of apparatuur. Dit kan leiden tot operationele problemen en verplicht AWZI's hun leidingen te vervangen of handmatig te verwijderen, wat aanzienlijke kosten met zich meebrengt. Na het verzamelen van gegevens over deze AWZI's realiseerden we ons dat vivianiet zich op verschillende plaatsen kon vormen: leidingen met onvergist slib, centrifuges, en warmtewisselaars. Interessant genoeg bleken de mechanismen van vivianietvorming op deze drie plaatsen te verschillen: ijzerreductie, pH-verhoging door CO2-stripping, en temperatuurafhankelijkheid van de oplosbaarheid van vivianiet. We konden preventie- en mitigatiestrategieën voor de AWZI voorstellen om deze problemen te verhelpen. Dit project heeft ons twee dingen geleerd. Ten eerste kun je veel ijzer doseren en geen problemen hebben met vivianietafzetting als je het ijzer op een verstandige manier doseert. Ten tweede denken we dat vivianiet-afzetting niet algemeen gerapporteerd wordt in de literatuur omdat men zich concentreert op struviet-afzetting. Toch komen vivianietafzettingen vaker voor dan men denkt.

Dit proefschrift heeft aangetoond dat vivianiet een belangrijke rol speelt in anaerobe omgevingen die ijzer en fosfor bevatten. Magnetische extractie is een goede optie om vivianiet terug te winnen, wat aantoont dat interdisciplinaire samenwerking (afvalwaterbehandeling +

mineraalverwerking in dit geval) kan leiden tot grote wetenschappelijke doorbraken. Deze aanpak is veelbelovend en komt steeds dichter bij de markt, wat zeer opwindend is. Na de afscheiding is de valorisatie van het vivianiet een cruciaal punt dat zal moeten worden onderzocht om de technologie levensvatbaar te maken. Dit project heeft antwoorden gegeven op verschillende vragen en heeft ons geholpen de mysteries rond vivianiet beter te begrijpen. In het algemeen heeft het nog meer vragen doen rijzen (die toekomstige PhD's zullen behandelen), en dat is uiteindelijk waar het bij onderzoek allemaal om draait.

## Résumé vulgarisé de cette thèse

Les engrais sont vitaux pour notre société puisque nous les utilisons pour faire pousser des plantes. Ces plantes peuvent produire des fruits et légumes pour notre propre consommation, ou des aliments pour les animaux, qui finissent eux-mêmes dans nos assiettes. En bref, nous avons besoin d'engrais pour produire notre nourriture, et nous en utilisons une quantité croissante avec l'augmentation de la population. Le phosphore (P) est un constituant essentiel des engrais et un élément indispensable pour tout organisme vivant puisqu'il est présent dans l'ADN. L'approche actuelle consiste à miner la roche phosphatée pour en extraire le phosphore et produire des engrais. Cette stratégie est la seule option dont nous disposons à ce jour pour produire du phosphore en grande quantité, mais elle est polluante et les ressources ne sont pas inépuisables. Dans notre société, nous essayons de remplacer les énergies fossiles par des énergies renouvelables. Cependant, cela ne peut pas être fait pour le phosphore ; rien ne peut le remplacer. Nous devons donc trouver des alternatives pour obtenir du phosphore sans endommager davantage la planète.

Après que nous nous soyons alimentés, le phosphore se retrouve dans nos excréments et est acheminé vers les stations d'épuration municipales (STEP). Là, du fer (Fe) peut être ajouté aux eaux usées. Il va se lier fermement au phosphore sous forme de solide (le phosphore arrive sous une forme dissoute dans une STEP). Toutes les matières solides, y compris le phosphate lié au fer, sont séparées de l'eau épurée et collectées sous forme de boue. Si vous laissez la boue vieillir quelques jours, un minéral composé de phosphate de fer appelé vivianite se formera en raison de la réduction du fer (processus chimique au cours duquel une molécule/un atome gagne des électrons). Dans une station d'épuration, les boues sont souvent conservées pendant 20 à 30 jours à 37°C dans une grande cuve appelée digesteur. Dans le digesteur, la matière organique est décomposée par des bactéries pour produire du méthane, qui peut être utilisé comme énergie. En raison de l'absence d'oxygène et de la longue durée de stockage des boues, un digesteur est un excellent endroit pour la formation de vivianite. En observant au microscope des boues digérées (contenant du fer), on peut voir des particules bleues qui se détachent du fond brun/noir : c'est de la vivianite ! Mon prédécesseur Philipp Wilfert a montré que plus de 80 % du phosphore présent dans les boues pouvait être présent sous forme de vivianite s'il y avait suffisamment de fer. Par conséquent, se concentrer sur la récupération de la vivianite est une option prometteuse pour récupérer le phosphore des boues.

La vivianite ne se trouve que sous forme de minuscules cristaux (20-200μm) dans les boues, ce qui rend sa récolte compliquée avec les techniques conventionnelles basées sur la gravité, comme les hydrocyclones. Par conséquent, j'ai étudié la cristallisation de la vivianite pendant mon doctorat pour comprendre comment faire grossir les particules afin qu'elles soient plus faciles à séparer. Il s'est avéré que c'était un projet très compliqué et qu'il pourrait être difficile de produire de grosses particules de vivianite dans les conditions de pH et de concentration que l'on trouve dans les stations. Heureusement, les techniques basées sur la gravité n'étaient pas la seule option pour séparer la vivianite puisque ce minéral a des propriétés paramagnétiques, ce qui signifie que les aimants puissants l'attirent.

La première partie de mon projet consistait à montrer que la vivianite pouvait effectivement être extraite des boues avec un séparateur magnétique « fait-maison ». A partir de là, deux axes de recherche étaient intéressants à poursuivre. Premièrement, il était vital de s'assurer que suffisamment de phosphore était présent sous forme de vivianite dans les boues puisque seul le phosphore présent comme vivianite peut être récupéré magnétiquement. Deuxièmement, le système devait être démontré à plus grande échelle et optimisé.

L'un de nos partenaires, "Brabantse Delta", a augmenté le dosage du fer dans l'une de ses stations d'épuration (Nieuwveer) pendant que la récupération magnétique de la vivianite y était testée. Cela nous a permis de faire d'une pierre deux coups : étudier la production de vivianite en augmentant le dosage de fer tout en améliorant la technologie. Au cours de son doctorat, Philipp a montré que plus le rapport Fe/P est élevé dans les boues, plus la quantité de phosphore présent sous forme de vivianite est élevée. Cependant, son étude a été réalisée sur différentes STEP sans modification de leur dosage de fer alors que nous avons pu suivre "en direct" ce qui s'est passé après l'ajout de fer à Nieuwveer. Pendant l'augmentation du dosage de fer, tout le fer supplémentaire ajouté a été transformé en vivianite, ce qui était une excellente nouvelle. En outre, un dosage plus élevé de fer a permis de réduire la concentration de phosphore dans l'effluent et la concentration de $H_2S$ dans le biogaz (on s'y attendait mais c'était quand même bien de le confirmer). L'étude a également mis en évidence qu'un dosage plus élevé de fer n'entravait pas le fonctionnement normal de la STEP.

La comparaison de nos résultats avec les études précédentes a montré qu'avant que la vivianite puisse se former, le fer réagit avec le sulfure dans un rapport de 1:1. Cela indique que pour maximiser la quantité de phosphore présente sous forme de vivianite, un rapport Fe/P de 1,5 (la vivianite est composée de trois fer et de deux phosphates ; 3/2=1,5) n'est pas suffisant ; 1,5-2 pourrait être nécessaire s'il y a beaucoup de sulfure.

En parallèle de cette étude, Wokke Wijdeveld et son équipe ont utilisé un séparateur magnétique (une technologie de l'industrie minière) dans la même STEP. L'installation pilote pouvait traiter $1m^3$/h de boues digérées, soit l'équivalent des boues produites par 20 000 personnes (deux fois la population de ma belle vallée en France). Il a montré que la séparation de la vivianite était meilleure qu'avec le séparateur de laboratoire « fait maison », principalement grâce à la pulsation de la boue et à l'utilisation de matrices de tiges d'acier magnétisées. En faisant circuler la boue trois fois dans le séparateur, environ 80% de la vivianite a pu être récoltée. Globalement, plus de 60 % du phosphore présent dans les eaux usées influentes a pu être recueillis sous forme de vivianite, ce qui est mieux que les 10 à 30 % obtenus par la récupération de struvite (une autre approche de récupération des minéraux phosphorés). En outre, ce pourcentage de récupération a satisfait au seuil (>50%) de la future législation allemande qui est la plus stricte à l'heure actuelle.

Aux Pays-Bas, seulement 75% des boues sont digérées, ce qui signifie qu'il est important d'étudier également la récupération de vivianite à partir de boues non digérées. À ce stade du projet, nous savions que la vivianite se formait après 20 à 30 jours dans des conditions anaérobies dans un digesteur. En collaboration avec Wout Pannekoek de "Waterschapsbedrijf Limburg", nous avons découvert que le fer présent dans les boues fraîchement formées était réduit très rapidement lorsqu'elles étaient stockées dans des conditions anaérobies : tout le fer

était entièrement réduit après 2 ou 3 jours. Ceci est intéressant car la vivianite ne peut se former qu'à partir de la forme réduite du fer ($Fe^{2+}$). On peut donc en déduire que la plupart de la vivianite qui se formerait après le temps de rétention typique d'un digesteur (20-30 jours) était déjà formée après 2-3 jours. En d'autres termes, s'il y a suffisamment de fer dans une boue, quelques jours de stockage sans oxygène suffisent pour former une quantité significative de vivianite. Cela signifie qu'un digesteur n'est pas nécessaire pour récupérer le phosphore avec l'approche de la formation de vivianite.

Comme expliqué précédemment, il y a beaucoup de phosphore dans les excréments humains, mais en Europe, le fumier animal en contient quatre fois plus. Si nous pouvions recycler le phosphore présent dans les boues et le fumier, nous n'aurions plus besoin d'importer du phosphore. Dans le fumier, le phosphate est présent principalement sous forme de phosphate de magnésium et d'ammoniac (struvite) et de phosphate de calcium. La struvite est un minéral phosphoré thermodynamiquement stable dans les environnements réduits (comme les boues et le fumier). Si du fer est ajouté au fumier, on peut s'attendre à ce que la vivianite se forme en priorité comparé aux autres minéraux phosphatés. Par conséquent, nous avons développé un projet avec Chris Schott dans lequel nous avons étudié la formation de vivianite dans le fumier de porc après ajout de fer. Il s'est avéré que la plupart du phosphore pouvait être transformé en vivianite lorsqu'un rapport Fe/P de 4-5 était utilisé. Ce rapport est beaucoup plus élevé que celui nécessaire dans les boues (1.5-2), et nous pensons que c'est parce que le fer se lie à la matière organique avant de former la vivianite. Après avoir montré que la vivianite se formait, nous avons pu l'extraire du lisier de porc avec le même dispositif « fait maison » que celui utilisé pour les boues digérées. Ce projet était passionnant car il a montré que la vivianite pouvait également être utilisée pour récupérer le phosphore du fumier. Toutefois, la quantité de fer à utiliser doit être réduite pour que le processus soit économiquement viable. Ce sera un axe de recherche intéressant pour un prochain projet de doctorat.

La partie la plus originale de mon doctorat ne consistait pas à recueillir la vivianite mais à comprendre pourquoi elle se forme parfois à des endroits indésirables dans les STEP. Après avoir discuté avec plusieurs STEP, nous avons réalisé que beaucoup d'entre elles souffraient d'entartrage à la vivianite, c'est-à-dire de la formation d'une couche dure de vivianite sur les parois des tuyaux ou des équipements. Cela peut entraîner des problèmes de fonctionnement et obliger les STEP à changer leurs tuyaux ou à les nettoyer manuellement, ce qui représente un coût important. Après avoir collecté des données sur ces STEP, nous avons réalisé que la vivianite pouvait se former à différents endroits comme dans les tuyaux transportant des boues non digérées, les centrifugeuses utilisées pour enlever l'eau des boues non digérées et les échangeurs de chaleur où circulent les boues digérées. Il est intéressant de noter que les mécanismes de formation de la vivianite semblent différer dans ces trois endroits: réduction du fer, augmentation du pH due à l'extraction du $CO_2$ et dépendance de la solubilité de la vivianite à la température. Nous avons aussi pu proposer des stratégies de prévention/atténuation pour les STEP afin de remédier à ces problèmes. Ce projet nous a appris deux choses. Premièrement, vous pouvez doser beaucoup de fer et ne pas avoir de problèmes d'entartrage de la vivianite si le fer est dosé de manière judicieuse. Deuxièmement, l'entartrage de la vivianite n'a pas été largement rapporté dans la littérature parce que les gens

sont obnubilés par l'entartrage de la struvite. Cependant, la formation de tartre de vivianite est plus fréquente qu'on ne le pense.

Cette thèse a montré que la vivianite est un acteur clé dans les environnements anaérobies contenant du fer et du phosphore. L'extraction magnétique est une bonne option pour récupérer la vivianite, ce qui montre qu'une collaboration interdisciplinaire (traitement des eaux usées + traitement des minéraux dans ce cas) peut conduire à de grandes percées scientifiques. Cette approche est prometteuse et se rapproche du marché, ce qui est très excitant. Après sa séparation, la valorisation de la vivianite est un point crucial qui devra être étudié pour rendre cette technologie viable. Ce projet de thèse a apporté des réponses à plusieurs questions et nous a permis de mieux comprendre les mystères entourant la vivianite. Dans l'ensemble, il a soulevé encore davantage de questions (auxquelles les futurs doctorants s'attaqueront), ce qui est, en fin de compte, le but de la recherche.

# Contents

# Chapter 1: Introduction

**1**

## 1.1. Phosphorus/phosphate

### 1.1.1. What is it?

Phosphorus is the element with the atomic number 15 and with the symbol P. This element was discovered in 1669 by Henning Brandt (merchant and alchemist) when he evaporated urine residue (Gleason 2007). How amazing is it that the discovery of phosphorus was related to human wastes and that nowadays, its presence in wastewater gave the purpose for this thesis?! The name phosphorus comes from the Greek phosphoros, meaning "light-bearer" since white phosphorus glows in the dark due to its chemiluminescent properties. Phosphorus was sometimes called the "Devil's Element" because of its ability to burst into flame, its supernatural glow, and the fact that it was the 13th discovered element (Helmenstine 2019).

Phosphorus is the $11^{th}$ most abundant element in the earth's crust (0.1%) and the $17^{th}$ most abundant in the entire universe (Kwok 2012). The two main elemental forms of phosphorus are white and red phosphorus. Due to its instability, white phosphorus can be used to produce weapons and is used to make red phosphorus during an exothermic reaction. Red phosphorus is used as a reductive agent during the synthesis of methamphetamine (Skinner 1990), as all the Breaking Bad fans know. Fortunately, not all phosphorus is used for destructive applications. For example, red phosphorus can be a component of some flame retardants (Fu et al. 2017). Even though some applications exist for elemental phosphorus, it is mainly known under its oxidized form composed of phosphorus and oxygen: phosphate ($PO_4^{3-}$).

Phosphate is widely present in living species and represents around 3% of human body weight (Cohn and Dombrowski 1971). Most of it is present in our teeth and bones as calcium hydroxyapatite ($Ca_3(PO_4)_2)_3Ca(OH)_2$ (Lohman et al. 2005). Also, phosphate is a building block for DNA molecules participating in the reproduction of the cells and occupies a central role in the cells energy metabolism. In solution, phosphate is called orthophosphate ($PO_4^{3-}$) and can bind up to 3 protons depending on the pH. The pKa of the couple [$HPO_4^{2-}/H_2PO_4^-$] being 7.2, phosphate solutions an attractive buffer since their pH can be adjusted to neutral levels to mimic a human body's conditions.

### 1.1.2. Phosphorus is an essential fertilizer ingredient

Besides breathing and drinking, one of the crucial human needs (and pleasures) is to eat. Fertilizers are widely used to produce the increasing amount of food needed to match the growing population (Scholz et al. 2013). Phosphorus is an essential and not replaceable component of those fertilizers (Blackshaw et al. 2009, Childers et al. 2011). The primary phosphorus source is phosphate rock, a mineral obtained through mining, similarly to many other elements like gold, iron, or copper. More than 80% of the mined phosphate rock is used for fertilizer application (Van Kauwenbergh, 2010).

The world's phosphate rock production increased from 6 Mt in 1961 (Scholz et al. 2013) to 45 Mt of phosphorus in 2016 (De Boer et al. 2018), essentially due to the rising world population. It can be noted that the amount of phosphate rock consumed per person tends to reduce in developing countries since the end of the last century. The main reasons for this decrease seem to be better utilization of the phosphate rock combined with the progressive enrichment of soil stocks of phosphorus due to inputs of fertilizers and animal manures (Scholz et al. 2013).

Currently, 70% of the known in-land reserves are present in Morocco, while Europe bears minimal reserves and strongly depends on imports (Cordell et al. 2015). Whether we will run out of phosphorus rock in the coming decades is a constant point of discussion and mainly originates from the difficulty of estimating phosphorus reserves (Scholz et al. 2013, Van Kauwenbergh, 2010, Cordell et al. 2009). What is more certain is that rock mining is environmentally unfriendly since it releases heavy metals which pollute soil, air, and water (Cordell et al. 2015, El Zrelli et al. 2018). Because it is (potentially) limited, non-renewable, and harmful to the environment, alternatives to phosphate rock need to be found (Scholz et al. 2013).

### 1.1.3. Secondary phosphorus sources

To find those secondary phosphorus sources, we need to look in the direction of what we call "wastes": animal and human feces/urine (Barnett et al. 1994, Damalerio et al. 2019). It is funny to realize that even though the benefits of their soil amendments are known and utilized for thousands of years, these resources are called waste streams. Historically, agricultural soils have been amended with animal and human excreta for their fertilizing properties since they contain high concentrations of nitrogen, phosphorus, potassium, all essential elemental for plant growth.

Unfortunately, the application of sewage sludge (the final product of human excreta treatment) is not always possible. Since 1986, the use of sewage sludge in agriculture is regulated in Europe, and certain requirements (dry matter, organic matter, heavy metals, nutrient contents…) need to be met (Pescod 1992). New concerns about pathogens, micropollutants or heavy metals, and the regional excess of nutrients led some European countries like the Netherlands to stop spreading it on fields.

Animal manure is generally considered safer to return to the land, but other concerns limit its land application. Due to the unequal distribution of the intensive farming zones, some spatial imbalances in manure (and phosphorus) production are created. For example, demand exceeds supply in Africa and Australia, while supply exceeds demand in the Netherlands and North America (Cordell and White 2013). Consequently, 30-40% of the animal produced in the Netherlands needs to be transported to regions with nutrient deficits (Leenstra et al. 2014).

Yearly, around 1400 Mtons of animal manure are produced in Europe (European Commission 2014), roughly accounting for 1.4Mt of phosphorus. Over the same period, about 0.4Mt of phosphorus ended up in wastewater treatment plants (WWTP) (Van Dijk, 2016). Considering that Europe approximately imports 1.6 Mt of phosphorus as fertilizer per year (Schoumans, 2015), it can be seen that manure and wastewater represent a consequent reserve of phosphorus. The efficient recycling of the phosphorus they bear could cover a big part of the European demand. The work describes in this thesis will mainly focus on phosphorus recovery from sewage sludge. Before the phosphorus can be recovered, it needs to be removed from wastewater at wastewater treatment plants.

**1**

## 1.2. Municipal wastewater treatment

### 1.2.1. Why do we clean wastewater?

First of all, let us remember that it is all about health and water. Water is one of the most precious resources on the planet, and we need to protect it. Every day, we use a massive amount of freshwater: 10 billion tons. It is estimated that a person consumes on average 167 liters of water per day just for the production of the items we use (paper, clothes…). Around 80-90% of the freshwater is used in agriculture since food production requires a considerable amount of it (3500 liters per person per day!) (The World Counts 2021). For example, 1kg of grain requires a ton of water to grow. Cheese requires seven times more water than grain, and beefsteak 16 times more than grain. Everybody likes to compare to Olympic swimming pools, so I will follow the trend: feeding and maintaining a cow before killing it to produce 200kg of beefsteak requires more water than contained in an Olympic swimming pool! Even though water is present everywhere and seems like an unlimited resource, it is important to know that only 2.5% of the water on earth is freshwater (1.7% in the form of ice) while salty water completes the balance. It is estimated that we only have 18 years of freshwater supply available (The World Counts 2021). That makes a good reason to adjust our water consumption and recycle the water we already use, partly present as wastewater.

Yearly, around 380 billion tons of wastewater are produced and need to be cleaned (Mateo-Sagasta et al. 2015). Considering that 80% of the diseases are waterborne, according to WHO, it is easy to understand why wastewater treatment is necessary. The main objective of wastewater treatment is to produce an effluent that can be safely discharged in natural waters without causing any harm to the ecosystems and that can later be reused. Evidence of wastewater collection was found Middle-East around 2500 BC and in Rome with the building of an elaborated sewer system around 400 BC. The first proof of wastewater treatment was found in writing from ancient Greece around 1500 BC, describing a process involving charcoal filtration and exposure to sunlight. The construction of centralized sewage treatment started in the late 19th century, mainly in the United Kingdom and the United States. New sewage collection were also developed at that time to separate sewage and rainwater and not overload WWTP. Nowadays, wastewater originates from household waste collection, industrial streams (often pre-treated on-site), water intrusions in the sewer network, and rainwater. This thesis mainly focuses on municipal wastewater (toilet, shower, kitchen….etc). Wastewater is a very complex matrix that is composed of a multitude of elements (Table 1. 1). Three major contaminants need to be removed from wastewater before discharge: carbon, nitrogen, and phosphorus.

The main problem with the release of active organic matter in the natural waters is that it would consume the oxygen present in water, which is detrimental to aquatic life. The organic matter present in wastewater is denoted as Chemical Oxygen Demand (COD) and represents the oxygen necessary to fully oxidize (and thereby remove) the organic matter to $CO_2$ and $H_2O$. Around half of the organic matter can be degraded by bacteria, provided that they receive sufficient oxygen. This fraction is called the biodegradable oxygen demand (BOD). The rest of the COD is formed by non-biodegradable carbon and the newly produce microbial cell mass and is removed as excess sludge. While phosphorus and nitrogen are essential in fertilizer,

their presence in natural water is only wanted in small quantities. They cause eutrophication that can be characterized by an algae bloom detrimental to the ecosystems. Some of the algae, for example the blue-green algae, can be very toxic and would prevent water consumption and recreational activities (Skulberg et al. 1984). Since phosphorus is believed to be the limiting nutrient compared to ammonium-nitrogen, its removal is of paramount importance (Smith et al. 1999). Other contaminants like micropollutants, microplastics, or resistant genes also require attention. Many of the current WWTPs are not designed to remove those compounds but can partly remove them.

|  | Low | Typical | High |
|---|---|---|---|
| pH | 6.5 | 7.5 | 8.5 |
| P-PO$_4$ (mg P/L) | 1 | 5 | 15 |
| COD (g/L) | 0.2 | 0.5 | 2.0 |
| Mg$^{2+}$ (mg/L) | 1 | 15 | 60 |
| SO$_4^{2-}$ (mg S/L) | 10 | 30 | 60 |
| Na$^+$ (mg/L) | 40 | 100 | 400 |
| Cl$^-$ (mg/L) | 30 | 300 | 600 |
| Ca$^{2+}$ (mg/L) | 10 | 60 | 150 |
| K$^+$ (mg/L) | 10 | 20 | 35 |
| N-NH$_4^+$ (mg N/L) | 10 | 35 | 75 |
| Alkalinity (mg/L CaCO$_3$) | 50 | 200 | 550 |
| HCO$_3^-$ (mg/L) | 20 | 90 | 350 |
| VFA (mg/L HAc) | 10 | 30 | 120 |

*Table 1. 1: Composition of municipal wastewater (more details in Chapter 8)*

## 1.2.2. Process overview

The main process involved in the wastewater treatment is to separate the wastewater into two fractions: the clean liquid phase, and a solid phase called sludge, containing all the unwanted material. The operation of an advanced WWTP can be decomposed into four sections: the primary treatment, which removes the solids particles and a part of COD, the secondary treatment that focuses on the removal of nitrogen, phosphorus, and COD, the optional tertiary treatment dealing with effluent polishing and advanced treatment and the solid treatment that aims at solids conditioning for their safe disposal/reuse. A scheme of a conventional WWTP organization can be seen in Figure 1. 1.

## 1.2.3. Primary treatment

The wastewater us collected and carried to the WWTP through the sewer network. The flow coming to the installation is the influent. The first step of the process is the primary treatment, which aims to remove a maximum of solids present in the influent. Such solids are typically sand, natural residues like branches, and human-made wastes like paper (or even mattresses?!). Those solids can be detrimental to the rest of the process, provoking blockages of the units or the pumps and need to be removed before any further treatment can occur. The bigger solids are removed with sieves while the sand and grit are removed in grit chambers, functioning on

**1**

such solids' quick settling. The next unit is usually a clarifier or sedimentation tank that works on the particles' settling to separate liquid from solids. These units are the ones that make a WWTP easily identifiable from a plane. These basins present very low turbulence and a few hours of retention time to allow optimal sedimentation. Besides, oils will float on the surface of the clarifier and will be removed by slow scrapping. A well-operated primary sedimentation unit can remove 50-70% of the suspended solid and 25-40% of the BOD (Metcalf & Eddy). Coagulants like iron can improve primary sedimentation by increasing the flocs' size to ease their settling and reduce the load to be treated by the secondary treatment. The mix of solids collected at the bottom of the primary settlers is called the primary sludge.

## 1.2.4. Secondary treatment

### 1.2.4.1. COD removal

The secondary treatment, sometimes referred to as the biological treatment, is the most important place of a WWTP. During this step, the remaining COD, nitrogen, and phosphorus are removed. The configuration of WWTP can significantly vary, but the processes mainly involve microorganisms to degrade the pollutants. In the influent wastewater, a concentration of 0.5-1 g/L of COD can be expected. Two main routes are used to destroy dissolved and suspended organic matter by bacteria: transformation into $CO_2$ and water or accumulation by the microorganisms that will later settle and end up in the sludge. The destruction of organic matter involves a wide variety of microorganisms, each of them degrading a specific type of organic form. The activated sludge units are aerated to provide enough energy to these organisms to accomplish their destruction process. The aeration also mixes the activated sludge to increase the contact between the organic matter and the microorganisms and prevent the biomass's settling. In aerated zones, around half of the COD is transformed into biomass while the other half is consumed as energy. The aeration represents approximately 50% of a WWTP cost and needs to be carefully controlled. The bacteria present in the activated sludge systems can bind to each other by producing a sticky polysaccharide. These agglomerates of bacteria are called flocs, and their considerable size (50-200μm) allows them to sediment in the secondary clarifier, where the biomass is removed as excess sludge. A part of the sludge is recirculated to the beginning of the secondary process to reuse its bacterial community.

### 1.2.4.2. Nitrogen removal

The removal of nitrogen from wastewater also heavily relies on biological activity. In the influent wastewater, nitrogen is mainly present as ammonia $NH_4^+$ at a concentration of 10-75 mg/L (see Chapter 8). Its removal consists of two steps called nitrification and denitrification, which will convert ammonia to gaseous nitrogen, safely released into the atmosphere. In the first stage of the process, nitrification, ammonia is oxidized to nitrite ($NO_2^-$) and later to nitrate ($NO_3^-$) by bacterial action. Around 4 g of oxygen and 7 g of alkalinity (as $CaCO_3$) are necessary to provide the bacteria sufficient energy to realize this conversion. Alkalinity can be seen as the buffer capacity of water, its ability to neutralize acid (Chapter 8). After ammonia is transformed to nitrate, it needs to be reduced to gaseous nitrogen. For this reduction process, around 4g of organic matter is required per gram of $NO_3^-$-N to serve as an electron donor. Sicne most of the BOD has already been removed in the activated sludge process sludge is recirculated at the start of the activated sludge process to furnish organic matter for the reduction process.

Figure 1.1: Scheme of a conventional WWTP. All rights and credit go to Rebeca Pallarès Vega for the realization of my favorite representation of a WWTP.

**1**
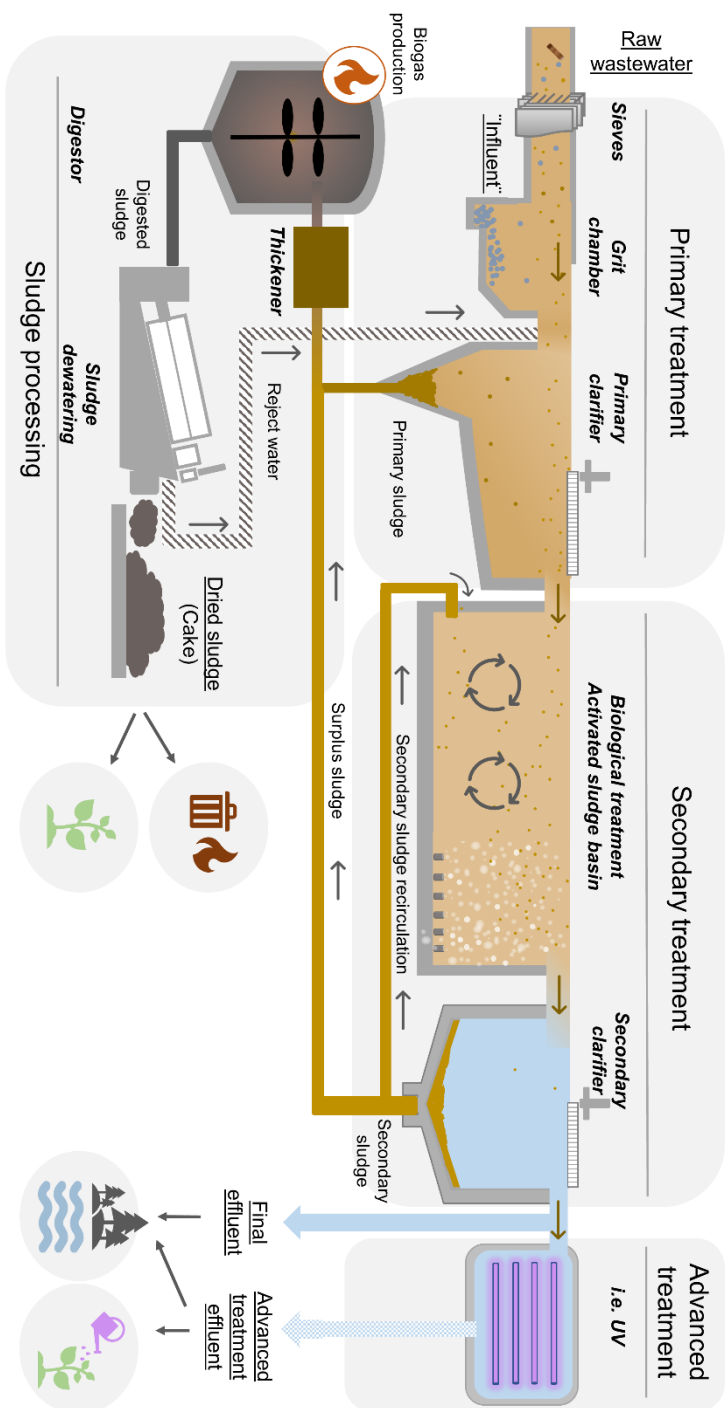
This reduction process takes place in the absence of oxygen, in zones called anoxic (no oxygen, but nitrate). Denitrification produces around 3.5 g of alkalinity that can be used for the nitrification process. It is sometimes hard to understand the order in which these processes are taking place in a full-scale installation because of the numerous recirculated streams. A process called anammox (based on the name of the bacteria) can simultaneously transform ammonia and nitrite into nitrogen gas without nitrate's production. This process can achieve the same results as the conventional nitrification/denitrification process without organic matter input and half the alkalinity and oxygen requirement. Unfortunately, the anammox does not perform well at low temperatures (<20°C) occurring during the cold season due to its slow growth. A part of the ammonia present in the wastewater will also end up in the newly formed biomass, as organic nitrogen.

### 1.2.4.3. Phosphorus removal

Phosphorus removal from wastewater is essential since its presence even at low concentrations (0.01 mg/L) can cause eutrophication. The phosphorus concentration in the raw sewage is typically 5-15 mg/L, mainly composed of orthophosphate, and typically needs to be brought to 0.1-2 mg/L depending on the legislation. Stringent phosphorus effluent limits will usually be implemented in areas where the water bodies are considered more sensitive, like the Baltic Sea. While the particulate phosphorus removal mechanism is essentially done by settling the particles in the biomass (by coagulation), dissolved phosphate treatment can be performed either biologically or chemically.

The Enhanced Biological Phosphorus Removal (EBPR) strategy was developed in the 1960s and relies on the accumulation of phosphate by specific microorganisms. The Phosphorus Accumulating Organisms (PAO's) are growing and assimilating the soluble phosphate as polyphosphate in their cells when aerobic conditions are present. The energy necessary for polyphosphates' formation originates from the oxidation of the previously stored intracellular polyhydroxy butyrate (PHB) and glycogen. In addition to phosphate, the bacteria absorb magnesium and potassium to stabilize the negative charge of the phosphate (Jardin et al. 1994). The PAO's are the bacteria that can store the most energy in a wastewater treatment system, and they can be selected over other bacteria. To do so, anaerobic (no dissolved oxygen nor nitrate) zones are present at the beginning of the activated sludge processes. There is a lot of organic matter (another reason sludge is recycled) on which bacteria can feed, but no oxygen to produce enough energy to store this organic matter. Due to their ability to hold a lot of energy, the PAO's can destroy the polyphosphates present in their cells, harvest their binding energy, and feed on organic matter to accumulate it as PHB. In short, PAO's consume BOD and release phosphate in anaerobic conditions. In aerobic conditions, they accumulate phosphate while consuming oxygen. This reversible process is a strength of EBPR and a weakness since phosphate will be released as soon as anaerobic conditions occur. It can easily happen during sedimentation, for example. Compared to the chemical phosphorous removal (described below), the EBPR strategy offers a reduced sludge volume and decreased chemical cost. However, it may require metal salts support to reach very low phosphorus levels (Morse et al. 1997).

The Chemical Phosphorus Removal (CPR) strategy relies on the precipitation of the soluble phosphate (and the coagulation of the particulate phosphate) with either aluminum or iron salts.

Phosphate has a stronger affinity to aluminum than iron, allowing a good phosphate removal, but making it difficult to recover phosphate from aluminum phosphate minerals. The choice between those two salts mainly depends on their regional availability. In Europe, iron salts are generally cheaper and, therefore, more widely used (Korving et al. 2019). Besides, more stringent limits of aluminum discharge can exist in some countries due to its toxicity (e.g., in the United Kingdom). It has also been noticed that a few mg/L (1-10mg/L, according to Wilfert et al. 2015) of iron could already be present in the influent wastewater and could potentially participate in the phosphate removal process. The form under which iron phosphates are present in activated sludge is still not very clear nowadays. They could be present as adsorbed phosphate on iron oxides/hydroxides or iron phosphate minerals. These species are transformed into the more stable vivianite mineral when reductive conditions are present (Wilfert et al. 2016). The speciation of the iron phosphate minerals especially seems of interest to better understand the phosphorus removal process. Things can get even more complicated considering that ferrous iron salts (usually cheaper than ferric iron) are often dosed in aerated sections to be oxidized to $Fe^{3+}$, which presents better flocculation ability due to its higher charge. The type of iron phosphate formed and the removal process is suspected to depend on the kind of iron salt used and the WWTP process flow. However, vivianite appeared to be a prominent iron phosphate mineral in digested sludge (and in stored excess sludge) whether Fe(II) or Fe(III) salts were dosed (Wilfert et al. 2018).

It seems that CPR can reach lower phosphorus limits in the effluent (0.1mg/L) than EBPR (0.5mg/L), making it the preferred strategy for the countries with more stringent legislation. For example, it is not rare to find WWTPs with molar Fe:P>2 in countries bordering the Baltic Sea. It can also be noted that metal salts are often used to support biological phosphorus removal, for example, when lower phosphorus limits need to be met during warmer seasons. Whether the phosphorus is removed biologically or chemically, it ends up in the sludge in the biomass or present as metal phosphate minerals, which will have its importance for the rest of this thesis. After the secondary treatment, most pollutants have been passed from the liquid phase to the solid phase. The separation of these two phases is performed during the secondary sedimentation by another clarifier. The solids collected in this clarifier are called the secondary sludge and will generally be mixed with the primary sludge to be stabilized for safe disposal, often by digestion (explained later).

## 1.2.5. Tertiary treatment

The liquid phase (called effluent) is relatively clean after the secondary treatment and can often be safely discharged. In some installations, tertiary treatment is performed to polish the effluent, for example, to further remove nutrients or emerging contaminants. This treatment may be necessary if the water is meant to be reclaimed or is containing a high load of emerging pollutants that are not treated by conventional wastewater treatment. Such compounds can be, for instance, micropollutants or pharmaceuticals. Techniques like ozonation, UV treatment, and chlorination are among the possible strategies (Gerba and Pepper, 2019).

**1**

### 1.2.6. Solid stabilization and disposal

The solid phase is made from the primary and secondary sludge, and sometimes external sludge originating from neighbouring WWTP. This slurry can be referred to as mixed sludge or surplus sludge and contains all the unwanted material and contaminants removed from the wastewater that have not been oxidized. The final sludge should be compact to be transported and stable to prevent the release of pollutants. The disposal method will set the goals for the sludge conditioning methods applied at the wastewater treatment. The most common disposal routes are landfilling, incineration, agricultural use, or composting. Thickening, stabilization, and dewatering are three widespread processes used for on-site sludge conditioning. Stabilization of the sludge is commonly done by aerobic or anaerobic sludge digestion. Around 75% of the sewage sludge produced in the Netherlands stabilized by (aerobic or anaerobic) digestion (Unie van Waterschappen 2018). Aerobic digestion uses microorganisms, supplied with oxygen at ambient temperature, to degrade organic matter into $CO_2$.

The more widely used anaerobic digestion operates at 20-30 days of solids residence time in the absence of oxygen and allows energy production as biogas. This process is also biological but operates around 37°C (mesophilic digestion) or 55°C (thermophilic digestion) for the appropriate microorganisms to function correctly. During this thesis, most of the installations encountered function with mesophilic anaerobic digestion. Some WWTPs are energy self-sufficient thanks to their biogas production. The formation of biogas is achieved by the sequential destruction of the organic matter to Volatile Fatty Acids (VFA), further decomposed into $CH_4$ and $CO_2$. Biogas formation also results in the production of $H_2S$ gas that is smelly, can cause corrosion, and needs to be treated before using the biogas. One of the common strategies to capture $H_2S$ is to add iron to the digester, showing the ubiquity of iron in wastewater treatment processes.

Sludge pre-treatments like Thermal Hydrolysis Process (THP) are recently gaining more interest since they improve dewaterability and partially degrade the organic matter, making biogas production more effective in the subsequent anaerobic digestion. These processes are operating at high temperatures (>150°C) and several bars of pressure. Before being transported for disposal, the sludge volume (digested or not) needs to be dramatically reduced to save transportation costs. The solid content is typically increased from 3-5% to 20-30% (23% is typical in the Netherlands, Unie van Waterschappen 2018) using belt-thickening or centrifugation, supported by polymer addition for improved flocculation. The sludge disposal costs approximate 400€/ton dry solid in the Netherlands and represent a significant cost of a WWTP operation since more than 300 000 tons of dry sludge are produced every year in the Netherlands (Unie van Waterschappen 2018). Incineration of dewatered sludge was further developed in recent years since it dramatically reduces the sludge volume as ashes. Still, installations are expensive to build, and sewage sludge is not accepted in all incineration plants. Sludge contains valued compounds for agriculture and can be employed as organic fertilizer and partly replace commercial fertilizers. However, its use is strictly regulated, which led some countries like the Netherlands to abandon this option. Landfilling is another possible route for sludges with high contaminant concentration but is already forbidden in several European countries (Kemira Handbook 2020).

**1**

Wastewater is widely collected in Europe, with 95% of the household being connected to a collection system in 2014 (European Commission 2017). Most of this wastewater is treated, and the processes to treat the major pollutants are commercially available and optimized for a wide range of applications. Since their removal is well-developed in industrialized countries, the focus of recent years has been on valorizing the waste produced at the WWTPs. Around 90% of the phosphorus present in a WWTP influent ends up in the sludge, either stored in the PAO's or as metal phosphates, making sludge an attractive target for its recovery (Egle et al. 2016).

## 1.3. Phosphorus recovery technologies

The current more widely (and easiest) option to reuse the phosphorus from sewage sludge is by using the stabilized sludge in agriculture (Kabbe 2019). This practice may be abandoned in the future due to concerns about emerging pollutants such as antibiotic resistant genes. The phosphorus need of the crops and the land are not always considered (e.g. FeP is not very bioavailable). In this case, application on land is a form of landfilling rather than phosphorus recycling. Therefore, alternatives for the recovery of the phosphorus in a purer form have to be developed. Transportation of a more concentrated phosphorus product would also be cheaper and equalize the regional imbalances (Wilfert et al. 2015).

In a WWTP, there are opportunities to recover phosphorus at four different steps in the process (Egle et al. 2016, Kabbe 2019, Chrispim et al. 2019):

- From the effluent, if phosphorus has not been precipitated during the wastewater treatment process (e.g., Ravita process, Rossi et al. 2018).
- From dewatered sludge, by land application or ash leaching after incineration.
- From reject water (liquid fraction of the digested sludge) by struvite crystallization if EBPR process is used.
- From the digested sludge as struvite if EBPR is employed, or as vivianite if CPR with iron is used (this thesis).

The most commonly used strategies to recover phosphorus from wastewater are via struvite crystallization from reject water, and ash leaching after icineration of the dewatered sludge. The different phosphorus recovery technologies are presented in the next sections along with their advantages and disadvantages, based on the stream they are applied to: effluent, dewatered sludge, reject water and digested sludge.

### 1.3.1. From the effluent

One of the recent innovations is the recovery of phosphorus from the effluent of WWTPs with a unit located at the very end of the treatment process. This technology is limited to the phosphorus that reaches the effluent (soluble phosphorus), and therefore, a limited amount of phosphorus needs to be removed in the waterline. The phosphorus can, for example, be recovered from the effluent by adsorption on reusable iron-based compounds (Drenkova-Tuhtan et al. 2017). This strategy is rather used as effluent polishing to meet stringent discharge limits than recover phosphorus for the moment. For this approach, the reusability of the adsorbent is crucial for economic viability. If the recovery from the effluent is sought, organic coagulants should be preferred to efficiently settle the sludge flocs since they do not interact

**1**

with phosphorus. Aluminum or iron salts can be added to the effluent to produce pure phosphorus precipitates that gravity-based techniques can recover. For example, the Ravita approach allows the recovery of 70% of the influent phosphorus by precipitation in the effluent. In this case, disk filtration is used to recover the sludge (Rossi et al. 2018). Post-precipitation processes produce a phosphate sludge that is poor in pathogens and micropollutants (that remain in the "organic" sludge). Besides, the savings in aeration costs (up to 10-25%) and a reduction of the sludge volume (10-20%) are two other advantages of this technology (Rossi et al. 2018). Piloting this technology revealed that the floc formation is the most critical aspect of this technology since bad flocculation complicated the sludge recovery (Rossi et al. 2018). A drawback of the technologies targeting phosphorus recovery from WWTP effluents is that wastewaters containing a high share of particulate phosphate or dissolved metals are not suited for this process. Also, PAO's need to be avoided to maximize the phosphorus in the effluent, which seems challenging in a standard activated sludge process for nitrogen removal. Most of these technologies are currently used at intermediate TLR (pilot-scale), and their full-scale feasibility is yet to be proven.

### 1.3.2. From the dewatered sludge

The principal phosphorus recovery technology after dewatering is from ash processing after mono-incineration. The high temperatures reached during incineration make the ashes free of organics, micropollutants, bacteria, or pathogens, which is a strong point of this approach (Liu et al. 2021). Besides, the volume reduction offered by incineration is economically attractive. During incineration, the organic matter will be burnt (<1% remains), concentrating the phosphorus to around 10% of the solids (against 2-3% in dewatered sludge solids) (Kabbe et al. 2020). Mono incineration (only sewage sludge) is essential to prevent the dilution of phosphorus in the ashes but is more expensive and is especially relevant for infrastructures processing a lot of sludge (Egle et al. 2016, Chrispim et al. 2019). Otherwise, additional transportation costs have to be taken into account, and this can reduce the interest in this technology. Nevertheless, sludge incineration is increasingly used in Europe and is the only sludge disposal route in the Netherlands and Switzerland. Around half of the sludge is incinerated in Germany, and more incineration infrastructures are currently being built (Kabbe 2019).

Once the phosphorus is concentrated in the ashes, there are two ways to recover it: thermal treatment or dissolution and subsequent recovery by precipitation or ion exchange. The most straightforward process is the thermal treatment of the ashes (e.g., MEPHREC). First, the ashes are mixed with sodium or magnesium sulfate and heated at a temperature higher than 1000°C, evaporating some heavy metals like cadmium, lead, zinc, or mercury. The resulting P-rich slag needs further treatment before being reused because it still contains high concentrations of iron or aluminum. However, phosphorus is more bioavailable in this form than in ashes (soluble in citric acid) due to the formation of magnesium and calcium phosphate phases (Adam et al. 2009). The product could be blended in NPK fertilizer. While the investment costs of this technology are lower, the metal salts cannot be recovered. (Adam et al. 2009)

The second option is the dissolution of the ashes and the subsequent phosphorus recovery. Two routes are currently used to leach the phosphorus from the ashes: acidic or alkaline

treatment. In the first case, inorganic or organic acids are used to efficiently dissolve phosphorus (80-100%) (Chrispim et al. 2019, Liu et al. 2021). The main drawback of this approach is the simultaneous release of heavy metals. Technologies like liquid-liquid separation or cationic exchange membranes were used to remove the heavy metals, but never at full scale due to their price and complexity (Liu et al. 2021). Further research needs to be undertaken in this direction. The second strategy is to use alkaline solutions, producing leachates with lower heavy metals contents. However, the phosphorus release will be lower than with the acidic route (<70%) since MgP and CaP are not soluble at high pH. The formation of more stable CaP and MgP phases during sludge incineration can also explain this low recovery (Ovsyannikova et al. 2019). Sludge coagulated with iron or aluminum salts is a better target for the alkaline route due to the solubility at high pH or FeP and AlP. Sequential extraction is an exciting approach to combine high phosphorus release and low heavy metal recovery but requires more development (complexity, more solvents required, efficiency depends on the feedstock used) (Liu et al. 2021). After phosphorus leaching, precipitation is employed to recover the phosphorus as salt, typically struvite of calcium phosphate that can be used as fertilizer. The leaching approach presents the advantage that iron and aluminum salts can be recovered after leaching and reprocessed for further reuse. Phosphorus recovery from incineration ashes is already mature, and processes like Tetraphos and Ash2Phos are available on the market.

### 1.3.3. From the reject water

During anaerobic digestion, phosphorus is released from the biomass and can reach several hundreds of mg/L. After dewatering, the liquid fraction is therefore rich in phosphate, ideal for recovery by precipitation. Since this stream contains ammonia (released during biomass digestion), the recovery as struvite $MgPO_4NH_4*6H_2O$ is an attractive option (Peng et a. 2018). Initially, the interest in struvite crystallization came from the need to solve a problem. Large build-ups of struvite scaling were occurring in WWTP using EBPR, especially in dewatering centrifuges, and required heavy maintenance. The control of struvite scaling by chemical dosing was the starting point to the study of struvite formation and the development of various technologies targeting struvite recovery (Le Corre et al. 2009). Several processes (e.g., Ostara, Nuresys, Phospaq, Struvia, Phosphogreen) are based on magnesium addition to rejected water and precipitation of struvite pellets in engineered reactors. Nowadays, moer than 20 different systems based on struvite recovery exist (Kabbe et al. 2019).

The precipitation of struvite from reject water produces high-quality struvite that can be used directly as fertilizer or raw material for the fertilizing industry (Peng et al. 2018). Struvite is known as a slow-release fertilizer, ideal for the slow assimilation of nutrients by some crops (Chrispim et al. 2019). However, while standard fertilizers present a weight N/P ratio of around 5, the ratio in struvite is ten times lower. In some cases, when only phosphorus is required, the presence of nitrogen can limit the applicability of struvite. When metal salts are added to the wastewater treatment process, phosphate is not released during anaerobic digestion but is firmly bound to the iron or aluminum. Therefore, phosphorus recovery from reject water is not feasible for installations using CPR. The recovery yield is also lower for WWTPs using CPR to support EBPR or treating wastewater containing iron. The fact that only a part of the phosphate is released during anaerobic digestion limits phosphorus recovery via struvite

precipitation to 10-30% of the phosphorus in the WWTP influent, representing its biggest disadvantage (Wilfert et al. 2015).

### 1.3.4. From the digested sludge

Currently, not many technologies allow the recovery of phosphorus from digested sludge. The precipitation of struvite and its recovery by settling is possible (e.g., Airprex) (Chrispim et al. 2019). Still, the crystallization in a sludge environment increases the risk of contaminant inclusion in the product (especially organics). With this recovery approach, magnesium salts need to be added and the pH increased (by $CO_2$ stripping) to promote struvite crystallization. Since phosphorus can be bound to other cations like calcium and iron, this technology often requires a redissolution step to maximize the phosphorus available for struvite precipitation (Remy et al. 2016). In this case, heavy metals can be released from the sludge and need to be removed. This technology's primary economic driver is the digested sludge's improved dewaterability after struvite settling (Bergmans et al. 2013). Roughly 75% of this process's cost savings originate from the improved dewaterability leading to lower transport and sludge disposal cost (Kemira Handbook 2020). This approach presents a clear economic interest for sludge reduction but produces a low-quality product. Similar to the recovery of struvite from reject water, this approach's efficiency is limited by the amount of phosphorus bound to aluminum or iron in the digested sludge. Besides, the struvite is recovered from the sludge via gravity settling, meaning that only the biggest crystals can be recovered, leading to extraction efficiency lower than 50%. Saerens et al. 2021 reported a total phosphorus recovery from the influent of 5% based on a full-scale installation.

Currently, no fully developed technology is available to recover phosphorus from digested sludge of WWTP using the CPR strategy. Phosphorus recovery from aluminum-coagulated sludge did not attract much attention since aluminumphosphate precipitates are complicated to separate from the sludge. More research was carried out on phosphorus recovery from iron-coagulated sludge, which is the main topic of this thesis. The primary studied approach is the release of the phosphate from the sludge by sulfide or pH adjustment. While actively investigated, these methods are not present at full-scale scales due to their low recovery or substantial chemical costs. Wilfert et al. 2020 showed that 60-90% of the phosphorus could be released from various iron phosphates by sulphide addition. However, they observed solubilization of only 30% of the phosphorus after sulphide addition to digested sludge. The low recovery was assumed to be due to the rebinding of the released phosphates to other cations present in the soluble phase of the sludge.

As discussed above, the mechanism of phosphorus removal by iron addition in the waterline is widely used, but its fundamentals are complex and not fully understood. Wilfert et al. 2015 discussed that the phosphorus removal mechanism could be based on several iron phosphate species. Such compounds could be ferric phosphate complexes and phosphates adsorbed on iron oxides. After a detailed study of the excess and digested sludge at two WWTPs, they noticed that Fe(II) dominated the iron pool and that vivianite ($Fe(II)_3(PO_4)_2*8H_2O$) was a major iron phosphate species in all the samples (Wilfert et al. 2016). At this point, they hypothesized that vivianite was an important mineral in the WWTPs dosing iron and that vivianite could play an essential role in phosphorus recovery from iron-coagulated sludges.

Further study of excess sludges showed that vivianite was present, but no clear correlation with the composition of the sludges could be made (Wilfert et al. 2018). This research brought to light an interesting finding: the share of phosphorus present as vivianite increased with the molar Fe/P ratio in these sludge. At Fe/P ratios above 2, 70-90% of the phosphorus was present as vivianite, showing the potential for phosphorus recovery if vivianite can be extracted from digested sludge. In Wang et al. 2019 the formation of vivianite in activated sludge was relatively quick and connected to the biological reduction of iron. It was hypothesized in Wilfert et al. 2018 that vivianite could form in the treatment line persist through the oxygenated zones. Finally, Philipp Wilfert showed that the particles of vivianite could be separated from digested sludge thanks to their paramagnetic properties.

## 1.4.    Vivianite: a few words about the start of the show

Vivianite is an iron-phosphate mineral that was named after the English mineralogist John Henry Vivian. In the scope of this thesis, the most important characteristic of vivianite is his paramagnetism, which means that vivianite is weakly attracted by an applied magnetic field, but does not possess a permanent magnetic field itself.

Vivianite is colorless at first and progressively turns dark blue when oxidizing. The oxidation of vivianite can be oxygen or light-induced and is therefore complicated to prevent (this will have its importance later). Because of its gradual darkening, vivianite was used by some tribes to catch evil spirits. The freshly extracted vivianite was relatively clear and supposed to be kept at home to help absorb the evil spirits, which would provoke the darkening of the protective stone. Of course, a new vivianite gem had to be bought when the old one would have become dark because saturated with bad energy (and so unusable). Its spiritual nature is reinforced by its presence on the bones of some corpses buried in iron-rich waterlogged soils (or coffins). Vivianite is a relatively rare mineral but is the most stable iron phosphate in anaerobic environments. Therefore, its presence is widely reported in lake sediments, forest soils, or clays.

Because of its nice color, vivianite has been used as a blue-grey pigment, mainly by Dutch painters such as Johannes Vermeer and Rembrandt van Rijn. Due to its rarity, only 70 paintings containing vivianite could be identified (Čermáková et al. 2013). The degradation of vivianite over time could make its identity complicated to track. The decomposition of vivianite to yellow species (iron oxides) provoked some paintings' sky to turn yellow over the years. From a more spiritual aspect, vivianite gems help focus on goals and their realization and prevent burn-out. It seems evident that it is the perfect gem to get when navigating through a Ph.D.

**1**

## 1.5.    Motivation of the research axis of this thesis

At the beginning of my Ph.D., it was known that vivianite was an essential mineral in phosphorus recovery from iron-coagulated sludge. The first evidence that it could be recovered magnetically was just found when I started my journey. Therefore, the first objective was to prove that the separation could be done at lab-scale. Following this proof of principle study, the up-scaling of the technology was the next challenge. It mainly consisted in two research axis: the maximization of the vivianite content at full-scale and the upscaling of the vivianite magnetic recovery.

Since the interest in vivianite was relatively new, another foreseen challenge of my Ph.D. was the quantification of vivianite in sludge. Mössbauer spectroscopy was an available analytical tool focusing on iron species but was not widely used on sludge samples. This aspect was a constant point of attention during my Ph.D and our approach constantly evolved and improved over time.

The vivianite particles found in digested sludge so far were relatively small (20-200µm). A main goal of my research was to understand the crystallization of vivianite and find a way to grow bigger particles that would allow (cheap) gravity-based separation. It turned out that it was very challenging at the typical pH of wastewater, which is discussed in Chapter 9.

While vivianite formation in digested sludge attracted some attention following the work of my predecessor at Wetsus, Philipp Wilfert, its occurrence in excess sludge was not deeply studied. The extent to which vivianite could form was never studied. Besides forming in sludge, vivianite can form problematic scaling, which was scarcely reported in the literature. We suspected that vivianite scaling occurred more widely than the lack of information in the literature suggested and that the study of its formation could bring new insights.

Since vivianite is a thermodynamically stable mineral and can be recovered magnetically, its potential to recover phosphorus from other sources was studied. Considering that animal manure represents a significant secondary phosphorus source in the Netherlands, the formation and extraction of vivianite in this new substrate were investigated.

## 1.6. Thesis outline

In **chapter two**, the proof of principle of the extraction of vivianite from digested sludge was given. It opened a new phosphorus recovery route from digested sludge.

In **chapter three**, the iron dosing was increased for three months at the full-scale WWTP of Nieuwveer. It showed that vivianite could be efficiently formed by increased iron dose without being detrimental to the WWTPs functioning.

In **chapter four**, vivianite could be magnetically recovered from digested sludge at pilot-scale, which posed the first stone for further developing the Vivimag technology.

In **chapter five**, iron was added to undigested sludge, kept under anaerobic conditions for a few days. A significant quantity of vivianite formed after 2-4 days of residence time, showing the potential for vivianite recovery for plants without digester.

In **chapter six,** it appeared that vivianite scaling is more common than the scarce mentions in the literature suggested. Vivianite scaling prevention and phosphorus recovery can go hand in hand.

In **chapter seven**, iron was added to pig manure which resulted in vivianite formation. The vivianite could later be recovered magnetically, suggesting a new route for phosphorus recovery from animal manure.

In **chapter eight**, literature was reviewed to estimate the composition of the liquid phase of the different streams in a WWTP and to deduct their ionic strength. It suggested that, despite its importance in wastewater treatment, the accurate determination of this parameter is often overlooked.

In **chapter nine**, the findings of this thesis were evaluated to discuss the bottlenecks of the vivianite recovery approach and the things that did not work during this thesis. Lastly, an outlook was given on the future of phosphorus recovery and the opportunities that may arise.

**1**

# References

Adam, C., Peplinski, B., Michaelis, M., Kley, G., & Simon, F.-G. (2009). Thermochemical treatment of sewage sludge ashes for phosphorus recovery. Waste Management, 29(3), 1122–1128. doi:10.1016/j.wasman.2008.09.011.

Barnett, G. M. (1994). Phosphorus forms in animal manure. Bioresource Technology, 49 (2), 139–147 DOI: 10.1016/0960-8524(94)90077-9.

Bergmans, B. J. C., Veltman, A. M., van Loosdrecht, M. C. M., van Lier, J. B., & Rietveld, L. C. (2013). Struvite formation for enhanced dewaterability of digested wastewater sludge. Environmental Technology, 35(5), 549–555. doi:10.1080/09593330.2013.837081

Blackshaw, R. E.; Molnar, L. J. (2009). Phosphorus fertilizer application method affects weed growth and competition with wheat. *Weed Science*, 57 (3), 311–318.

Chrispim, M. C., Scholz, M., Nolasco, M.A. (2019). Phosphorus recovery from municipal wastewater treatment: Critical review of challenges and opportunities for developing countries, *Journal of Environmental Management,* Volume 248, 109268, ISSN 0301-4797, https://doi.org/10.1016/j.jenvman.2019.109268.

Čermáková, Z., Hradilová, J., Jehlička, J., Osterrothová, K., Massanek, A., Bezdička, P., & Hradil, D. (2013). Identification of vivianite in painted works of art and its significance for provenance and authorship studies. *Archaeometry*, 56, 148–167. doi:10.1111/arcm.12067.

Childers, D. L., Corman, J., Edwards, M., Elser, J. J. (2011). Sustainability challenges of phosphorus and food: Solutions from closing the human phosphorus cycle. *Bioscience*, 61 (2), 117–124 DOI: 10.1525/bio.2011.61.2.6.

Cohn, S.H., Dombrowski, C.S. (1971). Measurement of total-body calcium, sodium, chlorine, nitrogen, and phosphorus in man by in vivo neutron activation analysis. *J Nucl Med*. Jul;12(7):499-505. PMID: 5092227.

Cordell D, White S. (2013). Sustainable phosphorus measures: strategies and technologies for achieving phosphorus security, *Agronomy*. 3(1):86-116. https://doi.org/10.3390/agronomy3010086.

Cordell, D. (2015). Tracking phosphorus security: indicators of phosphorus vulnerability in the global food system. *Food Security*, 7 (2), 337–350.

Damalerio, R. G., Belo, L. P., Orbecido, A. H., Pausta, C. M. J., Promentilla, M. A. B., Razon, L. F., Eusebio, R. C. P., Saroj, D., Beltran, A. B., Orbecido, A., (2019). Phosphorus recovery from wastewater and sludge. *Matec Web of Conferences*, 268, 06016–06016 DOI: 10.1051/matecconf/201926806016.

De Boer, M. A., Wolzak, L., & Slootweg, J. C. (2018). Phosphorus: Reserves, Production, and Applications. *Phosphorus Recovery and Recycling, 75–100.* doi:10.1007/978-981-10-8031-9_5.

Drenkova-Tuhtan, A., Schneider, M., Franzreb, M., Meyer, C., Gellermann, C., Sextl, G., Mandel, K. & Steinmetz, H. (2017). Pilot-scale removal and recovery of dissolved phosphate from secondary wastewater effluent reusable ZnFeZr adsorbent $Fe_3O_4/SiO_2$ particles with magnetic harvesting. *Water Research* 109, 77–87.

Egle, L., Rechberger, H., Krampe, J., & Zessner, M. (2016). Phosphorus recovery from municipal wastewater: An integrated comparative technological, environmental and economic assessment of P recovery technologies. *Science of The Total Environment*, 571, 522–542. doi:10.1016/j.scitotenv.2016.07.019.

El Zrelli, R., Rabaoui, L., Daghbouj, N., Abda, H., Castet, S., Josse, C., van Beek, P., Souhaut, M., Michel, S., Bejaoui, N. (2018). Characterization of phosphate rock and phosphogypsum from gabes phosphate fertilizer factories (se Tunisia): high mining potential and implications for environmental protection. *Environmental Science and Pollution Research*, 25 (15), 14690–14702 DOI: 10.1007/s11356-018-1648-4.

European Commission (2014). Collection and analysis of data for the control of emissions for the spreading of manure. Available at: https://ec.europa.eu/environment/air/pdf/Final%20Report.pdf.

European commission (2017). Ninth Report on the implementation status and the programs for implementation (as required by Article 17) of Council Directive 91/271/EEC concerning urban waste water treatment.

Fu, S., Song, P., Liu, X. (2017). 19 - Thermal and flame retardancy properties of thermoplastics/natural fiber biocomposites. *Advanced High Strength Natural Fibre Composites in Construction*, 479-508, https://doi.org/10.1016/B978-0-08-100411-1.00019-4.

Gerba, P., Pepper, I. (2019). Environmental and Pollution Science, 3rd ed, *Academic Press*. https://doi.org/10.1016/C2017-0-00480-9.

**1**

Gleason, W. (2007). An introduction to phosphorus: History, production, and application. *JOM*, 59(6), 17–19. doi:10.1007/s11837-007-0071-y.

Helmenstine, A. M. (2021) "10 Fun and Interesting Phosphorus Facts." ThoughtCo, Feb. 16, 2021, thoughtco.com/interesting-phosphorus-element-facts-3862735.

Jardin, N., Pöpel, H. J. (1994). Phosphate release of sludges from enhanced biological p-removal during digestion. *Water Science and Technology*, 30(6), 281–292. doi:10.2166/wst.1994.0279.

Kabbe, C. (2019). Global compendium on phosphorus recovery from sewage/sludge/ash.

Kemira handbook (2020). About water treatment.

Korving, L., van Loosdrecht, M., Wilfert, P. (2019) Effect of iron on phosphate recovery from sewage sludge. In: Ohtake H., Tsuneda S. (eds) *Phosphorus recovery and recycling*. Springer, Singapore. https://doi.org/10.1007/978-981-10-8031-9_21.

Kwok, S. (2012). Organic matter in the universe. Wiley-VCH, Weinheim.

Le Corre, K. S., Valsami-Jones, E., Hobbs, P., & Parsons, S. A. (2009). Phosphorus Recovery from Wastewater by Struvite Crystallization: A Review. *Critical Reviews in Environmental Science and Technology*, 39(6), 433–477. doi:10.1080/10643380701640573.

Leenstra, F. R., Vellinga, T. V., Neijenhuis, F., & de Buisonje, F. E. (2014). Manure : a valuable resource. *Wageningen UR Livestock Research*.

Liu, H., Hu, G., Alper Basar, I., Li, J., Lyczko, N., Nzihou, A., Eskicioglu, C. (2021). Phosphorus recovery from municipal sludge-derived ash and hydrochar through wet-chemical technology: A review towards sustainable waste management, *Chemical Engineering Journal,* Volume 417, 129300, ISSN 1385-8947, https://doi.org/10.1016/j.cej.2021.129300.

Lohman, T., Going, S., Wang, Z. (2005). Human body composition, *Human Kinetics*, volume 918.

Mateo-Sagasta, J., Raschid-Sally, L., & Thebo, A. (2015). Global Wastewater and Sludge Production, Treatment and Use. *Wastewater, 15–38.* doi:10.1007/978-94-017-9545-6_2.

Metcalf, W., Eddy, C. (2003). Metcalf and Eddy Wastewater Engineering: Treatment and Reuse, in *Wastewater Engineering: Treatment and Reuse* McGraw Hill. New York, NY. https://doi.org/10.1016/0309-1708(80)90067-6.

Morse, G., Brett, S., Guy, J., Lester, J. (1998). Review: Phosphorus removal and recovery technologies. *The Science of The Total Environment*, 212(1), 69–81. doi:10.1016/s0048-9697(97)00332-x

Ovsyannikova, E., Arauzo, P.J., Becker, G., Kruse. A. (2019). Experimental and thermodynamic studies of phosphate behavior during the hydrothermal carbonization of sewage sludge, *Sci. Total Environ.* 692 (2019) 147–156, https://doi.org/10.1016/j.scitotenv.2019.07.217.

Ott, C., & Rechberger, H. (2012). The European phosphorus balance. *Resources, Conservation and Recycling*, 60, 159–172. doi:10.1016/j.resconrec.2011.12.007.

Peng, L., Dai, H., Wu, Y., Peng, Y., & Lu, X. (2018). A comprehensive review of phosphorus recovery from wastewater by crystallization processes. *Chemosphere*, 197, 768–781. doi:10.1016/j.chemosphere.2018.01.098.

Pescod, M.B., (1992). Wastewater treatment and use in agriculture. Consulted last on 24/03/2021 at http://www.fao.org/3/T0551E/t0551e08.htm#TopOfPage

Qu, J., Wang, H., Wang, K., Yu, G., Ke, B., Yu, H.-Q., Ren, H., Zheng, X., Li, J., Li, W., Gao, S., Gong, H. (2019). Municipal wastewater treatment in China: Development history and future perspectives. *Frontiers of Environmental Science & Engineering*, 13(6). doi:10.1007/s11783-019-1172-x.

Remy, C., Boulestreau, M., Warneke, J., Jossa, P., Kabbe, C., Lesjean, B., (2016). Evaluating new processes and concepts for energy and resource recovery from municipal wastewater with life cycle assessment. *Water Sci. Technol.* 73, 1074–1080. https://doi.org/10.2166/wst.2015.569.

Rossi, L., Reuna, S., Fred, T., & Heinonen, M. (2018). RAVITA Technology – new innovation for combined phosphorus and nitrogen recovery. *Water Science and Technology*, 78(12), 2511–2517. doi:10.2166/wst.2019.011.

Saerens, B., Geerts, S., Weemaes, M. (2021). Phosphorus recovery as struvite from digested sludge – experience from the full scale, *Journal of Environmental Management*, Volume 280, 111743, ISSN 0301-4797. https://doi.org/10.1016/j.jenvman.2020.111743.

Scholz, R. W., Ulrich, A. E., Eilittä, M., & Roy, A. (2013). Sustainable use of phosphorus: A finite resource. *Science of The Total Environment*, 461-462, 799–803. doi:10.1016/j.scitotenv.2013.05.043.

Schoumans, O. F., Bouraoui, F., Kabbe, C., Oenema, O., & van Dijk, K. C. (2015). Phosphorus management in Europe in a changing world. *Ambio*, 44(S2), 180–192. doi:10.1007/s13280-014-0613-9.

Skinner, H. (1990). Methamphetamine synthesis via HI/red phosphorous reduction of ephedrine. *Forensic Science International*, 48 128-134.

Skulberg, O.M., Codd, G.A., Carmichael, W.W., (1984). Toxic blue-green algal blooms in Europe: a growing problem. *Ambio* 13, 244-247.

Smith, V. H., Tilman, G. D., Nekola, J. C. (1999). Eutrophication: impacts of excess nutrient inputs on freshwater, marine, and terrestrial ecosystems. *Environmental Pollution*, 100(1-3), 179–196. doi:10.1016/s0269-7491(99)00091-3.

The World Counts last consulted on 25/03/2021 at https://www.theworldcounts.com/stories/average-daily-water-usage

Unie van Waterschappen (UvW), 2018. Last consulted on the 20/04/2021 at https://www.waterschapsspiegel.nl/wp-content/uploads/2019/09/Bedrijfsvergelijking-Zuiveringsbeheer-2018.pdf

Van Kauwenbergh, S.J., (2010). World phosphate rock reserves and resources. *Fertilizer outlook and technology conference*. Georgia, USA.

Wilfert, P., Kumar, P. S., Korving, L., Witkamp, G.-J., van Loosdrecht, M. C. M. (2015). The relevance of phosphorus and iron chemistry to the recovery of phosphorus from wastewater: a review. *Environmental Science & Technology*, 49 (16), 9400–9414. doi:10.1021/acs.est.5b00150.

Wilfert, P., Mandalidis, A., Dugulan, A. I., Goubitz, K., Korving, L., Temmink, H., Witkamp G.J., Van Loosdrecht, M. C. M. (2016). Vivianite as an important iron phosphate precipitate in sewage treatment plants. *Water Research,* 104, 449–460.

Wilfert, P., Korving, L., Dugulan, I., Goubitz K., Witkamp, G. J., Van Loosdrecht M.C.M. (2018). Vivianite as the main phosphate mineral in digested sewage sludge and its role for phosphate recovery. *Water Research,* 144, 312-321.

Wilfert, P., Meerdink, J., Degaga, B., Temmink, H., Korving, L., Witkamp, G. J., van Loosdrecht, M. C. M. (2020). Sulfide induced phosphate release from iron phosphates and its potential for phosphate recovery. *Water Research*, 171, 115389. doi:10.1016/j.watres.2019.115389

# Chapter 2: Magnetic separation of vivianite from digested sewage sludge: The proof of principle
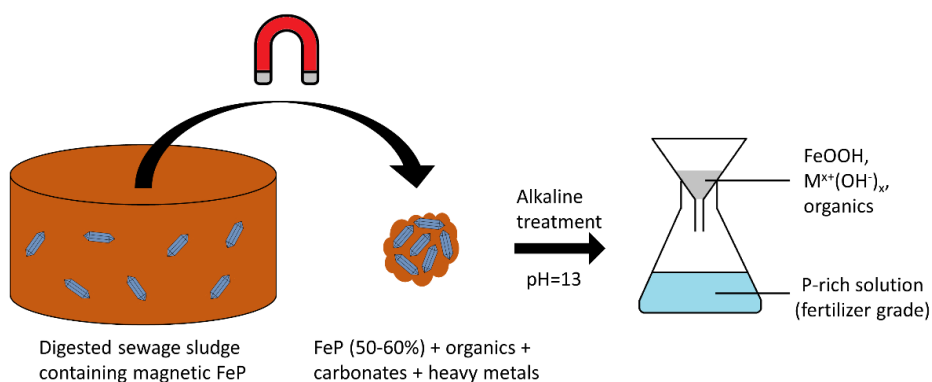
**2**

**Highlights**

- For the first time, vivianite was separated from sludge via a wet magnetic technique.

- The product contained vivianite (50-60%), organic matter (20%), quartz, and siderite.

- Phosphorus was recovered and purified from vivianite through an alkaline treatment.

- After purification, heavy metal contents are in line with those in phosphate rock and future legislation.

**2**

## Abstract

To prevent eutrophication of surface water, phosphate needs to be removed from sewage. Iron dosing is commonly used to achieve this goal either as the main strategy or in support of biological removal. Vivianite ($Fe(II)_3(PO_4)_2*8H_2O$) plays a crucial role in capturing the phosphate. If enough iron is present in the sludge after anaerobic digestion, 70 to 90% of total phosphorus can be bound in vivianite. Based on its paramagnetism and inspired by technologies used in the mining industry, a magnetic separation procedure has been developed. Two digested sludges from sewage treatment plants using chemical phosphorus removal were processed with a lab-scale Jones magnetic separator, emphasizing the characterization of the recovered vivianite and the P-rich caustic solution. The recovered fractions were analyzed with various analytical techniques (e.g., ICP-OES, TG-DSC-MS, XRD, and Mössbauer spectroscopy). The magnetic separation showed a concentration factor for phosphorus and iron of 2-3. The separated fractions consist of 52% to 62% of vivianite, 20% of organic matter, less than 10% of quartz, and a small quantity of siderite. More than 80% of the phosphorus in the recovered vivianite mixture can be retrieved via an alkaline treatment. At the same time, the formed iron oxide has the potential to be reused. Moreover, the trace elements in the P-rich caustic solution meet the future legislation for recovered phosphorus salts and are comparable to the usual content in Phosphate rock. The efficiency of the magnetic separation and the advantages of its implementation in WWTP are also discussed in this paper.

**2**

## 2.1. Introduction

Phosphorus is an essential element for life and is responsible for various functions in both humans and plants. Particularly for plants, it is a major nutrient and is often spread onto soils in phosphate fertilizer (Childers et al. 2011). The source for the phosphate in fertilizer is primarily from mining phosphate rock. This process is environmentally unfriendly, and the resources are becoming depleted, whereas human demand is increasing due to the rise of the population (Ridder et al. 2012). In parallel with being a necessary nutrient, phosphorus can also cause eutrophication if released in excess into water bodies, obliging Waste Water Treatment Plants (WWTPs) to remove it before discharging the effluents in natural streams. (Yang et al. 2008).

Currently, there are two main methods for advanced phosphorus removal in treatment plants: enhanced biological phosphorus removal (EBPR) and Chemical Phosphorus Removal (CPR). Iron is usually dosed in CPR mainly to remove the phosphorus. It also helps control the sulfide production and acts as a coagulant to facilitate sludge dewatering while being a cost-effective chemical. Furthermore, iron can already be present in the influent wastewater depending on its origin, meaning that phosphorus could already be partially bound to iron before the dosing step. Iron can also enhance the flocculation/coagulation of suspended particles in wastewater and thereby play a key role in future energy-producing WWTPs (Wilfert et al. 2015).

It is estimated that 370 kton of phosphorus per year ends up in the sludge of the European WWTPs (Van Dijk, 2016). By utilizing this resource, up to 20-30% of the fertilizer demand of Europe could be met (Schoumans, 2015). Hence, various technologies have been developed to serve this purpose, ranging from the direct use of sewage sludge on farmland to more advanced methods such as recovery from incinerated sewage sludge ash or recovery as struvite (Egle et al. 2016). There have not been many technologies proposed serving treatment plants using CPR without the requirements for incineration. Incineration is often disapproved by the public and capital intensive as it requires expensive infrastructures.

In WWTPs dosing iron, several researchers reported the presence of the iron phosphate mineral vivianite ($Fe_3(PO_4)_2.8H_2O$). Frossard et al. 1997 discovered sand-sized to silt-sized vivianite in sludge, while Seitz et al. 1973 observed it in dried sewage sludge. Nriagu and Dell 1974 evaluated that vivianite was the most thermodynamically stable iron phosphate mineral in reductive environments (e.g., sediments, sludge). More importantly, vivianite should preferably form over struvite during sludge digestion, according to thermodynamic evaluations. Wilfert et al. 2016 observed this in two WWTPs where vivianite was found as the dominant iron phosphate mineral in the digested sludge. In line with the findings of Poffet et al. 2008, this study also showed that Fe(III) compounds are reduced and transformed to vivianite in the activated sludge tanks even though Fe(III) was dosed. Additionally, Wilfert et al. 2018 suggested that after digestion, between 70-90% of the total amount of phosphorus present in sludge can be bound to vivianite provided the dosing of iron is high enough.

With such a high fraction of phosphorus potentially present as vivianite, there is an opportunity to recover phosphorus from sludge by extracting vivianite. It is especially interesting considering that only 10-50% of the total phosphorus in the influent can be recovered via struvite precipitation (Cornel and Schaum, 2009). Interestingly, vivianite is a

paramagnetic mineral with a magnetic susceptibility varying from 0.8 to 1.7 $10^{-6}$ m$^3$/kg (Minyuk et al. 2013). Vivianite is the main paramagnetic compound in sludge besides some other iron-bearing species. Magnetic separation would, therefore, provide a selective way to recover vivianite from sludge.

Seitz et al. 1973, already designed an experimental set-up to separate vivianite from dried sludge powder using magnetic attraction. Other devices from the mining industry like the Frantz separator were used to extract magnetic fractions from streams but never tested to extract vivianite from sludge. These separators can only work with dry materials, and the separation of vivianite from sludge was not achieved with high efficiency (Bouderbala, 2016). Another device having the potential for this extraction process is the Jones separator, a high-intensity magnetic separator that can be used directly with wet sludge (Wills and Napier-munn, 2006). In this study, a device mimicking the working mechanism of the Jones separator was used to extract vivianite from sludge. The objective of this study was to provide the proof of principle that this technique can work and investigate the composition of the extracted fraction. The magnetic separation of ferrite sludge from wastewater has already been studied earlier (Barrado et al. 1999) but is different from the technique studied here. Vivianite is paramagnetic and not ferromagnetic, which makes its separation more challenging.

## 2.2. Materials and methods

### 2.2.1. WWTPs and sample handling

For this research, digested sludges from 2 WWTPs have been used. One was sampled in Dokhaven (The Netherlands) and the other in Espoo (Finland). Both plants rely on CPR by dosing iron salts in different molar ratios to phosphate, which impacts the quantity of vivianite formed. After sampling, the sludges were kept in polyethylene bottles of 1L and stored in a 4°C fridge. Before analysis, the sludges were sieved with a 1 mm sieve to remove any large particles in the sludge. No particular precautions were taken to maintain the anaerobicity of the feed samples considering that the sludge buffers oxygen, and oxidation of vivianite should be slow in these conditions. A relatively pure (~ 95 % as determined with ICP-OES) vivianite scaling found in a heat exchanger from the WWTP of Venlo (The Netherlands) has been used as a comparison during the study. More information about the sieved and non-sieved sludges can be found in Supplementary information.

### 2.2.2. Magnetic separation and phosphorus release

#### 2.2.2.1. Definitions

In this study, the initial mix from which the product is extracted is called the feed. The magnetic fraction containing the vivianite is the concentrate, while the non-wanted part is the tailing. The grade is the purity of the concentrate in terms of dry weight. The amount of a compound ending up in the concentrate compared to its quantity in the feed is called the grade. The yield is defined as the quantity of concentrate compared to the feed in terms of dry weight.

#### 2.2.2.2. Device description

A lab-scale replicate of the separator (μ-Jones) has been designed to investigate the application of this system to sludge (Figure 2.1). The μ-Jones consists of two steel plates with seven vertical 4 cm-high/1.5 mm long teeth. The ridges are 2 mm away from each other and made

**2**

magnetic with 2*3 Nd-Fe-B permanent magnets of ~1.3 T (creating a magnetic field of ~1.3 T on the ridge and ~ 0.3 T in-between the teeth). The μ-Jones is put in water until the teeth are entirely submerged to increase the contact time between the teeth and the sludge. An aluminum tray was designed to collect the solids as soon as they are released from the teeth. Further information about the working principle of a full-scale Jones separator can be found in Wills and Napier-Munn, 2006.
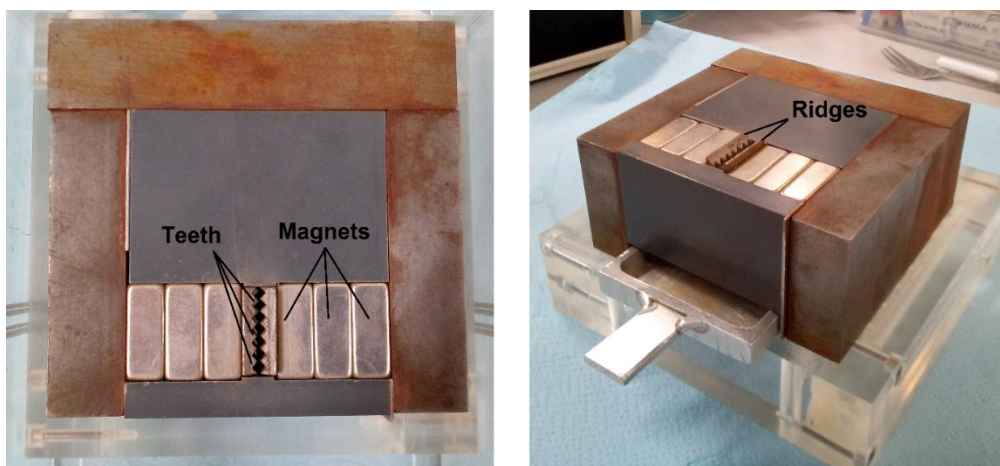


*Figure 2.1: μ-Jones top view (left) and side view (right).*

The sludge is continuously mixed for homogenization, and 20 mL/min are pumped on the teeth (Figure 2.1). The sludge from Finland was pumped for 30 seconds and the sludge from the Netherlands 45 seconds to obtain a similar quantity of concentrate because the amount of iron in the Finish sludge is higher. To wash away a maximum of non-magnetic residues stuck in the teeth (mainly organic matter), Milli-Q water (MQW) was pumped at 20 mL/min for 30 seconds. Finally, the μ-Jones was removed from the water, and a stronger flow of MQW was sent through the teeth with a squeeze bottle to free all the material attached to the ridges.

The wet concentrate was introduced in 50 mL tubes to be centrifuged at 3750 rpm for 30 min as a post-treatment. The pellets were then vacuum-dried at 30°C for 1-2 days. Around 250 mL (Finnish) and 500 mL (Dutch) of sieved sludge were necessary to separate 1 g of dried material. Feed samples were directly poured into a petri dish after sieving and vacuum dried at 30°C. All the materials (including the scaling) were then ground and stored in 15 mL plastic tubes without precaution toward exposure to oxygen or light. Once extracted from the sludge, vivianite is not protected anymore and can easily be oxidized (McCammon et al. 1980, Čermáková et al. 2013).

### 2.2.2.3. *Release of phosphorus from vivianite*

An alkaline treatment was used to release phosphate from vivianite. 20 mg of concentrate was introduced in 10 mL of Ultratrace water (Sigma-Aldrich) under stirring, and 0.2 mL of 7.5 M ultra-trace NaOH was added, giving an OH⁻/Fe molar ratio excess of 5 - 10. The release solution is let to stir for 2h to be sure that the reaction is over. A change of color can be

observed from transparent to the characteristic rust-brown of $Fe(OH)_3$. The precipitates were removed by 0.45µm filtration, and the filtrate was analyzed for elemental composition.

## 2.2.3. Analyses

### 2.2.3.1. XRD

The sample was filled in a 0.7 mm glass capillary and tamped so the solid settles. No precautions toward oxygen-free conditions have been taken. Just before measurement, the capillaries were sealed with a burner and mounted in a sample holder. The device used was a PANalytical X´Pert PRO diffractometer with Cu-Ka radiation (5-80 º2θ, step size 0.008º). The fitting was realized with the software Origin Pro 9.

### 2.2.3.2. SEM-EDX

The apparatus is a JEOL JSM-6480 LV scanning electron microscope (SEM) equipped with an Oxford Instruments x-act SDD energy dispersive x-ray (EDX) spectrometer. The accelerating voltage used is 15.00 kV for a working distance of 10 mm. A 10 nm-layer of gold is deposited on the sample with a JEOL JFC-1200 fine coater to make the surface electrically conductive. The software used is JEOL SEM Control User Interface for the SEM and Oxford Instruments Aztec for the EDX data processing.

### 2.2.3.3. Mössbauer spectroscopy

The sample weight was adjusted to have 15 mg of $Fe/cm^2$. Transmission $^{57}Fe$ Mössbauer absorption spectra were collected at 300 K and 77 K with a conventional constant-acceleration spectrometer using a $^{57}Co$ (Rh) source. Velocity calibration was carried out using an α-Fe foil. The Mössbauer spectra were fitted using the Mosswinn 4.0 program (Klencsár 1997).

### 2.2.3.4. TG-DSC-MS

To evaluate the vivianite and the organic share in the samples, Thermo Gravimetry equipped with Differential Scanning Calorimetry and a Mass Spectrometer (TG-DSC-MS) were used. The apparatus is a STA 449 F3 Jupiter for the simultaneous TG-DTA/DSC and QMS 403C Aëolos for the MS detector, both from NETZSCH Gerätebau GmbH. 40mg of sample is introduced in the oven, which follows a continuous heating ramp of 10°C/min from 40°C until 550°C, under an Argon atmosphere.

### 2.2.3.5. Digestion

All the solid samples have been destroyed by microwave digestion to perform liquid analyses. The digestion takes place in an Ethos Easy from Milestone with an SK-15 High-Pressure Rotor. 10 mg of solid are introduced in a Teflon vessel in which 10 mL of ultrapure $HNO_3$ (64.5 – 70.5% from VWR Chemicals) is poured. The digester is set to reach 200 °C in 15 min, run at this temperature for 15 min, and cool down for 1h.

### 2.2.3.6. ICP-OES/MS

The elemental composition was measured via Inductively Coupled Plasma (Perkin Elmer, type Optima 5300 DV) with an Optical Emission Spectroscopy as detector (ICP-OES). The device was equipped with an Autosampler, Perkin Elmer, type ESI-SC-4 DX fast, and the data were processed with the software Perkin Elmer WinLab32. The rinse and internal standard solution were respectively 2% of $HNO_3$ and 10 mg/L of Yttrium.

ICP-OES does not allow to determine concentrations < 0.05ppm, so another ICP equipped with a Mass Spectrometer detector (ICP-MS) was also used. The device is a PlasmaQuant MS from Analytik-Jena and was used with three different analytical methods, depending on the element studied: with He (120 mL/min), with $H_2$ (80 mL/min), or without gas (ng). Y and In were used as the internal standard in both gas modes, whereas Sc and Y were used in no gas mode.

The samples from the phosphate release experiments were not digested before the analysis but only filtered with a 0.45μm filter to remove the precipitates. More details about the ICP-MS method can be found in Supplementary information.

## 2.3. Results

The magnetic separation of vivianite from digested sludge was performed, and the feeds and concentrates were analyzed to evaluate the separation. A relatively pure vivianite scaling sample from a WWTP plant in Venlo was used as reference material. The names and descriptions of the samples are presented in Table 2.1.

*Table 2.1: Sample names and description*

| Sample name | Description |
|---|---|
| Feed NL | Sieved digested sludge from Dokhaven (NL) with a molar Fe/P ratio of 0.99 |
| Feed FI | Sieved digested sludge from Espoo (FI) with a molar Fe/P ratio of 2.19 |
| Conc. NL | Magnetic fraction (concentrate) obtained from the processing of Feed NL |
| Conc. FI | Magnetic fraction (concentrate) obtained from the processing of Feed FI |
| Scaling | Vivianite scaling of a purity >95% of vivianite harvested in Venlo (NL). This scaling is used as a reference for "pure" vivianite produced in sewage sludge. |

### 2.3.1. Solid analysis

#### 2.3.1.1. XRD

Vivianite was detected in all five samples described in Table 2.1 and was the only crystalline phase observed in all cases except for Feed NL (presence of quartz detected). All the peaks could be assigned in the diffractograms obtained for the scaling and Conc. FI. In contrast, one, three, and four peaks remain unidentified for Conc. NL, Feed NL, and Feed FI, respectively. The bump between 15-40° that is usually associated with amorphous material is absent for the concentrates and the scaling. The diffractogram can be found in Supplementary information.

#### 2.3.1.2. SEM-EDX

SEM-EDX showed that iron and phosphorus were not homogeneously distributed. They were clustered in specific overlapping places presenting sheet or needle-shaped crystals (5–15 μm), agglomerated into bigger particles (30-100 μm) (Figure 2.2). All the particles had a Fe/P ratio of 1.2-1.9, close to vivianite (1.5) (Table 2.2). Mg, Ca, and Al were homogeneously distributed in the sample while S and Si formed small clusters.

*Table 2.2: Molar ratio of the Fe/P overlapping particles found in the samples (EDX results)*

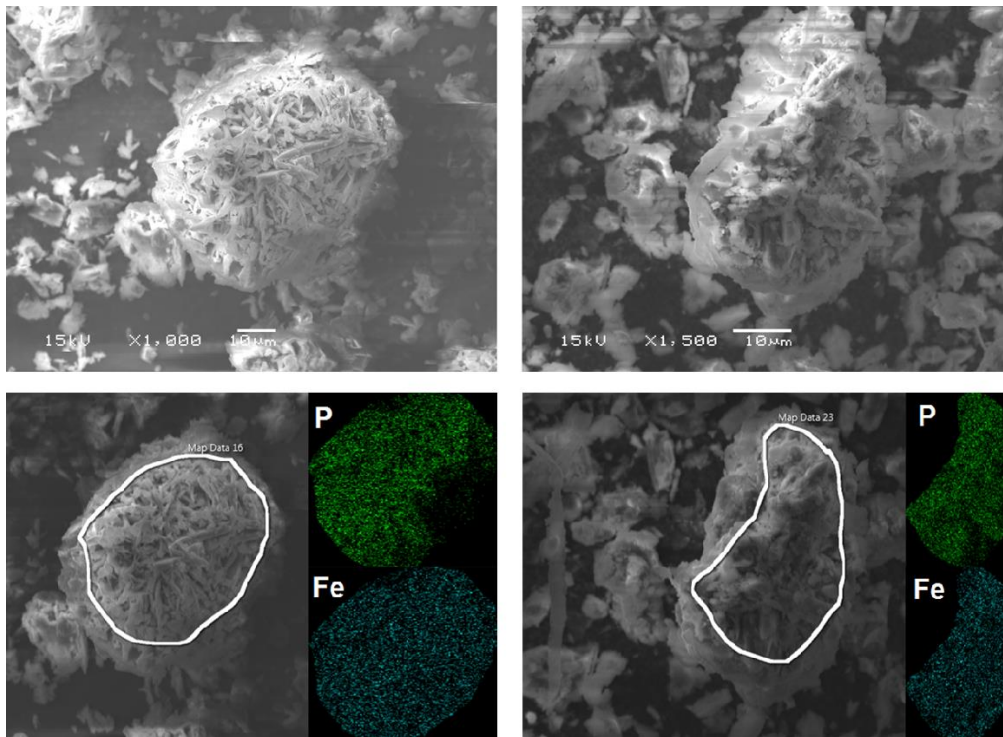|  | Scaling | Feed NL | Feed FI | Conc. NL | Conc. FI |
|---|---|---|---|---|---|
| Molar Fe/P ratio | 1.8 | 1.2 | 1.6 | 1.4 | 1.9 |



*Figure 2.2: SEM pictures (top) and corresponding EDX maps (bottom) of the concentrates from Finland (left) and the Netherlands (right)*

### 2.3.1.3. *Mössbauer spectroscopy*

In Table 2.3, $Fe^{3+}$ stands for oxidized iron either in the vivianite structure or as another iron (III) species. $Fe^{II}$ stands for low-spin iron compounds (typically pyrite). In the crystalline structure of vivianite, $Fe^{2+}$ ions can occupy the center of three octahedrons formed by water molecules and oxygen atoms. Two positions are equivalent and named $Fe^{2+}$ Vivianite B in Table 2.3, while the third is unique and called $Fe^{2+}$ Vivianite A (Grodzicki and Amthauer 2000). Other crystalline iron phases were not identified (Figure 2.3).

*Table 2.3: Mössbauer data for the 5 samples at 300K. Spectral contribution error are ±3%.*

| Sample | T (K) | IS (mm·s-1) | QS (mm·s-1) | Γ (mm·s-1) | Phase | Spectral contribution (%) |
|--------|-------|-------------|-------------|------------|-------|---------------------------|
| Scaling | 300 | 0.33 | 0.88 | 0.54 | $Fe^{3+}$ | 32 |
| | | 1.22 | 2.40 | 0.36 | $Fe^{2+}$ Vivianite A | 27 |
| | | 1.22 | 2.96 | 0.36 | $Fe^{2+}$ Vivianite B | 41 |
| NL conc. | 300 | 0.34 | 0.88 | 0.49 | $Fe^{3+}/Fe^{II}$ | 35 |
| | | 1.26 | 2.35 | 0.39 | $Fe^{2+}$ Vivianite A | 25 |
| | | 1.23 | 2.95 | 0.39 | $Fe^{2+}$ Vivianite B | 40 |
| FI conc. | 300 | 0.38 | 0.82 | 0.53 | $Fe^{3+}/Fe^{II}$ | 70 |
| | | 1.25 | 2.09 | 0.39 | $Fe^{2+}$ Vivianite A | 16 |
| | | 1.19 | 2.95 | 0.39 | $Fe^{2+}$ Vivianite B | 14 |
| NL feed | 300 | 0.36 | 0.85 | 0.53 | $Fe^{3+}/Fe^{II}$ | 66 |
| | | 1.27 | 2.31 | 0.31 | $Fe^{2+}$ Vivianite A | 13 |
| | | 1.22 | 2.97 | 0.31 | $Fe^{2+}$ Vivianite B | 21 |
| FI feed | 300 | 0.38 | 0.87 | 0.57 | $Fe^{3+}/Fe^{II}$ | 61 |
| | | 1.21 | 1.99 | 0.43 | $Fe^{2+}$ Vivianite A | 27 |
| | | 1.14 | 2.81 | 0.43 | $Fe^{2+}$ Vivianite B | 12 |
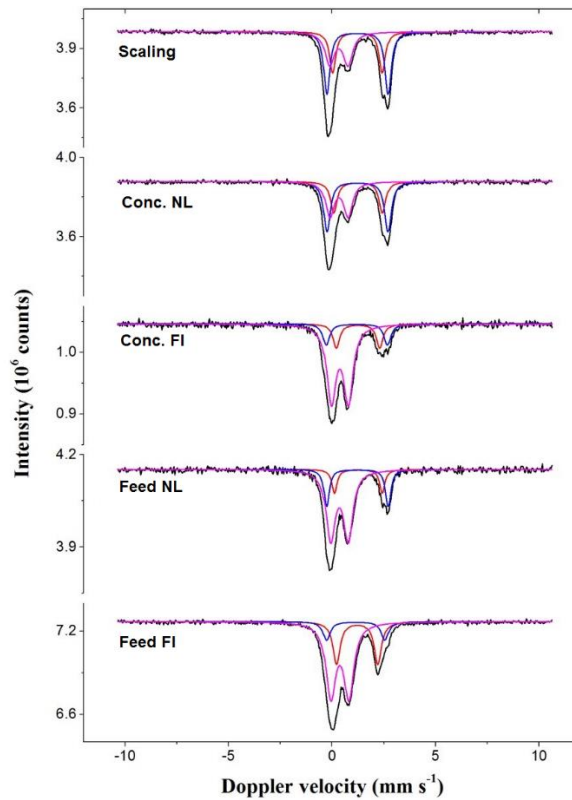


*Figure 2.3: Mössbauer spectra obtained at 300K with the signal of $Fe^{3+}/Fe^{II}$ in pink, $Fe^{2+}$ Vivianite A in red, $Fe^{2+}$ Vivianite B in blue, and the sum of the spectrum in black.*

## 2.3.1.4. TG-DSC-MS

The TG analysis of the scaling presented a weight decrease of 25% before 200 °C while 5% is lost between 200 °C and 550 °C. The other samples presented two weight decreases, the first being steeper for the concentrates than for feed samples. The temperature intervals for the loss of water and $CO_2$ (blue and orange curves in Figure 2.4) were slightly different for each sample (Table 2.4). Based on the MS signal and the results for the scaling, the first weight decrease could be attributed to the evaporation or 7 of the 8 $H_2O$ of vivianite. In contrast, the second decrease should account for the last $H_2O$, the organic fraction, and other unidentified minor phases.

Table 2.4: Weight losses during the 1st and the 2nd decrease in TG analysis (after vacuum oven drying)

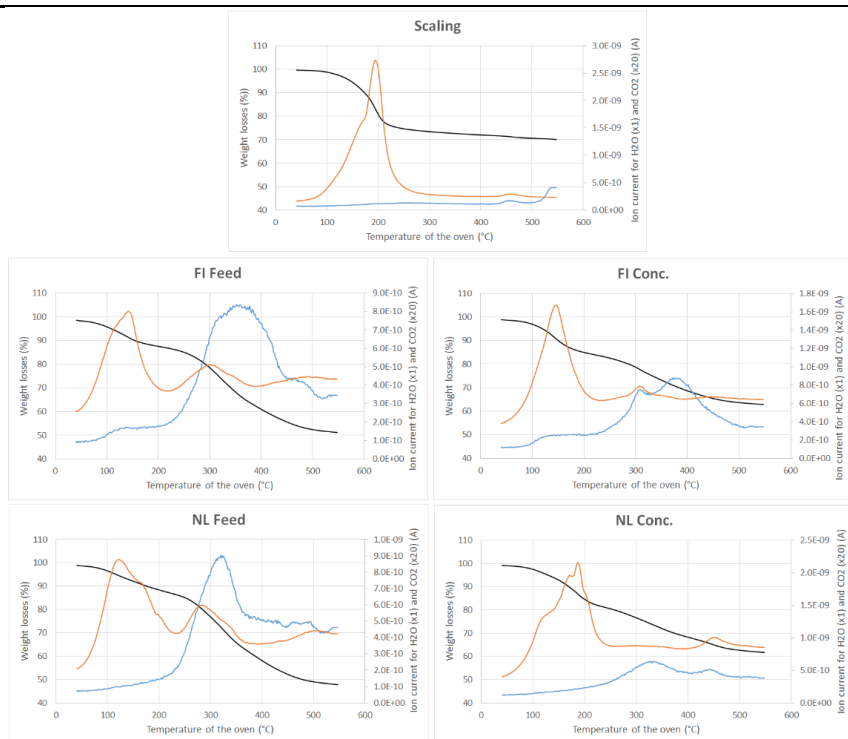| Sample | 1st decrease (% of weight lost) | 2nd decrease (% of weight lost) |
|---|---|---|
| Scaling | 25 (40-220 °C) | 5 (220-550°C) |
| Feed FI | 10 (40-200 °C) | 36 (200-550°C) |
| Feed NL | 12 (40-220 °C) | 40 (220-550°C) |
| Conc. FI | 14 (40-200 °C) | 23 (200-550°C) |
| Conc. NL | 17 (40-200 °C) | 20 (200-550°C) |



Figure 2.4: TG-DSC-MS spectra for the scaling, both feeds and concentrates. In black the weight losses, in orange the Mass Detector signal for $H_2O$ and blue for $CO_2$

### 2.3.2. Elemental composition: ICP-OES/MS

The elemental composition of all samples was determined after microwave digestion. The major elements detected were iron, phosphorus, and calcium for both feeds, with twice as much iron in FI Feed than NL Feed due to the higher iron dosing. The quantity of iron and phosphorus increased by a factor 2-3 after separation while the other elements' share was reduced (Table 2.5).

Table 2.5: Elemental composition of the feeds, concentrates, and scaling measured by ICP-OES. nd: not detected because the concentration was below the LOQ of the device.

| Samples | Weight content (mg/kg dry solid) | | | | | | | | | | | |
|---|---|---|---|---|---|---|---|---|---|---|---|---|
| | Fe | P | Ca | Mg | Al | S | K | Zn | Si | Cu | Na | Mn |
| FI Feed | 120 | 28 | 27 | 4 | 6 | 9 | 11 | 1 | 8 | nd | nd | nd |
| FI Conc. | 236 | 65 | 17 | 3 | 5 | 6 | 2 | 1 | 6 | 1 | nd | nd |
| NL Feed | 64 | 37 | 36 | 3 | 6 | 21 | 10 | 1 | 7 | 1 | 7 | nd |
| NL Conc. | 195 | 77 | 20 | 8 | 5 | 10 | 2 | 1 | 6 | 1 | nd | 2 |
| Scaling | 308 | 119 | 10 | 11 | nd | 2 | nd | nd | nd | nd | nd | 3 |

Table 2.6: Elemental composition of the feeds, concentrates, and scaling measured by ICP-MS. nd: no data, meaning below LOQ. Data no shown: $Mg>790$, $Al>790$, $Mo<10$, $Ag<10$, $Sn<30$, $Rb<10$, $Li<5$ mg/kg of dry solids.

| Samples | Weight content (mg/kg dry solid) | | | | | | | | | | | |
|---|---|---|---|---|---|---|---|---|---|---|---|---|
| | Cr | As | Mn | Co | Ni | Cu | Zn | Sn | Ba | Pb | Na | Ce |
| FI Feed | 33 | 9 | 252 | 9 | 33 | 378 | 725 | 27 | 114 | 15 | >790 | 75 |
| FI Conc. | 25 | 8 | 414 | 9 | 398 | >790 | 414 | 18 | 94 | 8 | nd | 51 |
| NL Feed | 51 | 40 | 635 | 6 | 42 | 685 | >790 | 26 | 400 | 113 | >790 | 13 |
| NL Conc. | 60 | 18 | >782 | 9 | 91 | 710 | 648 | 18 | 240 | 82 | 240 | 11 |
| Scaling | nd | nd | >782 | 32 | 79 | 17 | 268 | nd | nd | 3 | nd | nd |

ICP-MS was used in complement of ICP-OES to reach lower concentrations. The limit of quantification (LOQ) was established by setting a threshold of 20% to the relative standard deviation (RSD) of the calibration curve for each element (EPA publication SW-846). Only results above the LOQ are presented in Table 2.6. For these analyses, the device encountered analytical problems measuring Si, S, K, Ca, and Ti. As observed by ICP-OES, most elements are reduced in concentration after magnetic separation.

*Table 2.7: Elemental composition of the release solution for both concentrates measured by ICP-OES. nd: no data, meaning below LOQ*

| Sample | Weight content (g solubilized element/kg of dry matter) | | | |
|---|---|---|---|---|
| | Al | P | S | Si |
| FI Conc. release | 2 | 60 | 5 | 1 |
| NL Conc. release | 2 | 70 | 7 | Nd |

After the alkaline release of phosphorus from the concentrates and filtration, only 4 elements can be detected in the filtrate by ICP-OES (Table 2.7). This result is confirmed by the small number of elements detected by ICP-MS in further experiments (Table 2.8). The device encountered problems measuring Si, S, K, Ca, and Ti for these measurements.

*Table 2.8: Elemental composition of the release solution for both concentrates measured by ICP-MS*

| Sample | Weight content (mg solubilized element/kg dry matter) | | | | | | | |
|---|---|---|---|---|---|---|---|---|
| | As | Mn | Ni | Cu | Zn | Mo | Sn | Fe |
| FI Conc. release | 3 | 3 | 91 | 196 | 25 | 2 | 11 | 281 |
| NL Conc. release | 13 | 9 | 12 | 114 | 34 | 3 | 9 | 184 |

## 2.4.  Discussion

The objective of this chapter was to prove that magnetic extraction of vivianite from sludge is possible and selective using a lab-scale magnetic separator that mimics the working principle of large-scale wet magnetic separators. As a proof of concept study, a pure product rather than a high yield was sought to selectively extract vivianite to study and understand how vivianite is present in digested sewage sludge. Three main points will be discussed in the following section:

- The magnetic separation performances
- The composition of the magnetic concentrate in terms of vivianite content and side products.
- The valorization possibilities of the concentrate with an emphasis on its transformation into a fertilizing material

The sample names and descriptions are indicated in Table 2.1.

*Table 2.9: Vivianite, organics, and quartz content of the feeds and concentrates (processed data from Table 2.3, Table 2.4, Table 2.5, and Table S2.6)*

| % of dried matter | Vivianite* | Organics** | Quartz** |
|---|---|---|---|
| FI Feed | 7 - 23 | 40 | 8 |
| FI Conc. | 52 | 20 | 8 |
| NL Feed | 6 - 30 | 40 | 4 |
| NL Conc. | 63 | 20 | 7 |

\* For the concentrates, the content has been determined with ICP-OES assuming that all the phosphorus is bound to vivianite which should be the major (if not the only) magnetic P-specie in the sample. For the Feeds, this hypothesis is not applicable considering the diversity of phosphorus compounds in sludge (CaP, organic P, struvite, FeP). Therefore, a range is given with the minimum determined by Mössbauer and the maximum by ICP-OES.

\*\* Details of the determination of the content stand in Supplementary information.

The composition of the magnetic fraction and the digested sludge were compared to evaluate the potential of the magnetic separation. The vivianite content in the magnetic concentrates was reliably estimated with ICP-OES and TG-DSC-MS (see further in the discussion). Mössbauer spectroscopy cannot differentiate the fraction of oxidized vivianite from other $Fe^{3+}$ bearing compounds present in sludge. The samples were exposed to oxygen during the separation and sampling handling, resulting in some oxidation of the vivianite. Therefore, in this case, Mössbauer spectroscopy underestimated the vivianite content and gave the minimum rather than the exact content. The maximum vivianite content could be obtained by hypothesizing that all the phosphorus measured by ICP-OES in the samples was vivianite. A combination of Mössbauer spectroscopy and ICP-OES gave a range of vivianite content in the digested sludge (Table 2.9).

*Table 2.10: Spectral contribution of both $Fe^{2+}$ sites of vivianite at 300K and site ratio (processed data from Table 2.3).*

| Sample | $Fe^{2+}$ Vivianite A (%) | $Fe^{2+}$ Vivianite B (%) | Ratio B/A |
|---|---|---|---|
| NL Conc. | 25 | 40 | 1.6 |
| FI Conc. | 9* | 14 | 1.6 |
| NL Feed | 13 | 21 | 1.6 |
| FI Feed | 7* | 12 | 1.7 |

\* The QS of Vivianite A (Table 2.3) is lower than it should (~2.1 instead of ~2.4 mm/s) for these samples indicating a possible interference with the siderite (QS ~ 1.8 mm/s) present as well. Therefore, the contribution of siderite (calculated further in the discussion) is deducted from this signal, giving a spectral contribution of 9% (instead of 16%) and 7% (instead of 27%) for FI Conc. and FI Feed, respectively.

Earlier, more detailed studies on the vivianite content of the same sludges (Wilfert et al. 2018) estimated the phosphorus present as vivianite at 65% and 85% of the total phosphorus (average value from their measurements) in NL Feed and FI Feed, respectively. Based on the elemental composition of these sludge in Table 2.5, the vivianite weight content could be estimated at 20 % for both sludges. This result suggests that the magnetic separation concentrates the vivianite by a factor of 2-3, which is promising at this stage. The magnetic separation also reduced the organic content from 40% to 20% (Table 2.9). The remaining could be the organic matter that seemed to trap the vivianite crystals, as suggested by Figure

2.2 and Frossard et al. 1997. The persistence of quartz even after magnetic separation was surprising, considering that quartz is not paramagnetic. It could act as a nucleation center for vivianite and may be present in its structure and be extracted with it.

Since the concentration of heavy metals is relevant for the valorization of the magnetic concentrate, the concentration factor of the heavy metals during the separation was studied. Our study showed that the magnetic separation reduces the heavy metal to phosphorus ratio (Supplementary information). However, this is not the case for the cations Mn, Ni, Mg, and Cu that remained similar or increased. The authors see two possible explanations for the persistence of these elements in the magnetic fraction: they could form other magnetic compounds than vivianite or substitute $Fe^{2+}$ in the structure of vivianite. Vivianite is known to have a structure allowing substitution of its $Fe^{2+}$ atoms by other divalent cations (Rothe et al. 2016 and Taylor et al. 2008). At ambient temperature, two $Fe^{2+}$ occupy the two octahedral sites B, while one $Fe^{2+}$ occupies the octahedral site A. Therefore, the ratio ($Fe^{2+}$ Vivianite B / $Fe^{2+}$ Vivianite A) given by Mössbauer should be 2 for pure vivianite (McCammon et al. 1980, Mori and Ito 1950). Divalent cations substitute preferentially in site B, decreasing this ratio (Manning et al. 1991). The samples showed ratios <2 suggesting the presence of impurities (Table 2.10). This ratio is an interesting indicator to assess the purity of the vivianite, but oxidation of the mineral complicates the evaluation. Rouzies and Millet 1993 and McCammon et al. 1980 consider that oxidation happens preferentially in site A, increasing the ratio. The antagonist effects of the oxidation and the impurities make a quantitative approach impossible in the case of samples exposed to air, as was the case in this study.

A deeper characterization of the magnetic fractions has been realized to assess the purity of the product. First of all, vivianite was identified in the magnetic concentrates by Mössbauer spectroscopy and XRD. Crystals showing a Fe/P ratio close to 1.5 (as in pure vivianite) were also observed by SEM-EDX (Table 2.2). Moreover, as observed in Figure 2.2, the morphology of these crystals agreed with the sheet/needle-shaped appearance of vivianite already reported by several authors (Zelibor et al. 1988, Taylor et al. 2008).

*Table 2.11: Vivianite content in the concentrates estimated with different analytical methods (processed data from Table 2.3, Table 2.4, and Table 2.5)*

| Content (weight % of dried matter) | Conc. NL | Conc. FI |
|---|---|---|
| ICP-OES | 63 | 52 |
| TG-DSC-MS | 68 | 56 |
| Mössbauer | 38 | 17* |

* see explanation below Table 2.10

The quantification of vivianite is complicated, and, therefore, ICP-OES, TG-DSC-MS, and Mössbauer spectroscopy were used together to give the best result possible (Table 2.11). A first estimate of the vivianite content could be made based on the elemental composition (ICP-OES) by hypothesizing that all the phosphorus was bound to vivianite in these samples. It seems like a reasonable assumption since vivianite should be the major (if not the only) magnetic P-compound in sludge. Additionally, TG-DSC-MS was used. This method was based on the dehydration process of vivianite, which loses its eight crystal water with

temperature increase. The vivianite scaling used as a reference (Table 2.1) had seven of its eight crystal water evaporating in the temperature range 40-200°C (Figure 2.4). The vivianite content in the concentrates is estimated by matching the weight decrease in this temperature range to the loss of 7 water molecules (Table 2.4). In complement, Mössbauer spectroscopy was used. It can detect the $Fe^{2+}$ ions of vivianite but is unable to quantify them after they oxidize to $Fe^{3+}$, even though they are still present in the structure of vivianite. This is because the signal of $Fe^{3+}$ in vivianite overlaps with other oxidized iron phases and low-spin iron like in pyrite (Nishihara, Y., & Ogawa, S. 1979) and cannot be isolated. Therefore, only the contribution of $Fe^{2+}$ can be taken into account to estimate the vivianite content, giving a conservative estimate for the vivianite content. No precautions toward oxidation were taken during magnetic separation and sample handling. Thus, the $Fe^{3+}$ content in any recovered vivianite will be significant, explaining the low vivianite content obtained with Mössbauer in Table 2.11. ICP-OES and TG-DSC-MS seemed appropriate to estimate the vivianite content in the magnetic fraction, while Mössbauer spectroscopy requires extreme precaution toward oxidation to be reliable.

*Table 2.12: Organic matter, FeCO₃, and quartz content measured in both magnetic concentrates*

| Content (weight % of dried matter) | Organic matter* | FeCO₃* | Quartz* |
|---|---|---|---|
| FI Conc. | 20 | 3.3 | 8 |
| NL Conc. | 19 | 0.3 | 7 |

* Details of the determination of the content are in Supplementary information.

Vivianite accounts for 50-60% of the weight of the magnetic fractions, so 40-50% are left to determine. Organic matter, quartz, and carbonates (likely to be siderite $FeCO_3$) were also found, and their estimated content is listed in Table 2.12. TG-DSC-MS quantified organic matter with the mass loss due to pyrolysis and gasification before 550°C (responsible for the second weight drop in Table 2.4). The quartz content was considered to be equal to the residue after microwave digestion. SEM EDX confirmed this residue contained mainly silica and oxygen. The carbonate quantity was estimated based on the $CO_2$ release from the sample after acid addition to the sample. Methods and results are detailed in Supplementary information.

The iron content in the magnetic fraction is high compared to the phosphorus content (Table 2.5), and the presence of vivianite cannot alone explain it. Therefore, other iron species must have been extracted together with vivianite. No other iron compound was positively identified by XRD or Mössbauer, indicating a low content, a small size or/and an amorphous nature of these iron compounds. The carbonates found in the magnetic fractions are likely to be $FeCO_3$ (siderite) (Supplementary information); not only is it a magnetic species (Frederichs et al. 2003), but it is also the possible reason for the interference observed with Mössbauer spectroscopy (see explanation below Table 2.10). Pyrite, another magnetic compound, can potentially be present in the magnetic fraction and could account for 3-5% of the dried weight if we consider that the sulfur quantified by ICP-OES is present in the form $FeS_2$. SEM-EDX also revealed some Fe/S clusters (results not showed), which support this hypothesis. As mentioned above, pyrite is a low-spin iron and cannot be distinguished from $Fe^{3+}$ species by Mössbauer, explaining why it has not been identified with certainty. Other Fe-species like

FeOH's should be present in the magnetic fraction to account for the rest of $Fe^{3+}$ detected by Mössbauer.

In conclusion, the magnetic fractions contain organic matter (20%), quartz (7-8%), pyrite (3-5%), siderite (0.3-3%) and other not identified compounds. Most importantly, the vivianite content is estimated to be around 50% of the concentrate. It shows the feasibility to magnetically concentrate vivianite, albeit that further work needs to be done to improve the purity of the concentrate and the yield.

Once vivianite is recovered from sludge, several valorizations may be foreseen. If a high-grade concentrate could be obtained, high-value applications could be considered. Using vivianite in the art to create pigments or as a component in the lithium-ion batteries are two such high-value possibilities (Čermáková et al. 2013, Recham et al. 2009). Several studies have already investigated the direct use of vivianite as a slow P-release fertilizer and its advantage for Fe-poor soils (Fodoué et al. 2015, Rombolà et al. 2007). However, they worked with natural vivianite and not vivianite from sewage, which might bear heavy metals, possibly limiting direct use. On the other hand, their presence could also benefit some plants requiring micronutrients like Cu or Zn.

*Table 2.13: Comparison of the concentration of 5 heavy metals present in the P-rich solutions with typical values for P-Rock and future recovered phosphorus salts legislation (processed results from Table 2.8).*

| Elements (mg/kg of P)* | As | Cd | Cr | Cu | Ni | Pb | Zn |
|---|---|---|---|---|---|---|---|
| PFC 1(C)1** | 87 | 130 | 13 | 4000 | 650 | 100 | 10000 |
| P-rock*** | 65 - 95 | 110-270 | 500 - 2000 | <2000 | < 180 | 50 - 100 | <2000 |
| P-rich solution from NL Conc. | 185 | < 195 | < 25 | 1600 | 180 | < 25 | 500 |
| P-rich solution from FI Conc. | 55 | < 250 | < 30 | 3300 | 1500 | < 35 | 420 |

*These seven elements have been studied because they are the ones that will be regulated by the European commission for the product from recovered phosphorus (Joint Research Centre 2018). Hg is missing, but the ICP-MS used was no able to measure it.

**The product after post-treatment of the P-rich solution falls into the category of recovered phosphorus salts as described in a proposal from December 2018 (Joint Research Centre 2018). This document refers to heavy metal limits for future Product Fertilizer Categories (PFC's, in this case, PFC 1(C)1: Inorganic Macronutrient Fertilizer) in a proposed and by EP amended revision of the fertilizer Ordinance. A product containing 35% of $P_2O_5$ is considered as a reference in the present study, which is the minimum phosphate content for this category. The phosphorus content is 15.3% of the weight.

***Dittrich and Klose 2008 give the typical amount of heavy metals in the P-rock from Morocco, which is taken as an indicator in this study considering that the country holds around 70% of the world's phosphate rock. The phosphorus content of these rocks is taken from Tahib 2015. The phosphorus content is 13.9% of the weight.

If the purity of the concentrate is too low for direct application, a post-treatment is required to crack vivianite and recover the phosphorus and the iron. With this objective, the magnetic concentrate was put in an alkaline solution that broke down the vivianite and released phosphorus into the solution. At the same time, iron and the other heavy metals precipitated as hydroxides. The precipitates were filtered out, and around 90% of the phosphorus from vivianite was recovered in the liquid fraction.

The heavy metal concentrations in these P-rich solutions were in line with the future legislation on recovered phosphorus salts and the typical concentration in P-rock for most of the elements considered (except Ni in FI Conc. and As in NL Conc.) (Table 2.13). The analytical method for Cd and Cr needs to be further developed to lower the limit of quantification. Concentrations of organic micro pollutants, macroscopic impurities, and pathogens have not yet been considered, and this requires further evaluation in the future. The P-rich solution could be used as liquid fertilizer or be further processed by adding Calcium to precipitate calcium phosphate. The iron hydroxide precipitate could be reused in the steel industry or transformed to iron chloride by dissolution in hydrochloric acid. In the last case, the heavy metals in the iron residue may require removal.

Through the magnetic separation and the alkaline treatment, 16-32% of phosphorus has been recovered from the digested sludge. This is a promising result for a first proof of concept, the objective of this study, considering that the digested sludge was not optimized for maximum vivianite formation. Further optimization is needed to increase the phosphorus recovery and make this approach economically relevant. Firstly, the vivianite content in the digested sludge needs to be maximized (which was not the case for the NL sludge). Increasing the iron dosing could convert 70-90% of the phosphorus in the digested sludge into vivianite (Wilfert et al. 2018), making it available for magnetic separation. Secondly, recovery and grade can be improved using a device in which the magnetic field and separation matrix can be adjusted (use of rods instead of teeth, for instance). The influence of these parameters on the separation efficiency is described in Finch and Wills, 2015.

Not only could this technology allow to recover phosphorus as vivianite, but its implementation at WWTPs could reduce the quantity of sludge to dispose of and increase the heating value of this waste sludge by decreasing its mineral content. The first estimates showed that these benefits, especially the expected reduction of the sludge volume, are in balance with the investment and operation costs of a magnetic separator (Wilfert 2018b). Pilot plant operations will have to confirm the economic benefits of the approach further. A direct land application of this sludge with a lower phosphorus content would also be easier considering phosphorus limitations in soil. Finally, better control of the vivianite precipitation through iron dosing could minimize scaling, a severe problem for WWTPs. These advantages could help make the process economically viable and boost the change to a circular economy for phosphorus.

## 2.5. Conclusion

Vivianite is the most prominent phosphorus sink in digested sewage sludge and can contain between 70-90% of the total phosphorus provided enough iron is present in the sludge. This study proved for the first time the feasibility of the extraction of this mineral with wet magnetic separation technologies. The separated vivianite had a grade of 50-60%, and the recovered P-rich solution presented heavy metals concentrations in line with recovered phosphorus legislation. As a proof of concept, this is a promising result. However, additional research and development is necessary to improve the phosphorus recovery efficiency, for instance, through the increase of the iron dosed to maximize vivianite formation (Chapter 3) and optimize its magnetic separation from digested sludge (Chapter 4).

## Acknowledgments

## References

Barrado, E., Prieto F., Ribas J., Lopez F.A. (1999). Magnetic separation of ferrite sludge from a wastewater purification process. *Water air and soil pollution*, 115(1), 385-394.

Bouderbala, A. (2016). Magnetic separation of vivianite from sewage sludge. Master's thesis realized at Wetsus in cooperation with the Paris Region Institut for Applied Science (Institut Francilien des Sciences Appliquées).

Čermáková. Z., Švarcová. S., Hradil. D., Bezdicka. P. (2013). Vivianite: A historic blue pigment and its degradation under scrutiny. *Science and Technology for the Conservation of Cultural Heritage*, 75-78.

Childers, D., Corman, J., Edwards, M., Elser, J. (2011). Sustainability Challenges of Phosphorus and Food: Solutions from Closing the Human Phosphorus Cycle. *BioScience*, 61(2), 117–124.

Cornel, P., Schaum, C., (2009). Phosphorus recovery from wastewater: needs, technologies and costs. *Water Science & Technology*, 59(6), 1069–1076.

Dittrich, B., & Klose, R. (2008). Schwermetalle in Düngemitteln. *Landesamt Für Umwelt, Landwirtschaft Und Geologie*, 3

Egle, L., Rechberger, H., Krampe, J., & Zessner, M. (2016). Phosphorus recovery from municipal wastewater: An integrated comparative technological, environmental and economic assessment of P recovery technologies. *Science of the Total Environment*, 571, 522–542.

Finch, J. and Wills, B.A., (2015). Chapter 13: Magnetic and Electrical Separation. *Wills Mineral Processing Technology, 8th Edition.*

Fodoué, Y., Nguetnkam, J. P., Tchameni, R., Basga, S. D., & Penaye, J. (2015). Assessment of the Fertilizing effect of Vivianite on the Growth and yield of the Bean "phaseolus vulgaris" on Oxisoils from Ngaoundere. *International Research Journal of Earth Sciences*, 3(4), 18-26.

Frederichs, T., von Dobeneck, T., Bleil, U., & Dekkers, M. J. (2003). Towards the identification of siderite, rhodochrosite, and vivianite in sediments by their low-temperature magnetic properties. *Physics and Chemistry of the Earth*, 28(16–19), 669–679.

Frossard, E., Bauer, J.P., Lothe, F. (1997). Evidence of vivianite in FeSO4-flocculated sludges. *Water research*, 31(10), 2449–2454.

Grodzicki, M., Amthauer. G. (2000). Electronic and magnetic structure of vivianite : cluster molecular orbital calculations. *Physics and Chemistry of the minerals*, 27(10), 694–702.

Klencsár, Z. (1997). Mössbauer spectrum analysis by Evolution Algorithm. Nuclear Instruments and Methods in Physics Research Section B: Beam Interactions with Materials and Atoms 129(4), 527–533.

Manning, P. G., Murphy, T. P., & Prepas, E. E. (1991). Intensive formation of vivianite in the bottom sediments of mesotrophic Narrow Lake, Alberta. *Canadian Mineralogist*, 29, 77–85.

**2**

McCammon, C. A., & Burns, R. G. (1980). The oxidation mechanism of vivianite as studied by Mossbauer spectroscopy. *American Mineralogist*, *65*(3–4), 361–366.

Minyuk, P. S., Subbotnikova, T. V., Brown, L. L., & Murdock, K. J. (2013). High-temperature thermomagnetic properties of vivianite nodules, Lake El'gygytgyn, Northeast Russia. *Climate of the Past*, *9*(1)

Mori, H., & Ito, T. (1950). The structure of vivianite and symplesite. *Acta Crystallographica*, 3(1), 1–6.

Nishihara, Y., & Ogawa, S. (1979). Mössbauer study of [57]Fe in the pyrite-type dichalcogenides-isomer shift of divalent iron in low spin state. *Le Journal de Physique Colloques*, *40*(C2).

Nriagu, J. O., & Dell, C. I. (1974). Diagenetic Formation of lron Phosphates in Recent Lake Sediments. *American Mineralogist*, 59, 934–946.

Poffet, M. S., Käser, K., & Jenny, T. A. (2008). Thermal runaway of dried sludge granules in storage tanks. *CHIMIA International Journal for Chemistry,* 62(1), 29–34.

Recham, N., Armand, M., Laffont, L., Tarascon, J.-M. (2009). Eco-Efficient Synthesis of LiFePO4 with Different Morphologies for Li-Ion Batteries. *Electrochemical and Solid-State Letters,* 12(2), A39-44.

Ridder, M., de Jong, S., Polchar, J., Lingemann, S. (2012). Risks and Opportunities in the Global Phosphate Rock Market. PDF document. Available at: http://www.phosphorusplatform.eu/images/download/HCSS_17_12_12_Phosphate.pdf Consulted on the 06/06/2018

Rombolà, A. D., Toselli, M., Carpintero, J., Quartieri, M., Torrent, J., Marangoni, B. (2007). Prevention of Iron - Deficiency Induced Chlorosis in Kiwifruit (Actinidia deliciosa) Through Soil Application of Synthetic Vivianite in a Calcareous Soil, *Journal of plant nutrition*, 26(10-11), 2031-2041.

Rothe, M., Kleeberg, A., & Hupfer, M. (2016). The occurrence, identification and environmental relevance of vivianite in waterlogged soils and aquatic sediments. *Earth-Science Reviews*, 158, 51–64

Rouzies, D., & Millet, J. M. M. (1993). Mossbauer Study of Synthetic Oxidized Vivianite at Room-Temperature. *Hyperfine Interaction.,* 77(1–2), 19–28.

Schoumans, O. F., Bouraoui, F., Kabbe, C., Oenema, O., & van Dijk, K. C. (2015). Phosphorus management in Europe in a changing world. *Ambio,* 44(2), 180–192.

Seitz, A., Riedner, J., Malhotra, K., Kipp, J. (1973). Iron-Phosphate Compound Identification in Sewage Sludge Residue. *Environmental Science and Technology*, 7(4), 354–357.

Taib, M. (2014). The mineral industries of Morocco and western Sahara. *U.S. Geological survey mineral yearbook,* 59.1-59.13

Taylor, K. G., Hudson-Edwards, K. A., Bennett, A. J., & Vishnyakov, V. (2008). Early diagenetic vivianite ($Fe_3(PO4)_2*8H_2O$) in a contaminated freshwater sediment and insights into zinc uptake: A μ-EXAFS, μ-XANES and Raman study. *Applied Geochemistry,* 23(6)

Test Methods for Evaluating Solid Waste, Physical/Chemical Methods, EPA publication SW-846, Third Edition, Final Updates V (2015), Method 60-10-D

Van Dijk, K. C., Lesschen, J. P. and Oenema, O. (2016). Phosphorus flows and balances of the European Union Member States. *Science of the Total Environment*, 542, 1078–1093.

Wilfert, P., Kumar, P. S., Korving, L., Witkamp G.J., Van Loosdrecht, M. C. M. (2015). The relevance of Phosphorus and iron chemistry to the recovery of phosphorus from wastewater. *Environmental Science and Technology,* 49(16)

Wilfert, P., Mandalidis, A., Dugulan, A. I., Goubitz, K., Korving, L., Temmink, H., Witkamp G.J., Van Loosdrecht, M. C. M. (2016). Vivianite as an important iron phosphate precipitate in sewage treatment plants. *Water Research,* 104, 449–460

Wilfert, P., Korving, L., Dugulan, I., Goubitz K., Witkamp, G. J., Van Loosdrecht M.C.M. (2018). Vivianite as the main phosphate mineral in digested sewage sludge and its role for phosphate recovery. *Water Research,* 144, 312-321

Wilfert, P. (2018b). Thesis: Phosphate recovery from sewage sludge containing iron phosphate.

Wills, B.A.; Napier-Munn, T.J. (2006). Will's Mineral Processing Technology:An Introduction to the Practical Aspects of Ore Treatment and Mineral Recovery.

Yang, X., Wu, X., Hao, H., He, Z. (2008). Mechanisms and assessment of water eutrophication. *Journal of Zhejiang University SCIENCE B,* 9(3), 197–209.

Zelibor, J. L., Senftle, F. E., & Reinhardt, J. L. (1988). A proposed mechanism for the formation of spherical vivianite crystal aggregates in sediments. *Sedimentary Geology,* 59(1–2), 125–142.

## Supplementary information

The Fe/P molar ratio increases after digestion partly due to extra iron added just before digestion in Dokhaven. For Espoo, iron-rich secondary sludge was sampled and combined with primary settled sludge in the digester, which explains this increase.

*Table S2.1: Characteristics of the studied WWTPs (data from Wilfert et al. 2017)*

| WWTP | Fe dosing strategy | Solid Retention Time (days) | | | Fe/P molar ratio | | Capacity (p.e. in 150g TOC/day) |
|---|---|---|---|---|---|---|---|
| | | A-stage | B-stage | Digester | Before digestion | After digestion | |
| Dokhaven (AB plant) | Fe (III) salts in A-stage | 0.3 | 5.5 | 35 | 0.85 | 1.07 | 564,000 |
| Espoo (CPR) | Fe (II) salts | 6-10 (1 step) | | 13-14 | 2.19 | 2.40 | 321,045 |

Characteristics of both sludges are given in Table S2.2. It is interesting to notice that the molar Fe/P ratio decreases by ~10% after sieving. The pH has been measured by potentiometry, while Total Solid (TS) and Volatile Solid (VS) have been determined following standard methods (APHA, AWWA, WEF 1998). ICP-OES has determined total phosphorus and iron concentration after $HNO_3$-assisted microwave digestion.

*Table S2.2: Characteristics of the sieved sludges used in the experiments*

| Parameter | Dokhaven (NL) | Espoo (FI) |
|---|---|---|
| pH | 7.6 | 7.3 |
| TS (g/kg sludge) | 22 | 24 |
| VS (g/kg sludge) | 14 | 14 |
| Total phosphorus concentration (mg P/ kg sludge) | 58 | 30 |
| Total iron concentration (mg Fe/ kg sludge) | 103 | 119 |
| Molar Fe: P ratio | 1.0 | 2.2 |

**Theoretical evaluation of the magnetic separation**

Two basic phenomena determine the separation of magnetic particles from the slurry. First of all, the particles need to reach the teeth as the sludge is poured into the μ-Jones. Then they need to stick to it without being dragged by the slurry. In our experiments, the average velocity for particles of 10-100 μm of diameter (hypothesis based on the authors' SEM-EDX observations) toward the magnetic plate of the separator is 3 mm/s. This is high enough to reach the teeth for a classic residence time of a few seconds. Secondly, once attached, the particles need to stick to the wall without being dragged by the slurry. By studying the forces applying on a magnetic particle attached to the teeth, it is possible to determine the maximum feeding flow rate to use before detaching them. The following calculations indicate that a flow rate lower than 28.2 mL should not detach vivianite particles bigger than 10μm.

As the slurry flows along the surface at a high magnetic gradient, the paramagnetic particles in the slurry are attracted towards the surface by a force

$$F_{magnetic} = \mu_0 \rho_p V_p \chi_p H \nabla H \qquad (S2.1)$$

Here, $\mu_0 = 4\pi\ 10^{-7}$ Tm/A is a universal constant of the laws of magnetics, $H$ (A/m) is the magnetic field, and $\nabla H$ (A/m$^2$) is its gradient. The particle is defined by its density $\rho_p$ (kg/m$^3$), its magnetic susceptibility $\chi_p$ (m$^3$/kg) and its volume $V_p$ (m$^3$). As the paramagnetic particles travel towards the surface, they experience a drag force. Since the speed $\Delta v$ of the particle towards the surface is typically of the order of 1 mm/s or less, and particles are 10-100 micron in diameter, Stokes' formula can estimate the drag on the particle:

$$F_{drag} = 3\pi\eta\Delta v D_p \qquad (S2.2)$$

Here, $\eta$ (kg/m*s) is the dynamic viscosity of the slurry and $D_p$ (m) is the diameter of the particle. Small fines in a liquid very quickly reach a velocity at which drag and external forces are at equilibrium, and so the equations above can be used to estimate $\Delta v$ for a spherical particle,

$$\Delta v = \frac{\mu_0 \rho_p D_p^2 \chi_p H \nabla H}{18\eta} \qquad (S2.3)$$

Magnetic susceptibilities of Vivianite nodules were found to vary in the range from 0.8 to 1.7 $10^{-6}$ m$^3$/kg by Minyuk et al. 2013. Conservatively assuming the lower value, a density for Vivianite of 2300 kg/m$^3$, and a viscosity of the slurry of twice that of water, 2 $10^{-3}$ kg/m.s, the speed of 10 micron diameter Vivianite particles towards the surface can be estimated as

$$\Delta v = 6\ 10^{-18}\ A^{-2} m^4 s^{-1}\ H \nabla H \qquad (S2.4)$$

Target slurries contain organic fibers of up to 1mm length, and so the channels for the slurry should leave at least a space of 2 mm between surfaces to avoid blocking. Still, this means that an average field of $10^6$ A/m and an average field gradient of $0.5*10^9$ A/m$^2$ (i.e., varying by $0.5*10^6$ A/m over 1 mm from the center of the channel towards the surface) would result in a particle speed of 3 mm/s. This is more than enough for all such particles to reach the surface for a typical residence time of one or more seconds. Field conditions like these do not require superconducting magnets or steel wool. They can be met by Jones separators with electromagnets and grooved plates, which has the advantage of low investment cost and simple channel geometries that do not easily block.

Once the magnetic particles have reached the surface, they should stick there and not be carried along the surface by the drag of the slurry. The Reynolds number of the flow in the channels formed by the surface is typically below 100, so the friction of the slurry flow per unit area of the coating of magnetic particles on the surface of the channels is

$$f_{friction\ slurry} = \frac{8\eta v}{D} \qquad (S2.5)$$

Here v (m/s) is the velocity of the slurry past the surface, and D (m) is the diameter of the channel. The friction of the surface of a particle is proportional to the magnetic force pulling the particle to the surface:

$$F_{friction\ surface} = fF_{magnetic} = f\mu_0\rho_pV_p\chi_pH\nabla H \qquad (S2.6)$$

Since $F_{friction\ surface} > A_p f_{friction\ slurry}$, where $A_p$ is the part of the surface covered by a single particle, the magnetic field should be strong enough to fix the magnetic particles to the surface:

$$H\nabla H > \frac{8\eta A_p v}{f\mu_0\rho_pV_p\chi_pD} \qquad (S2.7)$$

Taking again the values for Vivianite as above and estimating f=0.5, while conservatively taking $A_p = 5D_p^2$, we get:

$$H\nabla H > 1.7\ 10^{15}\ A^2m^{-4}s^1\ v \qquad (S2.8)$$

With v≈0.1 m/s, this means that, again, Jones separators will do well.

For a full coating of particles $A_p = 5D_p^2$ is a very conservative estimate since it would be expected that each particle covers roughly its square diameter of the surface. However, for a single particle sticking from the surface, this estimate is probably more appropriate.

Table S2.3: Forces applying on vivianite depending on the flow rate

| Total flow | Drag + gravity force on particles near the wall (pN) | | | Magnetic stick force on the wall (pN) | | |
|---|---|---|---|---|---|---|
| mL/min | 10 µm | 20 µm | 30 µm | 10 µm | 20 µm | 30 µm |
| 7.8 | 45 | 207 | 525 | 142 | 1130 | 3820 |
| 16.2 | 83 | 360 | 869 | 142 | 1130 | 3820 |
| 24.0 | 122 | 513 | 1210 | 142 | 1130 | 3820 |
| 32.4 | 160 | 666 | 1560 | 142 | 1130 | 3820 |
| 40.2 | 198 | 819 | 1900 | 142 | 1130 | 3820 |

Table S2.4: Ratio of the drag and stick forces depending on the flowrate

| Total flow | Ratio of drag and stick | | |
|---|---|---|---|
| mL/min | 10 µm | 20 µm | 30 µm |
| 7.8 | 0,32 | 0,18 | 0,14 |
| 16.2 | 0,59 | 0,32 | 0,23 |
| 24.0 | 0,86 | 0,45 | 0,32 |
| 32.4 | 1,13 | 0,59 | 0,41 |
| 40.2 | 1,40 | 0,72 | 0,50 |

Under all these assumptions, it can be seen in Table S2.4 that a flow rate lower than 24 mL/min should allow all the particles >10 µm to stick to the walls of the µ-Jones (ratio <1). The exact cut-off for these particles is 28.2 mL/min.

**2**

## Viability of magnetic separation

Experiments were performed to test the viability of magnetic separation of vivianite from sludge. The four tested flow rates are lower than the 28.2 mL/min cut-off previously determined to ensure that the separation will work and separate particles smaller than 10 μm. The separation protocol was the same as described in the Material & Methods section, with the difference that the flow rate varied and that the pouring time was 30 seconds for both sludges.
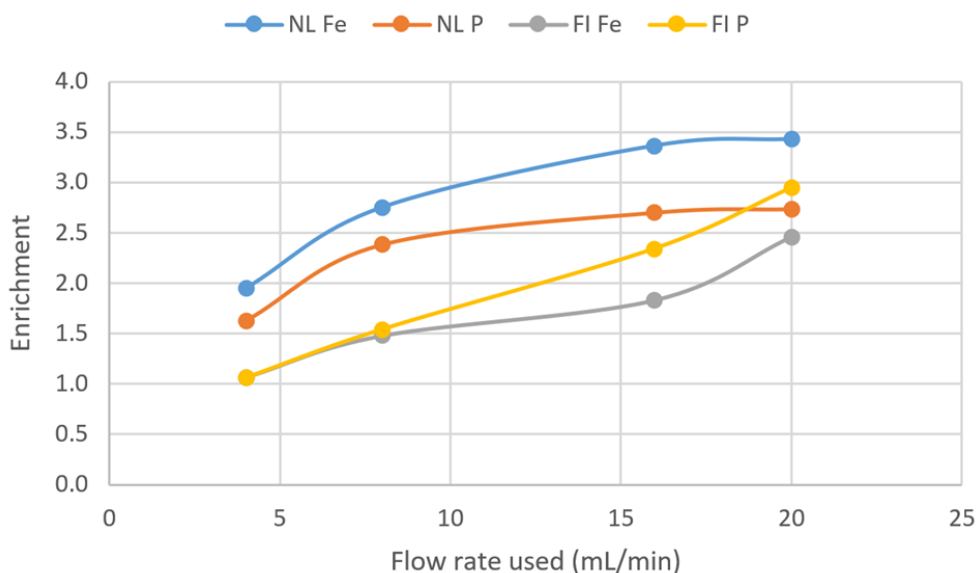


*Figure S2.1: Enrichment for phosphorus and iron for both sludge at four different flow rates (The enrichment defines the ratio of the weight content of a iron and phosphorus before and after magnetic separation)*

First of all, the separation works for flowrates below 20 mL/min which is in the expected range obtained by theoretical modeling. Indeed, from a certain flow rate, the drag force exerted by the slurry on a particle stuck on the surface becomes higher than the one retaining it against the wall. Figure S2.1 shows that for both sludges the enrichment increases for both iron and phosphorus with the flow rate. This is in line with the expectations since non-magnetic impurities are more likely to be flushed out at higher flow rates. The enrichment shows a saturation around 20 mL/min for the Dutch sludge which is not the case for the Finnish sludge (Figure S2.1). The maximum magnetic species may have been extracted from the Dutch sludge while a longer pouring time may be needed for the Finnish sludge. It is in accordance with the higher Fe/P ratio of the Finnish sludge, suggesting that a bigger magnetic fraction, containing siderite ($FeCO_3$), pyrite or/and FeO's, is present.
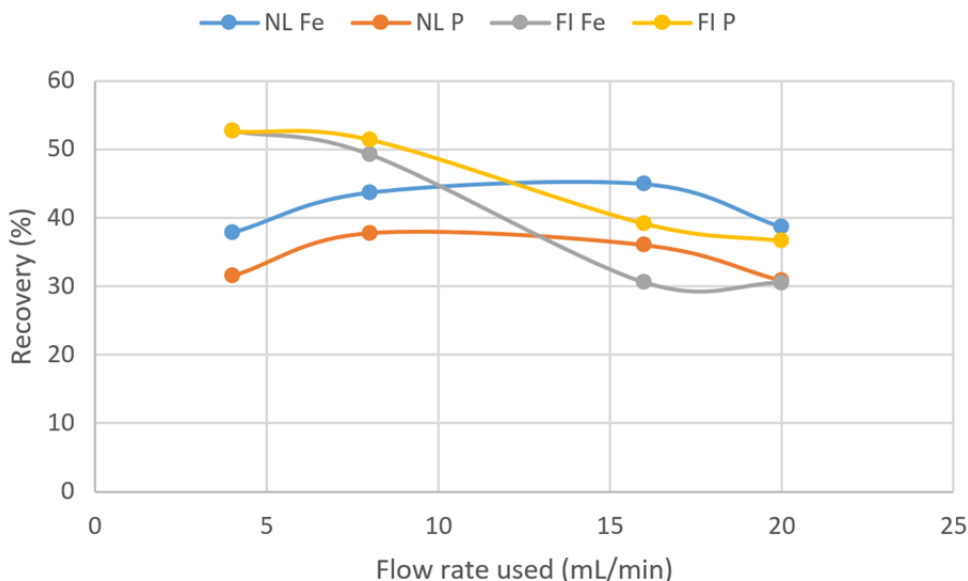
*Figure S2.2: Recovery of phosphorus and iron for both sludge at four different flow rates*

Aside from the enrichment, the recovery of phosphorus and iron has been measured as well. The recovery decreases with the flow rate for the Finnish sludge for both elements while it remains rather stable for the Dutch feed (Figure S2.2). Higher streams reduce the part of non/less-magnetic material susceptible to be retained which explains the behavior of the Finnish sludge. 20 mL/min was the highest flow rate tested. Even though it gave lower recovery, it gave the purest product with lower organic matter content and impurities like calcium, sulfur, and silicon. Determining the quantity of vivianite present in the concentrate is easier with a purer sample. Therefore, 20 mL/min have been chosen as the working flow rate

## Carbonate determination

The carbonate content in the sample has been estimated using µGC. First, 20 mg of solid is added to a 25 mL glass vial. 1 mL of HCl 9% (VWR Chemicals) is quickly poured on the powder, and the jar is immediately closed with a rubber stopper. After 10 minutes, 10 mL of the gas phase is withdrawn and quickly introduced in a µGC for $CO_2$ determination. The device is a Varian CP 4900 equipped with a Thermal Conductivity Detector. The column used is a PoraPlot U of 10 m long with Helium as a carrier. The data processing is realized with the software GC solution. A blank without any solid but only acid was also prepared.

The quantity of $CO_2$ released and the quantity of carbonate in the samples are presented in Table S2.5 (calculation below). There is significantly more carbonate in the samples from Finland (3-5% of dried solid) than the one from the Netherlands (< 1%). Independently from the sludge origin, the share of carbonate seems to decrease after magnetic separation. No $CO_2$ release has been observed in the case of the scaling sample.

**2**

*Table S2.5: Percentage of carbon dioxide evolution and FeCO₃ content assuming all evolved carbon dioxide was associated to FeCO₃*

| Sample | $X_{CO2}$ (%) | $X_{FeCO3}$ (%) |
|---|---|---|
| Blank | 0.1 | 0.1 |
| FI Feed | 1.3 | 4.9 |
| FI Conc. | 1.0 | 3.3 |
| NL Feed | 0.3 | 0.6 |
| NL Conc. | 0.2 | 0.3 |
| Scaling | 0.1 | 0.1 |

Hypothesizing the total reaction $FeCO_3 + 2HCl \rightarrow FeCl_2 + H_2O + CO_2$, the determination of the carbonate fraction can be done as follow:

$$n_{CO2} = \frac{(X_{CO2} - X_0) \times \rho_{air} \times V_{gas}}{M(CO_2)}$$

(S2.9)

1 mole of $FeCO_3$ releases 1 mole of $CO_2$, so:

$$n_{CO2} = n_{FeCO3}$$

(S2.10)

Giving finally:

$$X_{FeCO3} = \frac{n_{FeCO3} \times M(FeCO_3)}{m_{sample}}$$

(S2.11)

With:

$n_{CO2}$ the amount of substance of $CO_2$ released in the tube in moles

$X_{CO2}$ the $CO_2$ weight fraction of the gaseous phase in the tube

$X_0$ the $CO_2$ weight fraction of the blank

$\rho_{air}$ the density of air worth 1.20 g/L at the experimental conditions (20°C at sea level)

$V_{gas}$ the total volume of the gaseous phase in the tube worth 0.0240 L (1 mL of HCl in 25 mL tube)

$M(CO_2)$ the molar weight of $CO_2$ worth 44.0 g/mol

$n_{FeCO3}$ the amount of substance of $FeCO_3$ in the sample in moles

$X_{FeCO3}$ the $FeCO_3$ weight fraction of the solid

$M(FeCO_3)$ the molar weight of $FeCO_3$ worth 115.8 g/mol

$m_{sample}$ the weight of the sample introduced into the tube in g

## Quartz determination

It has been noticed that when a sufficient quantity (50 mg) of feed or concentrate is digested, an insoluble white solid remains. Quartz ($SiO_2$) is hard, or even impossible, to degrade with standard acid digestion. The solid fraction remaining after digestion was carefully collected by centrifugation and dried at 105 °C.

The undigested solid after digestion was isolated and analyzed by SEM-EDX. Silicon and oxygen were the main components of the sample (>80% of total weight) in a ratio close to $SiO_2$. However, some other elements were homogeneously distributed, ranging from sodium, aluminum and calcium at high concentrations, to iron, phosphorus, and copper at minor concentrations. The dry weight of the digestion residue was assumed to be entirely quartz for the calculations (Table S2.6).

*Table S2.6: Digestion residue (assumed to be quartz) content in both sludges*

| Sample | Average (% of vacuum dried matter) |
|--------|-------------------------------------|
| FI Feed | 8 |
| FI Conc. | 8 |
| NL Feed | 4 |
| NL Conc. | 7 |

*Table S2.7a: Elemental composition of the feeds, concentrates, and scaling measured by ICP-MS/OES*

| Sample | Weight content (g element/kg of P) | | | | | | | | | | | |
|--------|----|----|----|----|----|----|----|----|----|----|----|----|
| | Cr | As | La | Li | Mg | Al | Mn | Co | Ni | Cu | Cd | Ca |
| FI Feed | 1.2 | 0.3 | 1 | 0.1 | 140 | 215* | 9 | 0.3 | 1.2 | 13 | nd | 940* |
| FI Conc. | 0.4 | 0.1 | 0.4 | 0.1 | 43 | 71* | 6 | 0.2 | 6.2 | 15* | nd | 265* |
| NL Feed | 1.4 | 1.1 | 0.3 | 0.1 | 91 | 160* | 17 | 0.2 | 1.1 | 18 | nd | 968* |
| NL Conc. | 0.8 | 0.2 | 0.1 | 0.1 | 97* | 60* | 0.1 | 0.1 | 1.2 | 9 | nd | 259* |
| Scaling | nd | nd | nd | nd | 91* | 3 | 25* | 0.3 | 0.7 | 0.2 | nd | 80* |

nd: no data, meaning below LOQ of both ICP

* results from ICP-OES

*Table S2.7b: Elemental composition of the feeds, concentrates, and scaling measured by ICP-MS/OES*

| Sample | Weight content (g element/kg of P) | | | | | | | | | | | |
|---|---|---|---|---|---|---|---|---|---|---|---|---|
| | Zn | Mo | Ag | Sn | Ba | Pb | Na | Si | K | S | Rb | Ce |
| FI Feed | 26 | 0.2 | 0.1 | 0.9 | 4 | 0.5 | 107* | 278* | 380* | 303* | 0.4 | 2.6 |
| FI Conc. | 6 | 0.1 | nd | 0.2 | 1 | 0.1 | nd | 85* | 31* | 93* | 0.1 | 0.8 |
| NL Feed | 35* | 0.3 | 0.2 | 0.7 | 11 | 3.0 | 193* | 187* | 275* | 558* | 0.2 | 0.4 |
| NL Conc. | 8 | 0.1 | 0.1 | 0.2 | 3 | 1.1 | 3 | 72* | 23* | 124* | 0.1 | 0.2 |
| Scaling | 2 | nd | nd | nd | nd | 0.1 | nd | nd | nd | 14* | nd | nd |

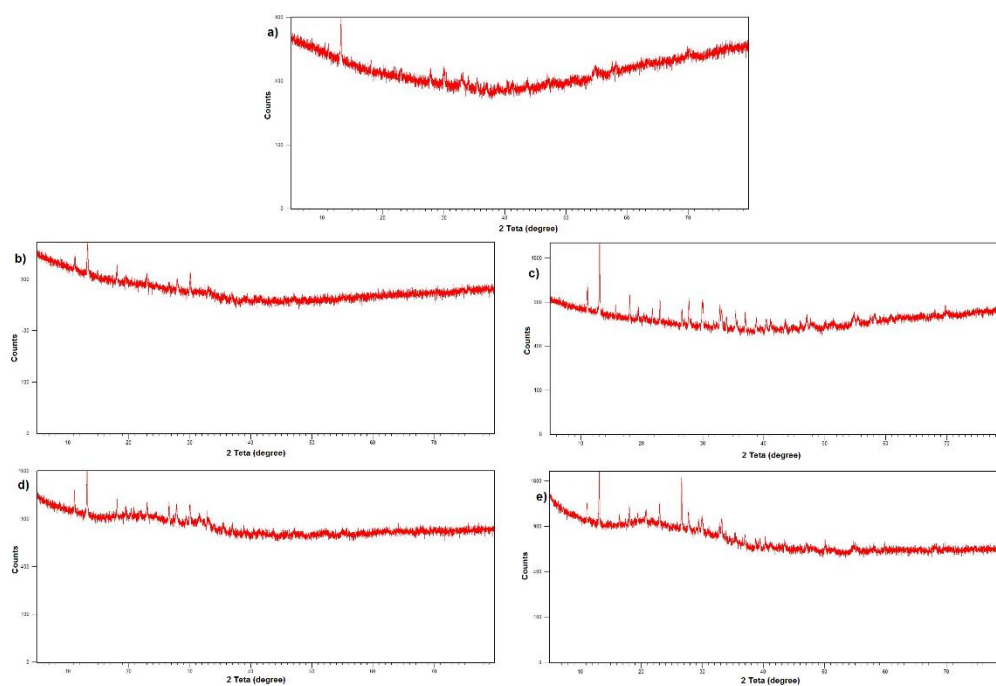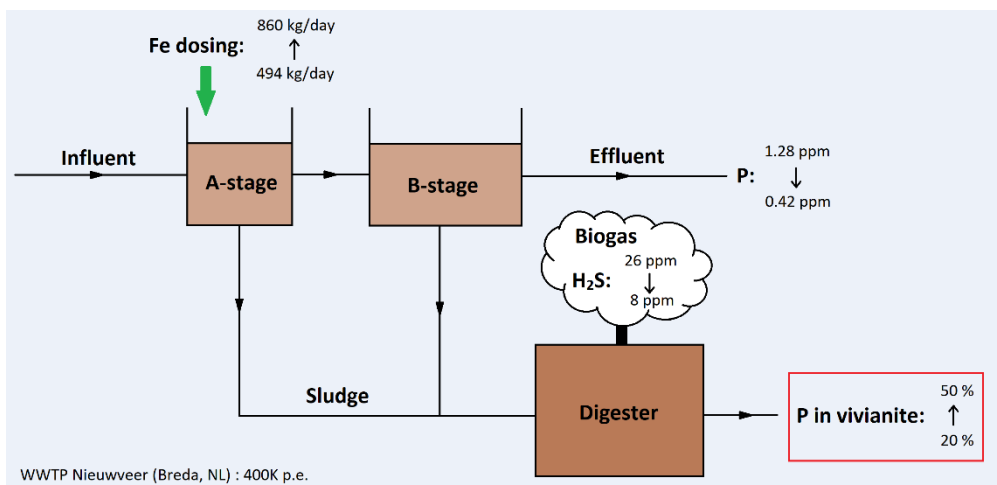nd: no data, meaning below LOQ of both ICP

* results from ICP-OES



*Figure S2.3: XRD diffractogram for a) the scaling, b) Conc. FI, c) Conc. NL, d) Feed FI and e) Feed NL*

# Chapter 3: Full-scale increased iron dosage to stimulate the formation of vivianite and its recovery from digested sewage sludge

**3**

**Highlights**

- Phosphorus recovery via vivianite can be enhanced through an increased iron dose.

- The additional dosed iron was nearly entirely transformed into vivianite.

- The extra iron dosing reduced the effluent phosphorus content to < 0.5 mg P/L.

- The different types of vivianite found suggest different formation mechanisms.

- The method for vivianite quantification with Mossbauer spectroscopy was improved.

Keywords: Phosphorus recovery, Waste Water Treatment Plant (WWTP), magnetic recovery, Mössbauer spectroscopy, X-Ray Diffraction (XRD), iron sulphide

**3**

## Abstract

The recovery of phosphorus from secondary sources like sewage sludge is essential in a world suffering from resource depletion. Recent studies have demonstrated that phosphorus can be magnetically recovered as vivianite ($Fe(II)_3(PO_4)_2*8H_2O$) from the digested sludge (DS) of Waste Water Treatment Plants (WWTP) dosing iron. To study the production of vivianite in digested sludge, the quantity of iron dosed at the WWTP of Nieuwveer (The Netherlands) was increased (from 0.83 to 1.53 kg Fe/kg P in the influent), and the possible benefits for the functioning of the WWTP were evaluated. Higher iron dosing is relevant for P-recovery and maximal recovery of organics from influent, e.g., biogas production. The share of phosphorus present as vivianite in the DS increased from 20% to 50% after the increase in iron dosing, making more phosphorus available for future magnetic recovery. This increase was directly proportional to the increase of iron in DS, suggesting that vivianite could be favored thermodynamically and kinetically. Interestingly, analyses suggest that several types of vivianite are formed in the WWTP and could differ in their purity, oxidation state, or crystallinity. These differences could have an impact on the subsequent magnetic separation. Following the iron dosing increase, phosphorus in the effluent and $H_2S$ in the biogas decreased: 1.28 to 0.42 ppm for phosphorus and 26 to 8 ppm for $H_2S$. No negative impact on nitrogen removal, biogas production, COD removal, or dewaterability was observed. Since quantification of vivianite in DS is complicated, previous studies were reviewed, and we proposed a more accurate Mössbauer spectroscopy analysis and fitting for sludge samples. This study is important from a phosphorus recovery point of view, but also because iron addition can play a crucial role in future resource recovery wastewater facilities.

## 3.1. Introduction

Phosphorus (P) is an essential nutrient for all living organisms and is a key element for global food production as it is widely used as fertilizer (Childers et al. 2011). Currently, the raw material for its production is mined phosphate rock. Unfortunately, the resources are scarce and concentrated in a few countries (Morocco holds 70% of the P-rock), making phosphorus a vulnerable resource (Cordell et al. 2015). This situation creates the need to exploit secondary sources of phosphorus like manure or sewage sludge (Ohtake et al. 2019).

The phosphorus present in wastewater is usually removed at the waste water treatment plant (WWTP). The most popular P-removal strategies are enhanced biological phosphorus removal (EBPR) and chemical phosphorus removal (CPR). The first relies on phosphate accumulating organisms, while the second involves iron dosing or, more rarely, aluminum dosing (Morse et al. 1998). While phosphorus removal technologies are well-established and widely applied, phosphorus recovery remains a challenge (Wilfert et al. 2015). The two main recovery routes are currently via struvite precipitation for WWTPs using EBPR and after incineration for those using CPR. However, both methods have limitations: the P-recovery percentage is low for the former (Cornel et al. 2009), and infrastructure costs are high for the second (Desmidt et al. 2015).

Recent studies indicate that the mineral vivianite ($Fe(II)_3(PO_4)_3*8H_2O$) is an important phosphorus sink in the digested sludge from CPR plants (Wilfert et al. 2016, 2018). Our team has demonstrated that the magnetic extraction of vivianite from DS is possible at lab scale, opening a possible new route for phosphorus recovery (Chapter 2). Wilfert et al. 2018 suggest that higher iron dosing could increase the conversion of the phosphorus in sludge into vivianite, increasing the share of magnetically recoverable phosphorus.

Besides its possible effect on vivianite production, increased iron dosing is in line with current trends in wastewater treatment. Northern European countries such as the UK and Germany have fixed low limits for phosphorus in WWTP effluent (0.15-0.3 ppm) that may decrease even further in the future (European Sustainable Phosphorus Platform 2019). Such low phosphorus levels can only be achieved by CPR, usually using iron salts (Suresh Kumar et al. 2019). Moreover, iron addition to the primary settler or the A-stage of a WWTP enhances primary sludge production, thus giving higher biogas yield after digestion (Li et al. 2005). It appears that the use of iron in wastewater treatment fits in the future of net energy-producing plants.

To verify the hypothesis of Wilfert et al. 2018, a controlled iron dosing increase was realized to investigate the actual effect of the iron dosing on vivianite production. To achieve this, the iron dosing was doubled at the Nieuwveer WWTP (The Netherlands), and the results are presented in this article. Special attention is given to the impact of the higher iron dosing on the integral parameters of the WWTP (e.g., phosphorus level in the effluent, biogas production, and N removal) to ensure that vivianite production is not achieved to the detriment of the WWTPs primary objectives and in the scope of future wastewater treatment.

## 3.2. Materials and methods

### 3.2.1. WWTP and iron dosing

The study took place at the AB plant in Nieuwveer (The Netherlands) (influent: 69.77m$^3$/day in 2018). There, a FeSO$_4$ solution is dosed in the aerated A-stage for phosphorus and COD removal. The Solid Retention Times (SRTs) are 0.72 days for the A-stage, 13 days for the B-stage, and 20 days for the anaerobic digester. This WWTP receives external sludge from other WWTPs at irregular intervals. The external sludges are mixed with the A and B sludges before being thickened and fed to the digester. The external sludge accounts for ~30% of the total sludge volume.

The quantity of FeSO$_4$ dosed in the A-stage was doubled for four months to study the influence of the iron dosing increase. The dosing can be broken down into 3 phases, as shown in Figure 3.1. Phase II with the highest iron dosing will be the studied period.
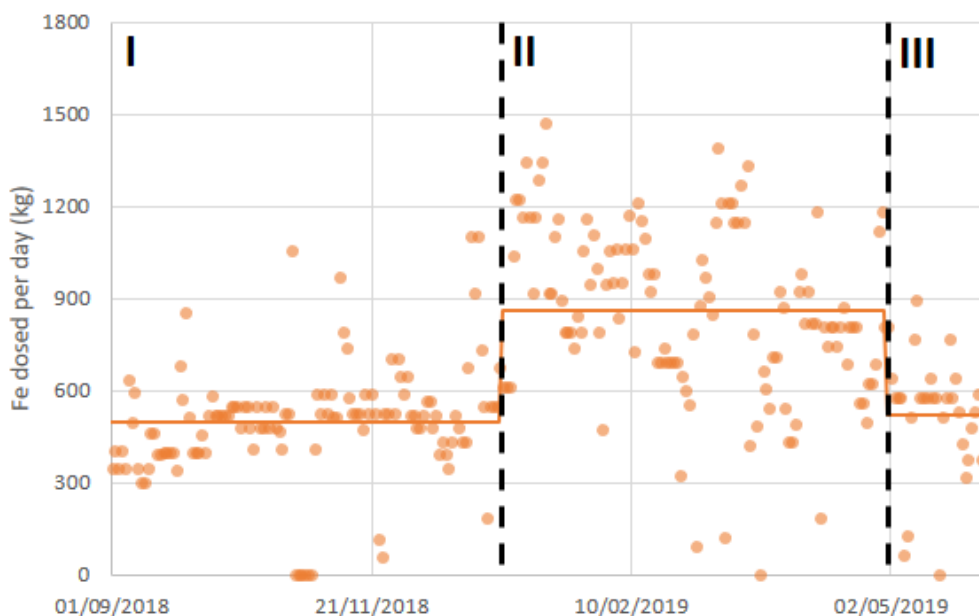


*Figure 3.1: Daily and average iron dosing before (Phase I: 494kg Fe/day), during (Phase II: 860kg Fe/day), and after the study (Phase III: 520 kg Fe/day).*

### 3.2.2 Sample handling

Four samples were taken every two weeks from the sludge line: the settled sludge from A-stage, the settled sludge from B-stage, the mixed A-stage, B-stage, and external sludge (MS) before digestion and the digested sludge (Figure S3.1). The sludge line was sampled twice in phase I, before starting the iron dosing as a reference and once in phase III. Eight other samples were taken at regular intervals for four months, after which time a steady-state should be reached in all the units (Table S3.1). Samples were poured to the brim into air-tight polyethylene bottles and stored in a 4°C fridge after 4 hours of transportation. At Nieuwveer, 1-2 mL of each sample was immediately filtered (0.45μm filter) and fixed with 0.05 mL of 0.5M HCl to prevent iron oxidation. These samples were analyzed with the ferrozine method

for iron speciation and ICP-OES for elemental composition. Sludge samples were centrifuged for 15 min at 3750 rpm. The cake was dried at 25°C in a fume hood for 48h for Total Solid (TS) measurement and later ground and digested for elemental composition and SEM-EDX. A part of the cake of the DS was dried in a glove box under anaerobic and light-free conditions to prevent vivianite oxidation for XRD (X-Ray Diffraction) and Mössbauer spectroscopy analysis. The drying of the sludge was done at room temperature to avoid the decomposition of vivianite.

### 3.2.3   Analyses

#### 3.2.3.1  Light microscopy & SEM-EDX

Around 0.1g of dried solid samples were ground for light microscopy and SEM-EDX analysis. The grinding was done to break the organic matter shell covering the vivianite crystals that prevented proper microscope observation. The light microscope used was a Leica MZ95 equipped with a Leica DFC320 camera.

The SEM-EDX apparatus was a JEOL JSM-6480 LV Scanning Electron Microscope (SEM) equipped with an Oxford Instruments x-act SDD Energy Dispersive X-ray (EDX) spectrometer. The working distance was 10mm for an accelerating voltage of 15.00 kV. Around 0.1g of dried samples were covered with a 10 nm-layer of gold using a JEOL JFC-1200 fine coater to make the surface electrically conductive. The software used was JEOL SEM Control User Interface for the SEM and Oxford Instruments Aztec for the EDX data processing.

#### 3.2.3.2  XRD

After being dried in the dark in an anaerobic chamber, the samples were introduced in a 0.7 mm glass capillary under anaerobic conditions and minimum light exposure. The samples were kept and transported in a sealed sample holder covered with aluminum foil. Just before measurement, the capillaries were sealed with a burner. The device used was a PANalytical X′Pert PRO diffractometer with Cu-Ka radiation (5-80º 2θ, step size 0.008º). The peaks assignment was realized with the software Origin Pro 9.

#### 3.2.3.3  Mössbauer spectroscopy

The samples were dried as explained in section 2.3.2 to prevent vivianite oxidation. Then, they were introduced in plastic rings sealed with Kapton foil and Epoxy glue to prevent oxygen exposure and wrapped in aluminum foil for light protection. The sample weight was adjusted to contain a maximum of 17.5 mg of $Fe/cm^2$. If the sample contained too much iron, it was diluted with inert carbon powder. Transmission $^{57}$Fe Mössbauer absorption spectra were collected at 300 K with a conventional constant-acceleration spectrometer using a $^{57}$Co (Rh) source. Velocity calibration was carried out using an α-Fe foil. The Mössbauer spectra were fitted using the Mosswinn 4.0 program (Klencsár 1997).

#### 3.2.3.4  Ferrozine method

First, 2mL of sample was filtered and fixed with HCl 0.1mL of 0.5M HCl directly at the WWTP to avoid iron oxidation/reduction and analyzed under anaerobic conditions 4h after sampling. The iron speciation was determined using the ferrozine method, as explained in Viollier et al. 2000. In brief, 1 mL of HCl-fixed sample was added into a cuvette to 0.1mL of

a ferrozine solution, which forms a pink complex with $Fe^{2+}$. The absorbance was measured at 562 nm after 15 minutes of reaction with a Shimadzu UV-1800 Spectrophotometer. Then, 0.15 mL of 1.4 M hydroxylamine was added to 0.8 mL of the complexed solution to reduce all the $Fe^{3+}$. The reduction took place for 12h to ensure that all the organically bound iron was reduced (Rasmussen and Nielsen, 1996). Finally, 0.05mL of 10M acetate buffer was added to the sample, and the final absorbance was measured. The $Fe^{2+}$ and $Fe^{3+}$ were calculated using these two absorbances.

### 3.2.3.5 Microwave digestion & ICP-OES

Solid samples were destroyed in an Ethos Easy digester from Milestone equipped with an SK-15 High-Pressure Rotor. Around 50 mg of dried solid was introduced in a Teflon vessel in which 10 mL of ultrapure $HNO_3$ (64.5 – 70.5% from VWR Chemicals) was poured. The digester reached 200 °C in 15 min, was run at this temperature for 15 min and was cooled down for 1h.

The elemental composition of the microwave digested samples and the filtered samples were measured via Inductively Coupled Plasma (Perkin Elmer, type Optima 5300 DV) equipped with an Optical Emission Spectroscopy (ICP-OES). An Autosampler, Perkin Elmer, type ESI-SC-4 DX fast was used, and the data were processed with the software Perkin Elmer WinLab32. The rinse and internal standard solution were respectively 2% of $HNO_3$ and 10 mg/L of Yttrium.

### 3.2.3.6 Global parameters of the WWTP

The operators of Nieuwveer on-site measured the following parameters of the WWTP:

- P effluent concentration (measured by Aquon according to the NEN norms)
- $H_2S$ content in the biogas (measured by INCA 4000 T101 from Union Instruments GmbH)
- COD removal (measured by Aquon according to the NEN norms)
- Biogas production (measured by ST51-FR32C00A flow meter from Fluid Components International LLC)
- Nitrogen removal (measured by Aquon according to the NEN norms)

## 3.3. Results & Discussion

Recovery of phosphorus via magnetic extraction of vivianite is a recent technique and is still in development. In Chapter 2, we reached the first milestone by maximizing the quantity of phosphorus present as vivianite. The results of Wilfert et al. 2018 had suggested that an increase in iron dosing could promote vivianite formation. However, they had conducted their study by examining sludge from 6 WWTPs with a fixed Fe/P ratio. To investigate the actual effect of the iron dosing on the vivianite content in the DS (vivianite content, efficiency of the dosing, delay required to form vivianite), therefore, a controlled iron dosing increase at a single WWTP is required.

The water authority Brabantse Delta made this research possible by increasing the iron dosing at the WWTP Nieuwveer (The Netherlands) from 0.83 to 1.53 kg Fe/kg P in the influent for four months. The effect of this increase on phosphate behavior and the integral operation of the treatment plant (e.g., phosphorus level in the effluent, biogas production, COD removal…)

was studied, and the results are discussed in this section. Since the strategy of recovering phosphorus as vivianite is novel, the analytical methods are still under development and subject to possible improvements. For this reason, the first part of the discussion is dedicated to the quantification of vivianite in digested sludge.

### 3.3.1. Quantification of vivianite in digested sludge: a short review and best practice

The major problem while studying vivianite in digested sludge is its quantification. Wilfert et al. 2018 used standard addition of synthetic vivianite together with XRD. A drawback of this method is its use of pure vivianite, even though the vivianite in sludge could be impure (Wilfert et al. 2016, Seitz et al. 1973). Moreover, XRD is unable to detect small or amorphous vivianite, which creates greater uncertainty. Despite these facts, XRD results were in line with Mössbauer results in their study, even though vivianite content was always estimated on the higher end with XRD.

Mössbauer spectroscopy can detect iron minerals independently of their size or crystallinity and is considered to be the best technique for vivianite quantification so far. Nevertheless, some discrepancies are present in the literature regarding sample handling and measuring and data fitting. These problems will be discussed below, and an improved practice for vivianite determination with Mössbauer will be proposed. To understand the data fitting for Mössbauer spectroscopy, it is important to know that a crystalline unit of vivianite bears three possible positions for iron: 1 octahedral site called site A and two equivalent octahedral sites called site B (Mori & Ito 1950). The most characteristic feature of vivianite is that it has two doublets for $Fe^{2+}$ present in site A (1 $Fe^{2+}$ ion) and site B (2 $Fe^{2+}$ ions). The Mössbauer parameters for these sites are well described and accepted in the literature: Site A (Isomer Shift (IS) = $1.2\pm0.1$ mm/s, Quadrupole Splitting (QS) = $2.4\pm0.1$ mm/s) and Site B (IS = $1.25\pm0.1$ mm/s, QS = $3.0\pm0.1$ mm/s) (McCammon et al. 1980, Rouzies & Millet 1993, Nembrini et al. 1983). Thus, the amount of $Fe^{2+}$ present in vivianite in a sample can be reliably quantified.

However, vivianite can easily be oxidized by oxygen and light (Čermáková et al. 2013, McCammon et al. 1980), leading to the transformation of a part of the $Fe^{2+}$ from both sites into $Fe^{3+}$. The signal of $Fe^{3+}$ in vivianite is difficult to distinguish from that of $Fe^{3+}$ species that can generally be present in sludge samples. Therefore, the samples are generally protected from oxidation as much as possible (Wilfert et al. 2018, Wang et al. 2019, this study) to prevent/minimize the oxidation of iron during sampling and handling. The samples can be studied by Mössbauer spectroscopy at temperatures from 4.2K to 300K. However, Wilfert et al. (2016, 2018) reported that measurements at 4.2K were not suitable for vivianite determination due to the complexity of the signal. Vivianite can be quantified at 100K (Wilfert et al. 2018, Wang et al. 2019), but these analyses do not seem to add any information to the quicker and easier analyses at 300K. Several researchers working with DS proposed measurements at 300K with a fitting with three doublets: $Fe^{2+}$ in site A, $Fe^{2+}$ in site B, and $Fe^{3+}/Fe^{II}$ accounting for all the $Fe^{3+}$ species (including $Fe^{3+}$ in vivianite) and low-spin $Fe^{2+}$ compounds like pyrite (Chapter 2, Frossard et al. 1997 and Wilfert et al. 2018). Vivianite is likely to be partly oxidized in DS, so its content was probably underestimated in these cases as the $Fe^{3+}$ in the oxidized vivianite will not be taken into account.

To overcome the neglect of $Fe^{3+}$ in the vivianite analysis, Rouzies & Millet 1993 proposed to fit the $Fe^{3+}$ in vivianite with three additional doublets. Because our samples could not be fitted this way, we synthesized vivianite and let it oxidize for 15 days. The resulting spectra could be fitted with the 2 $Fe^{2+}$ doublets of vivianite and one doublet (IS=0.46 mm/s and QS=0.63 mm/s), accounting for the oxidized iron in vivianite (Table S3.2). These parameters are in line with those reported by McCammon et al. 1980, Nembrini et al. 1983 and Rouzies & Millet 1993 (averaging the three doublets proposed for $Fe^{3+}$ in vivianite). The spectra of DS samples collected during the present study could successfully be fitted with four doublets: $Fe^{2+}$ site A, $Fe^{2+}$ site B, the proposed (IS=0.46 mm/s and QS=0.63 mm/s) doublet for $Fe^{3+}$ in vivianite, and a doublet accounting for the remaining $Fe^{3+}$ and low-spin $Fe^{2+}$. With this fitting, the quasi-inevitable oxidation of vivianite does not lead to a constant underestimation of its content.

To summarize, the authors propose a strategy where samples do not necessarily need to be protected from oxidation and are measured at 300K. The spectra should be fitted with 4 doublets: $Fe^{2+}$ site A (IS = 1.2±0.1 mm/s, QS = 2.4±0.1 mm/s), $Fe^{2+}$ site B (IS = 1.25±0.1 mm/s, QS = 3.0±0.1 mm/s), $Fe^{3+}$ in vivianite (IS=0.46 mm/s and QS=0.63 mm/s) and the remaining signal corresponding to other $Fe^{3+}$ species low-spin $Fe^{2+}$ like pyrite. These recommendations allow easier sample handling and higher accuracy of the vivianite quantification.

### 3.3.2. Iron dosing increase promotes quick and efficient vivianite formation in digested sludge

The primary objective of this study was to evaluate whether increased iron dosing would effectively increase the proportion of vivianite present in DS, as suggested by Wilfert et al. 2018. Figure 3.2 shows that the iron content in DS increased over time from 40mg/g until it reaches a steady state at around 65-70mg/g. Despite the doubling of the iron dosed (494 kg/day in phase I to 860 kg/day in phase II), the iron content in DS did not double. This may be the result of the mixing of on-site produced sludge with 30% of external sludge before digestion, which "dilutes" the Fe-rich produced sludge. It is important to verify that an increase of the vivianite content accompanies this iron increase in the DS.

First of all, XRD confirmed the presence of vivianite in all the samples (Figure S3.3). Also, modeling using Visual Minteq showed that the iron and phosphorus concentrations in the sludge liquor are above the saturation index for vivianite (Table S3.8). SEM-EDX analysis also showed particles with a sheet agglomerate structure, characteristic of vivianite, and an Fe/P ratio close to 1.5 (Figure 3.3) (Zelibor et al. 1988, Rothe 2016). The quantification of vivianite in the samples was performed according to the improved Mössbauer strategy described above. The results indicate that the vivianite content in DS increased from 50 to 150 mg/g of TS, following the increase of iron in DS (Figure 3.2). The fraction of phosphorus present as vivianite followed the same trend with an increase from 20% to 50% (Figure 3.2). This confirms the central research hypothesis of this study: an increase in iron dosing increases the proportion of phosphorus present as vivianite in DS.
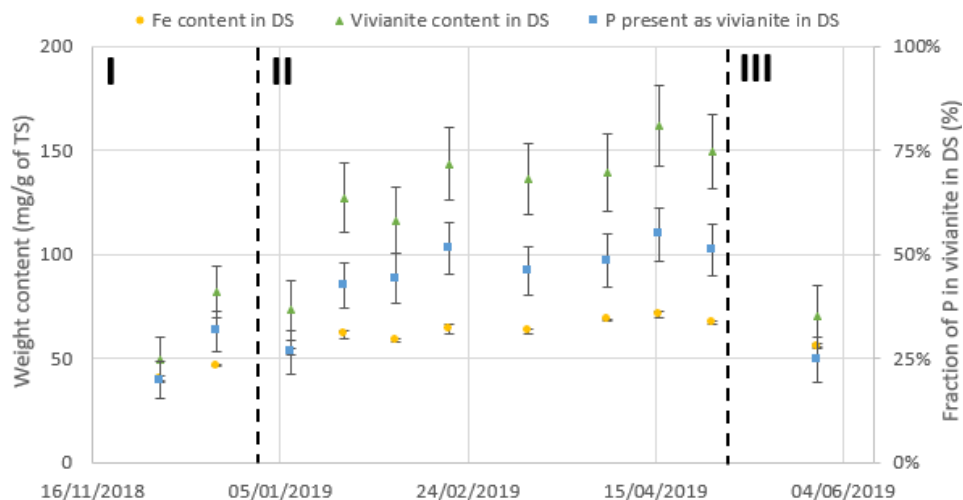
*Figure 3.2: Iron and vivianite content in the solid phase of the digested sludge of Nieuwveer (primary axis). Fraction of phosphorus in the solid phase of the digested sludge present as vivianite (secondary axis). (calculated from the Mössbauer results in Table S3.2 and the ICP-OES results in Table S3.3). I, II, and III correspond to the different iron dosing phases, as described in Figure 3.1.*

Interestingly, the increase in vivianite immediately followed the increase in iron content in sludge, indicating that the phosphorus present in digested sludge is quickly converted to vivianite. Nriagu et al. 1974 stated that vivianite is the most stable phosphorus mineral in a reducing environment (like DS). This result suggests that vivianite could also be kinetically favored.
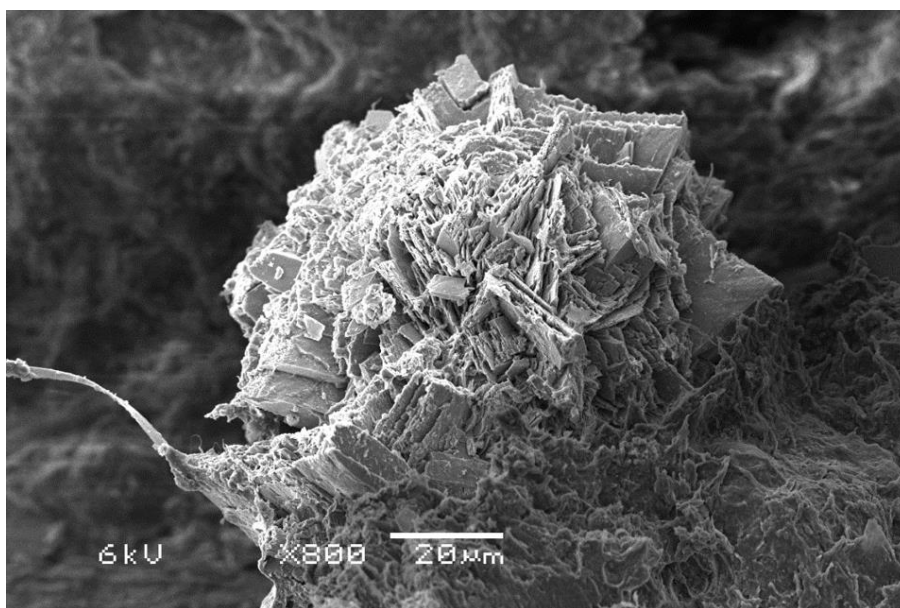


*Figure 3.3: Example of a vivianite particle found in the digested sludge (sample DS2) of Nieuwveer and observed by SEM.*

To confirm that this vivianite formation technique is efficient, it is essential to verify how much of the extra iron dosed is used to form vivianite. Firstly, mass balances show that >99% of the iron in the digested sludge can be found in the solid fraction (Table S3.11). Secondly, data in Figure S3.5 suggests that the iron content in vivianite increases linearly ($R^2$=0.86) with the iron content in DS. The slope of this line is 1.24±0.16, confirming that all the "extra" iron present in DS was present as vivianite. Moreover, a slope bigger than 1 suggests that some of the iron present in sludge in non-vivianite species was converted to vivianite as well. Such non-vivianite species could be iron oxides, $FeS_x$, or organically-bound iron, for example.

### 3.3.3. FeS compounds are forming before vivianite in digested sludge

The data obtained in this study follow the same trend observed in Wilfert et al. 2018 (Figure S3.4). The distribution of their data is broader since they used data from several studies, several plants, and different analytical methods and fitting. Their study showed that the fraction of phosphorus present as vivianite increased linearly with the Fe/P ratio and seemed to reach a plateau at Fe/P>1.5, which is the ratio in pure vivianite, due to limited phosphorus availability. For lower Fe/P ratios, the absence of vivianite is likely related to the lower solubility product for iron sulfide. The data of Wilfert et al. 2018 would seem to suggest that a Fe/P ratio of around 0.2-0.4 would be needed before vivianite precipitation occurred (x value for y=0 in Figure S3.4). Our set of data suggests, however, that a value of 0.5-0.6 is required. We hypothesize that these discrepancies are mainly due to the strong influence of the S content in sludge, which needs to be consumed before any iron is available for vivianite precipitation. This suggests that a comparison of data from different WWTPs would only be possible if the quantity of S were taken into account.
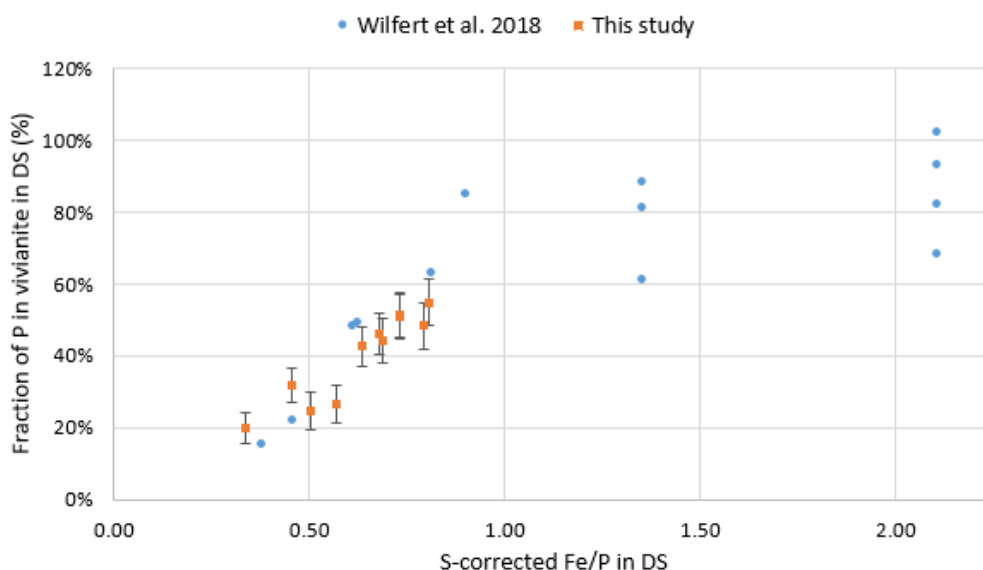


*Figure 3.4: Fraction of phosphorus in the solid phase of the digested sludge present as vivianite as a function of the S-corrected Fe/P molar ratio. Combined data from Wilfert et al. 2018 (6 different WWTPs) and the present study (calculation in Supplementary information). The S-corrected Fe/P ratio was calculated assuming that iron was first precipitating as FeS before vivianite. The data from Frossard et al. 1997 did not include S concentration, so they were not included.*

**3**

Accordingly, a S-corrected Fe/P ratio was calculated in our study, assuming that all the S was formed as FeS before vivianite. Even though $FeS_2$ is the most stable inorganic iron precipitate under anaerobic conditions (Pourbaix, 1963), pyritization is a slow process under digester conditions (Nielsen et al. 2005). Therefore, the meta-stable amorphous FeS could be a precursor to the formation of pyrite (Morse et al.1998, Dewil et al. 2009). This could explain why no trace of crystalline $FeS_x$ has been found in our samples by XRD.

The percentage of phosphorus in vivianite was plotted as a function of the S-corrected Fe/P, with data from both studies presenting less variation ($R^2$=0.86 for S-corrected Fe/P in Figure 3.4 and $R^2$=0.76 for uncorrected Fe/P in Figure S3.4). This suggests that the discrepancies observed were indeed related to the different sulphide content. The data for the S-corrected Fe/P ratio between 0 and 1 follow a linear trend (y=1.01x-0.21/$R^2$=0.86). This suggests that 100% of phosphorus will be present as vivianite for a S-corrected Fe/P ratio of 1.2, although the data with Fe/P>1 in Figure 3.4 contradict this presented. The proposed linear relation seems to be only valid for the low S-corrected Fe/P ratio (from 0 to 1, the authors suggest). This is due to the fact that a fraction of the phosphorus could be organically bound or precipitated with calcium or as struvite. The intercept with the X-axis indicates that a S-corrected Fe/P ratio of 0.2 is needed before the formation of vivianite. This suggests not only that S competes for iron, but another form also depletes iron before it can be available for vivianite precipitation. This part of the iron could be present as amorphous iron oxides/hydroxide (no crystalline FeO detected with XRD) and/or bound to humic substances (Abros'kina et al. 2016, Lovley et al. 1999).

Thermodynamic modeling suggests that vivianite, FeS, and iron oxides can form in the conditions of the Nieuwveer WWTP (Table S3.8). Strengite is often mentioned as one of the possible Iron phosphate minerals in wastewater and could form according to our modeling results. However, no trace of it has been found by XRD or Mössbauer spectroscopy. Visual Minteq does not consider some parameters (such as kinetics and activation energy) in its model, which can explain the discrepancies between the prediction and reality. For example, it is common that a mineral kinetically favored forms over a mineral thermodynamically favored (Brown et al. 1985). This could explain why strengite has never been found in previous studies within our group (Wilfert et al. 2015, 2018, Wang et al. 2019).

These observations lead to an important conclusion for WWTPs aiming to recover phosphorus via vivianite: the iron dosage needs to be adapted according to the sulphur content present in the sludge. More specifically, iron should be dosed in a molar ratio of 1:1 compared to the S in DS before any vivianite can be found in DS. This extra iron dosing required is not a waste as it will also help control $H_2S$ emission (see 3.3.5). In most cases, sulphide would have already been bound by iron; therefore, no extra iron is needed to compensate for S if one wants to increase the vivianite content.

### 3.3.4. There is evidence that different types of vivianite are formed

Several results from the current study suggest different kinds of vivianite formed in the WWTP at Nieuwveer. This finding is important since these vivianite species could have different properties, directly impacting their magnetic recovery. Different degrees of oxidation and impurity inclusion could lead to different types of vivianite. Indeed, vivianite can easily

be oxidized by light and oxygen (Čermáková et al. 2013, McCammon et al. 1980), and iron atoms in its structure can be replaced by other cations (Rothe et al. 2016, Seitz et al. 1973). Oxidation of vivianite and substitution of iron by a non-magnetic cation ($Mg^{2+}$, $Ca^{2+}$) modify the structure of vivianite (transition from crystalline to amorphous) and could impact its magnetic properties. Mössbauer results suggest that not all the vivianite formed in Nieuwveer is identical but do not allow a clear conclusion to be drawn about their characteristics (detailed discussion in Supplementary information).

In their study, Wilfert et al. 2018 used standard addition with XRD to quantify vivianite in DS as the XRD signal should be proportional to the quantity of vivianite. However, in the current study, the XRD signal stays relatively constant (Table S3.15) despite increased vivianite content in sludge. This result is surprising and suggests that the newly formed vivianite is different. As XRD can not detect it, this other vivianite could be smaller or amorphous.
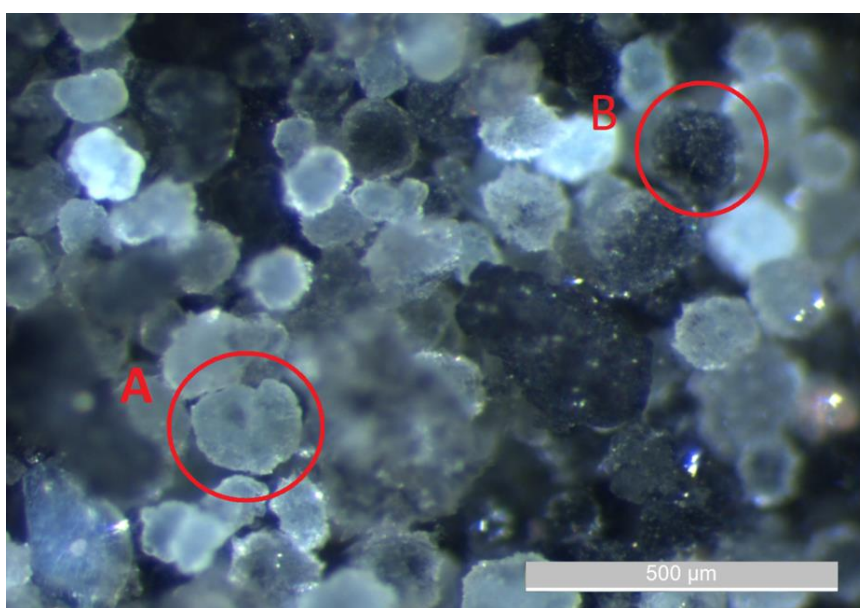


*Figure 3.5: Light-microscope picture of the vivianite extracted from the digested sludge from Nieuwveer with minimum oxygen and light exposure. This sample was magnetically separated at our pilot installation. Particle A: the light blue color suggests a small oxidation degree (these particles turned dark blue after more prolonged oxygen exposure). Particle B: the dark blue color suggests a high degree of oxidation.*

Light-microscope pictures of vivianite extracted from the DS at Nieuwveer showed that not all the vivianite particles are identical. A color gradient can be observed in Figure 3.5 and hints that some particles are more oxidized than others. Colorless when non-oxidized, vivianite becomes bluer with a higher degree of oxidation (Zelibor et al. 1988, Ogorodova et al. 2017). The oxidation of vivianite is accompanied by the departure of a proton from the vivianite structure, destabilizing its crystalline matrix. However, due to the anaerobic conditions in the digester, it is unlikely that vivianite oxidizes in this environment. It is possible that the dark blue crystals formed in the early stages of the WWTP and were oxidized in the aerated zones. Wilfert et al. 2018 already observed vivianite formation before digestion

in several WWTPs. Vivianite was also found in Nieuwveer in the B-stage and mixed sludge (Table S3.2). Almost all the soluble iron in the A-stage was $Fe^{2+}$, giving favorable conditions for vivianite formation (SI~3) (Table S3.8). In the B-stage, the concentration of $Fe^{2+}$ was low (~0.2 ppm), creating a barely saturated environment for vivianite formation (SI around 0). This suggests that the vivianite identified in the B sludge either forms in the A-stage and is transported to the B-stage afterward or forms slowly in the B-stage. This early formed vivianite will have been in oxidative conditions for enough time to be oxidized (SRT for B-stage: 16 days in Nieuwveer).

To summarize, there is clear evidence that different types of vivianite formed in Nieuwveer, but we could not identify their characteristics with certainty. From the results, we hypothesize that some vivianite forms early in the WWTP and has different characteristics (oxidation level, crystallinity) than the vivianite forming under anaerobic conditions in the digester. It is crucial to further study these vivianite species and their properties since they may influence their magnetic recovery.

### 3.3.5. Impact of increased iron dosing on the functioning of the WWTP

While increasing iron dosing favors vivianite formation, which is significant in terms of phosphorus recovery, this should no happen to the detriment of the global functioning of the WWTP. In this regard, the following integral parameters of the Nieuwveer WWTP were monitored: phosphorus in the effluent, $H_2S$ in the biogas, nitrogen removal, biogas production, COD removal, and dewaterability of the sludge. Since WWTPs are influenced by seasonal effects, the comparison was made to years with standard iron dosing, but for the same time period (period II: 01/01 to 30/04 as in Figure 3.1).
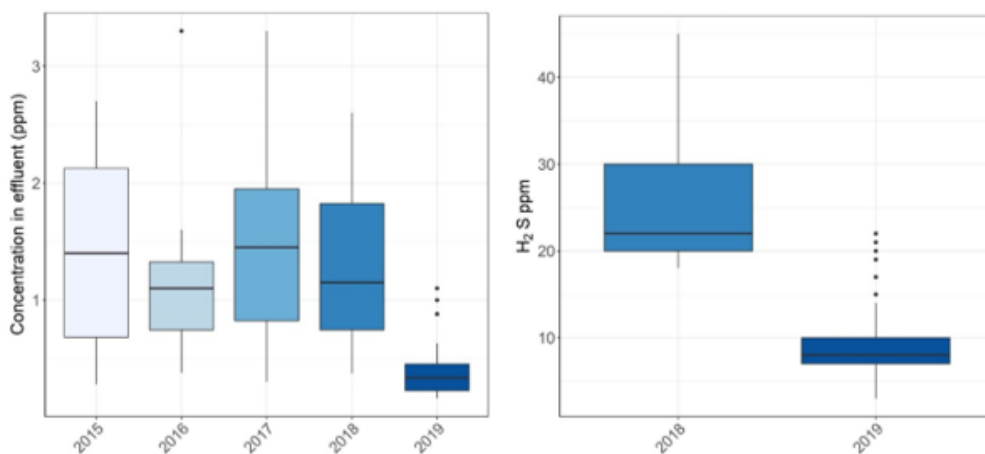


*Figure 3.6: Data for the Nieuwveer WWTP comparing the time with standard iron dosing (2015-2018) to the time with doubled iron dosing (2019) in January-April. Left: Phosphorus in the effluent. Right: $H_2S$ in the biogas (the position of the detector was changed in 2017, so the comparison is only possible for 2018 and 2019).*

First of all, total phosphorus concentrations in the effluent decreased after increasing the iron dosing. Figure 3.6 shows that it was reduced to an average of 0.42 mg/L during high iron dosing, compared to an average of 1.28 mg P/L for the four previous years in the same period.

Iron is dosed in the first place to remove phosphorus, so this observation is not surprising. Due to this decrease, the WWTP at Nieuwveer would be able to discharge its effluent in a more sensitive body of water closer to the plant and to improve water availability for agriculture in the region. High iron dosing and subsequent recovery of phosphorus through vivianite is, therefore, a promising technology for areas where strict effluent limits are applied, such as in countries bordering the Baltic Sea where stringent requirements for effluent phosphorus concentration can only be achieved by metal salt dosing (Suresh Kumar et al. 2019).

The quantity of $H_2S$ in the biogas was reduced in Nieuwveer to an average of 8 ppm under higher iron dosing compared to 26 ppm under standard iron dosing (Figure 3.6). This is in accordance with the observation that iron can be used to reduce the $H_2S$ in the biogas by binding it as $FeS_x$ (Gutierrez et al. 2010, Mamais et al. 1994). Despite a clear decrease of $H_2S$ in the biogas, an increase of S in the solid fraction of the DS is not noticeable. A mass balance of the S in the digester showed that this $H_2S$ reduction in the biogas corresponds to only 246 g of S per day. It represents 0.08% of the daily S load in the DS, explaining why an increase in the solid S was not noticeable in our measurements (Table S3.10). As discussed above, $FeS_x$ forms preferentially over vivianite, so we expected the soluble S pool to be already depleted before the increased iron dosing. The observed $H_2S$ decrease goes against this thought but can be explained by thermodynamic: as more iron is dosed, there is more soluble iron in the DS. Thus, soluble S decreases to keep the solid-liquid equilibrium for $FeS_x(s)$ (confirmed by ICP-OES in Table S3.7). The chemical potential theory says that the liquid and the gas phase need to be in equilibrium, which can only be matched if S in the gas phase ($H_2S$) decreases as well.

The data showed no significant change in the nitrogen removal performance of the WWTP after the increased iron dosing (Table 3.1). Also, no change in $NH_3$ removal was observed. This does not necessarily mean that the increased iron dosing has not affected the nitrogen cycle. Some possible impact of iron dosing are:

- Higher iron dosing could improve flocculation in the A-stage, allowing less COD to go to the B-stage, impairing the Nitrogen removal if not enough COD is present to perform denitrification.
- Excessive iron dosing could also have the opposite effect by destabilizing the flocs, allowing more COD to go to the B-stage and improving denitrification. According to Bratby et al. 2016, a concentration of $Fe^{2+}$ in the range of 0.8-80ppm allows good flocculation. Our measurements indicate values in this range (10-20ppm) in the A-stage, indicating that destabilization of the flocs is unlikely.
- Another point to consider is that 10-25% of the nitrogen is organically bound and will be flocculated in the A-stage (Henze et al. 2008), reducing the required COD in the B-stage.

In short, the nitrogen cycle could be affected in several contradictory ways by iron dosing, not leading to any significant difference. More detailed measurements would be necessary to obtain a more precise answer, but this was not the main objective of the current study.

*Table 3.1: Integral parameter of the WWTP Nieuwveer with standard iron dosing and increased iron dosing. The values presented are the average of January to April for 2015-2018 (standard iron dosing) and 2019 (increased iron dosing). Detailed comparisons are presented in Figure S3.7 for COD removal, N removal, Biogas production, and dewaterability. Daily measurments for H2S, COD and biogas. Weekly measurments for P and N. Monthly measurments for dewaterbaility.*

| Integral parameter | Unit | With standard iron dosing | With increased iron dosing |
|---|---|---|---|
| P in effluent | ppm | 1.28 | 0.42 |
| $H_2S$ in biogas | ppm | 26 | 8 |
| COD removal | % | 91.7 | 93 |
| N removal | % | 71.2 | 74 |
| Biogas production | $m^3$/kg dry solid | 442 | 418 |
| Dewaterability | kg PE/g of TS | 21.6 | 21.8 |

During increased iron dosing, COD removal was slightly improved from 91.7% to 93.0% (Table 3.1). The $Fe^{2+}$ dosed is oxidized in the A-stage to remove COD, as is commonly the case. However, 20-50% of the iron that arrives at the B-stage is still $Fe^{2+}$, and this suggests that the oxidation of the Fe(II) in the A-stage is not optimal (Table S3.6). $Fe^{2+}$ is a less strong coagulant than $Fe^{3+}$ due to its lower charge. Improved COD removal could still be possible if $Fe^{3+}$ were used in the A-stage or the oxidation of the $Fe^{2+}$ was improved. The water authority Brabantse Delta doses $Fe^{2+}$ salts in Nieuwveer because it is cheap and not to promote vivianite formation.

The higher iron dosing did not have a significant impact on biogas production (Table 3.1). No increase of A sludge production nor COD removal (~50%) in the A-stage was noticed despite more iron dosed, explaining why the biogas production did not increase. Moreover, the iron content jumped from 40 mg/g of TS for the 2015-2018 period (considered equal to the 04/12/2018 measurement) to an average of 65 mg/g for 2019 (Figure 3.2). This increase reduces the "digestible" content per tons of dry solid by 2-3%, contributing to less biogas production per dry weight of sludge.

Because the dewatered digested sludge is transported before incineration, the sludge volume needs to be minimized to reduce transportation costs. According to the results in Table 3.1, increased iron dosing had no measurable effect on the dewaterability of the digested sludge. The percentage of dry matter after dewatering of the digested sludge is comparable to other years, and the same quantity of polymer was used to achieve this dry matter content. However, no specific actions were taken to optimize the sludge dewatering during this test. Higher iron dosing slightly decreases the VSS in the sludge as it will increase the inorganic content of the sludge (more vivianite formed). The magnetic extraction of the formed vivianite reduces the inorganic content, leading to a higher VSS fraction, thus increasing the heating value of the sludge after dewatering.

In short, higher iron dosing did not appear to have any negative impact on the functioning of the WWTP in terms of N removal, dewaterability, biogas production, and COD removal (the latter showing slight improvement). On the contrary, it considerably reduced the phosphorus level in the effluent and the $H_2S$ content in the biogas.

### 3.3.6. Future perspectives for phosphorus recovery by magnetic extraction of vivianite

The magnetic extraction of vivianite from DS is possible (Chapter 2), and pilot plant tests for magnetic recovery were taking place in parallel to this study. This study confirmed that increasing iron dosing increases the share of phosphorus as vivianite and, thus, the share of recoverable phosphorus. According to Wilfert et al. 2018, neither the type of iron salt used nor the type of installation influences the quantity of phosphorus present as vivianite after digestion, suggesting that dosing will mainly depend on local aspects. A uniform guideline for practical implementation of higher iron dosing needs not to be given. The quantity of iron dosed should be adapted to the objective of the water authority in terms of phosphorus level in the effluent, $H_2S$ control, and vivianite production. WWTPs seeking to maximize phosphorus recovery as vivianite could aim at a S-corrected Fe/P ratio (see 3.3.3) in the digested sludge higher than 1.5 to convert more than 80% of the phosphorus into vivianite.

The cost increase associated with higher iron dosing is not negligible but can be offset by the savings in sludge disposal and better effluent quality. This is especially the case for countries with high sludge disposal costs where the land application of sludge is banned (e.g. The Netherlands). In the case of Nieuwveer, the increase in iron dosing was on average 366 kg Fe/day, corresponding to a cost of €304/day (based on a cost price of €0.83/kg for $FeSO_4 \cdot 7H_2O$ as paid by the WWTP). This WWTP produces 15 tons of dry solids per day with a disposal cost of around €277 per ton of dry solids (assuming 23% dry matter), leading to a daily cost of €4155 (SNB annual report 2018). Assuming that all the extra vivianite formed would be removed from the digested sludge, the amount of dry solid would be reduced by 10%, making a saving of €415 /day. Moreover, the oxygen required to oxidize the extra $Fe^{2+}$ dosed in the A-stage represents only 0.1% of the aeration necessary to treat the COD in Nieuwveer. As a result, no extra aeration costs are to be expected (Supplementary information).

In the case of WWTP Nieuwveer, 90% of the phosphorus present in the influent ended up in the sewage sludge at the higher iron dosage. These influent (~5 ppm) and effluent (~0.5 ppm) values are typical for sewage treatment plants in Northern Europe (Pons et al. 2004). The results of this study and Wilfert et al. 2018 indicate that if the iron dosage is adjusted to have a Fe/P molar ratio in digested sludge above 1.5, more than 80% of the phosphorus present in digested sludge can be present as vivianite. Our work on pilot scale magnetic separation of vivianite at Nieuwveer revealed that 70-80% of the vivianite in digested sludge could be recovered (unpublished results). Therefore, we expect that stimulation of vivianite formation combined with magnetic recovery from the sludge could recover 50-60% of the phosphorus present in the influent of the Nieuwveer sewage treatment plant. We believe that these results can be extrapolated for all WWTPs bearing an anaerobic digester.

In the future, vivianite recovery could be integrated with the dissolution of the vivianite by alkaline treatment (proof of principle in Chapter 2) to recover the phosphorus in any desired form and to enable the reuse of the iron in the next cycle of phosphate recovery at the WWTP. Also, vivianite extraction recovers the dosed iron and any iron that was present in the influent wastewater. This makes vivianite recovery of particular interest for WWTPs treating high-Fe

bearing industrial wastewater in areas with significant aerobic groundwater intrusion in the sewer network. In countries with strict effluent criteria, the iron dosage is already high (Fe/P ratio >1.5 is common). Therefore, the digested sludge from these types of plants is often suitable for direct vivianite recovery without additional iron dosing.

In addition to recovery of phosphorus and iron via an alkaline treatment, vivianite could be used as Fe-fertilizer for Fe-poor soils (Rombolà et al. 2007). Several high-value applications of vivianite could also be considered depending on its purity after separation. Using vivianite as a component in lithium-ion batteries or to create pigments are two such high-value possibilities (Recham et al. 2009, Čermáková et al. 2013).

## 3.4. Conclusion

The share of phosphorus present as vivianite in digested sludge could be increased from 20% to 50% by dosing more iron in the Nieuwveer WWTP, confirming our earlier hypothesis that high iron content in the sludge has a direct relation to a higher vivianite content (Wilfert et al. 2018). More importantly, all the additional iron that was dosed was used to produce vivianite quickly. This is an important finding as it suggests a way to efficiently increase phosphorus recovery potential via vivianite, for instance, via magnetic separation from digested sludge. Our analyses suggest that different types of vivianite mineral coexist in digested sludge. Further studies need to be carried out to characterize these minerals, as they could have implications for recovery methods for the vivianite (for instance, they may influence the magnetic properties of vivianite) and possible uses of the recovered vivianite.

A thorough study of the WWTP global parameters revealed that the increased iron dosing did not affect the functioning of the WWTP. Moreover, it effectively reduced the concentration of $H_2S$ in the biogas from 26 to 8 ppm, and more importantly, reduced the phosphorus in the effluent of the WWTP from 1.3 ppm to 0.4 ppm. This indicates that, especially if very low effluent phosphate is required, a combination of high iron dosing with vivianite recovery is a promising solution to recover phosphorus from DS.

## Acknowledgments

## References

Abros'kina, D.P., Fuentesb M., Garcia-Minab J.M., Klyainc O.I., Senikd S.V., Volkova D.S., Perminovaa I.V., and Kulikovaa N.A. (2016). The Effect of Humic Acids and Their Complexes with Iron on the Functional Status of Plants Grown under Iron Deficiency. *Eurasian Soil Science*, 49(10), 1099–1108.

Al-Borno, A., & Tomson, M. B. (1994). The temperature dependence of the solubility product constant of vivianite. *Geochimica et Cosmochimica Acta*, 58(24), 5373–5378.

Bratby, J. (2016). Coagulation and Flocculation in Water and Wastewater Treatment – Third Edition

Brown, M. E., Buchanan, K. J., and Goosen, A. (1985). Thermodynamically and kinetically controlled products. *Journal of Chemical Education,* 62(7), 575

Čermáková. Z., Švarcová. S., Hradil. D., Bezdicka. P. (2013). Vivianite: A historic blue pigment and its degradation under scrutiny. *Science and Technology for the Conservation of Cultural Heritage,* 75-78.

Childers, D., Corman, J., Edwards, M., Elser, J. (2011). Sustainability Challenges of Phosphorus and Food: Solutions from Closing the Human Phosphorus Cycle. *BioScience*, 61(2), 117–124.

Cordell, D., White, S. B. (2015). Tracking phosphorus security: Indicators of phosphorus vulnerability in the global food system. *Food Security*, 7(2).

Cornel, P., Schaum, C. (2009). Phosphorus recovery from wastewater: needs, technologies and costs. *Water Science and Technology*, 59(6), 1069− 1076.

Desmidt, E., Ghyselbrecht, K., Zhang, Y., Pinoy, L., Van der Bruggen, Bart, Verstraete, W., Rabaey, K., Meesschaert, B. (2015). Global Phosphorus Scarcity and Full-Scale P-Recovery Techniques: A Review. *Crit. Rev. Environ. Sci. Technol.*, 45(4), 336−384.

Dewil, R., Baeyens, J., Roels, J., Van de Steene, B. (2009). Evolution of the Total Sulphur Content in Full-Scale Wastewater Sludge Treatment. Environmental Engineering Science, 26(4).

European Sustainable Phosphorus Platform (2019). Report from of the "ESPP waste water phosphorus removal workshop" from November 2019 host by the University of Liège.

Frossard, E., Bauer, J.P., Lothe, F. (1997). Evidence of vivianite in FeSO4-flocculated sludges. *Water research*, 31(10), 2449–2454.

Gutierrez, O.; Park, D.; Sharma, K. R.; Yuan, Z. (2010). Iron salts dosage for sulfide control in sewers induces chemical phosphorus removal during wastewater treatment. *Water Research*, 44(11), 3467−3475.

Henze. M., Van Loosdrecht, M.C.M., Ekama, G.A., Brdjanovic, D. (2008). Biological Wastewater treatment: Principles, Modeling and design.

Klencsar, Z. (1997) Mössbauer spectrum analysis by evolution algorithm. *Nucl. Instrum. Methods Phys. Res. Sect. B Beam Interact. Mater. Atoms* 129 (4), 527-533.

**3**

Li, J. Effects of Fe(III) on floc characteristics of activated sludge. (2005) *J. Chem. Technol. Biotechnol.*, 80(3), 313−319

Liu, J., Cheng, X., Qi, X., Li, N., Tian, J., Qiu, B., Xu, K. Qu, D. (2018). Recovery of phosphate from aqueous solutions via vivianite crystallization : Thermodynamics and influence of pH. *Chemical Engineering Journal*, 349, 37–46.

Lovley, D.R. and Blunt-Harris, E.L. (1999). Role of Humic-Bound Iron as an Electron Transfer Agent in Dissimilatory Fe(III) Reduction, *Appl. Environ. Microbiol*. 65(9), 4252–4254.

Mamais, D., Pitt, P. A., Cheng, Y. W. (1994). Determination of ferric chloride dose to control struvite precipitation in anaerobic sludge digesters, Water Environmental Research 66(7), 912–918.

Manning, P. G., Murphy, T. P., & Prepas, E. E. (1991). Intensive formation of vivianite in the bottom sediments of mesotrophic Narrow Lake, Alberta. *Canadian Mineralogist*, 29, 77–85.

McCammon, C. A., & Burns, R. G. (1980). The oxidation mechanism of vivianite as studied by Mossbauer spectroscopy. *American Mineralogist*, 65(3-4), 361-366.

Mersmann, A. (2001). Crystallization Technology Handbook. Second Edition Revised and Expanded.

Mori, H., & Ito, T. (1950). The structure of vivianite and symplesite. *Acta Crystallographica*, 3(1), 1-6.

Morse, G.K., Brett, S.W., Guy, J.A., Lester, J.N. (1998). Review: Phosphorus removal and recovery technologies. *Science of the total environment*, 212(1), 69-81.

Nembrini, G.P., Capobianco J.A., Viel, M., Williams A.F. (1983). A Mössbauer and chemical study of the formation of vivianite sediments of Lago Maggiore (Italy). *Geochimica et Cosmochimica Acta*, 47(8), 1459-1464.

Nielsen, A.H., Lens, P., Vollertsen, J., Hvitved-Jacobsen, T. (2005). Sulphide-iron interactions in domestic wastewater from a gravity sewer. *Water Research*, 39(12), 2747-2755.

Nriagu, J. O. (1972). Stability of vivianite and ion-pair formation in the system $Fe_3(PO_4)_2$-$H_3PO_4H_3PO_4$-$H_2O$. *Geochimica et Cosmochimica Acta*, 36(4), 459-470.

Nriagu, J. O., & Dell, C. I. (1974). Diagenetic Formation of lron Phosphates in Recent Lake Sediments. *American Mineralogist*, 59, 934-946.

Ogorodova, L., Vigasina, M., Mel'chakova, L., Rusakov, V., Kosova, D., Ksenofontov, D., & Bryzgalov, I. (2017). Enthalpy of formation of natural hydrous iron phosphate: Vivianite. *Journal of Chemical Thermodynamics*, 110, 193-200.

Ohtake, H., Tsunade, S. (2019). Chapter 1: Development of Phosphorus recycling in Europe and Japan. *Phosphorus Recovery and Recycling*. 3-27

Pourbaix, M. (1963) Atlas of Electrochemical Equilibria. Gauthier-Villars, Paris.

Pons, M.N., Spanjers, H., Baetens, D., Nowak, O., Gillot, S., Nouwen, J., Schuttinga, N. (2004). Wastewater characteristics in Europe – A survey. *European Water Management Online.*

Prot, T., Nguyen, V.H., Wilfert, P., Dugulan, A.I., Goubitz, K., De Ridder, D.J., Korving, L., Rem, P., Bouderbala, A., Witkamp, G.J., Van Loosdrecht, M.C.M (2019). Magnetic separation and characterization of vivianite from digested sewage sludge. *Separation and Purification* (224)

Rasmussen, H., Nielsen, P., 1996. Iron reduction in activated sludge measured with different extraction techniques. *Water Research* 30 (3), 551-558

Recham, N., Armand, M., Laffont, L., Tarascon, J.-M., 2009. Eco-Efficient Synthesis of LiFePO4 with Different Morphologies for Li-Ion Batteries. *Electrochem. Solid-State Lett.* 12 (2), A39.

Rombolà, A. D., Toselli, M., Carpintero, J., Quartieri, M., Torrent, J., Marangoni, B. (2007). Prevention of Iron - Deficiency Induced Chlorosis in Kiwifruit (Actinidia deliciosa) Through Soil Application of Synthetic Vivianite in a Calcareous Soil, *Journal of plant nutrition*, 26(10-11), 2031-2041.

Rothe, M., Kleeberg, A., & Hupfer, M. (2016). The occurrence, identification and environmental relevance of vivianite in waterlogged soils and aquatic sediments. *Earth-Science Reviews*, 158, 51-64

Rouzies, D., & Millet, J. M. M. (1993). Mossbauer Study of Synthetic Oxidized Vivianite at Room-Temperature. *Hyperfine Interaction,* 77(1-2), 19-28.

Rosenqvist I.T., Formation of vivianite in Holocene clay sediments, *Lithos* 3 (1970) 327-334.

Seitz, A., Riedner, J., Malhotra, K., Kipp, J. (1973). Iron-Phosphate Compound Identification in Sewage Sludge Residue. *Environmental Science and Technology*, 7(4), 354-357.

SNB Annual report (2018). N.V. Slibverwerking Noord-Brabant.

Suresh Kumar, P., Korving, L., Van Loosdrecht, M. C. M., Witkamp G.J. (2019). Adsorption as a technology to achieve ultra-low concentrations of phosphate: Research gaps and economic analysis, *Water Research X*, 4.

Viollier, E., Inglett, P.W., Hunter, K., Roychoudhury, A.N., van Cappellen, P. (2000). The ferrozine method revisited: Fe(II)/Fe(III) determination in natural waters. *Appl. Geochem.* 15 (6), 785-790.

Wang, R., Wilfert, P., Dugulan, I., Goubitz, K., Korving, L., Witkamp, G. J., Van Loosdrecht M.C.M. (2019). Fe(III) reduction and vivianite formation in activated sludge, Separation Purification Technology, 220, 126-135.

Wilfert, P., Kumar, P. S., Korving, L., Witkamp G.J., Van Loosdrecht, M. C. M. (2015). The relevance of Phosphorus and iron chemistry to the recovery of phosphorus from wastewater. *Environmental Science and Technology,* 49(16).

Wilfert, P., Mandalidis, A., Dugulan, A. I., Goubitz, K., Korving, L., Temmink, H., Witkamp G.J., Van Loosdrecht, M. C. M. (2016). Vivianite as an important iron phosphate precipitate in sewage treatment plants. *Water Research,* 104, 449-460

Wilfert, P., Korving, L., Dugulan, I., Goubitz K., Witkamp, G. J., Van Loosdrecht M.C.M. (2018). Vivianite as the main phosphate mineral in digested sewage sludge and its role for phosphate recovery. *Water Research,* 144, 312-321

Zelibor, J. L., Senftle, F. E., & Reinhardt, J. L. (1988). A proposed mechanism for the formation of spherical vivianite crystal aggregates in sediments. *Sedimentary Geology,* 59(1-2), 125-142.
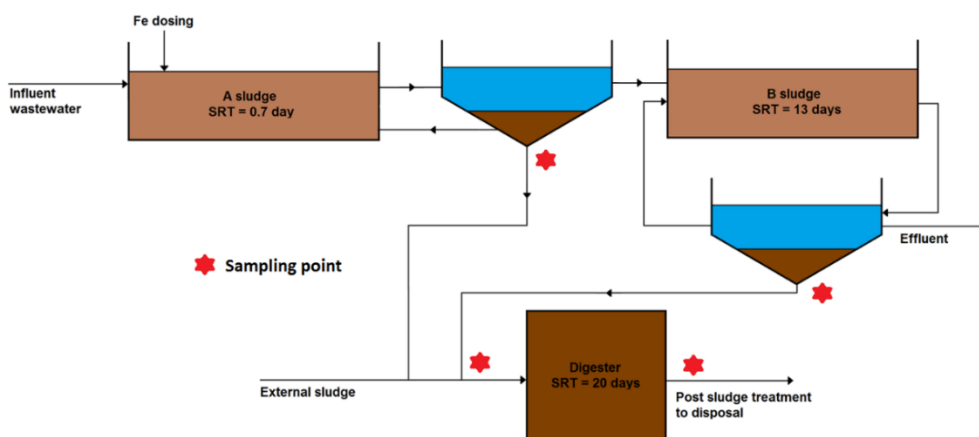
## Supplementary information



*Figure S3.1: Simplified flowchart of the WWTP Nieuwveer and sampling points*

*Table S3.1: Sampling dates of the WWTP Nieuwveer and corresponding iron dosing phase*

| Sample | 1 | 2 | 3 | 4 | 5 | 6 | 7 | 8 | 9 | 10 | 11 |
|---|---|---|---|---|---|---|---|---|---|---|---|
| Dosing phase | I | I | II | II | II | II | II | II | II | II | III |
| Date | 04/12 2018 | 19/12 2018 | 08/01 2019 | 22/01 2019 | 05/02 2019 | 19/02 2019 | 12/03 2019 | 02/04 2019 | 16/04 2019 | 30/04 2019 | 28/05 2019 |

**3**

Table S3.2: Mössbauer results for all solid samples from Nieuwveer studied. (DS=digested sludge, MS=mixed sludge, A=A-stage sludge, B=B-stage sludge). $Fe^{3+}/Fe^{II}$: $Fe^{3+}$ species other than vivianite and low-spin $Fe^{2+}$ compounds like pyrite. $Fe^{3+}$ (Viv. A+B): total $Fe^{3+}$ vivianite. $Fe^{2+}$ (Viv. A): $Fe^{2+}$ in the site A of vivianite. $Fe^{2+}$ (Viv. B): $Fe^{2+}$ in the site B of vivianite. The error on the spectral contribution is ±3%.

| Sample | Isomer Shift $(mm \cdot s^{-1})$ | Quadrupole Splitting $(mm \cdot s^{-1})$ | $\Gamma$ $(mm \cdot s^{-1})$ | Phase | Spectral contribution (%) |
|---|---|---|---|---|---|
| Synthetic vivianite | 0.46 | 0.63 | 0.52 | $Fe^{3+}$ (Viv. A+B) | 46 |
| | 1.17 | 2.48 | 0.37 | $Fe^{2+}$ (Viv. A) | 18 |
| | 1.22 | 2.99 | 0.37 | $Fe^{2+}$ (Viv. B) | 36 |
| DS1 | 0.31 | 0.82 | 0.55 | $Fe^{3+}/Fe^{II}$ | 59 |
| | 0.46 | 0.63 | 0.52 | $Fe^{3+}$ (Viv. A+B) | 13 |
| | 1.23 | 2.35 | 0.32 | $Fe^{2+}$ (Viv. A) | 16 |
| | 1.22 | 3.05 | 0.32 | $Fe^{2+}$ (Viv. B) | 12 |
| DS2 | 0.31 | 0.64 | 0.66 | $Fe^{3+}/Fe^{II}$ | 41 |
| | 0.46 | 0.63 | 0.52 | $Fe^{3+}$ (Viv. A+B) | 19 |
| | 1.22 | 2.43 | 0.33 | $Fe^{2+}$ (Viv. A) | 18 |
| | 1.25 | 2.97 | 0.33 | $Fe^{2+}$ (Viv. B) | 22 |
| DS3 | 0.31 | 0.41 | 0.62 | $Fe^{3+}/Fe^{II}$ | 54 |
| | 0.46 | 0.63 | 0.52 | $Fe^{3+}$ (Viv. A+B) | 12 |
| | 1.21 | 2.43 | 0.30 | $Fe^{2+}$ (Viv. A) | 18 |
| | 1.26 | 2.92 | 0.30 | $Fe^{2+}$ (Viv. B) | 16 |
| DS4 | 0.31 | 0.83 | 0.57 | $Fe^{3+}/Fe^{II}$ | 31 |
| | 0.46 | 0.63 | 0.52 | $Fe^{3+}$ (Viv. A+B) | 23 |
| | 1.22 | 2.42 | 0.33 | $Fe^{2+}$ (Viv. A) | 20 |
| | 1.24 | 2.97 | 0.33 | $Fe^{2+}$ (Viv. B) | 26 |
| DS5 | 0.31 | 0.56 | 0.72 | $Fe^{3+}/Fe^{II}$ | 34 |
| | 0.46 | 0.63 | 0.52 | $Fe^{3+}$ (Viv. A+B) | 24 |
| | 1.20 | 2.45 | 0.32 | $Fe^{2+}$ (Viv. A) | 17 |
| | 1.25 | 2.97 | 0.32 | $Fe^{2+}$ (Viv. B) | 25 |
| DS6 | 0.31 | 0.89 | 0.53 | $Fe^{3+}/Fe^{II}$ | 25 |
| | 0.46 | 0.63 | 0.52 | $Fe^{3+}$ (Viv. A+B) | 26 |
| | 1.21 | 2.42 | 0.34 | $Fe^{2+}$ (Viv. A) | 21 |
| | 1.24 | 2.96 | 0.34 | $Fe^{2+}$ (Viv. B) | 28 |

*Table S3.2: continued*

**3**

| Sample | Isomer Shift (mm·s$^{-1}$) | Quadrupole Splitting (mm·s$^{-1}$) | $\Gamma$ (mm·s$^{-1}$) | Phase | Spectral contribution (%) |
|---|---|---|---|---|---|
| DS7 | 0.31 | 0.86 | 0.56 | $Fe^{3+}/Fe^{II}$ | 28 |
|  | 0.46 | 0.63 | 0.52 | $Fe^{3+}$ (Viv. A+B) | 24 |
|  | 1.22 | 2.41 | 0.34 | $Fe^{2+}$ (Viv. A) | 19 |
|  | 1.24 | 2.95 | 0.34 | $Fe^{2+}$ (Viv. B) | 29 |
| DS8 | 0.31 | 0.89 | 0.59 | $Fe^{3+}/Fe^{II}$ | 32 |
|  | 0.46 | 0.63 | 0.52 | $Fe^{3+}$ (Viv. A+B) | 23 |
|  | 1.23 | 2.43 | 0.33 | $Fe^{2+}$ (Viv. A) | 19 |
|  | 1.25 | 2.97 | 0.33 | $Fe^{2+}$ (Viv. B) | 26 |
| DS9 | 0.31 | 0.85 | 0.57 | $Fe^{3+}/Fe^{II}$ | 24 |
|  | 0.46 | 0.63 | 0.52 | $Fe^{3+}$ (Viv. A+B) | 23 |
|  | 1.20 | 2.42 | 0.33 | $Fe^{2+}$ (Viv. A) | 22 |
|  | 1.23 | 2.92 | 0.33 | $Fe^{2+}$ (Viv. B) | 31 |
| DS10 | 0.31 | 0.80 | 0.55 | $Fe^{3+}/Fe^{II}$ | 26 |
|  | 0.46 | 0.63 | 0.52 | $Fe^{3+}$ (Viv. A+B) | 21 |
|  | 1.20 | 2.41 | 0.35 | $Fe^{2+}$ (Viv. A) | 22 |
|  | 1.23 | 2.93 | 0.35 | $Fe^{2+}$ (Viv. B) | 31 |
| DS11 | 0.31 | 0.86 | 0.59 | $Fe^{3+}/Fe^{II}$ | 59 |
|  | 0.46 | 0.63 | 0.52 | $Fe^{3+}$ (Viv. A+B) | 13 |
|  | 1.23 | 2.34 | 0.34 | $Fe^{2+}$ (Viv. A) | 15 |
|  | 1.26 | 2.93 | 0.34 | $Fe^{2+}$ (Viv. B) | 14 |
| MS2 | 0.31 | 0.61 | 0.67 | $Fe^{3+}/Fe^{II}$ | 51 |
|  | 0.46 | 0.63 | 0.52 | $Fe^{3+}$ (Viv. A+B) | 16 |
|  | 1.24 | 2.40 | 0.31 | $Fe^{2+}$ (Viv. A) | 14 |
|  | 1.26 | 2.92 | 0.31 | $Fe^{2+}$ (Viv. B) | 19 |
| MS6 | 0.31 | 0.41 | 0.59 | $Fe^{3+}/Fe^{II}$ | 76 |
|  | 0.46 | 0.63 | 0.52 | $Fe^{3+}$ (Viv. A+B) | 8 |
|  | 1.24 | 2.33 | 0.34 | $Fe^{2+}$ (Viv. A) | 7 |
|  | 1.26 | 2.89 | 0.34 | $Fe^{2+}$ (Viv. B) | 9 |
| A11 | 0.34 | 0.60 | 0.64 | $Fe^{3+}/Fe^{II}$ | 84 |
|  | 1.35 | 2.57 | 0.40 | $Fe^{2+}$ | 16 |
| B11 | 0.31 | 0.65 | 0.68 | $Fe^{3+}/Fe^{II}$ | 72 |
|  | 1.20 | 2.21 | 0.40 | $Fe^{2+}$ (Viv. A) | 9 |
|  | 1.25 | 2.82 | 0.40 | $Fe^{2+}$ (Viv. B) | 19 |

**3**

In the following Mössbauer spectra, the colored curves represent the following:

- Black: total spectrum
- Red: $Fe^{2+}$ in vivianite site A
- Blue: $Fe^{2+}$ in vivianite site B
- Pink: $Fe^{3+}$ in vivianite A+B
- Green: $Fe^{3+}/Fe^{II}$ for $Fe^{3+}$ compound excluding vivianite and low-spin $Fe^{2+}$ like pyrite
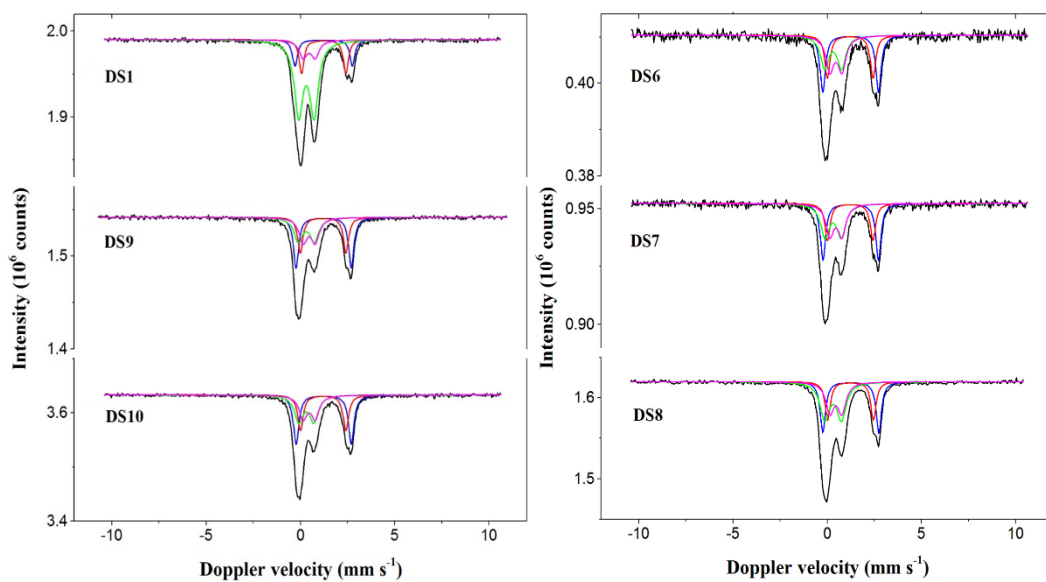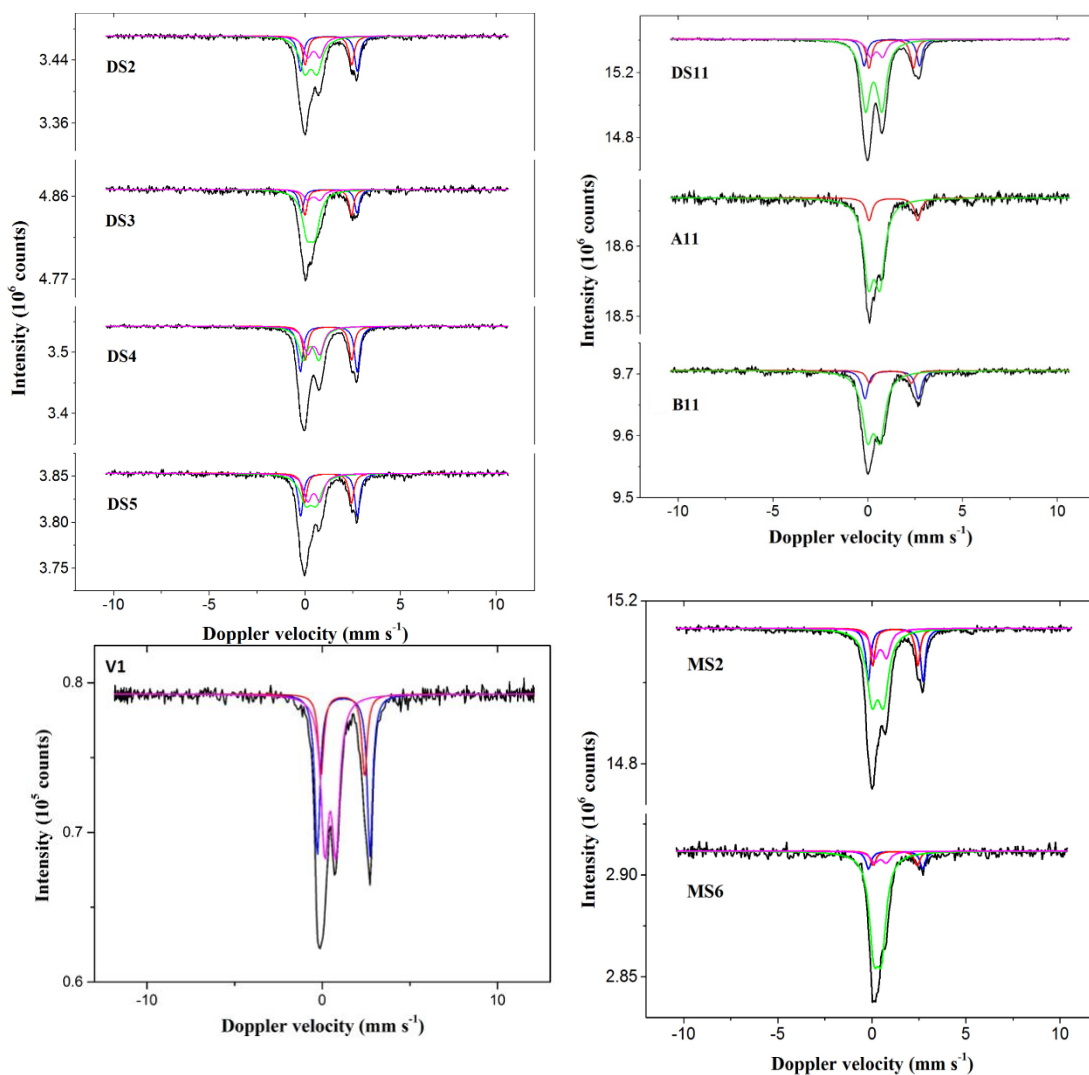
*Figure S3.2: Mössbauer spectra for all the DS samples, synthetic vivianite (V1), A11, B11, MS2 and MS6*
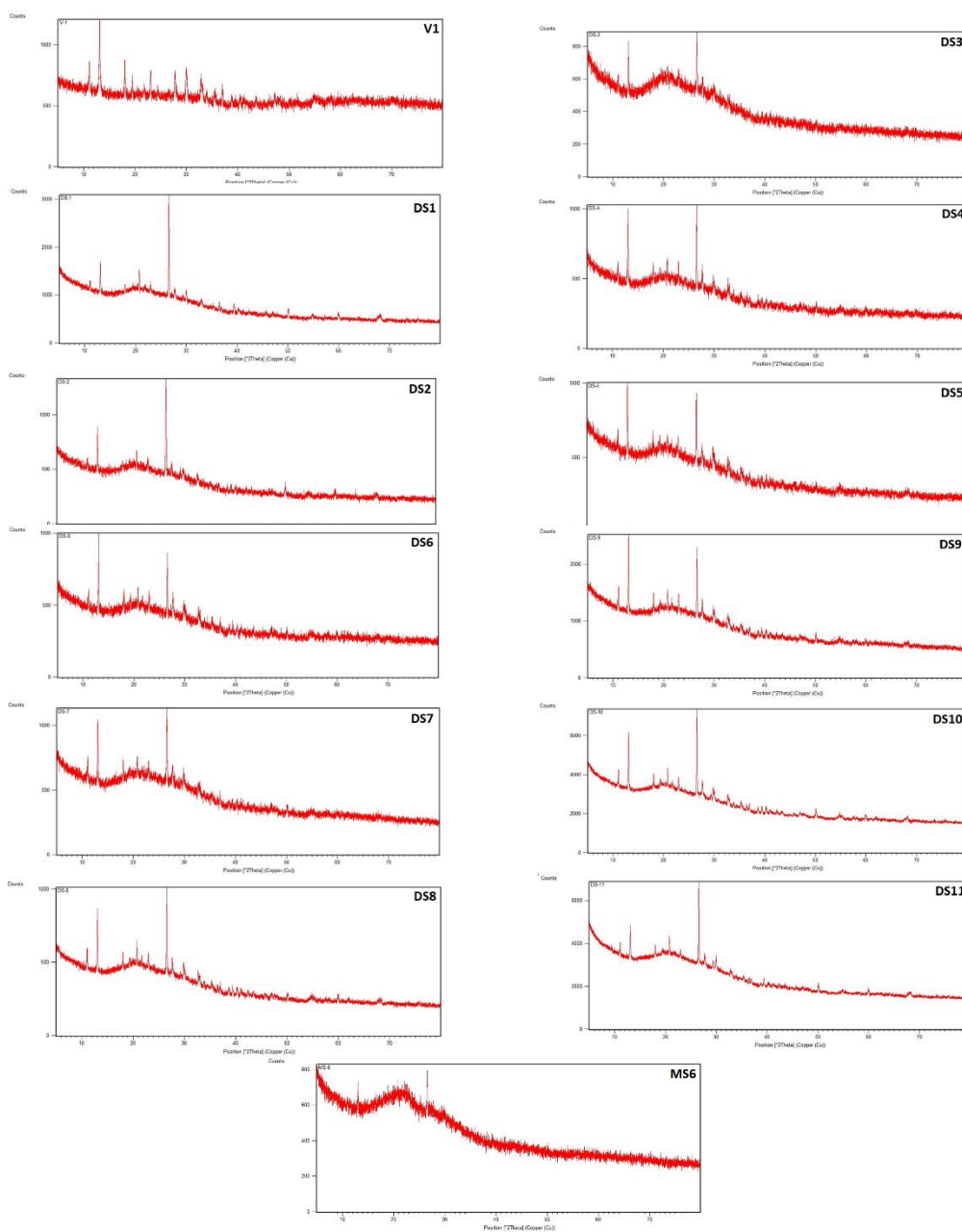
**3**



*Figure S3.3: XRD spectra for all the DS samples, synthetic vivianite (V1) and MS6*

*Table S3.3: Solid composition of the sludge A, B and digested measured by ICP-OES*

| Sludge sample | | Fe (mg/g TS) | P (mg/g TS) | S (mg/g TS) | Ca (mg/g TS) | Mg (mg/g TS) |
|---|---|---|---|---|---|---|
| 4-12-2018 | DS1 | 41 | 31 | 12 | 29 | 3,5 |
| 19-12-2018 | DS2 | 46 | 32 | 12 | 27 | 3,5 |
| 8-1-2019 | DS3 | 53 | 34 | 10 | 26 | 3,9 |
| 22-1-2019 | DS4 | 62 | 37 | 11 | 28 | 3,6 |
| 5-2-2019 | DS5 | 59 | 32 | 11 | 25 | 2,9 |
| 19-2-2019 | DS6 | 64 | 34 | 11 | 27 | 3,1 |
| 12-3-2019 | DS7 | 63 | 37 | 11 | 25 | 2,9 |
| 2-4-2019 | DS8 | 69 | 36 | 10 | 24 | 3,1 |
| 16-4-2019 | DS9 | 71 | 36 | 10 | 27 | 3,2 |
| 30-4-2019 | DS10 | 67 | 36 | 11 | 28 | 3,2 |
| 28-5-2019 | DS11 | 56 | 35 | 14 | 31 | 3,6 |
| 4-12-2018 | A1 | 22 | 16 | 7 | 19 | 2,3 |
| 19-12-2018 | A2 | 38 | 22 | 8 | 19 | 1,8 |
| 8-1-2019 | A3 | 34 | 18 | 6 | 16 | 1,3 |
| 22-1-2019 | A4 | 61 | 27 | 7 | 20 | 1,7 |
| 5-2-2019 | A5 | 49 | 22 | 6 | 15 | 1,4 |
| 19-2-2019 | A6 | 51 | 25 | 7 | 17 | 1,7 |
| 12-3-2019 | A7 | 41 | 19 | 6 | 11 | 1,4 |
| 2-4-2019 | A8 | 34 | 19 | 9 | 18 | 1,7 |
| 16-4-2019 | A9 | 46 | 23 | 7 | 19 | 1,6 |
| 30-4-2019 | A10 | 30 | 17 | 11 | 17 | 1,7 |
| 28-5-2019 | A11 | 25 | 15 | 11 | 20 | 1,7 |
| 4-12-2018 | B1 | 28 | 26 | 9 | 20 | 3,5 |
| 19-12-2018 | B2 | 29 | 24 | 8 | 16 | 2,6 |
| 8-1-2019 | B3 | 32 | 24 | 8 | 17 | 2,3 |
| 22-1-2019 | B4 | 36 | 25 | 8 | 16 | 2,4 |
| 5-2-2019 | B5 | 33 | 22 | 8 | 13 | 2,0 |
| 19-2-2019 | B6 | 38 | 23 | 8 | 15 | 2,2 |
| 12-3-2019 | B7 | 37 | 22 | 7 | 13 | 2,0 |
| 2-4-2019 | B8 | 44 | 24 | 7 | 17 | 2,5 |
| 16-4-2019 | B9 | 34 | 24 | 8 | 16 | 2,5 |
| 30-4-2019 | B10 | 42 | 28 | 8 | 18 | 2,5 |
| 28-5-2019 | B11 | 40 | 30 | 8 | 23 | 2,6 |

**3**

*Table S3.4: pH of the A, B, MS and digested sludge sample of Nieuwveer*

| Date | A | B | DS | MS |
|------|-----|-----|-----|-----|
| 4-12-2018 | 5,9 | 6,5 | 7,5 | ND |
| 19-12-2018 | 6,5 | 6,9 | 7,5 | 5,0 |
| 8-1-2019 | 6,5 | 6,9 | 7,7 | 5,2 |
| 22-1-2019 | 6,9 | 6,9 | 8,1 | 3,7 |
| 5-2-2019 | 6,9 | 7,1 | 8,2 | 4,6 |
| 19-2-2019 | 6,6 | 6,8 | 7,8 | 3,9 |
| 12-3-2019 | 8,2 | 8,2 | 8,5 | 4,6 |
| 2-4-2019 | 6,5 | 6,9 | 8,5 | 5,1 |
| 16-4-2019 | 7,1 | 7,5 | 8,3 | 3,9 |
| 30-4-2019 | 6,2 | 6,8 | 8,0 | 4,4 |
| 28-5-2019 | 6,3 | 7,3 | 8,2 | 4,7 |

*Table S3.5: Solid content (%) of the sludge sample of Nieuwveer*

| Date | A | B | DS | MS |
|------|-----|-----|-----|-----|
| 4-12-2018 | 1,1 | 0,8 | 4,7 | 12,9 |
| 19-12-2018 | 0,7 | 0,6 | 3,9 | 9,2 |
| 8-1-2019 | 1,0 | 0,6 | 4,0 | 7,5 |
| 22-1-2019 | 0,7 | 0,6 | 4,0 | 2,9 |
| 5-2-2019 | 0,9 | 0,7 | 3,7 | 1,3 |
| 19-2-2019 | 0,6 | 0,5 | 4,4 | 0,8 |
| 12-3-2019 | 1,1 | 0,8 | 3,7 | 3,4 |
| 2-4-2019 | 1,1 | 0,6 | 4,1 | 2,6 |
| 16-4-2019 | 0,6 | 0,4 | 4,3 | 1.0 |
| 30-4-2019 | 0,7 | 0,6 | 4,3 | 0,9 |
| 28-5-2019 | 0,9 | 0,4 | 4,0 | 1,5 |

*Table S3.6: Iron speciation in sludge A, B and digested in Nieuwveer obtained by the ferrozine method*

| Sample | $Fe^{2+}$ (ppm) | $Fe^{3+}$ (ppm) | Total Fe (ppm) |
|--------|-----------------|-----------------|----------------|
| A1 | 9,6 | 1,1 | 10,7 |
| A2 | 12,1 | -0,5 | 11,5 |
| A3 | 10,2 | 2,8 | 13,0 |
| A4 | 12,0 | 1,2 | 13,2 |
| A5 | 14,6 | 2,1 | 16,7 |
| A6 | 14,1 | 3,1 | 17,2 |
| A7 | 49,3 | 8,5 | 57,8 |
| A8 | 16,5 | 3,0 | 17,7 |
| A9 | 5,8 | 3.0 | 7,9 |
| A10 | 12,1 | 2.0 | 14,1 |
| A11 | 14,1 | 4,7 | 18,8 |
| B1 | 3,0 | 0,4 | 3,4 |
| B2 | 0,1 | 0,1 | 0,2 |
| B3 | 0,2 | 0,1 | 0,3 |
| B4 | 0,1 | 0,9 | 1,0 |
| B5 | 0,7 | 0,3 | 1,0 |
| B6 | 0,1 | 0,6 | 0,8 |
| B7 | 1,5 | 0,9 | 2,4 |
| B8 | 0,1 | 0,6 | 0,5 |
| B9 | 0,1 | 0,4 | 0,4 |
| B10 | 0,1 | 0,2 | 0,4 |
| B11 | 0,1 | 0,5 | 0,6 |
| DS1 | 0,5 | 5,4 | 5,9 |
| DS2 | 0,6 | 10,7 | 11,3 |
| DS3 | 0,1 | 10,6 | 10,6 |
| DS4 | 0,9 | 21,6 | 22,4 |
| DS5 | 0,9 | 22,3 | 23,2 |
| DS6 | 1,9 | 41,9 | 43,8 |
| DS7 | 46,6 | 15,5 | 62,2 |
| DS8 | 40,2 | 11,6 | 50,5 |
| DS9 | 1,2 | 24,4 | 28,0 |
| DS10 | 1,1 | 29,8 | 31.0 |
| DS11 | 0,5 | 22,9 | 23,4 |

*Table S3.7: Liquid fraction composition of the digested sludge obtained by ICP-EOS*

| DS | Fe (ppm) | P (ppm) | S (ppm) | Ca (ppm) | Mg (ppm) |
|------|------|------|------|------|------|
| DS1 | 5 | 91 | 12 | 66 | 8 |
| DS2 | 13 | 75 | 13 | 76 | 2 |
| DS3 | 10 | 71 | 9 | 65 | 17 |
| DS4 | 21 | 40 | 6 | 97 | 22 |
| DS5 | 43 | 44 | 6 | 131 | 27 |
| DS6 | 45 | 28 | 9 | 145 | 29 |
| DS7 | 52 | 50 | 4 | ND | 26 |
| DS8 | 50 | 57 | 5 | 126 | 28 |
| DS9 | 28 | 39 | 8 | 108 | 26 |
| DS10 | 30 | 52 | 9 | 96 | 25 |
| DS11 | 21 | 88 | 11 | 82 | 26 |

## Chemical Modeling

Thermodynamic evaluations were carried out with Visual Minteq to study the stable minerals that could form in the digested sludge under the pH and concentration conditions in the Nieuwveer WWTP. The saturation index, as defined in Mersmann 1995, indicates how thermodynamically favored a precipitation reaction is. For vivianite, its expression is:

$$SI = \log\left(\frac{IAP}{K_S}\right) \qquad \text{with} \qquad IAP = (\gamma_{Fe^{2+}} * C_{Fe^{2+}})^3 (\gamma_{PO_4^{3-}} * C_{PO_4^{3-}})^2$$

Where:

- SI is the saturation index
- $K_s$ is the solubility product of vivianite at 25°C worth $10^{-35.76}$ (Al Borno et al. 1994)
- $\gamma$ is the activity coefficient of the ion in solution in mol/L
- C the concentration of the ion in solution in mol/L

With this definition, a solid can theoretically form if its SI is >0. The higher the SI, the higher the chances of formation. Vivianite always presents a SI>0, which confirms that its formation is thermodynamically possible. Its SI values mainly comprise between 2 and 5, suggesting that it is the equilibrium zone for vivianite in digested sludge. Some discrepancies concerning the value of the pKs of vivianite can be found in the literature. While most researchers suggest a pKs value around 35-37 (Al Borno et al. 1994, Nriagu 1972, Rosenqvist 1970), Liu et al. 2019 proposed a higher value of ~40. Hypothesizing this value, the SI in our study would be significantly lower: between -2 and 1. Negative SI seems impossible considering that vivianite is forming in DS, indicating that the pKs given by Liu et al. 2019 may be overestimated. Therefore, we considered the pKs=35.76 from Al Borno et al. in our modeling.

It is interesting to note that the formation of amorphous FeS is also possible (SI>0). Another FeS$_x$ compound, greigite (Fe$^{(II)}$Fe$^{(III)}_2$S$_4$), known to be an amorphous intermediate to the formation of pyrite (Morse et al. 1998), is constantly saturated with SI values >25, and its presence cannot be excluded. Numerous iron oxides, including ferrihydrite, magnetite, or hematite, also have high SI (>7) and could be formed even though no clear evidence of their

presence was found. According to our simulation, the formation of struvite and strengite ($FePO_4*2H_2O$) is also thermodynamically possible, but XRD or Mössbauer found no trace of these compounds. Visual Minteq does not consider some parameters (like kinetics and activation energy) in its model, which can explain the discrepancies between the prediction and reality. For example, it is common that a mineral kinetically favored forms over a mineral thermodynamically favored (Brown et al. 1985).

In short, the SI values obtained in this simulation do not allow us to draw clear conclusions but support the presence of $FeS_x$ and the formation of vivianite over less favored phosphorus mineral as strengite or struvite.

**3**

*Table S3.8: Saturation index for the minerals suspected to be present in digested sludge calculated with Visual Minteq*

| Sample | Vivianite | Struvite | FeOOH | Srengite | FeS | Greigite |
|--------|-----------|----------|-------|----------|------|----------|
| DS1 | 2,4 | -0,3 | 5,9 | 5,3 | -0,3 | 26,7 |
| DS2 | 2,8 | -0,9 | 6,4 | 5,6 | -0,2 | 27,7 |
| DS3 | 0,4 | 0,2 | 6,5 | 5,2 | -0,9 | 26,4 |
| DS4 | 4,7 | 0,6 | 7,1 | 5,1 | 0,6 | 27,3 |
| DS5 | 4,6 | 0,7 | 8,8 | 4,8 | 0,6 | 27,2 |
| DS6 | 4,6 | 0,2 | 7,1 | 5,3 | 0,5 | 28,7 |
| DS7 | 10,2 | 1,0 | 7,1 | 4,1 | 1,8 | 21,8 |
| DS8 | 10,1 | 1,2 | 6,9 | 3,9 | 2.0 | 22,2 |
| DS9 | 5,2 | 0,9 | 7,2 | 4,6 | 0,9 | 27,8 |
| DS10 | 4,6 | 0,8 | 7,2 | 5,2 | 0,6 | 28,3 |
| DS11 | 3,9 | 1,0 | 7,1 | 5,1 | 0,4 | 27,9 |

*Table S3.9: Input data for Minteq modeling. P, $Mg^{2+}$, and S have been determined by ICP-OES. $Fe^{2+}$ and $Fe^{2+}$ have been determined by the ferrozine method. $NH_4^+$ value is an average of the online measurement realized by the operator of the WWTP on the period of study (Dec. 2018-Apr. 2019). Results of DS7 and DS8 are to be carefully considered as the WWTP Nieuwveer was having some maintenance in those periods.*

| (ppm) | pH | P | $Fe^{2+}$ | $Fe^{3+}$ | $Mg^{2+}$ | $NH_4^+$ | S |
|-------|------|-------|-------|-------|-------|-------|-------|
| DS1 | 7.48 | 90.79 | 0.47 | 5.41 | 7.75 | 250 | 11.79 |
| DS2 | 7.48 | 74.57 | 0.62 | 10.70 | 1.92 | 250 | 13.38 |
| DS3 | 7.69 | 71.13 | 0.07 | 10.57 | 16.53 | 250 | 8.86 |
| DS4 | 8.14 | 39.95 | 0.85 | 21.57 | 22.13 | 250 | 6.45 |
| DS5 | 8.19 | 43.51 | 0.91 | 22.25 | 26.52 | 250 | 5.93 |
| DS6 | 7.76 | 28.43 | 1.89 | 41.95 | 28.63 | 250 | 9.21 |
| DS7 | 8.45 | 50.45 | 46.63 | 15.53 | 26.08 | 250 | 4.29 |
| DS8 | 8.52 | 56.91 | 40.22 | 11.57 | 28.07 | 250 | 5.33 |
| DS9 | 8.30 | 38.73 | 1.24 | 24.38 | 26.26 | 250 | 8.41 |
| DS10 | 8.02 | 51.91 | 1.14 | 29.83 | 24.62 | 250 | 9.39 |
| DS11 | 8.16 | 87.86 | 0.52 | 22.90 | 25.65 | 250 | 10.92 |

*Table S3.10: Distribution of phosphorus, iron and sulphur in the digested sludge in December 2018 and from January to April 2019 (average values taken)*

| Period | gaz (kg/day) | Liquid (kg/day) | Solid (kg/day) |
|---|---|---|---|
| P (Dec. 2018) | 0,0 | 32 | 52 |
| Fe (Dec. 2018) | 0,0 | 3 | 720 |
| S (Dec. 2018) | 0,2 | 5 | 200 |
| P (Jan-Apr. 2019) | 0,0 | 19 | 590 |
| Fe (Jan-Apr. 2019) | 0,0 | 14 | 1050 |
| S (Jan-Apr. 2019) | 0,2 | 3 | 180 |

*Table S3.11: Average daily mass balance for iron and phosphorus for the period with standard iron dosing (Dec. 2018) and increased iron dosing (Jan.-Apr. 2019). The sum of the incoming streams (Influent, Dosing, and external sludge) is higher that of the discharge streams (effluent and digested sludge) and can be due to an overestimation of the iron and phosphorus in the external sludge (measured once by Wilfert et al. 2018).*

| kg/day | Fe | | P | |
|---|---|---|---|---|
| | Dec. 2018 | Jan.-Apr. 2019 | Dec. 2018 | Jan.-Apr. 2019 |
| Influent | 160 | 160 | 600 | 600 |
| Dosing | 560 | 860 | 0 | 0 |
| External sludge | 170 | 170 | 110 | 110 |
| Effluent | 15 | 20 | 70 | 30 |
| Digested sludge | 740 | 1090 | 570 | 620 |

*Table S3.12: Average concentration of iron and phosphorus in the influent and effluent for the period with normal iron dosing (Dec. 2018) and increased iron dosing (Jan.-Apr. 2019)*

| mg/L | Fe | | P | |
|---|---|---|---|---|
| | Dec. 2018 | Jan.-Apr. 2019 | Dec. 2018 | Jan.-Apr. 2019 |
| Influent | 1.9 | 1.9 | 7.2 | 7.9 |
| Effluent | 0.2 | 0.3 | 0.9 | 0.4 |
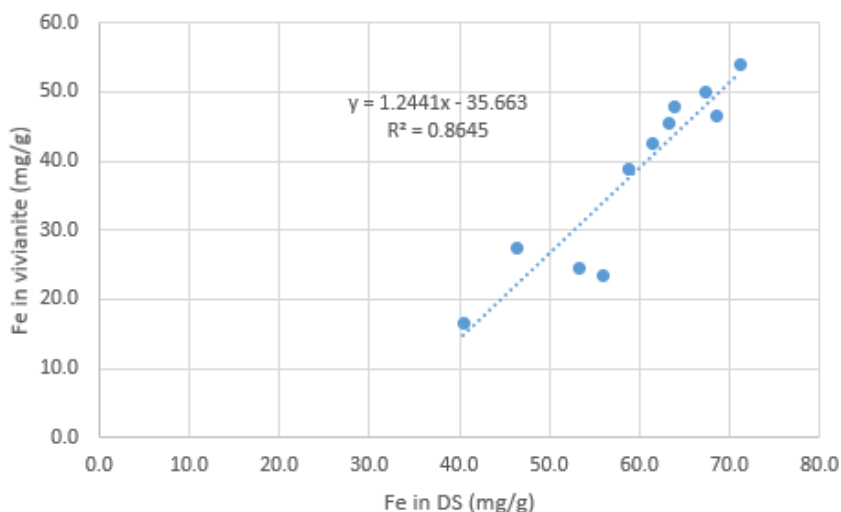
*Figure S3.4: Iron quantity in vivianite as a function of the iron content in the digested sludge of Nieuwveer.*

The intercept of the regression line with the X-axis suggests that 28±10 mg/g of iron is needed in sludge before seeing any vivianite formation. This value seems high but has a significant deviation, so further interpretation is risky.
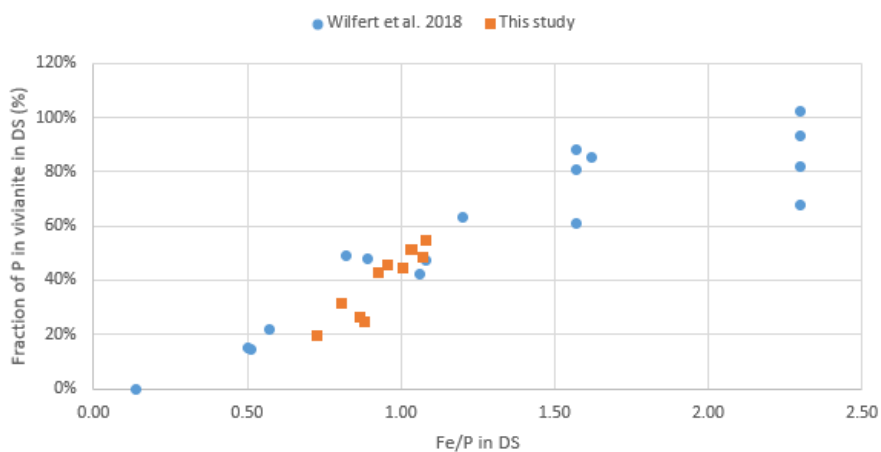


*Figure S3.5: Fraction of phosphorous present in vivianite as a function of the Fe/P molar ratio in the digested sludge of several WWTPs. Combined data from Wilfert et al. 2018 and the present study (data in Table S.1.13.*

*Table S3.13: Solid composition (ICP-OES & Mössbauer spectroscopy) of the digested sludge studied by Wilfert et al. 2016 & 2018, and in this study (calculated from Table S3.2 and Table S3.3).*

| Source | Sample | S (mg/g TS) | Fe (mg/g TS) | P (mg/g TS) | Fe in FeS (mg/g TS) | S-Corrected Fe/P | P in viv. (%) |
|--------|--------|------|------|------|------|------|------|
| W. 2015 | Leeuwarden | 9 | 41 | 39 | 8 | 0,46 | 22% |
| W. 2015 | Nieuwveer | 10 | 57 | 36 | 18 | 0,61 | 48% |
| W. 2018 | Leeuwarden | 6 | 43 | 48 | 11 | 0,38 | 15% |
| W. 2018 | Berlin | 26 | 104 | 35 | 46 | 0,90 | 85% |
| W. 2018 | Espoo | 8 | 135 | 32 | 14 | 2,11 | 102% |
| W. 2018 | Asten | 9 | 11 | 43 | 15 | -0,05 | 0% |
| W. 2018 | Cologne 300K | 8 | 101 | 36 | 14 | 1,35 | 61% |
| W. 2018 | Cologne 100K | 8 | 101 | 36 | 14 | 1,35 | 81% |
| W. 2018 | Cologne 4,2K | 8 | 101 | 36 | 14 | 1,35 | 88% |
| W. 2018 | Dokhaven | 11 | 74 | 37 | 20 | 0,82 | 63% |
| W. 2018 | Nieuwveer | 8 | 62 | 42 | 15 | 0,62 | 49% |
| W. 2018 | Espoo 300K | 8 | 135 | 32 | 14 | 2,11 | 82% |
| W. 2018 | Espoo 100K | 8 | 135 | 32 | 14 | 2,11 | 93% |
| W. 2018 | Espoo 4,2K | 8 | 135 | 32 | 14 | 2,11 | 68% |
| This study | DS1 | 13 | 41 | 31 | 22 | 0,34 | 20% |
| This study | DS2 | 12 | 46 | 32 | 20 | 0,45 | 32% |
| This study | DS3 | 11 | 53 | 34 | 18 | 0,57 | 27% |
| This study | DS4 | 11 | 62 | 37 | 19 | 0,64 | 43% |
| This study | DS5 | 11 | 59 | 33 | 19 | 0,69 | 44% |
| This study | DS6 | 11 | 64 | 35 | 19 | 0,73 | 51% |
| This study | DS7 | 11 | 63 | 37 | 19 | 0,68 | 46% |
| This study | DS8 | 10 | 69 | 36 | 18 | 0,79 | 48% |
| This study | DS9 | 11 | 71 | 37 | 18 | 0,80 | 55% |
| This study | DS10 | 11 | 67 | 36 | 20 | 0,73 | 51% |
| This study | DS11 | 14 | 56 | 35 | 24 | 0,50 | 25% |

The ratio of the spectral contribution Site B/Site A as given by Mössbauer spectroscopy (Table S3.2) can be used to evaluate these phenomena. At 300K, it has a value of 2 for pure vivianite, since two $Fe^{2+}$ occupy the two octahedral sites B, while one $Fe^{2+}$ occupies the octahedral site A (Mori & Ito 1950). Manning et al. 1991 showed that divalent cations substitute preferentially in Site B, decreasing the ratio. On the contrary, oxidation should occur more readily in Site A, increasing the ratio (Rouzies & Millet 1993, McCammon et al. 1980).
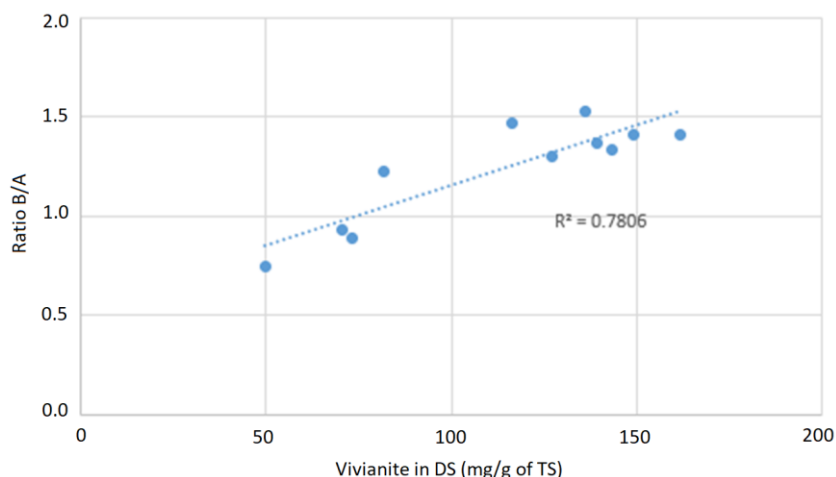
*Figure S3.6: Ratio between Site B and A as given by Mössbauer spectroscopy (Table S3.2), as a function of the vivianite content in the digested sludge of Nieuwveer*

Interestingly, the ratio Site B/Site A increased with the vivianite content in sludge (Figure S3.6). It can either suggest that the more vivianite in sludge, the more oxidized it is (1), or the more vivianite in sludge, the purer it is (2). We showed before that more vivianite was formed when the iron dosing was higher. Under these conditions, the saturation index for vivianite formation should be higher, so we can hypothesize that more vivianite formed before digestion. This early-formed vivianite goes through oxidative conditions and is, therefore, more likely to be oxidized, which goes in the direction of the case (1). However, the degree of oxidation as given by Mössbauer (Ratio $(Fe^{2+}A + Fe^{2+}B)/Fe^{3+}(A+B)$ in Table S3.2) stays constant with the vivianite content increase in DS, disproving the hypothesis (1). The amount of cations susceptible to replace iron in vivianite (Ca & Mg were the most present) stayed constant in the DS. We could imagine that if there is more vivianite in sludge, the impurities substituting iron should be more diluted in vivianite, supporting hypothesis (2). While iron dosing was increased, our team also operated a pilot installation in Nieuwveer to magnetically extract vivianite from the DS (unpublished results). The extracted vivianite (purity 55-80%) was analyzed for cations concentrations to confirm (2). From the cations II present (Ca, Mg, Mn…), only Mg concentration decreased as vivianite content increased while the other cations were not showing clear trends (Table S3.14).

*Table S3.14: Concentration of the most present ions in magnetic concentrates produced by our pilot plant in Nieuwveer*

| g/g of P | Ca | Cu | Mg | Mn | Zn |
|---|---|---|---|---|---|
| 14-jan | 0,16 | 0,00 | 0,12 | 0,01 | 0,01 |
| 6-feb | 0,30 | 0,01 | 0,10 | 0,01 | 0,01 |
| 8-mar | 0,18 | 0,00 | 0,07 | 0,01 | 0,01 |
| 9-apr | 0,22 | 0,00 | 0,07 | 0,01 | 0,01 |
| 21-may | 0,22 | 0,00 | 0,09 | 0,01 | 0,01 |

*Table S3.15: Peak height and crystallite size as measured by XRD for the samples of the digested sludge from Nieuwveer*

| Sample name | Date | Vivianite in DS (mg/g of TS) | Peak position (°2θ) | Peak height (cts) | Crystallite size (Å) |
|---|---|---|---|---|---|
| DS 1 | 4-12-2018 | 50 | 11,083 <br> 13,109 | 165 <br> 660 | 1100 |
| DS 2 | 19-12-2018 | 80 | 11,093 <br> 13,073 | 90 <br> 400 | 1200 |
| DS 3 | 8-1-2019 | 70 | 11,081 <br> 13,079 | 65 <br> 240 | 1200 |
| DS 4 | 22-1-2019 | 130 | 11,086 <br> 13,065 | 120 <br> 445 | 1100 |
| DS 5 | 5-2-2019 | 120 | 11,085 <br> 13,07 | 135 <br> 490 | 1400 |
| DS 6 | 19-2-2019 | 140 | 11,093 <br> 13,08 | 125 <br> 480 | 1200 |
| DS 7 | 12-3-2019 | 140 | 11,088 <br> 13,073 | 155 <br> 455 | 1400 |
| DS 8 | 2-4-2019 | 140 | 11,095 <br> 13,07 | 160 <br> 425 | 1200 |
| DS 9 | 16-4-2019 | 160 | 11,084 <br> 13,06 | 423 <br> 1385 | 1400 |
| DS 10 | 30-4-2019 | 150 | 11,087 <br> 13,062 | 273 <br> 927 | 1300 |
| DS 11 | 28-5-2019 | 70 | 11,094 <br> 13,101 | 174 <br> 524 | 1500 |

*Table S3.16: Dewaterability of the digested sludge for the period January-April at the WWTP Nieuwveer (TS stands for Total Solid content of the dewatered sludge and PE stands for PolyElectrolyte: Kemira superfloc C-62089 Cationic)*

| Year | 2015 | 2016 | 2017 | 2018 | 2019 |
|---|---|---|---|---|---|
| TS (%) | 21,4 | 22,6 | 20,2 | 22,3 | 21,8 |
| kg PE/g of TS | 10,4 | 10,8 | 12,1 | 11,3 | 10,8 |
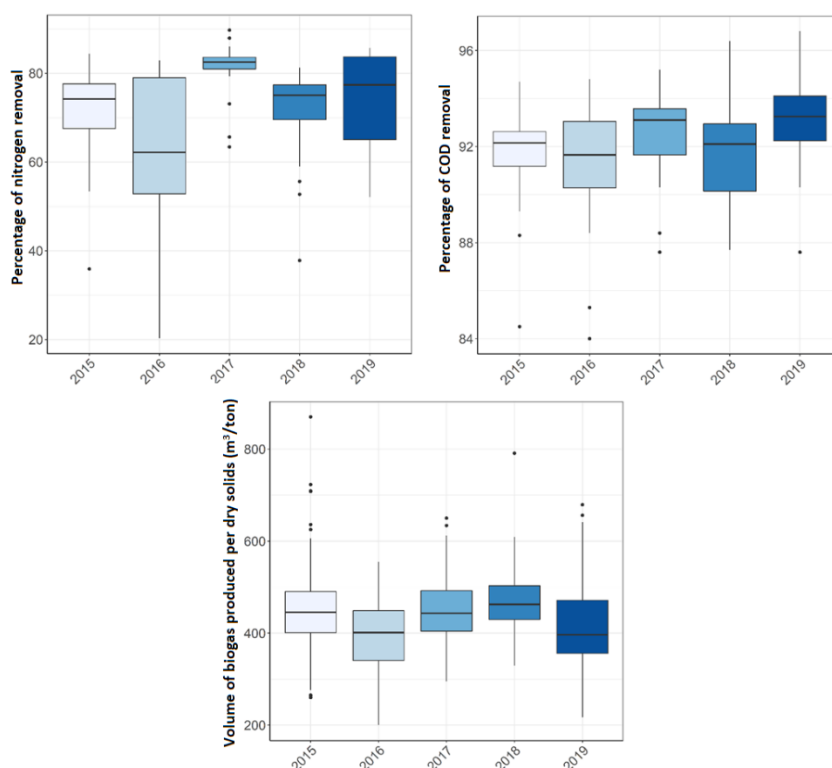
*Figure S3.7: Percentage of nitrogen removal, COD removed, and quantity of biogas produced for the plant Nieuwveer. Data comparing the time with standard iron dosing (2015-2018) to the time with doubled iron dosing (2019) on January-April.*

## Aeration energy

The following calculations show that the aeration energy necessary to fully oxidize the extra iron dosed in Nieuwveer (366kg/day) is negligible compared to the aeration necessary for the COD removal.

The equation of oxidation of $Fe^{2+}$ into $Fe^{3+}$ is:

$4H^+ + O_2 + 4Fe^{2+} = 4Fe^{3+} + 2H_2O$
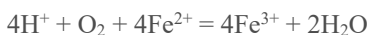
It means that 1 mole of oxygen is necessary to oxidize 4 moles of Fe2+ fully. Calculations give that to oxidize 366 kg of $Fe^{2+}$, 52.5kg of $O_2$ are necessary.

In the WWTP Nieuwveer, the average daily COD was 587 ppm $O_2$ for the period January-April 2019. The average flow rate on the same period being 76 273 m$^3$/day means that 44.8 tons of $O_2$ are necessary to entirely remove this COD. Considering that the plant COD removal is 93%, 41.7 tons of $O_2$ are used daily to treat the COD.

It means that the $O_2$ necessary to oxidize the extra $Fe^{2+}$ dose fully represents 0.1% of the $O_2$ used for COD removal, which is negligible

**3**

# Chapter 4: Pilot-scale magnetic recovery of vivianite from digested sewage sludge
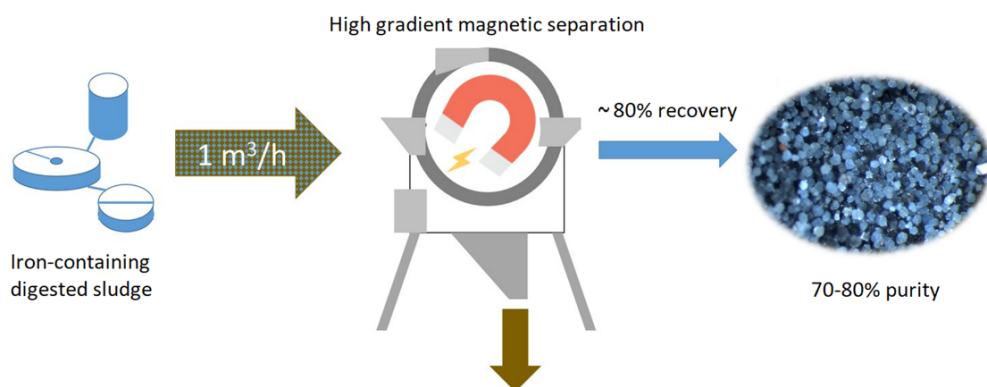


High gradient magnetic separation

1 m³/h

~ 80% recovery

Iron-containing digested sludge

70-80% purity

**4**

**Highlights**

- An urban mining concept is introduced to recover phosphorus from digested sludge

- A pilot-scale HGMS showed a vivianite recovery of 80% from digested sludge

- Vivianite recovery allows for 60% recovery of phosphorus from the influent wastewater

- The concentrate had a vivianite content of 800 mg/g and low heavy metal content

- This technology is more competitive than struvite recovery and is in line with future German legislation (>50% phosphorus recovery, <20mg/g P in solids).

*Wokke Wijdeveld (Wetsus) was the main contributor in the experiemnts and in the writing of the following chapter.*

**4**

## Abstract

Phosphorus is an essential resource for food production and the chemical industry. Phosphorus use has to become more sustainable and should include phosphorus recycling from secondary sources. About 20% of phosphorus ends up in sewage sludge, making this a substantial secondary phosphorus source. There is currently a technological gap to recover phosphorus from sludge locally at wastewater treatment plants (WWTP) that remove phosphorus by dosing iron. Vivianite ($Fe_3(PO_4)_2 \cdot 8(H_2O)$) is the main iron phosphate mineral that forms during anaerobic digestion of sewage sludge, provided that enough iron is present. Vivianite is paramagnetic and can be recovered using a magnetic separator. In this study, we have scaled up vivianite separation from lab-scale to bench- and pilot scale. Bench-scale tests showed good separation of vivianite from digested sewage sludge and that a pulsation force is crucial for obtaining a concentrate with a high phosphorus grade. A pilot-scale magnetic separator (capacity 1.0 $m^3$/h) was used to recover vivianite from digested sewage sludge at a WWTP. Recirculating and reprocessing sludge allows over 80% vivianite recovery within three passes. A concentrated P-product was produced with a vivianite content of up to 800 mg/g and phosphorus content of 98 mg/g. Phosphorus recovery is limited by the amount of phosphorus bound in vivianite and can be increased by higher iron dosing. With sufficient iron dosing, the Vivianite content can be increased, and subsequently, more phosphorus can be recovered. This would allow compliance with existing German legislation, which requires a phosphorus recovery larger than 50%.

## 4.1. Introduction

### 4.1.1. Incentive for recovery

Phosphorus is an essential resource for food production and the chemical industry. The primary source of phosphorus is phosphate rock. About 80% of mined phosphate rock $(Ca_{10}(PO_4)_6(OH)_2)$ is used in the fertilizer industry (Van Vuuren et al. 2010). Phosphate rock is a finite resource, and reserves are concentrated in a few countries (USGS, 2020). The EU has almost no phosphate rock reserves and depends therefore almost entirely on imports from other countries. This means there is a supply risk of phosphorus for the EU. Consequently, this is why the EU added phosphate rock and phosphorus to the list of critical raw materials in 2014 and 2017, respectively (European Commission, 2017, 2014). Hence, phosphorus use has to become more sustainable and should include phosphorus recycling from secondary sources. In 2005, the primary phosphorus import of the EU-27 was 1777 kton (van Dijk et al. 2016). Europe's Urban Waste Water Treatment Plants annually remove approximately 370 kton P by immobilization in the sewage sludge (van Dijk et al. 2016). Therefore, about 20% of imported phosphorus ends up in sewage sludge, making this a substantial secondary source of phosphorus and one of the largest secondary sources after animal manure (Cordell and White, 2013). In 2015, Switzerland implemented legislation demanding phosphorus recovery from sewage sludge by 2026, followed by Germany demanding 50% recovery in 2017 (Bundesamt für Umwelt, 2015; Bundesministerium für Umwelt, 2017).

### 4.1.2. Technological gap for decentralized phosphorus recovery at iron-dosing WWTPs

Land application of sewage sludge is the most straightforward and low-cost option to reuse phosphorus. Besides rising concerns about impurities in sludge such as micropollutants, pathogens, and heavy metals, the biggest challenge with direct land application of sewage sludge is the geographic imbalance of P. There are areas, for example in West-Europe, where there is a phosphorus surplus due to manure from livestock farming (MacDonald et al. 2011). Transporting sludge to areas with a P-deficit is economically and environmentally unthinkable due to transport costs and emissions. It is, therefore, desirable to recover a more concentrated phosphorus product.

Towards this end, phosphorus can be recovered in a centralized manner by incineration of the sludge followed by chemical leaching of phosphorus from the ash. Phosphorus recovery from sludge incineration ash has an advantage due to the economy of scale and high recovery efficiency (Korving et al. 2019). However, these technologies rely on expensive and strongly centralized infrastructure. Compliance with phosphorus recovery legislation alone will not be a sufficient reason to build sludge incinerators. Alternatively, phosphorus can be recovered at the wastewater treatment plant (WWTP) by separating P-bearing minerals from the sludge, i.e., struvite (Parsons and Doyle, 2002). P-recovery at the WWTP level is environmentally more beneficial than sludge incineration, although less phosphorus can be recovered. (STOWA, 2016)

The most favored advanced phosphorus removal technologies in municipal wastewater treatment are Chemical Phosphorus Removal (CPR) using iron or aluminium salts and

Enhanced Biological Phosphorus Removal (EBPR). EBPR plants have the option to recover a small fraction (10-30%) of the phosphorus from the sludge as struvite ($MgNH_4PO_4.6H_2O$) or calcium phosphate separation (Egle et al. 2016). There is currently a technological gap for CPR plants to recover phosphorus from the sludge directly at the WWTP.

### 4.1.3.   Vivianite recovery

The majority of WWTP in Europe utilize CPR (Korving et al. 2019). If iron salts are dosed for CPR, phosphorus precipitates as iron phosphate minerals and is immobilized in the produced sludge. This sludge is then often anaerobically digested for hygienisation and energy recovery via methane production. Iron can also be added in the treatment process as a coagulant to enhance primary sedimentation and thus biogas production or prevent hydrogen sulfide emissions (Charles et al. 2006; Ge et al. 2013).

Recently, research has shown that vivianite ($Fe_3(PO_4)_2 \cdot 8(H_2O)$) is the main iron phosphate mineral that forms during digestion of sewage sludge and that up to 80-90% of all phosphorus in digested sludge can be present as vivianite, provided that enough iron is present (Wilfert, 2018). Vivianite can be used as an iron fertilizer to prevent iron-chlorosis of crops like strawberries, olive trees, lupin, kiwi, grapevines, peach trees, and citrus trees growing on calcareous soils (Caballero et al. 2009; de Santiago et al. 2013; de Santiago and Delgado, 2010; Domenico Rombolà et al. 2003; Eynard et al. 1992; Rosado et al. 2002). Furthermore, vivianite can also be split via an alkaline treatment into a liquid phosphate fertilizer and an iron oxide precipitate (Chapter 2), which potentially can be reused as a raw material to produce iron salts for phosphate binding in sewage treatment plants, thus creating circular use of the dosed iron.
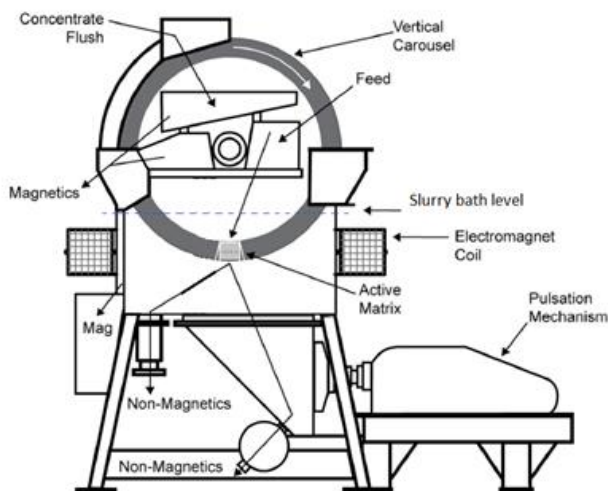


*Figure 4.1: SLon VPHGMS. Courtesy of Outotec.*

Vivianite recovery receives increasing interest as a novel approach to phosphorus recovery. However, recovery of vivianite from sewage sludge presents a separation challenge as the

vivianite particles are typically small, ranging from 10 to 200 µm. Vivianite is paramagnetic, and therefore a magnetic separation approach has been suggested and demonstrated at lab scale (Chapter 2). In this context, the application of industrial mining separators (i.e., High-Gradient Magnetic Separator), which are designed for extraction of paramagnetic minerals (Wills and Finch, 2016), allows for a clear pathway for upscaling of the vivianite recovery from digested sewage sludge. The SLon Vertically Pulsating High Gradient Magnetic Separator (VPHGMS) is widely used in the mining industry for ore concentration. Among other applications, the SLon separator has been used to concentrate fine particles such as hematite and ilmenite and desulfurization and dephosphorization of iron ore feeds prior to steelmaking (Xiong et al. 2015).

In a VPHGMS (Figure 4.1), to capture paramagnetic particles, a strong magnetic field is applied over a steel rod matrix which creates many points of high field gradient. These rods, in this way, attract paramagnetic particles, and non-magnetic particles are allowed to pass through the separator without being captured. Pulsation is achieved in the separation zone by an actuated diaphragm to assist in separation by agitating the sludge and keeping particles in a loose state. This minimizes the entrapment of particles and maximizes the usable surface area of the steel rods for magnetics collection (Wills and Finch, 2016).

This study evaluates the application of a VPHGMS for the separation of vivianite from digested sewage sludge. Firstly, a bench-scale VPHGMS was used for processing 0,5 L samples in batches to show the feasibility of the separation process. Secondly, a vivianite separation was studied at a pilot-scale VPHGMS installation at a WWTP in the Netherlands, which was able to process 1 m³/h of sludge continuously. Based on these studies, we evaluate the potential and further development of vivianite recovery by magnetic separation.

## 4.2. Materials and methods

### 4.2.1. Bench-scale magnetic separator SLon-100

A SLon-100 unit was provided by Outotec for the bench-scale tests. This machine is located in Outotecs R&D center in Frankfurt (Germany). The SLon-100 can process batch samples of 0.5 L, the magnetic field intensity is adjustable up to 1 Tesla, and steel rod matrices with different diameters can be utilized.

A steady flow of tap water of 4 L/h is created over the matrix, and pulsation is achieved with a diaphragm acted on by a motor. A digested sludge sample of approximately 0,5 L is then fed to the top of the machine, and the sludge is carried over the matrix by the water flow. The magnetic particles are retained by the magnetic field on the matrix, while the non-magnetics are carried out at the bottom of the machine. Table 4.1 provides an overview of the performed tests using the Slon-100.

*Table 4.1: Overview of bench-scale tests with SLon-100*

| Matrix rod diameter (mm) | Pulsation (Yes/No) | Magnetic field strength (T) |
|---|---|---|
| 1 | Yes | 1,0 |
| 1 | No | 1,0 |
| 1 | Yes | 0.9 |
| 2 | Yes | 1.0 |
| 2 | No | 1.0 |
| 2 | No | 0.5 |

## 4.2.2. Pilot plant installation

The pilot installation consisted of a SLon-750 VPHGMS and auxiliary equipment, namely a feed tank (1 m$^3$), tailings (=treated sludge) tank (1 m$^3$), and Dortmund type settler unit (1 m$^3$). Feed and tailings tanks were stirred. Worm pumps were used to supply the sludge. It was possible to reprocess tailings by cycling them back to the feed tank. Figure 4.2 shows a simplified flow scheme diagram of the installation.
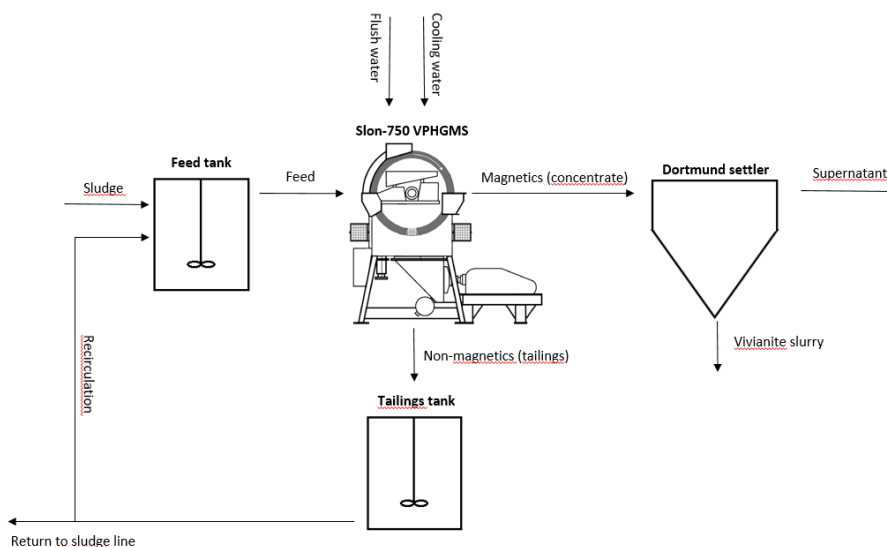


*Figure 4.2: Simplified flow scheme of pilot installation for Vivianite recovery deployed at the WWTP Nieuwveer (The Netherlands).*

## 4.2.3. WWTP Nieuwveer

The pilot study took place at WWTP Nieuwveer, the Netherlands, from 01/09/2018 till 30/06/2019. The WWTP has a size of 375.000 population equivalent (p.e.) with an average influent of 75.000 m$^3$/day. At the WWTP, Fe(II) is added in the aerated primary treatment for phosphorus removal. Sludge from primary and secondary treatment is anaerobically digested for 20 days. The digester receives sludge from other WWTPs, which accounts for about 30% of the total sludge load. During the pilot study, a parallel research on the influence of the iron

dosing increase on vivianite formation was performed (Chapter 3). The quantity of Fe(II) dosed in the A-stage was doubled for four months. The share of phosphorus present as vivianite in the digested sludge increased from 20% to 50% after increasing the iron dosing, making more phosphorus available for magnetic separation.

### 4.2.4. Pilot plant separation testing and sampling

Digested sludge with a dry matter content of typically 4% was tapped off from the main process before dewatering, sieved, and then fed to the pilot installation. Separation tests were performed to determine the separation performance with varying operational parameters. For each test, the parameters were set, and the magnetic separator was started. The feed was started through the SLon, and necessary adjustments were made to the outflow valves to maintain a steady slurry level in the separator and to achieve stable operation. Once this was achieved, the starting time was noted, and samples were taken every 15 minutes. On average, tests lasted 30 minutes to 1 hour, with 2 to 4 samples taken for the concentrate and tailings stream. The samples for each stream were then combined to decrease minor variations during the testing time. To determine dry solids percentage. Samples were dried in a Petri dish in a fumehood at room temperature to prevent loss of crystalline water from the vivianite structures.

### 4.2.5. Microwave digestion and ICP-OES analysis

The room temperature dried solid samples were digested in ultrapure $HNO_3$ (69%) in an Ethos Easy digester from Milestone equipped with an SK-15 High-Pressure rotor. The samples were placed in Teflon vessels, to which 10 ml of the $HNO_3$ was added. For digested sludge, 50 mg of sample was used, while for concentrate, 30 mg was used. The chosen digestion program heats the acid to 200°C in 15 minutes, maintains this temperature for 15 minutes, followed by a cool-down period of 1 hour.

The digested samples are then diluted and analyzed with Inductively Coupled Plasma (Perkin Elmer, type Optima 5300 DV) equipped with an Optical Emission Spectroscope (ICP-OES). A Perkin Elmer type ESI-SC-4 DX autosampler was used, and the data was processed with Perkin Elmer WinLab32. A solution of 10 mg/L Yttrium and a 2% $HNO_3$ solution were used as an internal standard solution and rinsing solution, respectively.

### 4.2.6. Mössbauer spectroscopy

The sample was put in a plastic ring sealed with Kapton foil and epoxy glue and wrapped in aluminium foil to prevent exposure to oxygen and light. The sample mass was adjusted with carbon powder to contain a maximum of 17.5 mg of Fe/cm$^2$. Transmission $^{57}$Fe Mössbauer absorption spectra were acquired at a temperature of 300 K with a conventional constant-acceleration spectrometer using a $^{57}$Co (Rh) source. Velocity calibration was performed using an α-Fe foil. The Mössbauer spectra were fitted using the Mosswinn 4.0 program (Klencsár, 1997).

### 4.2.7. Measures of separation

#### 4.2.7.1. *Grade*

Grade commonly refers to a particular element or mineral content in any stream, such as the feed and concentrate. The grade will be expressed in the weight ratio unit mg/g.

We adapted a method developed by Chapter 3 to determine the grade of vivianite in the sludge based on Mössbauer spectroscopy. Mössbauer spectroscopy can detect and speciate iron minerals very accurately and determine the part of the total iron in the sludge bound in vivianite. Using the data from Chapter 3 (experiment performed during the same period at the same location), the molar Fe:P ratio can be correlated to the amount of vivianite in the digested sludge, which is expressed as the percentage of phosphorus bound to vivianite. The following equation was derived from the data of Chapter 3.

$$P_{viv} = 0,98 \cdot Fe/P - 0,53 \pm 0,05 \qquad\qquad 4.1$$

$P_{viv}$ is the fraction of total phosphorus in the sludge that is immobilized in vivianite, and Fe/P is the molar iron to phosphorus ratio.

Another but less accurate approach is to estimate the vivianite grade of the concentrate purely based on the phosphorus content of the concentrate. Pure vivianite has a phosphorus grade of 12,35%. Therefore, dividing the phosphorus grade of the concentrate by this value will estimate the vivianite grade of the concentrate. Since vivianite is the only P-bearing magnetic mineral that is likely to be present, this is a reasonable approach, although some sludge and other impurities (potentially containing P) may also be entrained.

### 4.2.7.2. Recovery

The recovery is the percentage of the total element or mineral contained in the sludge recovered in the concentrate. The calculation requires the mass balance of the separation, as well as the grades of feed and concentrate:

$$R = \frac{c*C}{f*F} \qquad\qquad 4.2$$

where c is the grade (content) of element or mineral in the concentrate, f is the grade of the feed. C is the mass (or flowrate) of concentrate, and F the mass or flow rate of feed.

## 4.2.8. Response surface analysis

A wet magnetic separator has several operational parameters which influence the separation efficiency, and their net effect cannot be predicted in advance. Therefore, a response surface analysis was performed to determine the most relevant influences. The parameters and their expected effects on vivianite separation are as follows.

### 4.2.8.1. Pulsation frequency

Pulsation agitates the sludge and keeps particles in a loose state, which minimizes the entrapment of non-magnetic particles. Pulsation also maximizes the area of the steel rods that are used to trap magnetic particles. However, due to the pulsation drag forces, fine vivianite particles may not stay attached to the rods, which will decrease the recovery. The workings of the pulsation mechanism and the effect on fine vivianite particles suggest that there would be an optimum pulsation frequency.

### 4.2.8.2. Rod matrix diameter

In the magnetic separator, the applied magnetic field creates many points of high field gradient in the steel rod matrix to capture the vivianite particles. Agglomeration of the particles can occur if they are small and/or have a high magnetic susceptibility if the field is intense. This

effect can entrap sludge particles as well as bridge the gaps between magnetic poles, reducing the efficiency of separation. A smaller rod diameter results in a higher magnetic field gradient, which can increase this effect. Smaller diameter rods also have a smaller distance between them, which can increase the bridging effect. In general, this results in a higher recovery percentage for small rod diameters but a lower vivianite grade of the product, as more sludge particles are entrapped.

### 4.2.8.3. *Magnetic field intensity*

The magnetic field intensity should be high enough to ensure that a particle that collides with a matrix rod will remain attached to that rod. Any further increase of the field intensity will only retain particles with weaker magnetic properties (less pure) or entrap non-magnetic particles by agglomeration. Another adverse effect of high field intensity is that a high field strength can decrease the magnetic susceptibility of a particle if this particle shows some degree of magnetic ordering (Svoboda, 1994). The magnetic force on a particle is directly proportional to the magnetic field gradient in the separator and the magnetic susceptibility of the particle. Therefore, the net effect of increased field intensity can be a decrease in the magnetic force experienced by the particle. Applying the appropriate magnetic field is therefore crucial for a good separation performance.

The response surface analysis with different operating parameters was done on the 34 pilot-scale separation tests to investigate their effect statistically. A custom response surface design was defined using Minitabversion 18. As continuous factors were chosen molar Fe/P ratio of feed, Matrix rod diameter, Pulsation frequency, Magnetic field intensity, and Feed rate. The following levels were specified as low and high.

*Table 4.2: Low and high values for parameters used in response surface analysis*

| Factor | Name | Low | High |
|--------|------|-----|------|
| A | Molar Fe/P ratio feed | 0,82 | 1,12 |
| B | Matrix [mm] | 1 | 3 |
| C | Pulsation frequency [rpm] | 0 | 200 |
| D | Magnetic field [T] | 0,5 | 1,0 |
| E | Feed rate [$m^3$/h] | 0,5 | 1,0 |

The response surface results were then analyzed by plotting normal plots for 'Vivianite grade.'

'Vivianite recovery' 'P Recovery' 'P Grade' 'Fe Recovery' 'Fe Grade'.

A normal probability plot shows the standardized effects relative to a distribution fit line when all the effects would be 0. The standardized effects are t-tests that test the null hypothesis that the effect is 0. Positive effects have an increased response when the setting increases from a low to high value, whereas adverse effects would have a decreased response to this. The greater the magnitude of the effect, the further from 0 they are on the x-axis.

## 4.3.    Results and discussion

### 4.3.1.  Bench-scale tests: good separation of vivianite and pulsation is crucial

Digested sludge from WWTP Nieuwveer was subjected to a bench-scale separation test to evaluate the effect of pulsation, applied magnetic field strength, and matrix rod diameter. Figure 4.3 shows the bench-scale results with the Slon-100 machine in terms of recovery and grade of P.
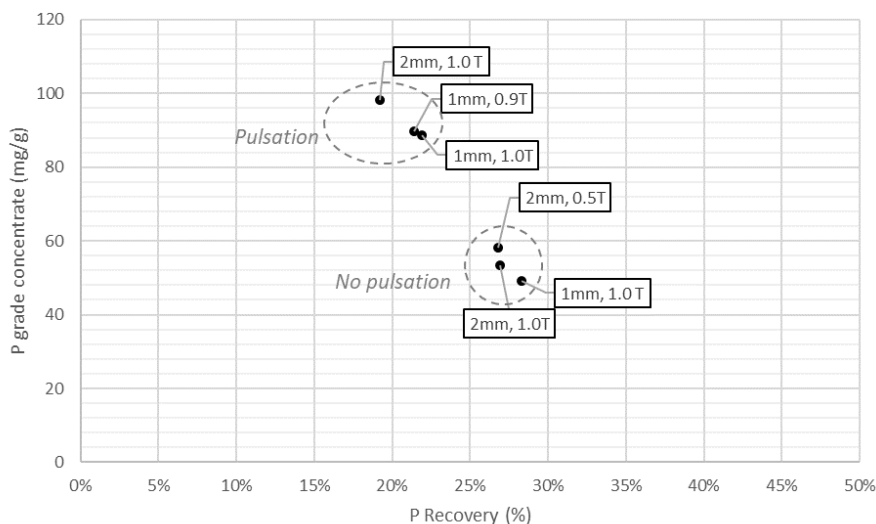


*Figure 4.3: Impact of pulsation in bench-scale magnetic vivianite separation expressed in phosphorus recovery and quality of recovered material. Labels show matrix rod diameter and magnetic field intensity in the magnetic separator. Pulsation enhances the grade of the recovered concentrate. A bigger rod diameter shows an increase in concentrate phosphorus grade and a decrease in phosphorus recovery.*

The results show that pulsation frequency has a significant effect on separation. With pulsation, the grade of the vivianite concentrate is significantly higher than without while the recovery decreases. Pulsation agitates the slurry and keeps particles in a loose state, which minimizes the entrapment of non-magnetic particles. Pulsation also maximizes the area of the magnetized rods that are used to trap magnetic particles. One would expect that pulsation increases the recovery. However, due to the pulsation drag forces, fine vivianite particles will likely not stay attached to the rods, which will decrease the recovery. The workings of the pulsation mechanism and the effect on fine vivianite particles already suggest that there would be an optimum pulsation frequency. Too much pulsation will remove fines, but not enough pulsation will entrap non-magnetic particles. Another more negligible effect that can be observed from the bench-scale separation tests is the effect of rod diameter. A bigger rod diameter shows an increase in grade and a decrease in recovery. With a bigger rod diameter, the distance between rods is larger, which will decrease the magnetic field gradient. The larger distance causes less entrapment by fines, and the decrease in field gradient will separate the more susceptible and purer vivianite, which will increase the concentrate grade.

The theoretical maximum phosphorus grade that can be reached is 123,5 mg/g, which is pure vivianite. The bench-scale separation tests showed promising results that vivianite can be recovered from sludge with a relatively high grade and establishes the potential for this technology on a large scale.

### 4.3.2. Pilot-scale separation tests show that over 80% of vivianite can be recovered in three passes.

Pilot testing was performed over nine months. The vivianite content of the sludge during the pilot testing varied between 44 and 148 mg/g, which immobilizes 18% to 54% of the phosphorus in the sludge in the form of vivianite, respectively. The variation in the vivianite content is due to the experimental increase and decrease of iron salt dosing during the same period as discussed in Chapter 3. During the operational period, 34 separation tests were performed with different operational parameters and varying vivianite content of the feed sludge. The results of all the separation tests are plotted in Figure 4.4.
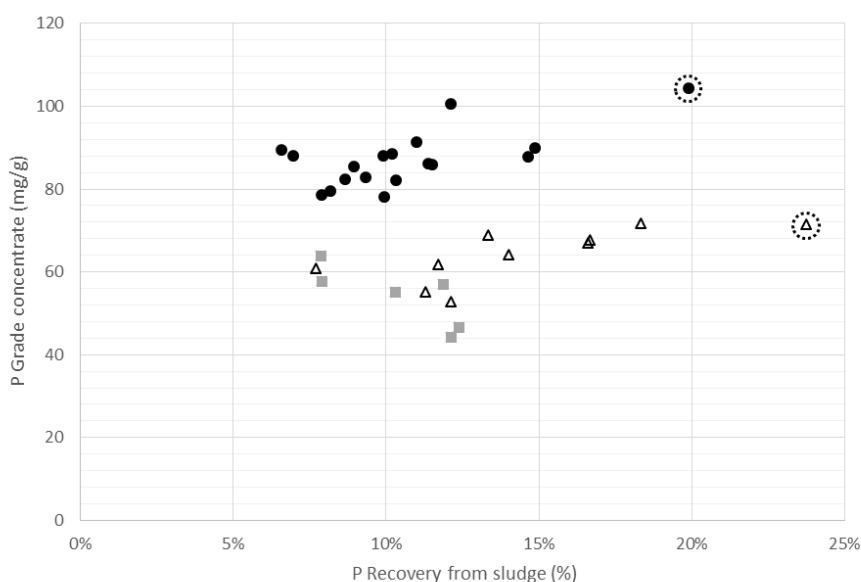


*Figure 4.4: Separation performance of all tests conducted with pilot-scale magnetic separator expressed in phosphorus recovery and quality of recovered material. The difference in steel matrix rod diameter is shown in the graph. Δ =1mm, ■=1,5mm ● = 3mm. Outliers are marked with a circle. With a larger rod diameter, the phosphorus grade of the concentrate increases.*

Table 4.3 shows additional detailed information for selected results with calculated vivianite recoveries and grades (full results are available in the supporting information).

*Table 4.3: Selected results of separation performance of pilot installation showing parameters used for maximum recovery, maximum grade, and long-term operation.*

| | Rod diameter (mm) | Field intensity (T) | Pulsation (rpm) | P grade (mg/g) | P recovery (%) | Vivianite grade (mg/g) | Vivianite recovery (%) |
|---|---|---|---|---|---|---|---|
| Max. recovery | 1 | 0,5 | 100 | 72 | 18 | 580 | 52 |
| Max. grade | 3 | 1 | 100 | 101 | 12 | 814 | 36 |
| Average of long-term operation | 3 | 1 | 100 | 91 | 12 | 735 | 31 |

### 4.3.3. Recirculation increased the vivianite recovery to over 80%

From separation testing, it was apparent that a 3 mm rod matrix performed better over time. Small diameter rods are more prone to bend and break under the influence of the strong magnetic field. A 1 mm diameter rod matrix is not recommended for industrial use by the machine supplier due to this reason (personal communication Outotec). Furthermore, a fine rod matrix is prone to blocking by coarse material, which was experienced during pilot testing. Additionally, a high-grade concentrate is desirable due to the transport costs of concentrate. This suggests using a big diameter rod matrix. Therefore, a 3 mm rod matrix is the best choice for the industrial application of this technology for vivianite recovery. However, a 3 mm rod matrix has a low vivianite recovery. Only about 30% of the vivianite in the sludge is recovered in one pass. To increase the recovery, tests were performed where sludge was processed by the magnetic separator in three separate passes, increasing the recovery with each pass. The results are shown in Table 4.4.

*Table 4.4: Recirculation test results of 17-1: matrix 3mm, pulsation 100 rpm, Field 1T, Feed rate 0.5 m³/h. Vivianite content in the sludge 73 mg/g dry. A total vivianite recovery of 81% from the original feed sludge was achieved in 3 passes.*

| Pass | Mass yield | Fe recovery from feed | P recovery from feed | Vivianite recovery from feed | Vivianite grade concentrate (mg/g) |
|---|---|---|---|---|---|
| 1 | 4% | 17% | 11% | 36% | 697 |
| 2 | 4% | 13% | 9% | 27% | 731 |
| 3 | 3% | 8% | 6% | 18% | 683 |
| Total | 11% | 38% | 26% | 81% | 705 |

With enough iron dosing (Fe/P=1.5-2), more than 80% of the phosphorus in the sludge can be immobilized in the form of vivianite (Wilfert et al. 2018, Chapter 3). If 80% of the vivianite is recovered, the total phosphorus recovery from sludge will be over 64%. This recovery potential is higher than that of struvite, which reaches typically only 10-30% of the total phosphorus load (Cornel and Schaum, 2009; Egle et al. 2016; Lodder et al. 2011) and complies

with existing legislation in Switzerland and Germany where 50% of phosphorus recovery from sludge is demanded.

### 4.3.4. The effect of parameters and their interaction is complex and can be optimized by response surface methodology.

As discussed in the materials and methods section, the following operational parameters are expected to influence the separation efficiency: pulsation frequency, rod matrix diameter, magnetic field intensity. A response surface analysis was done on the 34 pilot-scale separation tests to statistically investigate the effect of each of the operational parameters.

Normal plots for the standardized effect are given for the vivianite recovery in Figure 4.5 and vivianite grade in Figure 4.6.
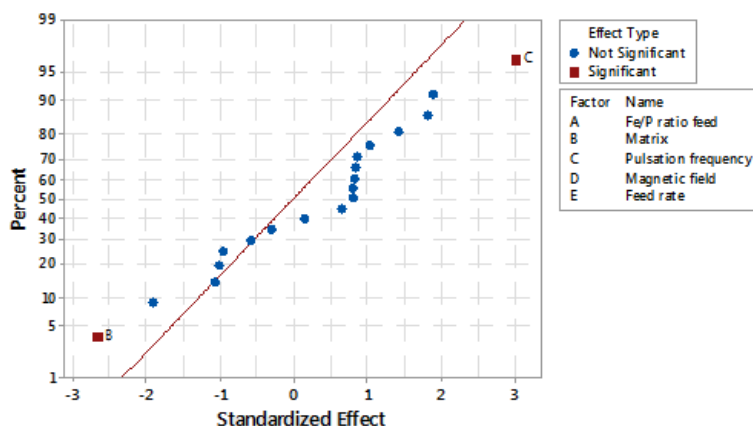


*Figure 4.5: Normal plot of the standardized effect on vivianite recovery(α=0,95). The significant effects are pulsation frequency (C, positive effect), and Matrix rod diameter (B, negative effect)*

The normal plots show that the pulsation frequency has the most significant effect on recovery, followed by the matrix rod diameter. The parameters or combinations thereof that significantly affect the vivianite grade of the concentrate, in order of magnitude, are pulsation frequency, combination pulsation frequency and magnetic field, combination pulsation frequency, and matrix rod diameter, and the combination of Fe/P ratio and magnetic field. The significance of the combination of pulsation frequency with the other parameters shows that the effect of pulsation is dependent on other parameters, for example, magnetic field, and could be optimized using response surface methodology. An interesting observation from the response surface analysis is the significant negative effect of the combination of Fe/P ratio and magnetic field. This means that if the Fe/P ratio increased and magnetic field strength increased, the vivianite grade of the concentrate decreased. The Fe/P ratio is increased by additional iron dosing. The newly formed vivianite from additional dosing could be present as finer particles, which can form flocs that entrap organics, lowering the concentrate vivianite grade. Another explanation that could add to this effect is that other iron minerals are formed, which are recovered in the magnetic fraction.
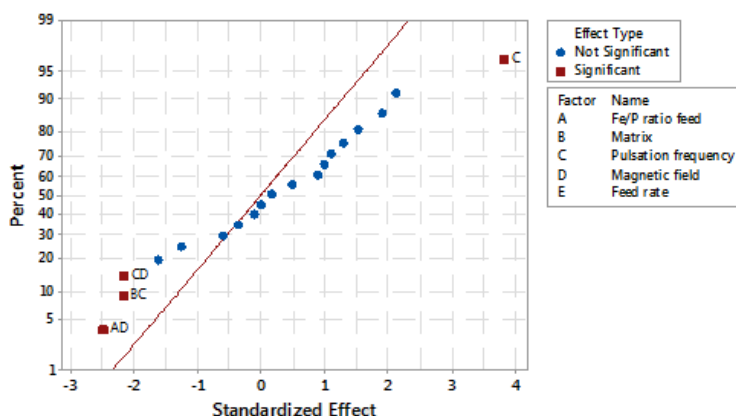
*Figure 4.6: Normal plot of the standardized effects on vivianite grade of the concentrate(α=0,95). The significant effects are Pulsation frequency (C, positive), a combination of pulsation frequency with magnetic field intensity (CD), a combination of pulsation frequency with matrix rod diameter(BC), and a combination of Fe/P ratio of the feed and magnetic field intensity(AD) (negative)*

### 4.3.5. A concentrated phosphorus product was produced by magnetic separation.

Mössbauer spectroscopy was performed on a sample of mixed concentrate from the pilot installation. The results showed that the vivianite grade of the concentrate was $710 \pm 40$ mg/g based on the iron speciation. It is known that iron can be replaced by other divalent ions (like Ca, Mg and Mn) in the vivianite structure, and therefore it is better to speak of vivianite-like structures (Wilfert et al. 2018). If we assume that the Ca, Mg, and Mn that we measured in the concentrate is in fact, replacing iron sites in the vivianite-like structures, then the vivianite grade will be higher as this part of the vivianite is not quantified by Mössbauer spectroscopy. The vivianite content of the concentrate would then be 800 mg/g. 96% of the phosphorus in the concentrate was bound to vivianite in this case. The total carbon content of the concentrate was 10%, the total nitrogen content was 1%. The phosphorus content of the concentrate is 9,8% P, or 22.4% $P_2O_5$ equivalent. Complete elemental analyses, including heavy metals, were performed on the concentrate and reported in the supplemental information. Heavy metal concentrations were in line and somewhat lower than earlier reported for lab-scale magnetic separation tests (Chapter 2).

### 4.3.6. Overview

The pilot tests were performed with a SLon-750 VPHGMS and were operated with feed flow rates of either 0.5 or 1 $m^3$/h of digested sludge that was tapped before the final dewatering of the sewage sludge. Sewage sludge presents a very different matrix compared to iron ore slurries that are typically treated in this type of separator. The viscosity of the treated digested sludge viscosity was comparable to these sludges (see SI) but had a significantly lower dry matter content (ca. 4% dry matter for digested sludge compared to 20-40% dry matter for iron ore slurries) (Xiong et al. 2015). For this sewage treatment plant (raw sewage inflow of 75.000

$m^3$/day), the total digested sludge production is roughly 16 $m^3$/h. Upscaling of the pilot system requires an increase in the ring diameter and/or the width of the ring. VPHGMS equipment is commercially available in capacities ranging from 10 to 1000 $m^3$/h iron ore slurry input. Therefore, it is more than large enough to treat the full capacity of this or even significantly larger sewage treatment plants and if recirculation is needed to maximize the recovery efficiency. Electrical consumption of the magnetic separator is around 1.5kW/$m^3$ of sludge which is comparable to the consumption of a typical dewatering operation.

An important aspect in a full-scale application is the potential effect of the magnetic separation on the dewaterability of the digested sludge. A lower dewaterability would imply higher sludge disposal volumes and associated disposal costs. Therefore, preliminary dewaterability tests were performed both in lab-scale experiments and at pilot scale using a decanter centrifuge. The results are reported in Supplementary information and show that there was a small negative effect on the dewaterability of the treated sludge. This effect will be compensated by reducing sludge volume that needs to be dewatered through the removal of vivianite from the sludge. Further optimization of the selection of the poly-electrolyte used for flocculation may further improve the dewatering.

This study shows that commercially available VHMGS-equipment can be used to "mine" this vivianite from the digested sewage sludge. Typically, sewage treatment plants remove 90% of all phosphorus from the sewage influent and concentrate it in the surplus sludge, often digested in the larger sewage treatment plants to produce biogas. If enough iron is dosed either in the main water line and/or in the sludge digester, then 80-90% of the phosphorus in the sewage sludge is present as vivianite (Wilfert 2018). The current study shows that a magnetic separation approach can recover 80% of this vivianite. Overall, this means that 60-64% of the phosphorus in the sewage influent can potentially be recovered as vivianite while recovering most of the dosed iron as well. Such an approach (called ViviMag) makes phosphorus recovery possible for sewage plants that employ chemical phosphorus removal, where currently this is not possible. The ViviMag approach would also have higher recovery efficiencies compared to struvite recovery approaches that are currently being implemented in sewage treatment plants applying enhanced biological phosphorus removal and typically show a recovery potential of 10-40% of the influent phosphorus (Korving 2019).

Future work should focus on further optimizing the magnetic separation to improve recovery efficiencies and purity of the magnetic concentrate. Suggestions were made for the main parameters to focus on: pulsation and rods diameter. Also, additional purification steps (for instance, a washing approach) can improve the purity of the recovered vivianite. Further research on splitting the vivianite into an iron phase and phosphate phase would make it possible to create circular use of iron salts for phosphorus recovery at a WWTP.

## 4.4.  Conclusions

Vivianite recovery is emerging as a promising approach for phosphorus recovery from sewage treatment plants employing iron salts for phosphorus removal. The tiny particle size of vivianite particles and the complex sludge matrix make an efficient separation challenging. Magnetic separation equipment commonly used in the mining industry efficiently extracted the paramagnetic vivianite from digested sludge, thus truly introducing "urban mining". With this approach, a recovery efficiency from digested sludge of 80% was achieved, making it possible to recover over 60% of the influent phosphorus load.  The recovered magnetic concentrate has a purity of up to 800 mg vivianite per gram (98 mg P/g) with low concentrations of heavy metals. The effect of the operational parameters on the separation performance is complex and was optimized by using response surface methodology.

**4**

### References

Bundesamt für Umwelt, (2015). Bericht über die Ergebnisse der Anhörung 20.

Bundesministerium für Umwelt, (2017). Verordnung zur Neuordnung der Klärschlammverwertung. *Bundesgesetzblatt*, 3465–3512.

Caballero, R., Pajuelo, P., Ordovás, J., Carmona, E., Delgado, A., (2009). Evaluation and correction of nutrient availability to Gerbera jamesonii H. Bolus in various compost-based growing media. *Sci. Hortic.* (Amsterdam). 122, 244–250. https://doi.org/10.1016/j.scienta.2009.05.010.

Charles, W., Cord-Ruwisch, R., Ho, G., Costa, M., Spencer, P., (2006). Solutions to a combined problem of excessive hydrogen sulfide in biogas and struvite scaling. *Water Sci. Technol*. 53, 203–210. https://doi.org/10.2166/wst.2006.198.

Cordell, D., White, S., (2013). Sustainable Phosphorus Measures: Strategies and Technologies for Achieving Phosphorus Security. *Agronomy* 3, 86–116. https://doi.org/10.3390/agronomy3010086.

Cornel, P., Schaum, C., (2009). Phosphorus recovery from wastewater: Needs, technologies and costs. *Water Sci. Technol*. 59, 1069–1076. https://doi.org/10.2166/wst.2009.045.

de Santiago, A., Carmona, E., Quintero, J.M., Delgado, A., (2013). Effectiveness of mixtures of vivianite and organic materials in preventing iron chlorosis in strawberry. *Spanish J. Agric. Res.* 11, 208–216. https://doi.org/10.5424/sjar/2013111-2671.

de Santiago, A., Delgado, A., (2010). Interaction between beet vinasse and iron fertilisers in the prevention of iron deficiency in lupins. *J. Sci. Food Agric*. 90, 2188–2194. https://doi.org/10.1002/jsfa.4068.

Domenico Rombolà, A., Toselli, M., Carpintero, J., Ammari, T., Quartieri, M., Torrent, J., Marangoni, B., (2003). Prevention of Iron-Deficiency Induced Chlorosis in Kiwifruit ( Actinidia deliciosa ) Through Soil Application of Synthetic Vivianite in a Calcareous Soil. J. *Plant Nutr.* 26, 2031–2041. https://doi.org/10.1081/PLN-120024262.

Egle, L., Rechberger, H., Krampe, J., Zessner, M., (2016). Phosphorus recovery from municipal wastewater: An integrated comparative technological, environmental and economic assessment of P recovery technologies. *Sci. Total Environ*. 571, 522–542. https://doi.org/10.1016/j.scitotenv.2016.07.019.

European Commission, (2017). Communication from the Commission to the European Parliament, the Council, the European Economic and Social Committee and the Committee of the Regions on the 2017 list of Critical Raw Materials for the EU. *Off. J. Eur. Union COM(2017),* 8.

European Commission, (2014). Communication from the Commission: On the review of the list of critical raw materials for the EU and the implementation of the Raw Materials Initiative. *Off. J. Eur. Union COM(2014)* 297 final.

Eynard, A., Campillo, M.C., Barrón, V., Torrent, J., (1992). Use of vivianite (Fe3(PO4)2.8H2O) to prevent iron chlorosis in calcareous soils. *Fertil. Res*. 31, 61–67. https://doi.org/10.1007/BF01064228.

Ge, H., Zhang, L., Batstone, D.J., Keller, J., Yuan, Z., 2013. Impact of iron salt dosage to sewers on downstream anaerobic sludge digesters: Sulfide control and methane production. J. *Environ. Eng*. (United States) 139, 594–601. https://doi.org/10.1061/(ASCE)EE.1943-7870.0000650.

Klencsár, Z., (1997). Mössbauer spectrum analysis by Evolution Algorithm. *Nucl. Instruments Methods Phys. Res. Sect. B Beam Interact. with Mater. Atoms* 129, 527–533. https://doi.org/10.1016/S0168-583X(97)00314-5.

Korving, L., Van Loosdrecht, M., Wilfert, P., (2019). Effect of Iron on Phosphate Recovery from Sewage Sludge, in: *Phosphorus Recovery and Recycling*. Springer Singapore, Singapore, pp. 303–326. https://doi.org/10.1007/978-981-10-8031-9_21.

Lodder, R., Meulenkamp, R., Notenboom, G., 2011. Fosfaatterugwinning in communale afvalwaterzuiveringsinstallaties. Stowa Rapp. 24, 102. https://doi.org/ISBN 978.90.5773.539.4, STOWA 2011-24.

MacDonald, G.K., Bennett, E.M., Potter, P.A., Ramankutty, N., (2011). Agronomic phosphorus imbalances across the world's croplands. *Proc. Natl. Acad. Sci*. 108, 3086–3091. https://doi.org/10.1073/pnas.1010808108.

Parsons, S.A., Doyle, J.D., 2002. Struvite formation, control and recovery. *Water Res*. 36, 3925–3940.

Prot, T., Nguyen, V.H., Wilfert, P., Dugulan, A.I., Goubitz, K., De Ridder, D.J., Korving, L., Rem, P., Bouderbala, A., Witkamp, G.J., van Loosdrecht, M.C.M., (2019). Magnetic separation and characterization of vivianite from digested sewage sludge. *Sep. Purif. Technol*. 224, 564–579. https://doi.org/10.1016/j.seppur.2019.05.057.

Prot, T., Wijdeveld, W., Eshun, L.E., Dugulan, A.I., Goubitz, K., Korving, L., Van Loosdrecht, M.C.M., (2020). Full-scale increased iron dosage to stimulate the formation of vivianite and its recovery from digested sewage sludge. *Water Res*. 115911. https://doi.org/10.1016/j.watres.2020.115911.

Rosado, R., Del Campillo, M.C., Martínez, M.A., Barrón, V., Torrent, J., (2002). Long-term effectiveness of vivianite in reducing iron chlorosis in olive trees. *Plant Soil* 241, 139–144. https://doi.org/10.1023/A:1016058713291.

Sahoo, B.K., Das, T.K., Gupta, A., De, S., Carsky, M., Meikap, B.C., (2017). Application of response surface analysis to iron ore slurry rheology using microwave pre-treatment. *South African J. Chem. Eng*. 23, 81–90. https://doi.org/10.1016/j.sajce.2017.03.002.

STOWA, (2016). Levenscyclusanalyse van grondstoffen uit rioolwater. Rapport 22, 181.

Svoboda, J., (1994). The effect of magnetic field strength on the efficiency of magnetic separation. *Miner. Eng.* 7, 747–757. https://doi.org/10.1016/0892-6875(94)90104-X.

USGS, (2020). Phosphate rock statistics and information. *Nat. Resour. U.S.-canadian Relations*, Vol. 2 Patterns Trends Resour. Supplies Policies 122–123.

van Dijk, K.C., Lesschen, J.P., Oenema, O., (2016). Phosphorus flows and balances of the European Union Member States. *Sci. Total Environ*. 542, 1078–1093. https://doi.org/10.1016/j.scitotenv.2015.08.048.

Van Vuuren, D.P., Bouwman, A.F., Beusen, A.H.W., (2010). Phosphorus demand for the 1970-2100 period: A scenario analysis of resource depletion. *Glob. Environ. Chang*. 20, 428–439. https://doi.org/10.1016/j.gloenvcha.2010.04.004.

Wei, P., Tan, Q., Uijttewaal, W., van Lier, J.B., de Kreuk, M., (2018). Experimental and mathematical characterisation of the rheological instability of concentrated waste activated sludge subject to anaerobic digestion. *Chem. Eng. J*. 349, 318–326. https://doi.org/10.1016/j.cej.2018.04.108.

Wilfert, P.., 2018. Phosphate Recovery From Sewage Sludge Containing Iron Phosphate. TU Delft. https://doi.org/10.4233/uuid:f3729790-0cfe-4f92-866b-eca3f2f2df24.

Wilfert, P., Dugulan, A.I., Goubitz, K., Korving, L., Witkamp, G.J., Van Loosdrecht, M.C.M., (2018). Vivianite as the main phosphate mineral in digested sewage sludge and its role for phosphate recovery. *Water Res*. 144, 312–321. https://doi.org/10.1016/j.watres.2018.07.020.

Wills, B.A., Finch, J.A., (2016). Magnetic and Electrical Separation. *Wills' Miner. Process. Technol*. 381–407. https://doi.org/10.1016/B978-0-08-097053-0.00013-3.

Xiong, D., Lu, L., Holmes, R.J., (2015). Developments in the physical separation of iron ore: Magnetic separation. Iron Ore *Mineral. Process. Environ. Sustain*. 283–307. https://doi.org/10.1016/B978-1-78242-156-6.00009-5.

**4**

Supplementary information

*Table S4.1: Complete results of pilot-scale separation testing*

| Date | Test nr. | Vivianite in feed | Fe/P ratio feed | Rod diameter | Pulsation frequency | Magnetic field | Feed rate | Fe Grade | Fe Recovery | P Grade | P Recovery | Vivianite grade | Vivianite recovery | Comments |
|---|---|---|---|---|---|---|---|---|---|---|---|---|---|---|
| dd-m-yyyy | | mg/g | | mm | rpm | T | m³/h | mg/g | % | mg/g | % | mg/g | % | |
| 14-1-2019 | 1901141 | 93 | 0,88 | 3 | 100 | 1,00 | 0,5 | 241 | 18,4% | 101 | 12,0% | 814 | 36% | |
| 17-1-2019 | 1901172 | 73 | 0,81 | 3 | 100 | 1,00 | 0,5 | 205 | 13,0% | 90 | 9,0% | 731 | 27% | |
| 17-1-2019 | 1901173 | 59 | 0,76 | 3 | 100 | 1,00 | 0,5 | 190 | 8,0% | 84 | 6,0% | 683 | 18% | recirculation |
| 17-1-2019 | 1901171 | 88 | 0,86 | 3 | 100 | 1,00 | 0,5 | 198 | 16,9% | 86 | 11,4% | 697 | 36% | recirculation |
| 17-1-2019 | 1901174 | 90 | 0,87 | 3 | 50 | 1,00 | 0,5 | 244 | 29,7% | 104 | 19,9% | 844 | 61% | |
| 23-1-2019 | 1901231 | 98 | 0,90 | 1 | 100 | 0,50 | 0,5 | 162 | 25,7% | 72 | 18,3% | 58 | 52% | |
| 23-1-2019 | 19012302 | 98 | 0,90 | 1 | 100 | 1,00 | 0,5 | 161 | 33,2% | 71 | 23,8% | 577 | 68% | |
| 24-1-2019 | 1901241 | 99 | 0,90 | 1 | 100 | 0,50 | 1,0 | 139 | 18,9% | 64 | 14,0% | 518 | 40% | |
| 24-1-2019 | 1901242 | 99 | 0,90 | 1 | 100 | 0,75 | 1,0 | 148 | 22,8% | 67 | 16,6% | 541 | 47% | |
| 24-1-2019 | 1901243 | 99 | 0,90 | 1 | 100 | 1,00 | 1,0 | 148 | 22,6% | 68 | 16,7% | 548 | 47% | |
| 29-1-2019 | 1901291 | 108 | 0,93 | 1 | 50 | 0,50 | 1,0 | 114 | 14,0% | 55 | 11,3% | 445 | 30% | |
| 29-1-2019 | 1901292 | 108 | 0,93 | 1 | 50 | 0,50 | 1,0 | 112 | 15,4% | 53 | 12,1% | 427 | 32% | |
| 6-2-2019 | 1902061 | 108 | 0,93 | 1 | 50 | 1,00 | 1,0 | 163 | 19,0% | 69 | 13,4% | 557 | 35% | |
| 8-2-2019 | 1902081 | 98 | 0,90 | 1 | 25 | 1,00 | 1,0 | 142 | 16,7% | 62 | 11,7% | 500 | 33% | |
| 8-2-2019 | 1902082 | 98 | 0,90 | 1 | 0 | 1,00 | 1,0 | 140 | 11,0% | 61 | 7,7% | 491 | 22% | |
| 8-3-2019 | 1903081 | 158 | 1,09 | 3 | 50 | 1,00 | 0,5 | 236 | 20,1% | 88 | 14,7% | 709 | 27% | |
| 8-3-2019 | 1903082 | 139 | 1,03 | 3 | 50 | 1,00 | 0,5 | 209 | 13,0% | 78 | 10,0% | 627 | 18% | recirculation |
| 8-3-2019 | 1903083 | 127 | 0,99 | 3 | 50 | 1,00 | 0,5 | 188 | 9,0% | 71 | 7,0% | 571 | 13% | recirculation |
| 14-3-2019 | 1903141 | 147 | 1,06 | 3 | 25 | 1,00 | 1,0 | 233 | 14,1% | 89 | 10,2% | 717 | 20% | |

*Table S4.2: Complete results of pilot-scale separation testing*

| Date | Test nr. | Vivianite in feed | Fe/P ratio feed | Rod diameter | Pulsation frequency | Magnetic field | Feed rate | Fe Grade | Fe Recovery | P Grade | P Recovery | Vivianite grade | Vivianite recovery | Comments |
|---|---|---|---|---|---|---|---|---|---|---|---|---|---|---|
| dd-m-yyyy | | mg/g | | mm | rpm | T | m³/h | mg/g | % | mg/g | % | mg/g | % | |
| 14-3-2019 | 1903142 | 147 | 1,06 | 3 | 75 | 1,00 | 1,0 | 246 | 15,6% | 91 | 11,0% | 740 | 22% | |
| 20-3-2019 | 1903201 | 168 | 1,12 | 3 | 75 | 1,00 | 0,5 | 236 | 19,3% | 89 | 14,9% | 727 | 26% | |
| 26-3-2019 | 1903261 | 160 | 1,10 | 3 | 50 | 1,00 | 0,5 | 208 | 13,4% | 78 | 10,0% | 632 | 18% | |
| 26-3-2019 | 1903262 | 160 | 1,10 | 3 | 50 | 1,00 | 1,0 | 240 | 9,6% | 88 | 7,0% | 713 | 13% | |
| 28-3-2019 | 1903281 | 152 | 1,07 | 3 | 100 | 1,00 | 0,5 | 232 | 16,1% | 86 | 11,5% | 695 | 22% | |
| 9-4-2019 | 1904091 | 146 | 1,05 | 3 | 100 | 0,75 | 0,5 | 227 | 13,5% | 88 | 9,9% | 712 | 20% | |
| 9-4-2019 | 1904092 | 146 | 1,05 | 3 | 50 | 0,75 | 0,5 | 201 | 10,7% | 78 | 7,9% | 635 | 16% | |
| 21-5-2019 | 1905211 | 101 | 0,90 | 3 | 50 | 0,80 | 0,5 | 188 | 11,9% | 79 | 8,2% | 644 | 23% | |
| 21-5-2019 | 1905212 | 101 | 0,90 | 3 | 100 | 0,80 | 0,5 | 200 | 13,9% | 83 | 9,3% | 671 | 26% | |
| 21-5-2019 | 1905213 | 101 | 0,90 | 3 | 150 | 0,80 | 0,5 | 201 | 15,5% | 82 | 10,3% | 664 | 29% | |
| 21-5-2019 | 1905214 | 101 | 0,90 | 3 | 200 | 0,80 | 0,5 | 208 | 13,5% | 8 | 9,0% | 690 | 25% | |
| 5-6-2019 | 1906051 | 82 | 0,84 | 3 | 100 | 0,80 | 0,5 | 194 | 13,5% | 82 | 8,7% | 666 | 29% | |
| 5-6-2019 | 1906052 | 82 | 0,84 | 3 | 100 | 0,80 | 1,0 | 216 | 10,5% | 89 | 6,6% | 724 | 22% | |
| 7-6-2019 | 1906071 | 77 | 0,83 | 1,5 | 100 | 0,75 | 1,0 | 144 | 11,9% | 64 | 7,9% | 516 | 28% | |
| 11-6-2019 | 1906111 | 82 | 0,84 | 1,5 | 100 | 0,75 | 0,5 | 120 | 16,5% | 57 | 11,9% | 461 | 40% | |
| 11-6-2019 | 1906113 | 82 | 0,84 | 1,5 | 100 | 0,50 | 0,5 | 116 | 14,3% | 55 | 10,3% | 447 | 35% | |
| 11-6-2019 | 1906114 | 82 | 0,84 | 1,5 | 50 | 0,50 | 0,5 | 88 | 15,9% | 44 | 12,1% | 357 | 41% | |
| 11-6-2019 | 1906115 | 82 | 0,84 | 1,5 | 50 | 0,75 | 0,5 | 93 | 16,3% | 47 | 12,4% | 377 | 42% | |
| 14-6-2019 | 1906141 | 74 | 0,82 | 1,5 | 100 | 0,75 | 1,0 | 124 | 11,6% | 57 | 7,9% | 467 | 29% | |

In municipal WWTPs, dewatering of the sludge is one of the most significant cost factors. The magnetic separation process alters the sludge by removing vivianite. It is crucial to investigate if there is an effect of vivianite removal on the dewaterability of the sludge. Firstly, tests were performed with a capillary suction time (CST) device. A CST measures how long it takes for water to drain from the sludge into a filter paper. Secondly, centrifuge tests were performed on a larger scale with polymer addition.

CST tests

*Table S4.3: Dewaterability of raw and treated sludge determined with capillary suction time.*

| Type of sludge | # of tests performed | Time per gram of dry matter (total avg.) (s) | Time per gram of dry matter (st.dev) | Dry solids content (total avg.) (%) |
|---|---|---|---|---|
| Raw | 4 | 66 | 6 | 4.1±0.1 |
| Sieved | 4 | 76 | 10 | 3.9±0.1 |
| Tailings | 4 | 82 | 15 | 2.6±0.5 |

Comparing the dewaterability of three sludge types (digested sludge, filtered, and tailings), it can be seen that dewaterability decreases with each operational step. Overall, the CST results show an impact on the sludge of decreased dewaterability regarding tailings compared to raw digested sludge. The CST results show high variation and uncertainty and are not an accurate method to determine dewaterability. To confirm the indication that dewaterability decreased, centrifuge tests were performed.

## Centrifuge tests

A GEA decanter UCD 205-00-32 was rented for two days to perform dewaterability testing. Digested sludge and sludge processed by the magnetic separator (of which part of the vivianite was removed) (tailings) were tested. The parameters that were used and dewaterability results can be seen in Table S4.5. The average results and the standard deviation are given in Table S4.4. The polymer used for decanting was Kemira Superfloc C62089.

*Table S4.4: Average centrifuge dewaterability results*

| Type of sludge | # of tests performed | Polymer used (average) g/ kg dry solids | Dry solids content reached (average) % |
|---|---|---|---|
| Digested (raw) | 4 | 12±1 | 25±1 |
| Tailings | 8 | 14±4 | 24±1 |

On average, more polymer was needed to dewater the sludge, and a lower dry solids content was reached. This shows that the magnetic separation of vivianite may decrease the dewaterability of the remaining sludge. However, there are fewer solids to dewater, which is an advantage. By optimization of the polymer used, the dewaterability of tailings might be improved.

*Table S4.5: Centrifuge dewaterability results.*

| Feed | Test | Feed rate | Revs | Internal revs | torque | PE feed | Dilution | | | |
|---|---|---|---|---|---|---|---|---|---|---|
| | | m³/h | rpm | rpm | | g/min | l/min | dilution | g PE / kg ds | ds% cake |
| | 1 | 1,4 | 5595 | 3,1 | 0,46 | 12,5 | 6,0 | 0,21% | 13 | 24,5% |
| Digested sludge | 2 | 1,4 | 5595 | 3,2 | 0,56 | 10 | 6,0 | 0,17% | 10 | 25,7% |
| | 3 | 1,7 | 5595 | 3,5 | 0,49 | 15 | 9,0 | 0,17% | 13 | 25,0% |
| | 4 | 1,6 | 5596 | 3,2 | 0,47 | 12,5 | 7,5 | 0,17% | 11 | 25,3% |
| | 1 | 1,5 | 5600 | 2,8 | 0,42 | 10 | 6,0 | 0,17% | 14 | 24,6% |
| | 2 | 1,5 | 5600 | 2,8 | 0,16 | 5 | 3,0 | 0,17% | 7 | 23,1% |
| | 3 | 1,5 | 5600 | 2,8 | 0,4 | 12,5 | 7,5 | 0,17% | 18 | 24,8% |
| Processed sludge (tailings) | 4 | 1,5 | 5600 | 2,8 | 0,33 | 15 | 9,0 | 0,17% | 22 | 24,8% |
| | 5 | 1,5 | 5600 | 2,7 | 0,29 | 7,5 | 4,5 | 0,17% | 11 | 22,6% |
| | 6 | 1,5 | 5600 | 2,6 | 0,46 | 10 | 6,0 | 0,17% | 14 | 25,2% |
| | 7 | 1,5 | 5600 | 2,6 | 0,42 | 10 | 6,0 | 0,17% | 14 | 25,2% |
| | 8 | 1,5 | 5600 | 2,6 | 0,4 | 9 | 5,0 | 0,18% | 13 | 24,0% |

## Theoretical evaluation of the magnetic separation

As the sludge flows along the surface at a high magnetic gradient, the paramagnetic particles in the slurry are attracted towards the surface by a force

$$F_{magnetic} = \mu_0 \rho_p V_p \chi_p H \nabla H \qquad (4.3)$$

Here, $\mu_0 = 4\pi\,10^{-7}$ Tm/A is a universal constant of the laws of magnetics, $H$ (A/m) is the magnetic field, and $\nabla H$ (A/m²) is its gradient. The particle is defined by its density $\rho_p$ (kg/m³), its magnetic susceptibility $\chi_p$ (m³/kg) and its volume $V_p$ (m³). As the paramagnetic particles travel towards the surface, they experience a drag force. The vertical pulsation of the sludge exerts an additional drag force. The drag on the particle can be estimated by Stokes' formula:

$$F_{drag} = 3\pi\eta\Delta v D_p \qquad (4.4)$$

Here, $\eta$ (kg/m*s) is the dynamic viscosity of the slurry and $D_p$ (m) is the diameter of the particle.

These formulas show the effect of viscosity on the separation performance. With a higher viscosity, the drag force on the particles by the sludge increases, and a longer residence time is needed for a particle to reach the magnetic surface. Also, a larger magnetic force is needed to keep the particle attached to the magnetic surface.

The viscosity of sewage sludge was measured using an Anton Paar MCR302 rheometer.

15 ml samples were used for the rheological measurement. The rheometer has two concentric cylinders (a rotating measuring bob and stationary cup) as a rotational Couette geometry. The CC27 system was used, having a 26.656 mm bob diameter and a 28.920 mm cup diameter. The measurement temperature was set at 20°C. Another test was performed at a temperature

of 35°C, which is generally the temperature of sludge exiting the digester. The viscosity was measured with shearing rates ranging from 0.01 s$^{-1}$ to 1000 s$^{-1}$, with a decreasing time interval from 10 s to 1 s, both varied logarithmic, as previously done by Wei et al. 2018. Before this, the material was pre-sheared for 90 seconds with a rate of 1000 min$^{-1}$ to reach a homogeneous sample distribution, and then paused for 30 seconds. The flow curves for both 20°C and 35°C samples are shown in Figure S4.1.
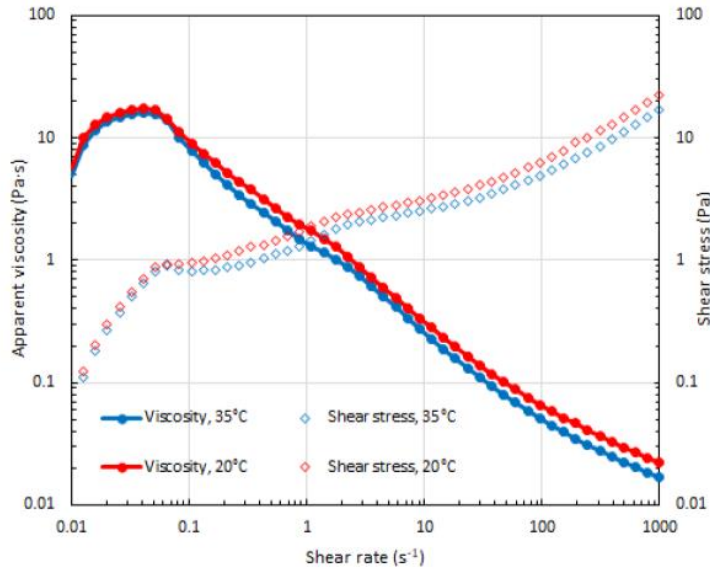


*Figure S4.1: Viscosity and shear stress of digested sewage sludge for 20 °Cand 35 °C*

It has been shown that digested sewage sludge displays shear-thinning behavior (Wei et al. 2018). This means that the viscosity of the sludge decreases with an increasing shearing rate. The measured rheology of this digested sludge agrees with the literature, as it also displays shear-thinning behavior.

The most common use of the VPHGMS is the beneficiation of low-grade (hematite) iron ore. The viscosity of digested sludge is comparable to that of hematite iron ore slurry (Sahoo et al. 2017). However, it must be noted that iron ore slurry processed with VHGMS typically has a much higher solids concentration of 20-40%. Digested sludge has a solids concentration of 4%, so the dry feed capacity for the purpose of treating digested sludge will be much lower.

*Table S4.6: Elemental composition of mixed vivianite concentrates from magnetic separation. Operational settings matrix 3mm, pulsation 100 rpm, Field 1T.*

| Element | Average (mg/kg) | Element | Average (mg/kg) |
|---|---|---|---|
| Aluminum | 4 | Lithium | <0,05 |
| Arsenic | <0,2 | Magnesium | 7 |
| Barium | 0.1 | Manganese | 1 |
| Berylium | <0,01 | Molybdenum | <0,05 |
| Boron | <0,05 | Nickel | <0,05 |
| Cadmium | <0,05 | Phosphorus | 95 |
| Calcium | 16 | Potassium | 0,7 |
| Cerium | <0,1 | Rubidium | <1 |
| Cesium | <2 | Selenium | <0,5 |
| Chromium | 0,05 | Silicon | 3 |
| Cobalt | 0,02 | Silver | <0,05 |
| Copper | 0,2 | Sodium | 0.7 |
| Gold | <1 | Sulphur | 5 |
| Iron | 250 | Tin | <0,05 |
| Lanthanum | <0,01 | Zinc | 0.5 |
| Total Carbon | 10 weight % | Total nitrogen | 1.1 weight % |

*Table S4.7: Heavy metal content of mixed vivianite concentrates from magnetic separation*

| Metal | Content (mg/kg dry matter) |
|---|---|
| Cadmium | 2 |
| Chromium | 80 |
| Mercury | 0,25 |
| Nickel | 40 |
| Lead | 50 |
| Arsenic | 4 |
| Copper | 220 |
| Zinc | 500 |

*Figure S4.2: Left : Slon-100 bench-scale VPHGMS. Picture courtesy of Outotec. Right: Slon-750 pilot-scale VPHGMS. Wokke (172cm) for scale.*
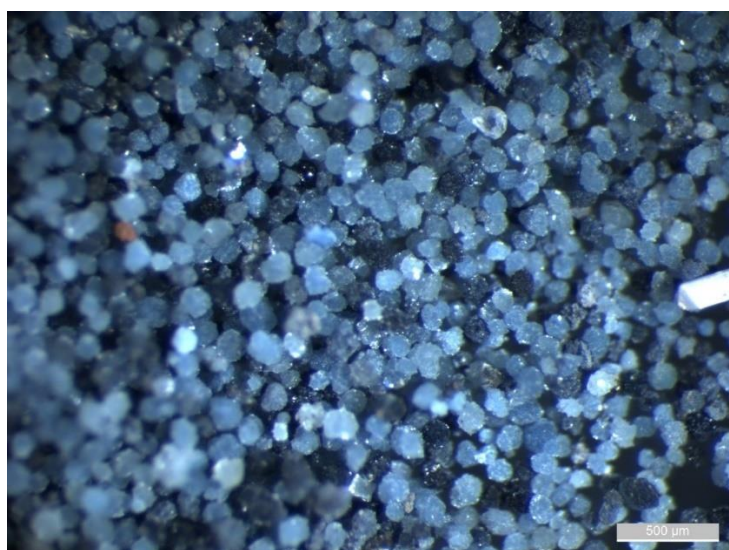


*Figure S4.3: Microscope picture of vivianite crystals magnetically recovered from digested sludge.*

# Chapter 5: Formation of vivianite in excess waste activated sludge and its correlation with Fe(III) reduction
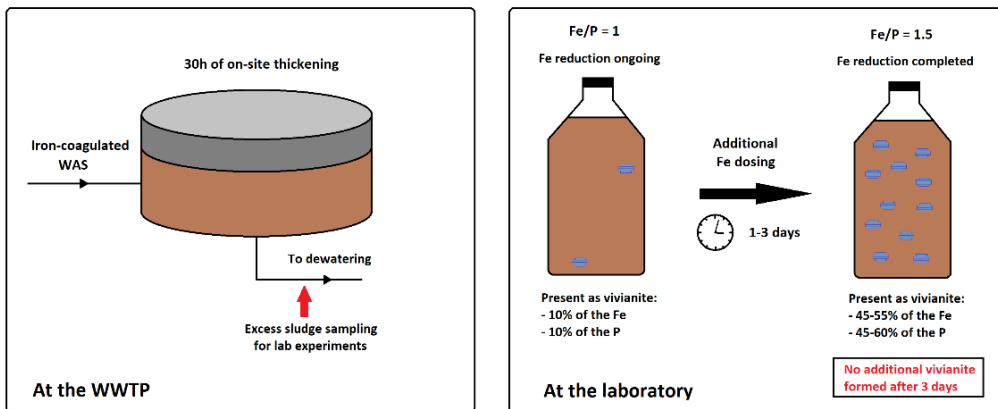
**Highlights**

- Iron reduction in excess activated sludge was completed after 2-4 days.

- Vivianite formation in excess activated sludge quickly followed iron reduction.

- Vivianite bore up to 55% of the iron and 60% of the phosphorus after 2-4 days of storage.

- Vivianite formation was almost completed after 2-4 days of storage.

- A sludge anaerobic digester is not necessary for the formation of vivianite in sewage sludge.

## Abstract

The iron phosphate mineral vivianite ($Fe_3(PO_4)_2 * 8H_2O$) received increasing attention since its ubiquity in digested sludge was shown in recent years. Vivianite can be magnetically extracted from digested activated sludge which opened a new route for phosphorus recovery. While its formation in digested sludge is regularly reported, it is not yet studied for fresh, undigested activated sludge. In particular, the extent to which vivianite could form during sludge storage is missing. The current research with full-scale WAS confirmed that the iron reduction rate in thickened sludge followed first-order rate kinetics with reduction rate constants of 0.03-0.05 $h^{-1}$. The reduction was completed after 2-4 days of anaerobic storage, and the vivianite appeared to form quickly from the pool of reduced iron made available. After sludge thickening at the WWTP (30 hours retention time), around 11% of the iron was vivianite. With subsequent 1-3 days of anaerobic storage, this fraction increased to 50-55%. After this storage, almost all the vivianite that could potentially form did form. The remaining iron was present as $FeS_x$, which preferentially formed over vivianite and soluble iron. This research concluded that efficient vivianite formation could be achieved without a sludge digester, showing phosphorus recovery potential from undigested sludge via vivianite recovery. Besides, the recovery of vivianite from undigested sludge presents advantages like the reduction of the sludge to dispose of and mitigation of the vivianite scaling formation.

**5**

## 5.1. Introduction

Phosphorus is an essential element for all living organisms. It is crucial in the energy metabolism (ATP), is vital for DNA and membrane lipid synthesis, and forms bones (Malhotra et al. 2018). The way phosphorus is produced nowadays through mining is not environmentally friendly, and the resources are depleting (Reijnders, 2014). The global reserves of phosphorus are estimated at $71*10^9$ metric tons, 70% of which being in Morocco and Western Sahara (Desmidt et al. 2014). In 2014 it was estimated that 180-190 million tons of phosphate rock are mined each year (Desmidt et al. 2014). Since Europe has no phosphorus reserves, its depletion is economically and politically disadvantageous due to future scarcity and dependence on the countries bearing the phosphate rock (Ott and Rechberger 2012). Society heavily relies on phosphorus, mainly because of its essential role in the agricultural and food production sector, although a fraction is also used in industrial processes (Withers et al. 2014). Around 80% of the mined phosphorus is used in the fertilizer industry (Van Vuuren et al.2010). A large fraction of the phosphorus ends up in the food, and after consumption, in the wastewater. Removal of phosphorus at Wastewater Treatment Plants (WWTPs) is essential since discharging too much phosphorus in surface water leads to eutrophication and harmful algal growth, causing hypoxia (Ryther and Dunstan 1971). Around 90% of the phosphorus in the influent of the WWTPs ends up in the sludge, which is, therefore, an interesting secondary source for phosphorus mining (Cornel & Schaum, 2009).

Phosphorus recovery from ash at central sludge mono-incinerations is well-developed and presents an interesting recovery of 60-90% of the phosphorus in the influent wastewater (Egle et al. 2016). However, decentralized phosphorus recovery would offer numerous advantages like better sludge dewatering, transportation costs reduction, and potentially reduced phosphorus scaling formation at the WWTP (Schemen 2017). Phosphorus recovery through struvite ($NH_4MgPO_4*6H_2O$) crystallization was one of the first decentralized methods developed where struvite can be used as a slow-release fertilizer (Partlan, 2018). A disadvantage of the struvite recovery approach is the limited phosphorus recovery, approximately 10-30% of the phosphorus in the influent (Wilfert et al. 2015). Moreover, this strategy is only applicable for WWTPs using Enhanced Biological Removal (EBPR).

Iron is commonly dosed in WWTPs using Chemical Phosphorus Removal (CPR) since it can remove phosphorus to a very low level. It is also beneficial for reducing hydrogen sulfide ($H_2S$) formation in biogas (Erdirencelebi and Kucukhemek 2018) and improve the flocculation of the sludge (Wilfert et al. 2015). The form of the precipitated iron phosphates has hardly been studied. Wilfert et al. 2016 showed that vivianite ($Fe_3(PO_4)_2*8H_2O$) was omnipresent in the sludge after anaerobic digestion. If the quantity of iron is high enough, vivianite can bear up to 70-90% of the phosphorus present in digested sludge (Wilfert et al. 2018). An increase of iron dosing in the waterline to minimize phosphate in the effluent showed quick and efficient vivianite formation in the digester (Chapter 3). Thanks to its paramagnetic properties' vivianite can be recovered from digested sludge via magnetic separation (Chapter 2, Salehin et al. 2020). This technology could recover more than 60% of the phosphorus from the influent wastewater at pilot scale (Chapter 4).

Iron reduction in iron-rich sludge kept under anaerobic conditions (like in digesters) is suspected to be the main trigger for vivianite formation (Azam and Finneran 2014, Zhang 2012, Wang et al. 2019, Chapter 3). However, the anaerobic residence time that is required for the optimum formation of vivianite is still unclear. Some research focused on the formation of vivianite in undigested sludge (Cheng et al. 2015) or septic water (Azam and Finneran 2014, Zhang 2012), but the majority of the studies were carried on digested sludge so far (Chapter 2 and 3, Wilfert et al. 2016, 2018, Frossard et al. 1997, Zhang et al. 2012, Roussel and Carliell-Marquet 2016). Digested sludge had a long anaerobic residence time (20-30 days) in a digester, which is favorable for vivianite formation. However, many WWTPs are not equipped with a digester while still dosing a high amount of iron. Therefore, it is crucial to study the possibility of vivianite recovery at WWTPs without digester since it represents an important part of the WWTPs. It may also be necessary concerning future developments related to resource recovery where organic substances (PHA, Kaumera) are produced from sewage sludge instead of producing biogas (Bengtsson et al. 2017, Wilfert et al. 2015).

Iron reduction in activated sludge kept under anaerobic conditions has already been studied (Nielsen et al. 1997, Rasmussen and Nielsen 1996). Recently, Wang et al. 2020 showed that the iron reduction was well-advanced after a day of storage in anaerobic conditions and that some vivianite could already form in this timeframe. However, vivianite formation at room temperature was never studied for residence times longer than a day since these conditions do not occur in standard WWTP operations (temperature and residence times are higher in anaerobic digesters). The current study investigates the correlation between iron reduction in thickened sludge and possible vivianite formation. This research was done with sludge obtained from a full-scale WWTP with chemical phosphate removal. The importance of these findings will be discussed in the scope of phosphorus recovery from undigested sludge.

## 5.2. Material & methods

### 5.2.1. Sludge samples

Thickened sludge from the WWTP Hoensbroek, operated by Waterschapsbedrijf Limburg (The Netherlands), was collected 30 minutes before the beginning of each experiment. The sludge was sampled from a tap downstream from the thickener. At this installation, iron is dosed in the aeration tank for phosphorus removal to achieve a phosphorus level of around 0.4ppm in the effluent. The surplus sludge goes to a thickener with a solid residence time of approximately 15 hours under regular operation but was 30h during the sampling period. In this thickener, external sludge from WWTP Abdissenbosch is added. The thickened sludge is then dewatered by centrifugation and transported for disposal. There is no sludge digester in WWTP Hoensbroek.

### 5.2.2. Method of lab experiments

Three experiments were carried out: a blank with no extra iron addition, a run with the addition of $FeCl_3$, and one with $FeCl_2$. The dosage of $FeCl_3$ or $FeCl_2$ was calculated on the sludge composition for all the phosphorus to precipitate as vivianite potentially. The quantity of iron added was calculated considering that iron will first precipitate as FeS and only then as

vivianite as suggested in Chapter 3. Unfortunately, the composition of the sludge changed right before the experiments' start (due to an unexpected higher thickening time of 30h instead of 15h), meaning that the iron added was not sufficient to convert all the phosphorus into vivianite.

Thickened sludge was poured until the brim in a 1L sealed bottle and kept under constant stirring at 1000-1200 rpm for the experiments' duration. Iron salts were added immediately after the initial sampling. Samples were taken at: 0 (before iron addition), 0.5, 1, 2, 4, 8, 24, 48, 72, 96, 168, 216 and 264 hours. Note that the sludge had a residence time of 30h in the thickener, so the actual anaerobic residence time of a sample is 30h more than its sampling time.

For each sample, pH and ORP were measured, and three homogenized sludge samples are taken:

- 25 ml of sludge was poured into a pre-weight aluminum tray and dried at ambient temperature. The solid content was determined, and a fraction of the sample was used for elementary composition analysis (Microwave digestion followed by ICP-OES). The samples were always dried at ambient temperature since higher temperatures can provoke the evaporation of the crystal water in vivianite, potentially damaging its structure (Chapter 2).
- 15 ml of sludge was centrifuged for 12 minutes at 4000 rpm, and the centrate was filtered with a 0.45 um hydrophilic filter. The phosphate and iron ($Fe^{2+}$ and $Fe^{3+}$) concentrations in the centrate were immediately measured with Hach-Lange kits (LCK 321). The cake was dried at ambient temperature and stored for microscope, XRD, and Mössbauer spectroscopy analyses.
- 4 ml of sludge was added to 16 ml of 0.5 HCl solution for the iron extraction, based on protocols described in Rasmussen and Nielsen 1996 and Nielsen et al. 1997. This solution was gently stirred for 15 minutes and filtered with a 0.45 um hydrophilic filter to determine the total phosphate and $Fe^{2+}/Fe^{3+}$ concentration in the whole sludge.

### 5.2.3. Analyses

Firstly, around 50 mg of powdered sample dried at room temperature was added in a Teflon vessel with 10 mL of ultrapure $HNO_3$ (64.5 – 70.5% from VWR Chemicals). The mixture was digested in an Ethos Easy digester from Milestone equipped with an SK-15 High-Pressure Rotor. It reached 200 °C in 15 min, stayed at this temperature for 15 min, and cooled down for 1h. The digestate was diluted, and their composition was evaluated with Inductively Coupled Plasma (Perkin Elmer, type Optima 5300 DV) equipped with an Optical Emission Spectroscopy (ICP-OES). The rinse and internal standard solution were respectively 2% of $HNO_3$ and 10 mg/L of Yttrium. The software Perkin Elmer WinLab32 was used for data processing.

Microscopy observations were performed on the samples dried without centrifugation to avoid embedding the crystals in the sludge matrix, making the observations challenging. The light microscope used was a Leica MZ95 equipped with a Leica DFC320 camera. The Scanning

Electron Microscope (SEM) apparatus was a JEOL JSM-6480 LV equipped with an Oxford Instruments x-act SDD Energy Dispersive X-ray (EDX) spectrometer. The accelerating voltage was 15 kV for a working distance of 10mm. Before measurements, 10 nm-layer of gold were deposited on the samples using a JEOL JFC-1200 fine coater to make the surface electrically conductive. The software used was JEOL SEM Control User Interface for the SEM and Oxford Instruments Aztec for the EDX data processing.

For XRD and Mössbauer spectroscopy measurements, the samples were centrifuged and the centrate removed before drying to avoid precipitation from the soluble ions during drying. The samples were then pulverized in a mortar for analysis. The XRD device was a Bruker D8 Advance diffractometer in Bragg-Brentano geometry with a Lynxeye position-sensitive detector, with Cu-Kα radiation, range 10-80°2θ, step size 0.008°. The Bruker DiffracSuite.EVA software vs 5.2 was used for the peak assignment and identification. Quantification was done with Profex-BGMN Rietveld software. While XRD only focuses on the crystalline fraction, Mössbauer spectroscopy detects the iron in both crystalline and amorphous forms and is, therefore, a practical way to quantify vivianite. The $^{57}$Fe Mössbauer absorption spectra were collected at 300 K with a conventional constant-acceleration spectrometer using a $^{57}$Co (Rh) source. The velocity calibration was carried out using an α-Fe foil while the fitting of the spectra was performed using the software Mosswin 4.0 was used (Klencsár 1997).

## 5.3.   Results and discussion

This study aimed to study the possibility of vivianite formation in excess activated sludge before anaerobic digestion. The iron reduction kinetics in thickened sludge dosed with iron salts was first investigated before looking at the correlation with vivianite formation. The interactions between iron and sulphur were also discussed. Finally, the opportunities for phosphorus recovery opened by this study were evaluated.

### 5.3.1.  Iron reduction

Anaerobic conditions were present in the three samples due to the oxygen consumption of the bacteria community and the absence of aeration. The ferric iron present in the liquid and the solid phase was progressively reduced. Figure 5.1 shows that when no iron or only ferrous iron was added, the reduction was completed within 24h, while it required 72h when additional ferric iron was added. The reduction kinetics were evaluated for the time 0-24h for the experiment without extra iron and the experiment with ferrous iron addition, and 4-72h when ferric iron was added to only consider the timeframe when the reduction takes place. The reduction followed a first-order kinetics in the three experiments (no additional iron $R^2$=0.84, ferrous addition $R^2$=0.99, ferric addition $R^2$=0.98, which agrees with previous studies (Wang et al. 2019, Hacherl et al. 2003) on the reduction of iron oxide/hydroxides). The first-order modeling allowed the reduction rate constants' determination at 0.03, 0.04, and 0.05 h$^{-1}$ for the experiment without additional iron, the addition of ferrous and ferric iron, respectively. Those values aligned with those of Wang et al. 2019 (k=0.05-0.06 h$^{-1}$), who worked with settled activated sludge. They also carried out autoclaved experiments that showed that the reduction

process was 95% biological-based. In the current study, the initial specific iron reduction rate was 0.9 g Fe/g VS*h (VS=Volatile solids) when no iron was added.

In comparison, it was 1.2 g Fe/g VS*h after both Fe(II) and Fe(III) dosing resulting in rate constants of $0.007h^{-1}$ in the three cases. These rates are the low range of the one previously observed by Nielsen et al. 1997, Rasmussen and Nielsen 1996, Wang et al. 2019, ranging from $0.007\text{-}0.07\ h^{-1}$. The low specific rate observed in the current study can be explained by the fact that the reduction was already well-advanced when the samples were collected after 30h of thickening (60-65% of the total iron were already Fe(II)). On the contrary, the samples collected in the other studies were fresh activated sludge in which Fe(III) would account for 70-90% of the total iron (Rasmussen and Nielsen 1996).
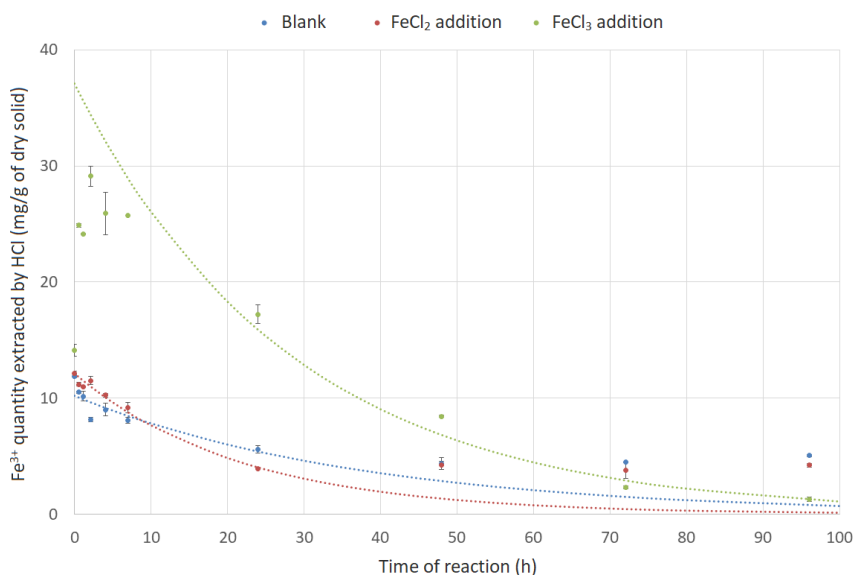


Figure 5.1: Evolution of the ferric iron concentration after HCl extraction. The low initial content of $Fe^{3+}$ can be explained by the 30h of thickening at the WWTP before the sampling, allowing Fe(III) to be partly reduced. The dash lines represent the first-order fit and are valid until the reduction is over (0-24h for no addition and Fe(II) addition and 4-72h for Fe(III) addition). The data for 172h, 216h, and 264h are not shown here since the iron concentration reached a steady state by that time. The total iron content in the samples is 38, 51, and 53 mg/g of dry solids for the experiment with no addition, Fe(II) addition, and Fe(III) addition.

The reduced ferric iron was essentially from the solid phase since the soluble Fe3+ in all three experimental conditions stayed around 5-20ppm (0.15-0.6 mg/g of dry solid), which was negligible compared to the total quantity of Fe(III) reduced (Figure 5.1). A part of the Fe(III) (1-3 mg/g of dry solids) persisted even after 11 days of experiments in anaerobic conditions, suggesting the presence of a minor and stable Fe(III) phase or partial oxidation of vivianite during sample manipulation. Extractions with HCl were used in this study to solubilize the iron present in the solid and study its oxidation degree. This method appeared to be suitable for this purpose since total iron recovery from the solids were 80±9%, 87±7%, and 86±9% for the case of no iron, ferrous and ferric additions, respectively. The iron recovery after HCl

extraction progressively increased with the time after which the sample was taken. Rasmussen and Nielsen 1996 reported similar findings with 80-90% of recovery during HCl extraction and slightly higher recovery in sludge stored anaerobically for two days than in fresh sludge. This suggests that the iron species became increasingly soluble in HCl over time, which agrees with the progressive formation of vivianite and FeSx, both soluble in HCl. In the current study, the iron compounds initially present in the thickened sludge and the Fe(III) compounds precipitated after the iron salts' addition were largely reduced in 2-4 days. It is important to note that not all iron sources are suitable for iron reduction and subsequent vivianite formation. Cheng et al. 2015 showed that ferrihydrite (added to digested sludge) could be reduced within five days while the more stable hematite stayed inert throughout 30 days of incubation in anaerobic conditions.

The current results confirm what was already observed in a few studies involving short-term experiments: the iron reduction is relatively quick in sludge systems under anaerobic conditions. Additionally, this study reveals that the iron reduction is completed after 2-4 days, depending on the iron source used. The following section evaluates the correlation between iron reduction and vivianite formation.

### 5.3.2. Vivianite formation

Vivianite has been widely reported as the dominant phosphate mineral in digested sludge (Chapter 2 and 3, Wilfert et al. 2016, 2018, Frossard et al. 1997, Zhang et al. 2012, Roussel and Carliell-Marquet 2016). Its formation in waste activated sludge (WAS) before digestion was more rarely discussed. Studies involving sludge before digestion mainly considered vivianite as a way to recover phosphorus after its release from WAS by pH modification (Cao et al. 2019, Li et al. 2020, Wu et al. 2020a). Some studies mentioned the presence of vivianite in sludge before digestion, mainly in surplus sludge (Wilfert et al. 2018, Wang et al. 2019, Chapter 3, Salehin et al. 2020). Still, these studies mainly focused on vivianite formation in digested sludge.

In the current study, the formation of vivianite in thickened sludge was evaluated after a few days of storage under anaerobic conditions and, for some experiments, after the addition of iron salts. Vivianite could be observed in all the samples (besides in the initial thickened sludge) by light microscope and SEM-EDX. The blue color of oxidized vivianite particles makes their identification relatively easy with a light microscope (Figure 5.2). The particles observed by SEM, composed of agglomerates of needles/plates (Figure 5.2), presented a similar morphology as vivianite observed in digested sludge (Wilfert et al. 2016, Chapter 3), lake sediments (Vuillemin et al. 2020), or synthesized vivianite (Zelibor et al. 1988). The EDX scans of those particles indicated that iron and phosphorus were the major elements present, with Fe/P molar ratios comprised between 1.3 and 1.7 (1.5 in pure vivianite).
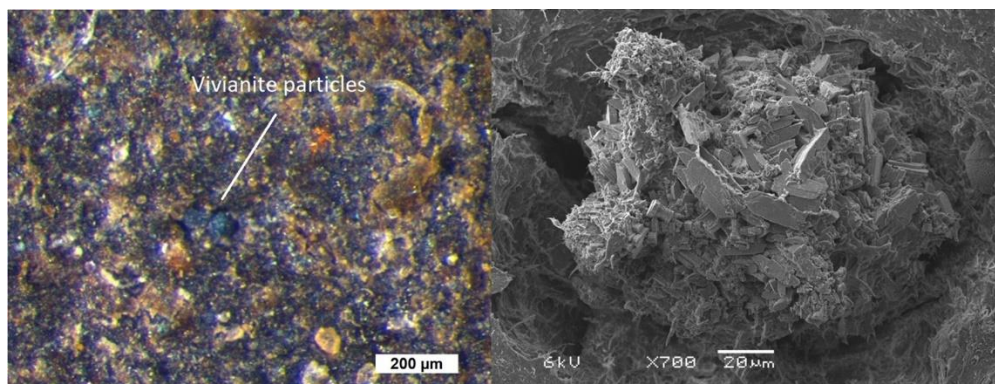
*Figure 5.2: Left: light microscope picture of blue vivianite crystals in the sample without extra iron addition after 24h / Right: SEM picture of a vivianite particle in the sample without extra iron addition after 24h.*

Frossard et al. 1997 reported that vivianite particles were smaller in non-digested sludge than after digestion. In the current study, the vivianite particles had a size in the range of 50-200 µm, which agrees with vivianite particles' size in digested sludge mentioned in the literature (Wilfert et al. 2018, Chapter 2). No significant size or morphology differences were observed depending on the time of sampling or oxidation degree of the iron salt used. Frossard et al. 1997 reported that vivianite was more crystalline after digestion, while Wu et al. 2020b observed that the iron phosphates were mostly amorphous in aerobic sludge with only a tiny fraction of vivianite. Mössbauer spectroscopy revealed that around 10% of the iron in the initial thickened sludge was vivianite. XRD did not detect any crystalline vivianite in this sample. It suggests that the vivianite formed in the initial stage of anaerobic storage (after 30h of thickening for this sample) could be composed of tiny crystals. XRD confirmed that vivianite was present in all the other samples. Additionally, the quantity of vivianite detected by XRD did not significantly increase between the time when the iron reduction was complete (24h or 72h according to Figure 5.1) and after 168h (Figure S5.1), which suggests that vivianite formation shortly followed iron reduction. It needs to be noted that the conclusions based on the XRD results are only made on the crystalline fraction of the sample and do not allow vivianite quantification.

### 5.3.3. Vivianite formation and iron reduction

Mössbauer spectroscopy is a powerful tool to analyze vivianite in sludge. This mineral gives two characteristic doublets, corresponding to the two sites where $Fe^{2+}$ can be present in the vivianite structure ($Fe^{2+}$ site A: Isomer Shift (IS) = 1.2 mm/s, Quadrupole Splitting (QS) = 2.4 mm/s and $Fe^{2+}$ site B: IS = 1.2 mm/s, QS = 3.0 mm/s, McCammon and Burns 1980, Rouzies and Millet 1993, Nembrini et al. 1983). During the present study, the samples could not be prepared under oxygen-free conditions at the WWTP site, and therefore, a part of the $Fe^{2+}$ got oxidized (Čermáková et al. 2013, McCammon and Burns 1980). Unfortunately, the signal of $Fe^{3+}$ atoms in vivianite is strongly overlapping with those of FeS compounds and other Fe(III) species present in sludge, making the quantification of $Fe^{3+}$ atoms in vivianite very complicated. We proposed in Chapter 3 to fit the $Fe^{3+}$ in vivianite as a doublet with the parameters IS=0.46 mm/s and QS=0.63 mm/s. Still, it led to incoherent results with the current

set of samples due to the higher share of oxidized vivianite (the samples in Chapter 2 and 3 were protected from oxygen as much as possible). Therefore, an alternative way of fitting was used. Since all samples were exposed to oxygen for the same amount of time during drying, sample storage, and preparation, it was assumed that the vivianite was oxidized to the same degree in all the samples. Previous research on natural (Dormann and Poullen 1980) and synthetic vivianite (Rouzies and Millet 1993) showed that vivianite oxidation reached a (meta)stable equilibrium when around 30% of the Fe(II) was oxidized. It agrees with the measurements of dozens of our samples of synthetic vivianite and vivianite extracted from digested sludge (unpublished data). Therefore, the share of the iron present as Fe(II) in vivianite was determined with Mössbauer spectroscopy and multiply by (0.3/0.7) to obtain the share of ferric iron present in vivianite.

Mössbauer spectroscopy revealed that the share of the iron present as vivianite significantly increased from 11% in the initial thickened sludge to 50-55% in the sludge sampled after 24h or 72h of additional anaerobic residence time (Figure 5.3 and Table S5.2). This percentage further increased by 10-15% after 168h for the sample without iron addition and with the addition of Fe(II) salt, while it stayed constant when Fe(III) was added. The sampling time of 24h (for no and Fe(II) addition) and 72h (for Fe(III) addition) correspond to the moment when the iron reduction was almost completed (Figure 5.1). The results show that 70-100% of the vivianite formed after 168h of anaerobic residence time was already formed after 24h or 72h. The fact that the vivianite formation was already so advanced after this time suggests that vivianite formation was strongly correlated to iron reduction.

Azam and Finneran 2014 and Zhang 2012 already noticed that phosphorus removal in septic water led to vivianite formation. Cheng et al. 2015 suspected that the Fe(III) reduction in WAS provoked vivianite formation (without solid evidence). Wang et al. 2019 investigated the iron reduction and confirmed that vivianite formed but stopped their experiment after 24h, not getting the opportunity to evaluate the maximal potential of vivianite in undigested sludge. The amount of vivianite formed compared to the theoretical maximum of vivianite could be calculated in the current study. Firstly, only the iron present as Fe(II) could potentially be vivianite (estimated by HCl extractions). Secondly, it was hypothesized that all the sulphur present in the sample would bind iron in a 1:1 molar ratio based on observations on digested sludge in Chapter 3. If the sum of the Fe(II) present as $FeS_x$, as vivianite, and in solution is equal to the total Fe(II) obtained by HCl extraction, it indicates that there are no other Fe(II) phases. Figure 5.3 shows that the sum of those 3 Fe(II) species is similar to the total Fe(II) in the samples with at least 24h of additional anaerobic stage, suggesting that the ferrous iron present in the solids are either vivianite or $FeS_x$. After 30h of sludge thickening (marked as 0h on Figure 5.3), not all the Fe(II) are accounted for (Total Fe(II)>soluble+vivianite+$FeS_x$), suggesting the presence of a ferrous species, intermediate to the formation of vivianite and ferrous sulphide.

From these observations, it can be concluded that more than 80% of the vivianite that could form (based on the pool of Fe(II) in the samples that are not present in $FeS_x$) was formed as soon as the iron reduction was completed. It suggests that a sludge digester is not necessary for vivianite formation. The fact that vivianite formation is already maximized after 24h in the sludge with no iron addition hints that the addition of iron early in the wastewater treatment

process could allow faster vivianite formation. The addition of iron in the waterline would also lead to a beneficial decrease of the soluble phosphate present in the effluent.
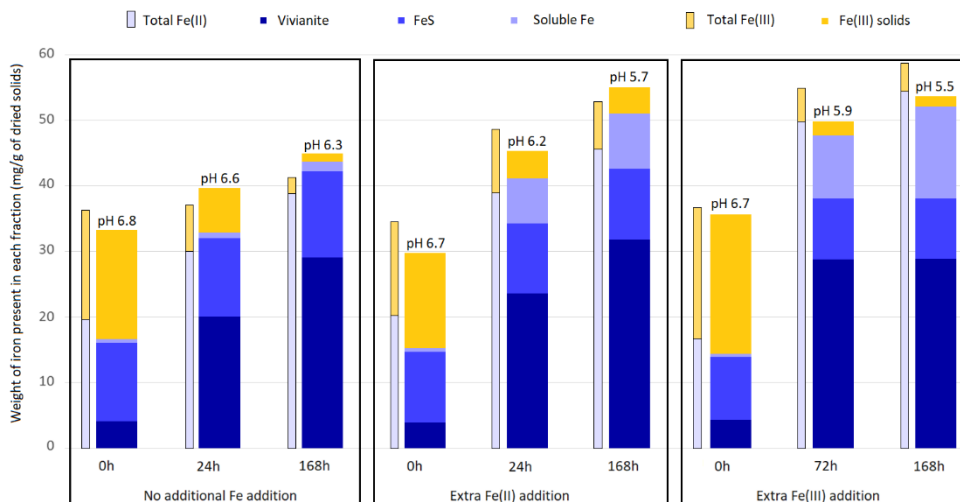


*Figure 5.3: Iron speciation (primary axis) and pH (secondary axis) in the seven samples analyzed. The quantification method for each iron fraction is described here. Vivianite: Mössbauer spectroscopy, FeS: assuming that all the sulphur in the solids bind iron in a 1:1 molar ratio, Fe(III): HCl extraction of the solids followed by ICP-OES, Soluble Fe: ICP-OES of the filtrate (>80% is $Fe^{2+}$). The vivianite quantity in the samples "0h, no additional Fe" and "0h, extra Fe(II)" were estimated based on the Mössbauer spectroscopy results of the sample "0h, extra Fe(III)". Note that all the samples were under anaerobic conditions in the sludge thickener for 30h before being sampled and used for the experiments; 0 h corresponds to 30h of thickening at the WWTP.*

Around 120 mg/g of vivianite would form in both sludges amended with iron, hypothesizing that all the additional iron would be transformed into vivianite. After 168h, the quantity of vivianite formed was 85 mg/g of dry solids when no iron or Fe(III) was added, 97 mg/g when Fe(II) was added. This shows that only a low share of the iron added is transformed into vivianite. Figure 5.3 indicates that this difference can mainly be explained by the lower pH of those sludges, resulting in 15-25% of the iron becoming soluble against less than 5% when no iron is added. Even though the additional iron is not immediately transformed into vivianite in those experiments, it does not mean that it is lost. The supernatant of the thickener would be recirculated in the WWTP, diminishing the iron quantity needed for phosphorus removal in the activated sludge and vivianite formation in the thickened sludge. Alternatively, different iron sources could be used to prevent the considerable pH decrease observed in these experiments. It is important to note that after 168h, around 50-55% of the phosphorus was bound as vivianite when no additional iron was dosed, while it accounted for 65-70% when extra iron was dosed. This increase is mainly due to the decrease in the initial phosphorus content of the sludge for the samples with iron addition.
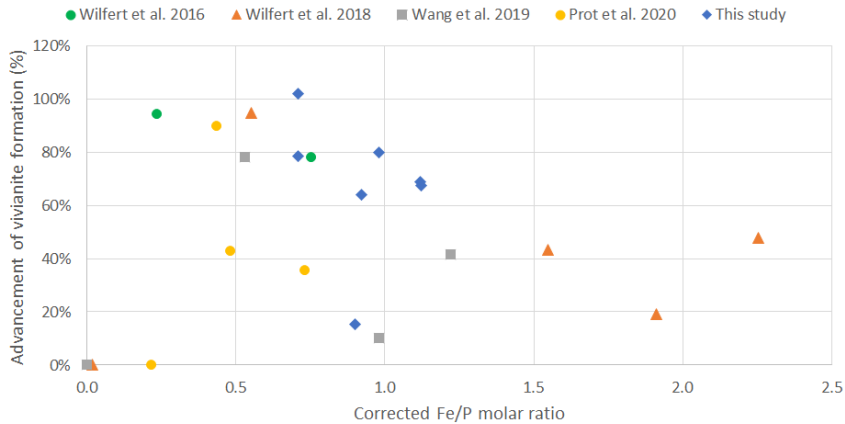
*Figure 5.4: Percentage of vivianite formed compared to the maximum vivianite that could form. The maximum vivianite that can form was calculated based on the elemental composition of the sludge assuming that FeS forms first, immediately followed by vivianite. The corrected Fe/P molar ratio is based on the total iron minus the iron precipitating as FeS. All the samples represented in the figure are undigested sludge.*

Wilfert et al. 2018 showed that the amount of phosphorus present as vivianite in digested sludge increases with the Fe/P ratio. They also noticed that no pattern could be seen in surplus sludge samples. Data from four studies quantifying vivianite in undigested sludge were plotted along with the current research data to study possible correlation. The advancement of the vivianite precipitation, defined as the amount of vivianite formed compared to the maximum vivianite expected, did not show a clear pattern either, and an even larger variation in the vivianite formation advancement (Figure 5.4). It is likely connected to the differences in times under which the samples were kept under anaerobic conditions, strongly impacting the share of iron reduced, and thus vivianite formation. For example, some of the samples in Figure 5.4 were WAS while others were surplus sludge, the second facing longer anaerobic retention times than the first. The share of iron present in the soluble phase (strongly depending on the pH) was not considered to calculate the vivianite formation advancement. Figure 5.4 also shows that it is not rare that more than 60% of the vivianite is already formed before digestion, strengthening the fact that anaerobic digestion is not necessary to form substantial quantities of vivianite.

## 5.3.4. The formation of sulphide does not provoke the destruction of the formed vivianite

Iron-sulphur interactions are essential in wastewater treatment. The addition of sulphide to digested sludge or activated sludge provokes phosphorus release (Wilfert et al. 2020, Lippens and de Vrieze 2019). It can also play a role in the chemical reduction of iron (Wilfert et al. 2020, Wang et al. 2019, Wilén et al. 2000). Since $FeS_x$ forms preferentially over vivianite during anaerobic digestion (Roussel and Carliell-Marquet 2016, Wilfert et al. 2018, Chapter 3), it can be concluded that $FeS_x$ is thermodynamically favored over vivianite. While a significant quantity of vivianite was formed after a few days of anaerobic residence time

(Figure 5.3), the progressive reduction of sulphate to sulphide could provoke the destruction of vivianite due to the higher affinity of iron to sulphide than to phosphate.

Reduction of sulphate by sulphate reducing bacteria is a prerequisite for the formation of $FeS_x$ and the destruction of vivianite (Rubio-rincón et al. 2017). Ingvorsen et al. 2003 showed that sulphate reduction begins as soon as anaerobic conditions are present, as observed for the iron reduction in this study. The sulphate reduction is linear in the first 4-5h after the anaerobic conditions start and only becomes exponential after this time (Ingvorsen et al. 2003). Based on the kinetic model proposed by Ingvorsen et al. 2003, more than 70% of the sulphate would already be reduced after 54h of anaerobic exposure. According to literature, the reduction of sulphate and the formation of vivianite should happen at the same time, so it could be hypothesiszed that the vivianite should not be destroyed because of subsequent ironsulphide formation. In the current study, a significant vivianite quantity was already formed after 54h (30h of thickening + 24h of experiment) (Figure 5.3). The fact that the vivianite quantity did not decrease after 198h of anaerobic residence time (30h of thickening + 168h of experiment) (Figure 5.3) reinforces this hypothesis.

### 5.3.5. The recovery of phosphorus from undigested sludge is relevant

According to the present study, a retention time of 2-4 days under anaerobic conditions in a sludge thickener or buffer tank would be sufficient for most iron to be reduced and for vivianite to form. In the WWTP of Hoensbroek, the Fe/P molar ratio in the thickener is 0.9-1.0 and was increased to 1.4-1.6 during lab-scale experiments. According to the stoichiometry of vivianite, a Fe/P molar ratio of 1.5 is necessary for maximal vivianite formation. Before any vivianite can form, 1 mole of iron is consumed per mole of sulphur in the sludge, assuming the same behavior as in digested sludge (Chapter 3). Considering this, the Fe/P molar ratio needed to achieve the stoichiometric formation of vivianite theoretically is 1.8 at the WWTP Hoensbroek.

According to Wilfert et al. 2018, the phosphorus quantity present as vivianite is limited to 70-90%, even at Fe/P molar ratio above 2, most likely due to a fraction of phosphorus present in the biomass. Therefore, a molar Fe/P ratio of 1.5 seems like a good alternative between a low quantity of vivianite formed and dosing excessive iron only to convert a small additional fraction of phosphorus to vivianite. If the WWTP Hoensbroek increased its iron dosage to match this ratio, it would correspond to an additional chemical cost of 45,000 € per year. Around 55% of the phosphorus would be present as vivianite based on the results of this study. Hypothesizing that the vivianite would be removed magnetically from the sludge with the same efficiency as the one shown at pilot-scale by Wijdeveld et al. 2021 (80% of vivianite recovery from digested sludge), less sludge would have to be disposed of. The sludge disposal costs saving in the Netherlands would approximate 108,000 € per year to recover 460 tons of vivianite per year, compensating the additional chemical costs (detailed calculation in Supplementary information). The operational costs and the commissioning of a larger thickener or an extra storage tank need to be considered to get a complete overview of the situation, but an entire economic study is not the scope of this research.

Besides the phosphorus recovery, the additional iron dosing and 2-4 days anaerobic retention time could present other advantages. Firstly, the recirculation to the waterline of the iron-rich

liquid fraction after thickening would lead to lower phosphorus in the effluent. Moreover, the additional iron earlier in the waterline would allow more time for vivianite to form whenever anaerobic/anoxic zones are encountered in the treatment, compared to dosing only in the thickener. Secondly, the reduction of the phosphorus content in the sludge is better for its valorization in cement kilns, according to Husillos Rodriguez et al. 2013, which is the current disposal route Hoensbroek WWTP dewatered sludge. It should be noted that the share of phosphorus present as vivianite would be higher than 60% with the same iron dosing if the pH would be higher since the saturation index of vivianite strongly depends on the pH (Liu et al. 2018). The addition of iron without a pH drop could be realized using other iron sources like drinking water sludge. A fermenting sludge at a pH<6 is favorable for the production of Volatile Fatty Acids (VFA) while inhibiting methanogenesis, making it a valuable feed for biobased industries (Kleerebezem et al. 2015), for example, for the production of polyhydroxyalkanoates (PHA) (Bengtsson et al. 2017).

It is essential to also take into consideration the effect that the iron dosing and the prolonged anaerobic retention time could have on vivianite scaling mitigation. Vivianite scaling is scarcely reported in the literature (Marx 2001, Shimada et al. 2011, Bjorn 2010, Pathak et al. 2018). Still, it appears that the problem is occurring to a vast extent, according to Chapter 6. It is especially the case in the WWTP of Hoensbroek, where scaling occurs in the pipeline between the thickener and the centrifuge, in the centrifuge itself, and the centrate pipe. Consequently, the centrifuge needs to be cleaned every 1-2 weeks, and the centrate pipe has to be cleaned or replaced every year. The iron reduction still ongoing after thickening appears to be an important trigger of the scaling formation (Chapter 6). The use of a longer residence time during thickening would promote vivianite formation and allow the iron reduction to be complete, which would help mitigate vivianite scaling.

## 5.4.  Conclusion

During this study, iron-containing WAS was sampled after 30h of thickening, and ferric or ferrous salts were added in some of the samples. The iron reduction and the vivianite formation were monitored in these samples. The iron reduction was completed after 2-4 days of total anaerobic storage (k=0.03-0.05 s$^{-1}$). The formation of vivianite was strongly correlated to the iron reduction since the share of iron present as vivianite increased from 10% (after 30h of thickening at the WWTP) to 50-55% (after 1-3 days of additional anaerobic storage) after most of the iron was reduced. It corresponded to 75-100% of the vivianite that could potentially form, taking into account the preferential formation of $FeS_x$. Up to 70% of the phosphorus could be present as vivianite after additional iron dosing, even though a part of the iron was still soluble due to the pH decrease. The central message of this research is that vivianite can form to a large extent not only in digested sludge but also in surplus WAS, opening the door for phosphorus recovery for WWTP not equipped with a sludge digester.

## Acknowledgments

**5**

## References

Azam, H. M., & Finneran, K. T. (2014). Fe(III) reduction-mediated phosphate removal as vivianite (Fe3(PO4)2·8H2O) in septic system wastewater. *Chemosphere*, 97, 1–9. doi:10.1016/j.chemosphere.2013.09.032.

Bengtsson, S., Werker, A., Visser, C., Korving, L. (2017). Stepping stone to a sustainable value chain for PHA bioplastic using municipal activated sludge. STOWA report.

Bjorn, A., (2010). Acid Phase Digestion at Derby STW - Context and preliminary optimisation results. Last consulted on 03/03/21 at https://www.atkinsglobal.com/~/media/Files/A/Atkins-Corporate/group/sectors-documents/water/library-docs/technical-papers/acid-phase-digestion-at-derby.pdf.

Cao, J., Wu, Y., Zhao, J., Jin, S., Aleem, M., Zhang, Q., Fang, F., Xue, Z., Luo, J. (2019). Phosphorus recovery as vivianite from waste activated sludge via optimizing iron source and pH value during anaerobic fermentation. *Bioresource Technology*, 122088. doi:10.1016/j.biortech.2019.122088.

Čermáková. Z., Švarcová. S., Hradil. D., Bezdicka. P. (2013). Vivianite: A historic blue pigment and its degradation under scrutiny. *Science and Technology for the Conservation of Cultural Heritage,* 75-78.

Cheng, X., Chen, B., Cui, Y., Sun, D., & Wang, X. (2015). Iron(III) reduction-induced phosphate precipitation during anaerobic digestion of waste activated sludge. *Separation and Purification Technology*, 143, 6–11. doi:10.1016/j.seppur.2015.01.002.

Cornel, P., & Schaum, C. (2009). Phosphorus recovery from wastewater: needs, technologies and costs. *Water Science and Technology*, 59(6), 1069–1076. doi:10.2166/wst.2009.045.

Desmidt, E., Ghyselbrecht, K., Zhang, Y., Pinoy, L., van der Bruggen, B., Verstraete, W., Rabaey, K., Meesschaert, B. (2014). Global phosphorus scarcity and full-scale P-recovery techniques: A Review. *Critical Reviews in Environmental Science and Technology*, 45(4), 336–384. doi:10.1080/10643389.2013.866531.

Dormann, J-L., Poullen, J-F. (1980). Étude par spectroscopie Mössbauer de vivianites oxydées naturelles. *Bulletin de Minéralogie*, 103, 6, 633-639. https://doi.org/10.3406/bulmi.1980.7431.

Egle, L., Rechberger, H., Krampe, J., & Zessner, M. (2016). Phosphorus recovery from municipal wastewater: An integrated comparative technological, environmental and economic assessment of P recovery technologies. *Science of The Total Environment*, 571, 522–542. doi:10.1016/j.scitotenv.2016.07.019.

Erdirencelebi, D., & Kucukhemek, M. (2018). Control of hydrogen sulphide in full-scale anaerobic digesters using iron (III) chloride: performance, origin and effects. *Water SA*, 44(2), 176. doi:10.4314/wsa.v44i2.04.

Frossard, E., Bauer, J. P., & Lothe, F. (1997). Evidence of vivianite in FeSO4-flocculated sludges. *Water Research*, 31(10), 2449–2454. doi:10.1016/s0043-1354(97)00101-2.

Hacherl, E. L., Kosson, D. S., & Cowan, R. M. (2003). A kinetic model for bacterial Fe(III) oxide reduction in batch cultures. *Water Resources Research*, 39(4). doi:10.1029/2002wr001312.

Husillos Rodríguez, N., Martínez-Ramírez, S., Blanco-Varela, M. T., Donatello, S., Guillem, M., Puig, J., Fos, C., Larrotcha, E., Flores, J. (2013). The effect of using thermally dried sewage sludge as an alternative fuel on Portland cement clinker production. *Journal of Cleaner Production*, 52, 94–102. doi:10.1016/j.jclepro.2013.02.026.

Ingvorsen, K., Yde Nielsen, M., & Joulian, C. (2003). Kinetics of bacterial sulfate reduction in an activated sludge plant. FEMS *Microbiology Ecology*, 46(2), 129–137. doi:10.1016/s0168-6496(03)00209-5.

Kleerebezem, R., Joosse, B., Rozendal, R., & Van Loosdrecht, M. C. M. (2015). Anaerobic digestion without biogas? *Reviews in Environmental Science and Bio/Technology*, 14(4), 787–801. doi:10.1007/s11157-015-9374-6.

Klencsár, Z. (1997). Mössbauer spectrum analysis by evolution algorithm. *Nuclear Instruments and Methods in Physics Research Section B: Beam Interactions with Materials and Atoms*, 129(4), 527–533. doi:10.1016/s0168-583x(97)00314-5.

Li, C., Sheng, Y., & Xu, H. (2020). Phosphorus recovery from sludge by pH enhanced anaerobic fermentation and vivianite crystallization. *Journal of Environmental Chemical Engineering*, 104663. doi:10.1016/j.jece.2020.104663.

Lippens, C., & De Vrieze, J. (2019). Exploiting the unwanted: Sulphate reduction enables phosphate recovery from energy-rich sludge during anaerobic digestion. *Water Research*, 163, 114859. doi:10.1016/j.watres.2019.114859.

Liu, J., Cheng, X., Qi, X., Li, N., Tian, J., Qiu, B., Xu, K., Qu, D. (2018). Recovery of phosphate from aqueous solutions via vivianite crystallization: Thermodynamics and influence of pH. *Chemical Engineering Journal*, 349, 37–46. doi:10.1016/j.cej.2018.05.064

Malhotra, H., Vandana, Sharma, S., & Pandey, R. (2018). Phosphorus nutrition: plant growth in response to deficiency and excess. *Plant Nutrients and Abiotic Stress Tolerance*, 171–190. doi:10.1007/978-981-10-9044-8_7.

Marx, J.J., Wilson, T.E., Schroedel, R.B., Winfield, G., Sokhey, A. (2001). Vivianite: Nutrient's removal hidden problem. *Proceedings of the Water Environment Federation*, 8, 378-388. doi:10.2175/193864701790861721.

McCammon, C. A., & Burns, R. G. (1980). The oxidation mechanism of vivianite as studied by Mossbauer spectroscopy. *American Mineralogist*, 65(3-4), 361-366.

Mejia Likosova, E., Keller, J., Rozendal, R. A., Poussade, Y., & Freguia, S. (2013). Understanding colloidal FeSx formation from iron phosphate precipitation sludge for optimal phosphorus recovery. *Journal of Colloid and Interface Science*, 403, 16–21. doi:10.1016/j.jcis.2013.04.001.

Nembrini, G.P., Capobianco J.A., Viel, M., Williams A.F. (1983). A Mössbauer and chemical study of the formation of vivianite sediments of Lago Maggiore (Italy). *Geochimica et Cosmochimica Acta*, 47(8), 1459-1464.

Nielsen, P. H., Frølund, B., Spring, S., & Caccavo, F. (1997). Microbial Fe(III) reduction in activated sludge. *Systematic and Applied Microbiology*, 20(4), 645–651. doi:10.1016/s0723-2020(97)80037-9.

Ott, C., & Rechberger, H. (2012). The European phosphorus balance. *Resources, Conservation and Recycling*, 60, 159–172. doi:10.1016/j.resconrec.2011.12.007.

Partlan, E., (2018). BlueTech Report on LIFT Water Technology Survey: Wastewater.

Pathak, B., Al-Omari, A., Smith, S., Passarelli, N., Suzuki, R., Khakar, S., DeBarbadillo, C. (2018). Vivianite occurrence and remediation techniques in biosolids pre-treatment process. *WEF Residuals and Biosolids Conference 2018.*

Prot, T., Nguyen, V. H., Wilfert, P., Dugulan, A. I., Goubitz, K., De Ridder, D. J., Korving, L., Rem, P.C., Bouderbala, A., Witkamp, G.J., van Loosdrecht, M.C.M (2019). Magnetic separation and characterization of vivianite from digested sewage sludge. *Separation and Purification Technology.* 224. ISSN 1383-5866. doi:10.1016/j.seppur.2019.05.057.

Prot, T., Wijdeveld, W., Eshun, L. E., Dugulan, A. I., Goubitz, K., Korving, L., van Loosdrecht, M. C. M. (2020). Full-scale increased iron dosage to stimulate the formation of vivianite and its recovery from digested sewage sludge. *Water Research*, 182. https://doi.org/10.1016/j.watres.2020.115911.

Prot, T., Korving, L., Dugulan, A.I., Goubitz, K., van Loosdrecht, M.C.M. (2021). Vivianite scaling in Wastewater Treatment Plants: occurrence, formation mechanisms and mitigation solutions, *Water Research*, in press. https://doi.org/10.1016/j.watres.2021.117045.

Rasmussen, H., & Nielsen, P. H. (1996). Iron reduction in activated sludge measured with different extraction techniques. *Water Research*, 30(3), 551–558. doi:10.1016/0043-1354(95)00203-0.

Reijnders, L. (2014). Phosphorus resources, their depletion, and conservation, a review. Resources, *Conservation and Recycling*, 93, 32–49. doi:10.1016/j.resconrec.2014.09.006.

Roussel, J. and Carliell-Marquet, C. (2016). Significance of vivianite precipitation on the mobility of iron in anaerobically digested sludge. *Frontiers in Environmental Science*. doi:10.3389/fenvs.2016.00060.

Rouzies, D., & Millet, J. M. M. (1993). Mössbauer study of synthetic oxidized vivianite at room temperature. *Hyperfine Interactions*, 77(1), 19–28. doi:10.1007/bf02320295.

**5**

Rubio-rincón, F., Lopez-vazquez, C., Welles, L., van den Brand, T., Abbas, B., van Loosdrecht, M.C.M., Brdjanovic, D. (2017). Effects of electron acceptors on sulphate reduction activity in activated sludge processes. *Applied Microbiology and Biotechnology*, 101 (15), 6229–6240. DOI: 10.1007/s00253-017-8340-3.

Ryther, J. H., & Dunstan, W. M. (1971). Nitrogen, Phosphorus, and Eutrophication in the Coastal *Marine Environment. Science*, 171(3975), 1008–1013. doi:10.1126/science.171.3975.1008.

Salehin, S., Rebosura, M., Keller, J., Gernjak, W., Donose, B. C., Yuan, Z., & Pikaar, I. (2020). Recovery of in-sewer dosed iron from digested sludge at downstream treatment plants and its reuse potential. *Water Research*, 115627. doi:10.1016/j.watres.2020.115627.

Schemen, R., (2017). Fosfor, de kansen en uitdagingen voor de waterschappen. STOWA. ISBN: 978.905773.743.5.

Shimada, T., Evers, M., White, J., Kaakaty, C., Sober, J., Kilian R. (2011). Detection and mitigation of vivianite scaling in anaerobic digesters. *Weftec 2011.*

Vuillemin, A., Friese, A., Wirth, R., Schuessler, J. A., Schleicher, A. M., … Kemnitz, H. (2020). Vivianite formation in ferruginous sediments from Lake Towuti, Indonesia. *Biogeosciences*, 17(7), 1955–1973. doi:10.5194/bg-17-1955-2020.

van Vuuren, D.P., Bouwman, A.F., Beusen, A.H.W. (2010). Phosphorus demand for the 1970-2100 period: A scenario analysis of resource depletion. *Global Environmental Change* 20, 428-439. https://doi.org/10.1016/j.gloenvcha.2010.04.004.

Wang, R., Wilftert, P., Dugulan, I., Goubitz, K., Korving, L., Witkamp, G., Van Loosdrecht, M.C.M., (2019). Fe(III) reduction and vivianite formation in activated sludge. *Separation and Purification Technology*. doi:10.1016/j.seppur.2019.03.024.

Wilén, B.-M., Lund Nielsen, J., Keiding, K., & Nielsen, P. H. (2000). Influence of microbial activity on the stability of activated sludge flocs. *Colloids and Surfaces B: Biointerfaces*, 18(2), 145–156. doi:10.1016/s0927-7765(99)00138-1.

Wilfert, P., Kumar, P. S., Korving, L., Witkamp, G.-J., & van Loosdrecht, M. C. M. (2015). The relevance of phosphorus and iron chemistry to the recovery of phosphorus from wastewater: A review. *Environmental Science & Technology*, 49(16), 9400–9414. doi:10.1021/acs.est.5b00150.

Wilfert, P., Mandalidis, A., Dugulan, A. I., Goubitz, K., Korving, L., Temmink, H., … Van Loosdrecht, M. C. M. (2016). Vivianite as an important iron phosphate precipitate in sewage treatment plants. *Water Research*, 104, 449–460. doi:10.1016/j.watres.2016.08.032.

Wilfert, P., Dugulan, A. I., Goubitz, K., Korving, L., Witkamp, G. J., & Van Loosdrecht, M. C. M. (2018). Vivianite as the main phosphate mineral in digested sewage sludge and its role for phosphate recovery. *Water Research*, 144, 312–321. doi:10.1016/j.watres.2018.07.020.

Wijdeveld, W.K., Prot, T., Sudintas, G., Kuntke, P., Korving, L., Van Loosdrecht, M.C.M., (2021). Pilot-scale magnetic recovery of vivianite from digested sewage sludge. Manuscript submitted.

Withers, P. J. A., Sylvester-Bradley, R., Jones, D. L., Healey, J. R., & Talboys, P. J. (2014). Feed the crop not the soil: Rethinking phosphorus management in the food chain. *Environmental Science & Technology*, 48(12), 6523–6530. doi:10.1021/es501670j.

Wu, Y., Cao, J., Zhang, T., Zhao, J., Xu, R., Zhang, Q., Fang, F., Luo, J. (2020a). A novel approach of synchronously recovering phosphorus as vivianite and volatile fatty acids during waste activated sludge and food waste co-fermentation: Performance and mechanisms. *Bioresource Technology*, 123078. doi:10.1016/j.biortech.2020.123078.

Wu, M., Liu, J., Gao, B., & Sillanpää, M. (2020b). Phosphate substances transformation and vivianite formation in P-Fe containing sludge during the transition process of aerobic and anaerobic conditions. *Bioresource Technology*, 124259. doi:10.1016/j.biortech.2020.124259.

Zelibor, J. L., Senftle, F. E., & Reinhardt, J. L. (1988). A proposed mechanism for the formation of spherical vivianite crystal aggregates in sediments. *Sedimentary Geology*, 59(1-2), 125–142. doi:10.1016/0037-0738(88)90103-0.

Zhang, X. (2012). Factors influencing iron reduction–induced phosphorus precipitation. *Environmental Engineering Science*, 29(6), 511–519. doi:10.1089/ees.2011.0114.
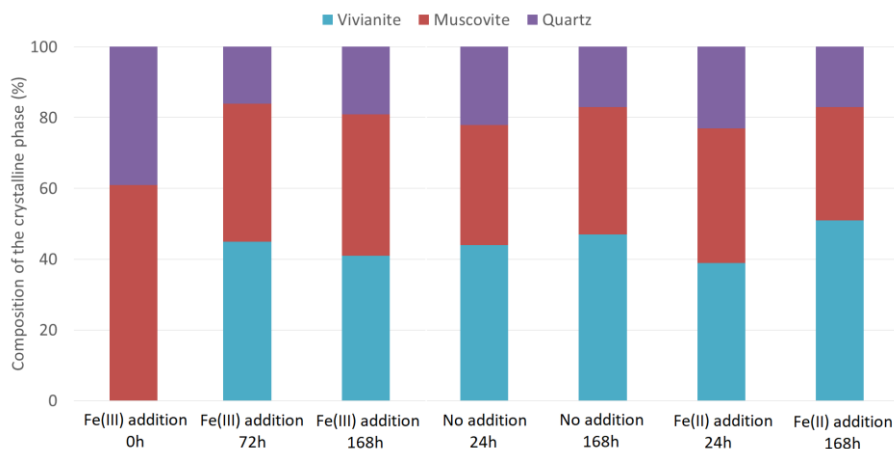
**5**

Supplementary information



*Figure S5.1: Composition of the crystalline phase by semi-quantitative XRD for the seven samples analyzed.*

*Table S5.1: Elemental composition of the samples used for analysis with light microscope and SEM-EDX. These samples were dried without liquid phase removal and represent the elemental composition of the liquid and the solid phase.*

| mg/g of dried solids | Fe | P | S | Ca | Mg |
|---|---|---|---|---|---|
| No addition 0h | 37 | 21 | 7 | 16 | 4 |
| No addition 24h | 37 | 21 | 7 | 16 | 4 |
| No addition 168h | 41 | 24 | 7 | 19 | 5 |
| Fe(II) addition 0h | 35 | 20 | 6 | 15 | 4 |
| Fe(II) addition 24h | 49 | 20 | 6 | 14 | 4 |
| Fe(II) addition 168h | 52 | 21 | 6 | 16 | 4 |
| Fe(III) addition 0h | 38 | 18 | 6 | 13 | 4 |
| Fe(III) addition 72h | 53 | 18 | 5 | 12 | 4 |
| Fe(III) addition 168h | 55 | 18 | 5 | 13 | 4 |
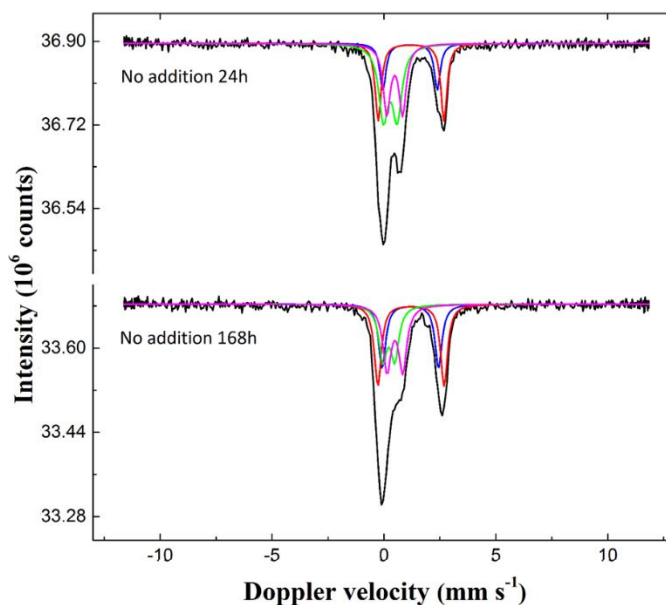
*Figure S5.2: Mössbauer spectra for the samples without iron salts addition after 30h of thickening and after 24h and 168h of additional anaerobic storage. The corresponding colors on the spectra are: Black, total signal; Blue, Vivianite site I; Red, Vivianite site II; Purple, $Fe^{3+}$ in vivianite; Green, FeS, and other minor Fe(III) compounds.*
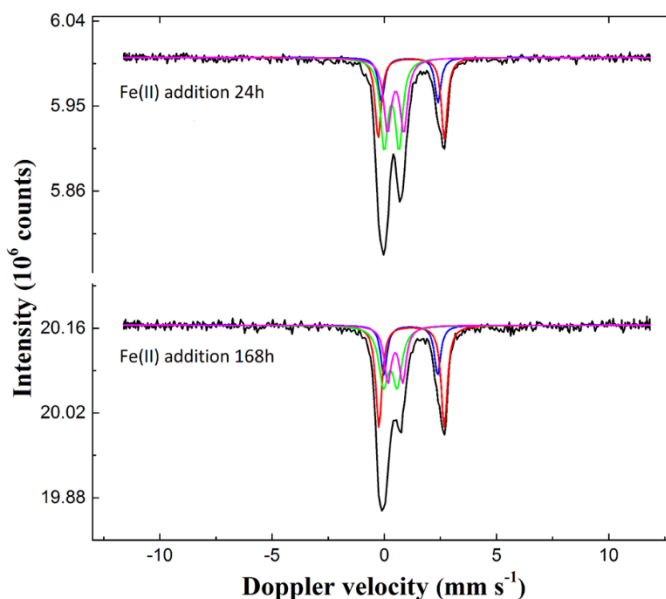


*Figure S5.3: Mössbauer spectra for the samples after the addition of Fe(II) salts after 30h of thickening and after 24h and 168h of additional anaerobic storage. The corresponding colors on the spectra are: Black, total signal; Blue, Vivianite site I; Red, Vivianite site II; Purple, $Fe^{3+}$ in vivianite; Green, FeS, and other minor Fe(III) compounds.*
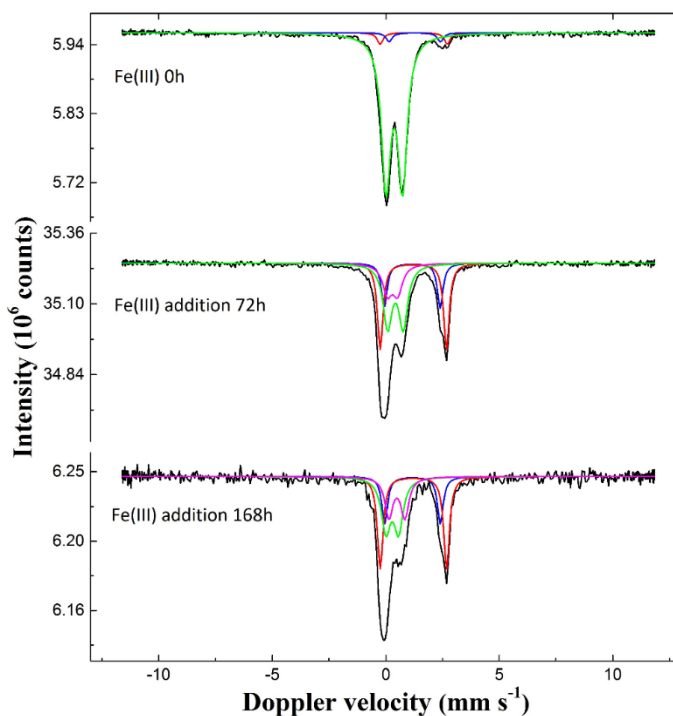
*Figure S5.4: Mössbauer spectra for the samples after the addition of Fe(III) salts after 30h of thickening and after 72h and 168h of additional anaerobic storage. The corresponding colors on the spectra are: Black, total signal; Blue, Vivianite site I; Red, Vivianite site II; Purple, $Fe^{3+}$ in vivianite; Green, FeS, and other minor Fe(III) compounds.*

Table S5.2: Mössbauer parameter fitting for the seven samples measured. Experimental uncertainties: Isomer shift: I.S. ± 0.01 mm s-1; Quadrupole splitting: Q.S. ± 0.01 mm s-1; Line width: Γ ± 0.01 mm s-1; Spectral contribution: ± 3%. *Value fixed during the fitting procedure. ^Constrain on vivianite sites I and II line width to be equal. Due to difficulty separating the signals from FeS and the Fe3+ in vivianite, it was assumed that 30% of the iron was oxidized in all the samples for the calculation carried out in the core of the article.

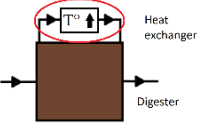| Sample | T (K) | IS (mm·s$^{-1}$) | QS (mm·s$^{-1}$) | Γ (mm·s$^{-1}$) | Phase | Spectral contribution (%) |
|---|---|---|---|---|---|---|
| Initial | 300 | 1.28 | 2.26 | 0.30* | $Fe^{2+}$ (Viv. A) | 3 |
|  |  | 1.23 | 2.96 | 0.30^ | $Fe^{2+}$ (Viv. B) | 4 |
|  |  | 0.37 | 0.73 | 0.50 | FeS/Fe(III) | 92 |
| No addition 24h | 300 | 1.17 | 2.43 | 0.33 | $Fe^{2+}$ (Viv. A) | 15 |
|  |  | 1.21 | 2.94 | 0.33^ | $Fe^{2+}$ (Viv. B) | 24 |
|  |  | 0.48 | 0.71 | 0.49 | $Fe^{3+}$ (Viv. A+B) | 26 |
|  |  | 0.28 | 0.62 | 0.51 | FeS/Fe(III) | 35 |
| No addition 168h | 300 | 1.18 | 2.52 | 0.37 | $Fe^{2+}$ (Viv. A) | 23 |
|  |  | 1.21 | 2.96 | 0.37^ | $Fe^{2+}$ (Viv. B) | 29 |
|  |  | 0.40 | 0.70 | 0.44 | $Fe^{3+}$ (Viv. A+B) | 27 |
|  |  | 0.22 | 0.53 | 0.44 | FeS/Fe(III) | 22 |
| Fe(II) addition 24h | 300 | 1.13 | 2.52 | 0.32 | $Fe^{2+}$ (Viv. A) | 14 |
|  |  | 1.20 | 2.95 | 0.32^ | $Fe^{2+}$ (Viv. B) | 25 |
|  |  | 0.50 | 0.73 | 0.41 | $Fe^{3+}$ (Viv. A+B) | 28 |
|  |  | 0.32 | 0.66 | 0.40 | FeS/Fe(III) | 33 |
| Fe(II) addition 168h | 300 | 1.17 | 2.39 | 0.33 | $Fe^{2+}$ (Viv. A) | 17 |
|  |  | 1.22 | 2.91 | 0.33^ | $Fe^{2+}$ (Viv. B) | 34 |
|  |  | 0.49* | 0.66 | 0.39 | $Fe^{3+}$ (Viv. A+B) | 21 |
|  |  | 0.27 | 0.61 | 0.50 | FeS/Fe(III) | 28 |
| Fe(III) addition 72h | 300 | 1.16 | 2.47 | 0.30 | $Fe^{2+}$ (Viv. A) | 16 |
|  |  | 1.22 | 2.92 | 0.30^ | $Fe^{2+}$ (Viv. B) | 31 |
|  |  | 0.43 | 0.69 | 0.47 | $Fe^{3+}$ (Viv. A+B) | 36 |
|  |  | 0.30 | 0.45 | 0.51 | FeS/Fe(III) | 17 |
| Fe(III) addition 168h | 300 | 1.18 | 2.45 | 0.30 | $Fe^{2+}$ (Viv. A) | 17 |
|  |  | 1.22 | 2.92 | 0.30^ | $Fe^{2+}$ (Viv. B) | 33 |
|  |  | 0.50* | 0.70* | 0.42 | $Fe^{3+}$ (Viv. A+B) | 20 |
|  |  | 0.29 | 0.56 | 0.48 | FeS/Fe(III) | 30 |

5
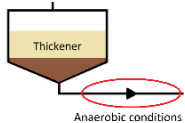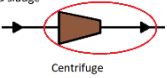
## Costs analysis

In Hoensbroek WWTP, the current yearly iron dosing is approximately 150 tons Fe/year. The sludge is composed of 3.7% of iron and 2.0% of phosphorus, and 6300 tons of dry matter are produced yearly. To reach a Fe/P molar ratio of 1.5, an additional 110 tons Fe/year would need to be added (the WWTP receives external sludge in its thickener). Around 15% of the iron in the thickened sludge would stay in the soluble phase due to the pH decrease after iron addition (6.3 with the current iron dosing and around 5.8 for a Fe/P=1.5 according to Figure 5.3 and would not contribute to vivianite formation. However, this iron fraction could be recirculated after thickening, reducing the iron requirement by 50 tons of Fe/year. It results in an annual cost of 45,000 € since Waterschapsbedrijf Limburg pays a price of 750€ per ton of iron. It represents a high cost but can be compensated by the reduction of the sludge to dispose of.

A Fe/P molar ratio of 1.5 coupled with 2-4 days of anaerobic storage time would lead to 55% of the total iron being present as vivianite (Figure 5.3). It corresponds to the formation of 570 tons of vivianite per year (5.4% of iron in the sludge solids for Fe/P=1.5). Yearly, the WWTP of Hoensbroek produces 6300 tons of dry matter. Assuming that the additional iron added (minus the soluble fraction) would form vivianite, which is likely according to this research, the WWTP would produce 6480 tons of dry matter per year. We hypothesize that the efficiency of the magnetic recovery of vivianite is similar to the one shown at the pilot scale in Chapter 4 (80% with digested sludge), resulting in the recovery of 460 tons of vivianite per year. Based on sludge disposal costs of 385€/ton dry matter in the Netherlands, according to Unie van Waterschappen, 2018, the savings would be around 108,000 €, compensating the expenses for the additional iron dosed. The price of a magnetic separator, the operational costs and the commissioning of a larger thickener need to be considered to get a complete overview of the situation, but an entire economic study is not the scope of this research.

**5**

# Chapter 6: Vivianite scaling in wastewater treatment plants: Occurrence, formation mechanisms, and mitigation solutions

**Highlights**

- Vivianite scaling is widely occurring in WWTPs, even though it is rarely reported.

- The iron reduction appears to be the cause of vivianite scaling in anaerobic equipment.

- pH increase is the main trigger for scaling around centrifuges treating raw sludge.

- Solubility of vivianite decreases when T>32°C, favoring scaling in heat exchangers.

- Proper sludge admixing and iron dosing are essential to mitigate vivianite scaling.

**6**

**Abstract**

The presence of soluble iron and phosphorus in wastewater sludge can lead to vivianite scaling. This problem is not often reported in the literature, most likely due to the difficult identification and quantification of this mineral. It is usually present as a hard and blue deposit that can also be brown or black, depending on its composition and location. From samples and information gathered in 14 wastewater treatment plants worldwide, it became clear that vivianite scaling is common and can cause operational issues. Vivianite scaling mainly occurred in 3 zones, for which formation hypotheses were discussed. Firstly, iron reduction seems to trigger scaling in anaerobic zones like sludge pipes, mainly after sludge thickening. Secondly, pH increase was evaluated as the primary cause for the formation of a mixed scaling (a majority of oxidized vivianite with some iron hydroxides) around dewatering centrifuges of undigested sludge. Thirdly, the temperature dependence of vivianite solubility appears to be the driver for vivianite deposition in heat exchangers around mesophilic digesters (37°C). Also, higher temperatures potentially aggravate the phenomenon, for instance, in thermophilic digesters. Mitigation solutions like the use of buffer tanks or steam injections are discussed. Finally, best practices for safe mixing of sludges with each other are proposed since poor admixing can contribute to scaling aggravation. The relevance of this study lies in the occurrence of iron phosphate scaling, while the use of iron coagulants will probably increase in the future to meet more stringent phosphorus discharge limits.

## 6.1.   Introduction

Wastewater treatment significantly developed in the last decades. In 2014, about 95% of the European population (EU 28) was connected to a wastewater collection system, accounting for around 517 million people (European commission 2017). Additionally, nutrient removal is practiced in 84.5% of the Wastewater Treatment Plants (WWTP) through tertiary treatment (European commission 2017). The current direction is to evolve from the standard wastewater treatment practice towards a Water Resource Recovery Facility (Solon et al. 2019). Specifically, sludge is increasingly used to produce biogas, while phosphorus can be recovered, for example, as struvite ($NH_4MgPO_4*6H_2O$) in installations where phosphorus is removed biologically (Partlan 2018).

Initially, the interest in struvite was not based on its recovery but the prevention of its presence as scaling. The occurrence of struvite scaling in WWTPs is long recognized in the literature (Rawn et al. 1939, Doyle et al. 2002) and is a plague. It can cause pipe diameter reduction, thus increasing the required pumping energy and eventually pipe replacement, among other problems (Parsons and Doyle 2002). Struvite scaling is predominantly reported in the dewatering units after digestion in WWTPs using Enhanced Biological Phosphorus Removal (EBPR), as phosphorus is released and solubilized during sludge digestion.

Another phosphorus mineral, vivianite ($Fe_3(PO_4)_2*8H_2O$), can also cause scaling problems in WWTPs. It provokes the same operational problems as described for struvite and can involve substantial maintenance costs. Vivianite recently received increased attention since it was recognized as the major phosphorus mineral in iron-coagulated digested sludge (Wilfert et al. 2018) and could be recovered by magnetic separation (Chapter 2). Due to its quick oxidation after exposure to air and light, vivianite scaling usually presents a blueish color, facilitating an easy identification (Čermáková et al. 2013, McCammon et al. 1980). Nonetheless, we believe that vivianite scaling is not always identified due to the general lack of information about its occurrence. Moreover, it is often misattributed to struvite scaling, which explains why vivianite scaling received little attention in the past. Twenty years ago, WWTP professionals started to report vivianite scaling in their installations (Marx 2001, Shimada et al. 2011, Bjorn 2010), but this type of scaling was never studied in depth.

The understanding and prevention of vivianite scaling is a relevant topic due to the current lack of information and the expected increased use of iron salts in the future. Indeed, Chemical Phosphorus Removal (CPR) or a combination of CPR and EBPR can achieve lower phosphorus levels in the effluent than EBPR alone (El-Bestawy et al. 2005, Kumar et al. 2018). Additionally, precipitation is proposed as an effective way to make WWTPs energy neutral or energy-producing. Therefore, the number of WWTPs relying on (partial) CPR strategy is expected to increase, as is already the case in North-West Europe (ESPP 2019), to comply with more stringent legislation for effluent quality. Furthermore, high iron dosages are essential to maximize the amount of phosphorus that is recoverable magnetically (Chapter 3). It is crucial to ensure that it is compatible with vivianite scaling prevention. It is possible that vivianite scaling is already widely occurring nowadays but without being identified. Vivianite identification is challenging without advanced techniques like Mössbauer spectroscopy since it can be highly oxidized and therefore become amorphous (Chapter 3).

We reviewed the information available in the literature for cases of WWTPs experiencing vivianite scaling. Since the data on vivianite scaling was limited in literature, information was also gathered from WWTPs suffering from vivianite scaling. In total, data from 14 WWTPs worldwide were collected to get a better overview of the situation. After identifying the preferential places for scaling, thorough analyses of several scaling samples were carried out. The possible formation mechanisms were discussed to finally evaluate several scaling mitigation strategies.

## 6.2.    Materials & Methods

### 6.2.1.  WWTPs studied

In total, information from 14 WWTPs has been gathered, some of them presenting several places where scaling was observed. Figure S6.1 depicts the location of these WWTPs and the type of information gathered.

### 6.2.2.  Analyses

The scaling samples were not protected from oxygen and were stored for up to 6 months before analysis. Visual observations suggested that the centre of the samples was relatively protected from oxidation since it kept the same color even after six months of storage, while the darkening of the samples from light to dark blue characterizes vivianite oxidation (Čermáková et al. 2013, McCammon et al. 1980). However, it cannot be completely excluded that the samples partly oxidized during their storage before the measurements. The samples were analyzed to determine their elemental composition and their phase composition. Besides, pH, iron, and phosphorus measurements were carried out in the sludge line of the WWTP of Hoensbroek (NL) of Waterschapbedrijf Limburg, using Hach-Lange kits. Chemical equilibrium modeling was conducted with the software Visual Minteq: the equilibrium reactions considered are detailed in Table S6.1.

#### 6.2.2.1.    *Elemental composition*

At first, 30-50mg of powdered sample was added to 10 mL of ultrapure $HNO_3$ (64.5-70.5% from VWR Chemicals) in a Teflon vessel. The powder was then digested in an Ethos Easy digester from Milestone equipped with an SK-15 High-Pressure Rotor. The digester reached 200 °C in 15 min, ran at this temperature for 15 min, and cooled down for 1h.

The elemental composition of the digestates was determined via Inductively Coupled Plasma (Perkin Elmer, type Optima 5300 DV) equipped with an Optical Emission Spectroscopy (ICP-OES). An Autosampler, Perkin Elmer, type ESI-SC-4 DX fast was used, and the data were processed with the software Perkin Elmer WinLab32. The rinse and internal standard solution were respectively 2% of $HNO_3$ and 10 mg/L of Yttrium.

#### 6.2.2.2.    *Solid characterization*

Firstly, a thin slice of each sample was cut with a scalpel for light microscope and SEM-EDX observation. The microscope used was a Leica MZ95 equipped with a Leica DFC320 camera. The SEM-EDX apparatus was a JEOL JSM-6480 LV Scanning Electron Microscope (SEM) equipped with an Oxford Instruments x-act SDD Energy Dispersive X-ray (EDX)

spectrometer. The accelerating voltage was 15.00 kV for a working distance of 10mm. The samples were covered with a 10 nm-layer of gold using a JEOL JFC-1200 fine coater to make the surface electrically conductive. The software used was JEOL SEM Control User Interface for the SEM and Oxford Instruments Aztec for the EDX data processing.

Then, the samples were pulverized in a mortar for XRD, Mössbauer spectroscopy, and carbonate analysis. Due to organizational changes in TU Delft, two XRD devices were used. The first one was a PANalytical X´Pert PRO diffractometer with Cu-Kα radiation (5-80°2θ, step size 0.008°). The peak assignment was realized using Origin Pro 9 (samples measured with this device: Venlo, Hoensbroek). The second device was a Bruker D8 Advance diffractometer Bragg-Brentano geometry and Lynxeye position-sensitive detector with Cu-Kα radiation (10-80°2θ, step size 0.008°). The peaks assignment was done with Bruker software DiffracSuite.EVA vs 5.2 (Samples measured with the second device: Spokane County, Amsterdam, Blue Plains, Turku).

In addition, Mössbauer spectroscopy was performed on a selection of samples to study the iron compounds, even those with an amorphous nature, which is not possible with XRD alone. The powdered samples were first introduced in plastic rings sealed with Kapton foil and Epoxy glue and wrapped in aluminium foil. If necessary, carbon powder was added to the sample to maintain a maximum iron quantity of 17.5 mg of $Fe/cm^2$. Transmission $^{57}Fe$ Mössbauer absorption spectra were collected at 300 K with conventional constant-acceleration spectrometer using a $^{57}Co$ (Rh) source. One sample (from Turku) was also analyzed at 4.2K to analyze the Fe(III) phases further. Velocity calibration was carried out using an α-Fe foil. The Mössbauer spectra were fitted using the Mosswinn 4.0 program (Klencsár 1997) and based on previous fittings of sludge samples as described in Wilfert et al. 2018 and Chapter 3.

Literature data on vivianite scaling are scarce and not detailed enough to understand the scaling formation mechanisms. Therefore, 10 WWTPs experiencing vivianite scaling were directly contacted to gather additional information and samples (Table 6.1 and Table 6.2). The collection of these data allowed the identification of the preferential vivianite scaling zones. The possible formation mechanisms were then proposed and correlated to the composition of the vivianite scaling samples. When necessary, more detailed analyses were carried out at the WWTPs to challenge the proposed formation mechanisms.

## 6.3. Results & Discussion

From the data collected at 14 WWTPs (Figure S6.1), five possible locations for vivianite scaling formation in a WWTP were identified. These locations are discussed in the following sections: in the anaerobic pipes and units before sludge digestion (6.3.1), around the dewatering centrifuges for undigested sludge (6.3.2), in the heat exchangers around anaerobic digestion (6.3.3), in zones where sludge with different characteristics are mixed together (6.3.4), and in digesters as settled particles (6.3.5). The possible mechanisms of formation of vivianite scaling are discussed, resulting in a proposal for strategies to prevent vivianite-related scaling.

Table 6.1: Inventory of the vivianite scaling observed by the WWTPs contacted during this study, as well as previously reported in the literature

| Hot-spot | WWTP | Zone description | Source | Composition (mg/g) | | | | | Phase identification | | | |
|---|---|---|---|---|---|---|---|---|---|---|---|---|
| | | | | Fe | P | Mg | Ca | S | XRD | Mössbauer | Light microscope/SEM-EDX | $CO_3$ (%) |
| Sludge transport or handling units under anaerobic conditions | Hoensbroek | Pipe after the thickener | This study | 309 | 95 | 4 | 8 | 41 | Vivianite | 72% vivianite Possible FeS mineral | Blue zone with Fe/P overlay Orange zone with Fe/S overlay | 0.1 |
| | Dokhaven | Sludge buffer tank for B-stage | This study | 319 | 123 | 9 | 8 | 2 | nd | nd | Blue crystals with the same structure as vivianite | 0.0 |
| | Venlo | Pipe after the thickener | Prot et al. 2019 (our study) | 308 | 119 | 11 | 10 | 2 | Vivianite | 68% vivianite | Layered blue scaling Homogeneous elemental distribution | nd |
| | Bosscherveld | Pipe after the thickener | This study | 191 | 97 | 3 | 47 | 3 | nd | nd | Blue crystal with the same structure as vivianite | 0.0 |
| | Blue Plains | In equipment pre-centrifuge | Pathak et al. 2018 | nd | | | | | Vivianite | nd | nd | nd |
| Pre-dewatering centrifuge | Hoensbroek | | This study | 259 | 112 | 2 | 44 | 2 | Vivianite | 23% vivianite | Major brown phase Minor blue phase Homogeneous elemental distribution | 0.2 |
| | Turku | | This study | 393 | 41 | 1 | 14 | 2 | Major amorphous phase Minor goethite | 70% Ferrihydrite 30% santabarbaraite | Brown amorphous phase More crystalline black phase Homo. elemental distribution | 0.5 |
| | Bosscherveld | Centrifuge tank and subsequent centrate pipe | This study | 282 | 107 | 6 | 9 | 2 | nd | nd | Layered black, brown, light-brown scaling with a blue layer on the inside | 0.2 |
| | Blue Plains | | This study | 307 | 109 | 2 | 23 | 1 | nd | nd | Major brown phase Minor blue phase Homogeneous elemental distribution | 0.3 |
| | Blue Plains | | Pathak et al. 2018 | nd | | | | | Minor vivianite Major amorphous phase | nd | nd | nd |

nd: no data means that the information was not available in the literature reference, or that we did not analyse the sample with this method

**6**

*Table 6.2: Inventory of the vivianite scaling observed by the WWTPs contacted during this study; as well as previously reported in literature.*

| Hot-spot | WWTP | Zone description | Source | Composition (mg/g) | | | | | XRD | Phase identification — Mössbauer | Light microscope/SEM-EDX | CO3 (%) |
|---|---|---|---|---|---|---|---|---|---|---|---|---|
| | | | | Fe | P | Mg | Ca | S | | | | |
| | Amsterdam | This study | | 298 | 129 | 18 | 11 | 3 | Baricite (impure vivianite) Quartz, low | 68% vivianite | Layered blue scaling Homogeneous elemental distribution | 0.0 |
| | Dallas | HE around the mesophilic digester | Shimada et al. 2011 | 122 | 23 | 6 | 7 | nd | | | Vivianite (method not mentioned) | nd |
| | Lübeck | Contact with the WWTP | | nd | | | | | | | Vivianite (visual observation and laboratory analysis) | nd |
| | Ejby Molle | Contact with the WWTP | | nd | | | | | | Vivianite (XRD) | | nd |
| Heat exchangers (HE) | Back's river | | Marx et al. 2001 | nd | | | | | | Vivianite (method not mentioned) | | nd |
| | Derby | HE around the mesophilic APD | Bjorn 2010 | nd | | | | | | Vivianite (method not mentioned) | | nd |
| | Nine Springs | HE around thermophilic digestion | Reusser 2009 | nd | | | | | | Vivianite (method not mentioned) | | nd |
| | Venlo | Cooling HE after THP | This study | 87 | 113 | 26 | 98 | 11 | | nd | Homogeneous black layer (amorphous) Homogeneous elemental distribution | 0.0 |
| | Blue Plains | Cooling HE after THP | This study | 319 | 118 | 10 | 3 | 8 | Baricite (impure vivianite) | 72% of vivianite | Blue zone with Fe/P overlay Orange zone with Fe/S overlay | 0.3 |
| Digester | Spokane County | Digester withdrawal | This study | 310 | 87 | 3 | 20 | 1 | Vivianite Rhodochrosite (possible siderite) | 45% vivianite 11% possibly siderite | Dark blue particles (microscopic structure of vivianite) Quartz like transparent particles Orange particles | 4.8 |
| | Blue Plains | Digester withdrawal | This study | 89 | 29 | 5 | 9 | 3 | nd | nd | Vivianite-like dark blue particles Quartz like transparent particles | nd |

nd: no data means that the information was not available in the literature reference, or that we did not analyse the sample with this method

### 6.3.1. Anaerobic zones

Our dataset indicates that one preferential place for vivianite scaling is pipes and storage tanks for waste sludge, where sludge is maintained under anaerobic conditions for several hours. In the WWTP of Blue Plains, scaling was observed in several units downstream of the sludge thickener (screens, flow meters, valves, centrifuge feed). The WWTP of Venlo also experiences scaling before the Thermal Hydrolysis Process (THP) installation, mainly in the pipes and sludge cutter after the thickener. At the WWTPs of Hoensbroek and Bosscherveld, a blueish scaling was observed in the pipes carrying the sludge from the thickener to the dewatering centrifuge. This scaling provoked operational issues, forcing the shut-down of centrifuges for cleaning while restricting the flow in the pipeline (Pathak et al. 2018).

XRD indicated that no other crystalline phases than vivianite were present in Hoensbroek and Venlo, while some quartz and siderite were also found in Blue Plains in 2 out of 6 samples (Pathak et al. 2018). While XRD is limited to analyzing the crystalline phases, Mössbauer spectroscopy allows to also quantify any amorphous Fe-compounds. Mössbauer spectroscopy revealed that vivianite accounted for 72% and 82% of the total weight of the scaling in Hoensbroek and Venlo, respectively. The unidentified part of the scaling could be other iron species like Fe(III) phases or a low-spin Fe(II) phase (typically FeS minerals) according to Mössbauer spectroscopy. These species could be iron oxides resulting from the aging of vivianite (Roldan et al. 2002). In Hoensbroek, the 4% of sulphur exactly accounts for the iron fraction not bound to vivianite if the formation of FeS is assumed, which is also in line with EDX results (Figure 6.1). The vivianite present in the scaling can be impure and include Mg and Ca in its structure, as noticed by Rothe et al. 2016 and Seitz et al. 1973. Therefore, we hypothesize that the scaling was actually composed of more than 72% (Hoensbroek) and 82% (Venlo) (value obtained assuming no iron substitution) of a vivianite-like mineral.
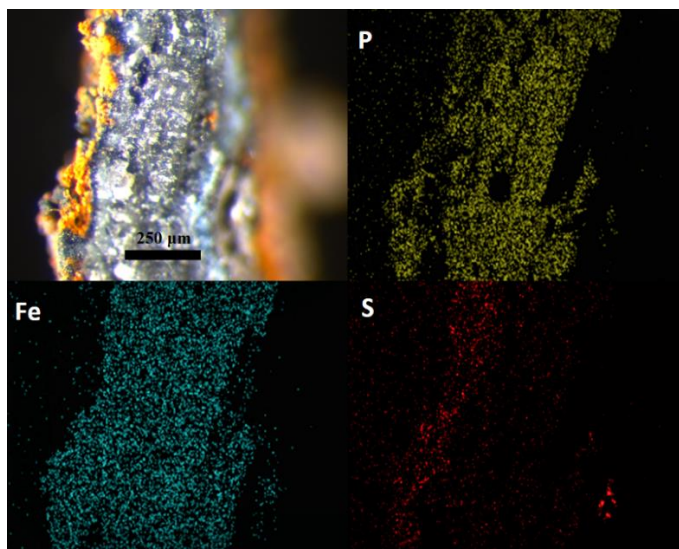


*Figure 6.1: Light microscope picture of the scaling in the anaerobic pipe of Hoensbroek (top left). Corresponding elemental distribution by EDX for Phosphorus (top right), iron (bottom left), and sulphur (bottom right). The blue phase of the microscope picture is vivianite (Fe and P overlap), while the orange phase is a FeS mineral (Fe and S overlap).*

Even though the different scalings do not have the exact same composition, we believe that the cause of their formation is identical. The scaling could result in the formation of stable nuclei on a surface (e.g., wall of a pipe) through primary heterogeneous nucleation, being the onset for further crystal (in this case scaling) growth (Mersmann 2001). Alternatively, agglomeration could be triggered by the deposition of small vivianite crystals (resulting from the previous nucleation) on the surface of the equipment or pipe. Turbulence in the pipe or equipment near the walls increases collision probabilities and forms an essential factor for this mechanism (Mersmann 2001). Fluid mechanics in the pipe system have been studied to discuss this point. The main findings are presented in this section, while the detailed calculation can be found in Supplementary information. In Hoensbroek, the activated sludge is brought to a thickener with a residence time of 13h before being pumped toward a centrifuge at a flow of 18.7 $m^3$/h via three consecutive pipes ($d_1$=0.2 m/$l_1$=30 m; $d_2$=0.1 m/$l_2$=5 m; $d_3$=0.08 m/$l_3$=16 m). Considering a power-law model approach, the flow regime is laminar in pipe 3 since Re<2100 (Ratkovich et al. 2013), so the flow is also laminar in pipe 1 and 2 since they have bigger diameters. This is in line with what is reported in the literature, where sludge flow in pipes is usually considered laminar (Slatter 2004, Haldenwang et al. 2012). A collision formation mechanism seems unlikely in a laminar regime since it would require some transversal vivianite particle movement. Moreover, light microscope/SEM observations of the sample from Hoensbroek and Venlo show a continuous crystalline matrix rather than an agglomeration of particles, indicating that a growth mechanism from soluble phosphorus and $Fe^{2+}$ is more likely (Figure 6.1).

Since the conditions are anaerobic between the thickener and the dewatering units, Fe(III) will be reduced to Fe(II), while phosphate could be released from the biomass. According to rate measurements by Wang et al. 2019, it takes around one day to reduce the majority of the Fe(III) present in activated sludge to Fe(II). Around two days are required to release the biggest fraction of the phosphate from the Phosphate Accumulating Organisms (PAO's) during thickening, according to Janssen et al. 2002. Considering that the typical sludge retention time in a thickener is a few hours, the release of phosphorus and iron will still be ongoing when the sludge leaves the thickener, allowing scaling growth. In iron-coagulated sludge (like in Hoensbroek), phosphorus is not only found in PAO's but also bound to iron. It is complicated to separately evaluate the phosphorus released from PAO's and Fe(III)P minerals. The study of the vivianite scaling formation was realized, assuming that iron is the limiting compound since phosphorus release mechanisms are more complex.

According to Wang et al. 2019, iron reduction follows a first-order kinetic with k=0.05 $h^{-1}$, so the quantity of iron reduced in the pipes is proportional to the sludge retention time for low retention times. From the sludge velocity profile in the pipes, the zone next to the pipe wall will present a much smaller velocity and so higher $Fe^{2+}$ concentration than in the bulk. We can assume that the formation of vivianite follows a wall-mechanism rather than a bulk-mechanism. Bigger pipes will see more iron being reduced compared to smaller pipes due to higher retention times. However, a big part of the $Fe^{2+}$ produced will not have time to diffuse to the pipe wall and will precipitate in the bulk, not causing scaling (Supplementary information).
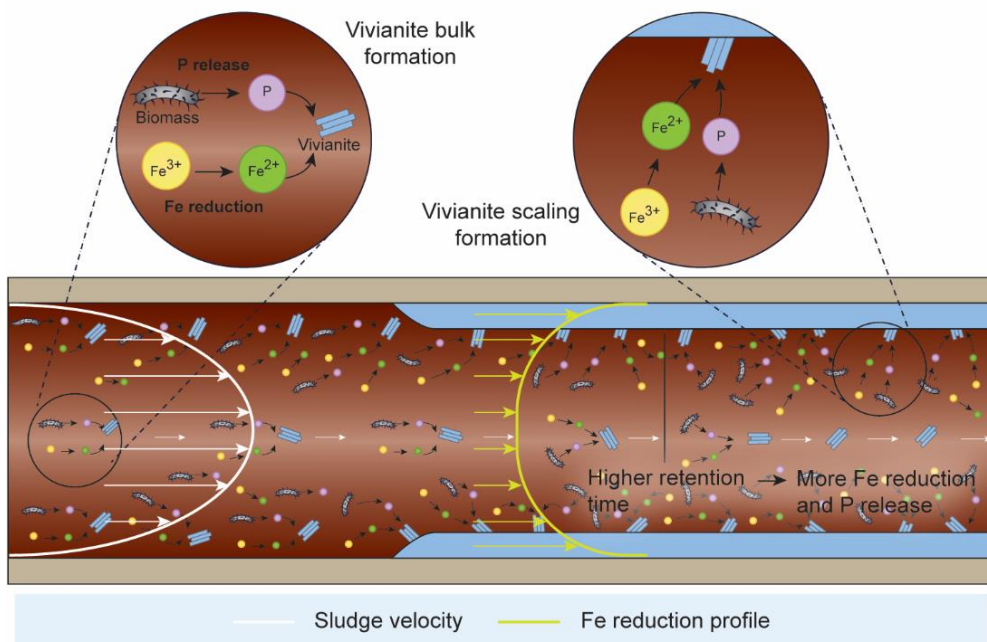
*Figure 6.2: Proposed formation mechanism of vivianite scaling in an anaerobic pipe. This figure highlights the difference between bulk and scaling formation and the importance of the sludge velocity and iron reduction profile.*

To summarize, the morphology of the scaling and the laminar flow regime suggest that the scaling found in the sludge transport or handling units under anaerobic conditions follows a growth mechanism rather than an agglomeration mechanism. We hypothesize that the iron reduction due to the anaerobic conditions is the driver for the scaling formation (Figure 6.2). Both low diffusion velocities and high iron concentrations near the walls suggest that a wall-mechanism growth is favored. These observations imply that larger diameter pipes may be better to use due to their lower wall area/volume ratio, even though they present higher sludge retention times. Iron reduction and phosphorus release will strongly contribute to the formation of vivianite scaling and are unavoidable. However, the iron reduction should be almost complete after 24h according to Wang et al. 2019. This means that allowing a fermenting sludge to rest in a unit bearing a high volume/surface ratio (e.g., a buffer tank) for a day could allow all the iron to be reduced and the main part of the vivianite to form in the bulk of the sludge, instead of creating problematic scaling in the units downstream. A small fraction of the vivianite could still scale on the wall of the buffer tank, but this should be manageable and is easily accessible for cleaning. Such buffer tank is used in the WWTP of Dokhaven (for a different purpose than scaling prevention). Vivianite scales were observed in this tank, but it is not a significant issue since it only requires a yearly cleaning. No scaling problem downstream from this tank has been reported, indicating that the addition of such a buffer tank may be a valid option for scaling prevention.

## 6.3.2. Dewatering units

According to the information collected, the worst occurrence of scaling was around centrifuges used for the dewatering of undigested sludge. The WWTPs of Hoensbroek, Bosscherveld, and Turku dewater their thickened sludge by centrifugation before sending it for disposal. The scaling occurs in Turku WWTP in the centrifuge and centrate pipe and is manageable with a manual cleaning being necessary 2-3 times per year, costing around 2000€/month (information obtained from the WWTP). The situation is more dramatic in Hoensbroek and Bosscherveld, where an important build-up of scaling, mainly composed of vivianite-based compounds, was observed in the centrifuge, the centrate box, and the centrate pipe. It forces a stoppage and cleaning of the centrifuge every 1-2 weeks and a yearly replacement of the centrate pipe in Hoensbroek. Scaling formation also happened in the WWTP of the Blue Plains in and downstream of the pre-dewatering centrifuge before THP. The build-up in the centrifuge increased torque and vibration, obliging operators to put the equipment out of service for manual cleaning (Pathak et al. 2018). Scaling formation in the centrifuge and the centrate pipes caused the most severe operational problems compared to the other scaling location.

Since the scaling observed in the centrifuges and the centrate pipes are similar in their elemental composition and microscopic structures (unpublished data), detailed analyses were only carried out on the samples found in the centrate pipes. The samples were quite different from the scaling found in the heat exchangers and the sludge transport pipes since the deposits were softer and mainly brown/black instead of blue. The scaling from Blue Plains, Hoensbroek, and Bosscherveld presented a similar elemental composition with 26-31% of iron, 10-11% of phosphorus, and 1-4% of calcium, which is close to the composition of vivianite (33% of iron, 12% of phosphorus) (Table 6.1). The samples were much more XRD-amorphous than the scaling found in other sections of the WWTPs, but XRD still managed to identify vivianite: impure in Hoensbroek and as a minor fraction in Blue Plains (Pathak et al. 2018).

Microscopic observations of these three samples revealed a structure with brown, black, and occasional blue layers suggesting a mix of species with vivianite not being the major compound (Figure 6.3). Surprisingly, EDX showed a homogeneous distribution of iron and phosphorus across the samples. The Mössbauer spectroscopy study of the centrate sample from Hoensbroek confirmed the presence of 23% of vivianite, accounting for only 30% and 25% of the iron and phosphorus in the sample, respectively. The 70% of remaining iron is present in Fe(III) minerals, according to Mössbauer spectroscopy. Based on the elemental composition close to the one of vivianite, we believe that vivianite originally formed and progressively oxidized (centrifuges are not protected from air intrusion), transforming into metavivianite ($Fe^{2+}Fe^{3+}_2(PO_4)_2(OH)_2 \cdot 6H_2O$) and then santabarbaraite (($Fe^{3+}$)$_3(PO_4)_2(OH)_3 \cdot 5H_2O$). The structure of the scaling from Bosscherveld supports this hypothesis: it presents a blue layer (vivianite) on the most freshly formed side of the scaling and brown/black Fe/P containing material (possibly metavivianite and santabarbaraite) more profound in the scaling (Figure 6.3).

Additionally, the EDX analyses revealed a homogeneous iron and phosphorus distribution across the entire sample. Oxidation of vivianite leads to the progressive destruction of its

crystalline structure, making the newly formed minerals undetectable by XRD (Dormann et al. 1980, Pratesi et al. 2003). The Mössbauer signals of the oxidation products of vivianite are close to the one observed in this study ($Fe^{III}$: δ=0.35-0.43 mm/s / QS=0.5-0.9 mms/s according to Dormann et al. 1980). However, they overlap with the signal of iron oxides, making it impossible to be attributed to metavivianite or santabarbaraite with certainty. Strengite is another possible Fe(III)P mineral, but the conditions in the centrifuge are not favorable for its formation (Wilfert et al. 2015, Pathak et al. 2018).
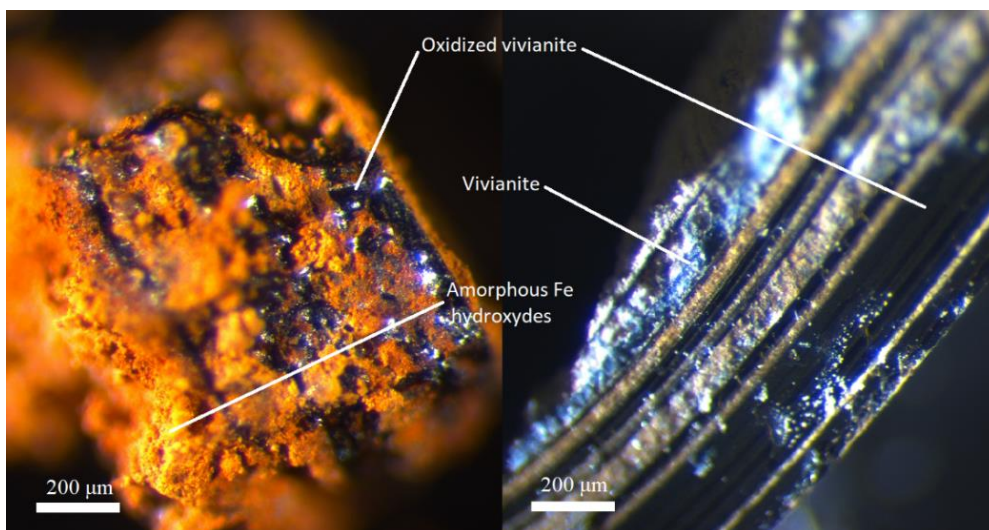


*Figure 6.3: Light microscope pictures of the scaling found in the centrate pipe of Turku (left) and Bosscherveld (right). Turku: slow formation mechanism dominated by ferrihydrite and a minor phase of fully oxidized vivianite (santabarbaraite). Bosscherveld: rapid formation mechanism dominated by vivianite; a fresh vivianite layer can be observed on the sludge side while oxidized vivianite is present on the pipe side.*

The sample from Turku is different in its composition (39% of iron, 4% of phosphorus, and 1% of calcium), appearance (major orange phase/minor black phase), and is fragile (Figure 6.3). Room temperature Mössbauer spectroscopy indicates that it is entirely composed of Fe(III) species (excluding the presence of vivianite and metavivianite) and contains ferrihydrite. Layered Iron hydroxide could be an intermediate since they are formed by oxidation of $Fe(OH)_2$ and inclusion of anions, and later form ferric oxyhydroxides under further oxidation (Refait et al. 1998). Phosphate adsorption alone cannot explain the 5% of phosphorus present in the sample since it would suggest a capacity five times higher (mg of P/g of Fe) than engineered Fe-adsorbents (Kumar et al. 2019). XRD indicated that the sample was mainly amorphous and could contain a small quantity of goethite, which agrees with Roldan et al. 2002, stating that vivianite oxidation results in the formation of poorly crystalline Fe(III) oxides, a polymorph of goethite. The 4.2K Mössbauer spectroscopy measurement (which allows Fe(III) phases speciation) reveals that a mix of 23% santabarbaraite and 77% ferrihydrite is possible (Figure 6.4 and Table S6.4).
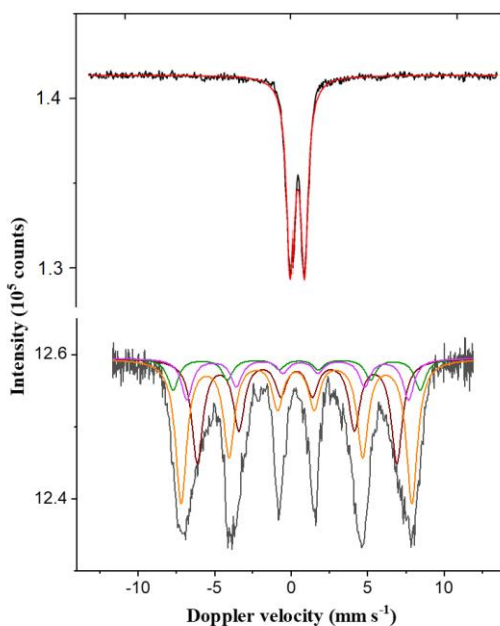
*Figure 6.4: Mössbauer spectra for the scaling in the centrate pipe of Turku at room temperature (top) and 4.2K (bottom). The top spectrum only reveals the presence of $Fe^{3+}$ compounds without possible speciation (red curve). The bottom spectrum reveals the presence of fully oxidized vivianite (santabarbaraite) (green and pink curves) and different ferrihydrite minerals with various degrees of crystallinity (orange and dark red curves). The fitting for low-temperature measurement was based on experiments realized with oxidized synthetic vivianite (results not shown). More information is available in Table S6.4.*

The scalings found in centrate pipes are mainly amorphous and rich in phosphorus and oxidized Fe. The major compounds seem to be oxidation products of vivianite (metavivianite and santabarbaraite). At the same time, Fe(III) oxides/hydroxides are also present (except for Turku's sample where Fe(III) oxides/hydroxides are the main fraction). A pH increase favors both the precipitation of vivianite and iron oxides/hydroxide and could be the primary mechanism explaining the formation of scaling around the centrifuge. Indeed, the pH increased by 0.3 during centrifugation in the WWTP of Blue Plains (Pathak et al. 2018) and Hoensbroek. The effect of pH on ferrihydrite precipitation is straightforward since its solubility directly depends on the third power of the $OH^-$ activity (Schwertmann 1991). The SI of vivianite is proportional to the square of the activity of $PO_4^{3-}$, which is increasing with the pH (Liu et al. 2018). During centrifugation, $CO_2$ stripping occurs due to the turbulences and the contact with air, which triggers the observed pH increase (Battistoni et al. 1997). This rise of pH is also the main mechanism triggering struvite scaling in post-digestion dewatering centrifuges (Doyle and Parsons 2002). Taking into account the composition of the sludge liquor just before centrifugation in Hoensbroek (P=8.6ppm / $Fe^{2+}$=27.4 ppm / $Fe^{3+}$=6.91 ppm / pH=6.9 / Ionic strength=0.02), an increase to pH 7.22 signifies a SI increase from 5.41 to 6.28 and 5.48 to 5.80 for vivianite and ferrihydrite, respectively. The SI values are high, which can be explained by an overestimation of $Fe^{2+/3+}$ in the sample. This overestimation is due to small colloidal iron

particles going through the pores of the 0.45 µm-filter. We experimentally confirmed this but at a later moment when the way of operation of the WWTP changed.

Since iron reduction is a relatively slow process (compared to the rapid pH increase during centrifugation), we consider that a certain steady-state toward vivianite formation is established before centrifugation. The concentrations of iron and phosphorus were decreased assuming vivianite and $Fe(OH)_2$ formation to match the equilibrium SI calculated above (5.41 and 5.48). Such equilibrium conditions at pH=7.22 are for P=5.1 ppm / $Fe^{2+}$=17.7 ppm / $Fe^{3+}$=3.4ppm, resulting in the formation of 28.3 mg/L of vivianite and 5.3 mg/L of ferrihydrite. It is clear that even a small pH increase can have an important effect on the precipitation of vivianite and ferrihydrite. From these calculations, it appears that the scaling would be composed of a majority of vivianite, which reinforces our hypothesis that vivianite was initially formed and oxidized, making it complicated to trace.

A second mechanism could also explain the formation of Fe(III) oxides: since the centrifuge is not protected from air intrusion, the soluble $Fe^{2+}$ could be oxidized, triggering the formation of poorly soluble $Fe(OH)_3$. Detailed calculations in Supplementary information reveal that Fe(II) oxidation is too slow to explain significant formation of Fe(III) to produce $Fe(OH)_3$. It seems, therefore, that this mechanism is much less important compared to vivianite formation, which is confirmed by the information collected from the WWTPs: the centrate scaling from Hoensbroek, Blue Plains, and Bosscherveld (containing a high quantity of Fe/P species) require regular cleaning, while the one in Turku (mainly iron oxide/hydroxide) only needs to be removed twice a year. The unique composition of Turku's sample may be explained by the high Fe/P molar ratio (1.75) used in this WWTP.

The reduction in the $Fe^{2+}$ concentration in the liquid phase of the sludge to the centrate (27.4 to 6.5 ppm) is much larger when compared to the reduction in the phosphorus concentration (8.6 to 4.7 ppm) and cannot be explained by the formation of vivianite. The authors believe that this is due to an overestimation of the soluble iron before centrifugation, as discussed above. Additionally, the extreme mixing conditions in the centrifuge may promote scaling formation. Indeed, the flow regime before the centrifuge is laminar, not allowing an optimal mixing of the ions, while centrifugation creates turbulent conditions. Yousuf et al. 2018 also showed that increased shear stress lowers the secondary nucleation (formation of crystals in the presence of parent crystals, Mersmann 2001) threshold by increasing the collision between particles. The presence of existing scaling and rough surfaces also promotes secondary nucleation.
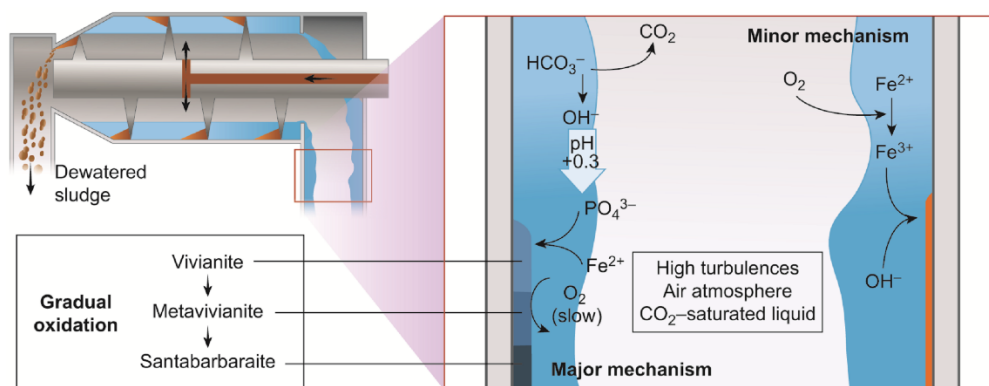
**6**

*Figure 6.5: Proposed formation mechanism of vivianite (major mechanism) and ferrihydrite (minor mechanism) in centrate pipes of pre-dewatering centrifuges. We assume that the formation mechanism is similar in the centrifuge itself. (vivianite: $Fe^{2+}_3(PO_4)_2 \cdot 8H_2O$, metavivianite: $Fe^{2+}Fe^{3+}_2(PO_4)_2(OH)_2 \cdot 6H_2O$, santabarbaraite: $(Fe^{3+})_3(PO_4)_2(OH)_3 \cdot 5H_2O$)*

From the information collected, it appears that scaling formation around centrifuges is mainly caused by a pH increase through $CO_2$ evolution in the centrate chamber and to a smaller extent by the oxidation of the soluble $Fe^{2+}$ (Figure 6.5). The large shear forces created by centrifugation can aggravate the scaling formation. Stripping some $CO_2$ in a tank before centrifugation to increase the pH would initiate controlled vivianite formation in the bulk and may reduce the scaling formation. Allowing a more extended time under anaerobic conditions for the sludge before centrifugation should also reduce soluble phosphorus and iron concentration. The addition of a buffer tank after the thickener could be a combined solution for the scaling around the centrifuge and in the anaerobic zones (discussed in 6.3.1).

No vivianite scaling was reported in post-digester centrifuges, indicating that a longer residence time could indeed be a suitable solution. Since the pH increase is due to $CO_2$ stripping, creating a $CO_2$-saturated atmosphere in the centrifuge could theoretically be an option to prevent it. More research needs to be undertaken to evaluate the feasibility of all these options. Counterintuitively, a higher iron/phosphorus molar ratio in the sludge may also reduce vivianite scaling formation. A higher iron dosing reduces the quantity of phosphorus present in the soluble phase, reducing the quantity of phosphorus available for precipitation. Therefore, the pH increase observed during centrifugation would provoke less vivianite scaling formation. For example, the iron dosage in Turku is high (Fe/P = 1.75), and the scaling only needs to be removed 2-3 times per year. On the contrary, WWTPs dosing less iron (Fe/P = 1.14 in Hoensbroek and 0.65 in Bosscherveld) need to remove the scaling every 1-2 weeks.

### 6.3.3. Heat exchangers

From the information gathered from WWTPs, and supported by literature, it appears that sludge heat exchangers are a common place for vivianite scaling to occur. In the case of the WWTPs of Lübeck, Ejby Mølle, and Amsterdam, a blue and hard scale was present in the sludge heat exchanger used for the heating of the mesophilic anaerobic digester. A similar situation was reported in the literature in several other WWTPs: inside and downstream of the digested sludge heat exchanger in Dallas (Shimada et al. 2011), in the heat exchanger around

the acid-phase digestion in Derby (Bjorn 2010) and the heating loop in Back's River WWTP (Marx et al. 2001). Problems at higher temperatures (especially in pasteurization units) have also been reported by Buchanan et al. 2014, Panter et al. 2013 and Reusser 2009. In the WWTP of Blue Plains and Venlo, scaling was found in the heat exchanger used to cool down the sludge after THP.
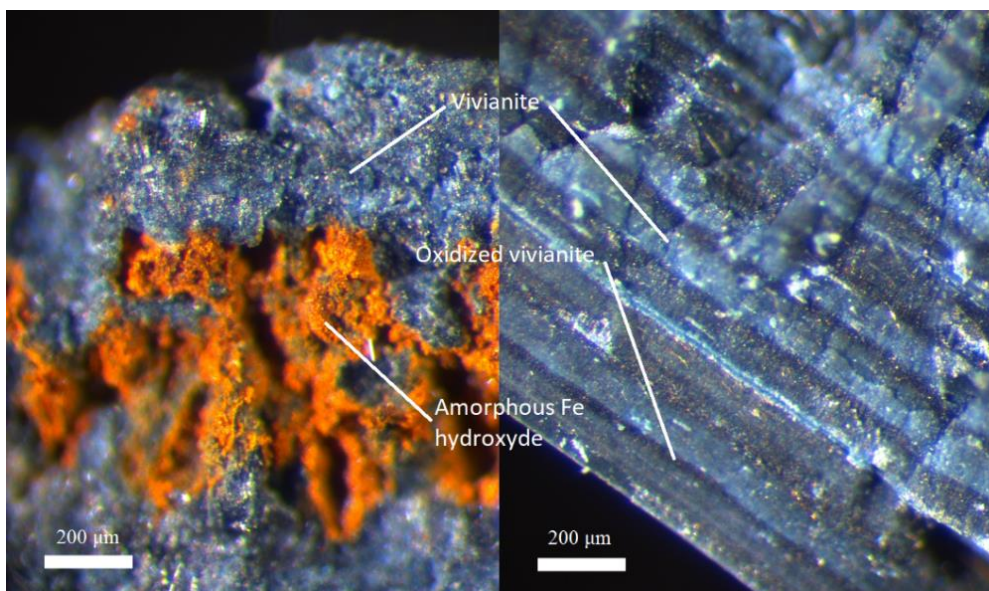


*Figure 6.6: Light microscope pictures of vivianite scaling found in the cooling heat exchanger after THP in Blue Plains WWTP (left) and the heating heat exchanger around the mesophilic digester of Amsterdam (right).*

The seven scalings found in heat exchangers used to warm up the sludge for mesophilic and thermophilic digestion were all reported to be vivianite: by "laboratory analysis" in literature (not specified, but probably XRD and elemental analysis), by visual observation in Lübeck (no sample was available, only picture), and by XRD in Amsterdam and Ejby Mølle. The scaling of Amsterdam was further studied by Mössbauer spectroscopy, which confirmed the presence of vivianite as 68% in weight (likely underestimated due to its partial oxidation). The macroscopic and microscopic observations of the scaling from Amsterdam show a crystalline hard and blue scale that seems to be purer (no other phase than vivianite visually observed) than the scaling found in sludge pipes or dewatering units (Figure 6.6). From the pictures available, the scalings from Lübeck and Ejby Mølle seem to have similar characteristics. This supposed high purity is supported by the elemental composition of the sample from Amsterdam: 30% of iron, 13% of phosphorus, and only 2% of magnesium and 1% of calcium as inorganic impurities.

It is interesting to note that $Mg^{2+}$ and $Ca^{2+}$ could be part of the structure of vivianite by substituting $Fe^{2+}$ (Rothe et al. 2016, Seitz et al. 1973). The scale formed in the heat exchanger after THP at Blue Plains WWTP presents a similar elemental composition with 32% of iron, 12% of phosphorus, 1% of magnesium, and 1% of sulphur. However, this sample is more fragile and composed of two main phases: a major blue and orange (Figure 6.6). Mössbauer

spectroscopy results confirmed that the blue phase is vivianite, accounting for 72% of the scaling weight (75% of the total iron). The remaining 25% of iron are Fe(III) species according to Mössbauer spectroscopy and could be a mix of iron oxides/hydroxides and metavivianite/santabarbaraite. The scaling found after THP in Venlo was black and had a completely different composition: 12% of phosphorus, 10% of calcium, 9% of iron, 2.5% of magnesium, and 1% of sulphur. No vivianite was present according to microscopic observations.

From the on-site observations described above, the temperature seems to promote vivianite scaling formation both when the sludge is heated up and cooled down. This is in line with the finding of Al Borno and Tomson 1994, who showed that vivianite solubility evolves hyperbolically in the function of the temperature (Figure 6.7). Their results indicate that vivianite was the most soluble, around 30-35°C, which is close to the temperature of operation of a mesophilic digester (37°C). The flow rate in heat exchanger is usually relatively high (60 m³/h for Amsterdam WWTP, for example), which, together with their geometry (spiral shape, corrugated tubes…), promotes turbulences (Alfa-Laval and Spiralex brochures) in order to prevent solid settling and thermal decomposition of organics (Lines 1991). If the flow is turbulent, a homogeneous temperature distribution can be expected in the bulk of the sludge. According to Guo, only a very thin layer of sludge near the wall (the boundary-layer) will have a lower velocity (and so higher temperature) than the bulk, as opposed to the more gradual velocity gradient existing for laminar flows (Figure S6.3). The exact temperature of the wall has not been calculated since the full description of the thermal situation was not the objective of this study.
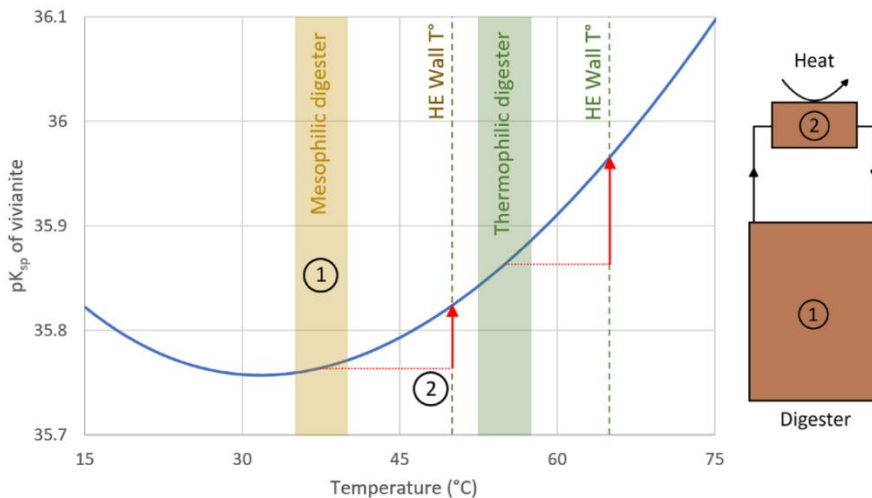


*Figure 6.7: Evolution of the negative logarithm ($pK_{sp}$) of vivianite in a function of the temperature. The figure was plotted following the relation obtained by Al Borno and Tomson 1994: $pKsp = -234.205 + 12{,}242.6/T + 92.510\, logT$, valid from 5 to 90°C. The figure also shows the temperature range in the mesophilic and thermophilic digester and the corresponding heat exchanger's wall temperature (considering heating fluid temperature of 60°C for mesophilic digester and 75°C for thermophilic digester).*

From the information we collected, the digested sludge is typically brought from 30°C to 38°C by a water stream decreasing from 60 to 55°C. According to Figure 6.7, the solubility product constant ($pK_{sp}$) of vivianite slightly increases from 35.738 to 35.766 between 30°C and 38°C. It translates into the precipitation of a maximum of 0.28 mg of vivianite per litre of sludge for a typical iron-coagulated digested sludge considered in Table S6.3 (P=30 ppm, $Fe^{2+}$=15 ppm, IS=0.05, pH=7). Considering the flowrate of the sludge in the heat exchanger of Amsterdam WWTP (60 $m^3$/h), it corresponds to the precipitation of 16.8 g of vivianite per hour in one heat exchanger. It seems unrealistic that all the vivianite formed in the heat exchanger would scale, so this value is likely overestimated. It is important to mention that iron was dosed in the sludge heating loop of the WWTP of Amsterdam, which undoubtedly contributed to scaling formation. Even though the turbulent flow regime suggests a bulk mechanism, it is interesting to study what can happen in the boundary layer of a heat exchanger.

At the exit of the considered counter-current heat exchanger, the water temperature is 60°C, while the temperature of the sludge is 38°C. Assuming that the wall temperature is the average of the temperature of the sludge and the heating water, eight times more vivianite (2.17 g/L of sludge) could potentially form at the wall at 50°C compared to the bulk at 38°C. In Derby WWTP, peaks to 85°C of the heating water were observed (and believed to aggravate the scaling), which would lead to the potential formation of 4.96 mg/L of vivianite (considering a wall temperature of 60°C). Figure 6.7 suggests that vivianite is more likely to form in the exit part of the heat exchanger where the sludge is the warmest, observed by Reusser 2009. The situation could be worse when the sludge is brought at a higher temperature (55°C). Heating sludge from 30°C to 55°C potentially produces 12 times more vivianite (3.4 mg/L) compared to heating up from 30°C to 38°C. Temperatures higher than 55°C cause severe vivianite scaling issues, particularly in the heat exchangers pre-pasteurization plants (Panter et al. 2013) and of a specific thermophilic digester configuration (Reusser 2009).

Salehin et al. 2019 did not find vivianite presence in digested sludge after THP by XRD. They concluded that vivianite formation was hindered by THP, suggesting that vivianite scaling would not occur after THP. However, our Mössbauer spectroscopy measurements revealed that vivianite accounted for 18% of the total solids in the post-THP digested sludge of Blue Plains WWTP, showing the possibility for vivianite to form. In the Cambi installation of Blue Plains WWTP, sludge after THP is cooled down from 160 to 41°C, first by pressure reduction from steam release followed by dilution with process water, and then with a heat exchanger. It can be hypothesized that the vivianite scaling observed was formed in the colder sections of the heat exchanger (with wall temperature <32°C according to Figure 6.7). Vivianite scaling in the cooling heat exchanger after THP could then occur in the cold sludge region, while the warmer region should be scale-free. In the case of Venlo WWTP, THP is followed by thermophilic digestion at 55°C. It is unlikely that the sludge temperature decreases below 32°C in the boundary layer under these conditions, so it seems logical that no vivianite scaling was found there.

From the different hot spots identified, vivianite scaling in the heat exchanger was the most commonly reported in the literature (Table 6.2). It could be because vivianite in heat exchangers is generally more recognizable ("clean" hard and blue scale), more accessible (compared to pipe inspection), and causing immediate operational issues (temperature losses

**6**

as observed by Shimada et al. 2011 and Reusser 2009). While the scaling in the heat exchanger was manageable in most installations using mesophilic digestion, it seems that it can be more severe in installation bringing sludges at higher temperatures. Vivianite scaling was observed in both tubular and spiral heat exchanger Lübeck WWTP, so it is complicated to say which type of heat exchanger would cause less trouble. Using steam injection instead of contact heat exchangers to promote bulk precipitation is sometimes used and could be an interesting alternative to reduce scaling (Buchanan et al. 2014, Panter et al. 2013). However, it involves more energy and on-site production of boiled feed water, making this strategy more complicated to apply. In general, maintaining a low (and constant) temperature difference between the sludge and the heating water to avoid high wall temperature seems to be the best solution to mitigate vivianite scaling (Reusser 2009, Bjorn 2010) but is more complicated at thermophilic temperatures. Iron salt addition or sludge admixing (see 6.3.4) in the heat exchanger loop can aggravate the problems further.

## 6.3.4. Sludge admixing

An additional point that requires attention to control scaling formation is how the different sludges are mixed together. Wastewater treatment produces different streams of sludge that will be brought together typically for pre-dewatering or digestion. Those sludges have different characteristics (pH, temperature, concentration of $Fe^{2+}$ and $PO_4^{3-}$), and when they are brought together, the saturation index (SI) of the mix can potentially be higher than the index of the individual sludges. This can be particularly the case when an already fermented sludge is mixed with a relatively fresh sludge. When a sludge ferments, pH drops (VFA production), $Fe^{2+}$ increases (dissolution of iron precipitates), and $PO_4^{3-}$ increases (poly-phosphate from PAO's hydrolysis). The difference of temperature between sludges can also be a factor triggering vivianite scaling. In Dallas WWTP, digester feed was periodically incorporated to recirculation sludge (Shimada 2011), which can aggravate the problem due to an increase of the saturation index because of influences on composition (pH, $Fe^{2+}$, $PO_4^{3-}$) and temperature. Similar mixing issues, in addition to an increased pH due to $CO_2$ stripping, were believed to aggravate vivianite scaling in Back River WWTP heating loop (Marx et al. 2001).

To conclude, mixing of different sludges can trigger or aggravate vivianite scaling. To prevent or at least mitigate vivianite scaling, it is essential to minimize the pH, temperature, and concentration differences between mixed sludges. This could be done by preferring continuous feed at a lower flowrate, over big periodical feed flows. More importantly, the place where the mixing occurs should be wisely chosen. The mixing of sludge should preferably happen in a unit where the volume to area ratio is high to favor bulk precipitation. The use of buffer tanks to allow the majority of the vivianite to precipitate seems ideal. On the contrary, we do not recommend mixing sludges in or before a unit where the surface/volume ratio is high (e.g., in the case of in-line mixing in pipes, heat exchanger, etc.).

## 6.3.5. Digester

Vivianite formation is promoted under anaerobic conditions due to the release of phosphate and the reduction of Fe(II), and anaerobic digesters are, therefore, a preferential formation site (Wilfert et al. 2018). Vivianite scaling could happen on the walls of digesters, similarly to struvite, but should not be so problematic due to the high volume/area ratio of digesters. The

authors think that the settling of vivianite particles in digesters is not likely to happen since vivianite particles have the same density as quartz but are usually smaller (100-150 μm maximum). We assume that digester mixing is generally engineered in a way that prevents settling of quartz and, similarly, settling of vivianite. Moreover, vivianite settling was never reported as an issue in any of the numerous digesters (bearing vivianite in their sludge) sampled by our team in previous studies (Wilfert et al. 2018). Blue Plains WWTP digester withdrawal contains some vivianite but does not accumulate, not creating issues.
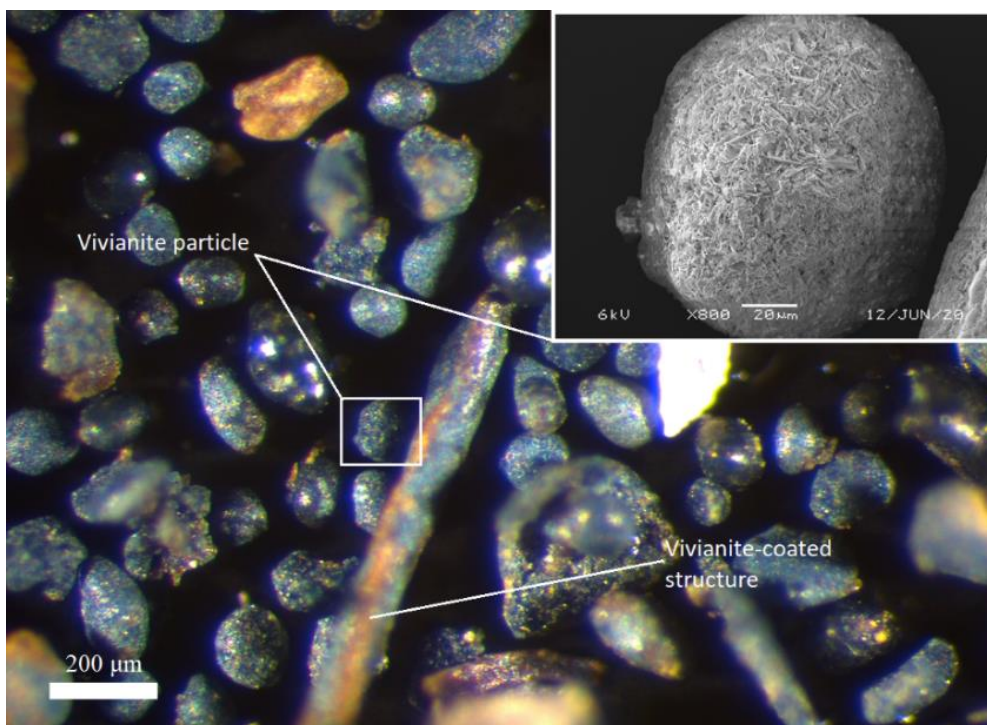


*Figure 6.8: Light microscope picture of the digester withdrawal obtained from Spokane County WWTP. EDX identified all the blue particles as vivianite, and a SEM picture of one of those is shown on the top right. The problem in Spokane County digester originated from the settling of free vivianite particles and not deposition of a continuous vivianite scaling.*

However, the WWTP of Spokane County experiences problems in its anaerobic digesters due to the accumulation of dark sand-like material, suspected to be vivianite (Figure 6.8). Each digester is mixed with an external draft tube designed to pull from the centre of the bottom section and feed at the top, but that needs to be reversed when too much material has accumulated. Additional mixing is provided by an internal jet mixing ring located at the bottom of each digester. This jet mixing system has experienced clogging, potentially also caused by material accumulation. This accumulation obliges the WWTP to drain the bottom of the digesters daily, losing a part of the valuable microbial community and involving heavy maintenance. Contrary to previously discussed scaling problems, the issue in Spokane County digesters was the settling of vivianite particles, not the deposition of a continuous vivianite layer. This case was investigated to confirm the presence of vivianite, understand the cause of the settling, and evaluate the uniqueness of this situation.

The digester withdrawal is composed of a majority of iron (32%) and phosphorus (9%), with 2% of calcium as the main other inorganic element. Mössbauer spectroscopy indicated that 45% of the sample is vivianite and may contain non-detected oxidation products of vivianite (metavivianite and santabarbaraite) since 37% of the phosphorus is still not attributed. XRD detected the presence of baricite $((Mg, Fe^{+2})_3(PO_4)_2 \cdot 8H_2O)$ that can be assumed to be impure vivianite and Rhodochrosite $(MnCO_3)$. The latter could be siderite $(FeCO_3)$ since Mn is absent from the sample and siderite has a similar XRD pattern as rhodochrosite (Anthony et al. 1990). Also, Mössbauer spectroscopy detects 11% of a Fe(II) phase with hyperfine parameters similar to siderite (Medina et al. 2006). The presence of siderite would also match with the 4.8% of $CO_3$ (equivalent to 9.6% of $FeCO_3$) detected by µGC. The microscopic observations reveal that most of the sample was composed of blue particles presenting a Fe/P overlap (Figure 6.8, EDX results not showed). These particles showed a similar structure (sheets agglomerate) as the vivianite particles found in digested sludge (Chapter 2, Wilfert et al. 2018 and 2020) but were free and more spherical (a longer retention time in the digester could promote erosion). The particles were not bigger (100-150 µm) than the largest particles usually encountered in digested sludge.

The terminal settling velocity of a vivianite particle of 150 µm of diameter was evaluated to be 2.27m/h (Supplementary information). This velocity is smaller than the one produced by the digester mixing (vertical velocity ~20 m/h), so we would not expect the particles to settle. However, vivianite does settle, and the turnover time for these digesters is 1h, which is in the high range compared to 4 digesters studied by Meroney et al. 2009 (24-54 min), suggesting a not sufficient mixing. From a discussion with the operators of the digesters of Spokane County, the mixing system is unique, and no other installations encountered similar settling problems. To conclude, the mixing design seems to be the primary cause of the problem.

For the specific case of Spokane County WWTP, the addition of an alternative mixing system to the existing installation could provide sufficient mixing and appear to be the most efficient solution but could be costly and complicated. The digester is emptied by an overflow at the top of the installation, which may not be optimal in this situation since the sludge is not homogeneous. Discharging from a lower point in the digester could help to prevent vivianite accumulation. More generally, it is interesting to note that working at higher solid content in a digester would increase the viscosity of the sludge and, therefore, lower the particle settling speed. For example, increasing the solid content from 2.5% (solid content in Spokane County WWTP) to 5% would decrease the settling velocity from 2.27 to 0.28 m/h (Supplementary information). Lastly, we noticed that vivianite was agglomerating on some particles in the digester withdrawal, increasing their size, and therefore, their settling potential (Figure 6.8). Accumulation of vivianite on sand particles (in a fluidized-bed reactor) was already proven possible by Priambodo et al. 2017. To avoid this agglomeration, solids, especially sand, should consistently be removed before digestion, so it is not used as a centre of agglomeration for vivianite.

### 6.3.6. Evaluation of the findings

From the information collected, it seems that vivianite scaling in WWTPs is occurring much more often than reported in the literature. From the five preferential scaling places studied,

three seem to be more common: 1. the anaerobic pipes and units before sludge digestion, 2. around the (pre-) dewatering centrifuges treating undigested sludge, and 3. in the heat exchangers around anaerobic digestion. Vivianite is usually the major component of the scaling in these three zones, with FeS and iron oxides/hydroxides being minor phases. In zone 2., vivianite gradually oxidizes to turn into amorphous metavivianite and santabarbaraite. The vivianite formation mechanism depends on the scaling place and can involve iron reduction, pH increase, or temperature changes. Different prevention solutions based on the formation mechanisms are proposed in Table 6.3.

*Table 6.3: Summary of the preferential scaling places, the scaling composition, their proposed formation mechanisms, and possible prevention methods.*

| Place where scaling occurs | Composition of the scaling | Formation mechanisms | Prevention methods |
|---|---|---|---|
| Anaerobic zones | Crystalline vivianite FeS (minor) | Fe(III) reduction coupled with phosphate release from biomass | Addition of a buffer tank to promote bulk precipitation before pumping the sludge. Prefer the use of large pipes |
| Dewatering units (for undigested sludge) | Vivianite (minor) Metavivianite and santabarbaraite (major) Fe oxides/hydroxides (generally minor) | Turbulences lead to $CO_2$ stripping, which increases the pH. Gradual oxidation of vivianite $Fe^{2+}$ oxidation ($Fe^{3+}$ has a low solubility) | Addition of a buffer tank to promote bulk precipitation before centrifugation. Centrifuging in $CO_2$-saturated atmosphere Centrifuging in $O_2$-free atmosphere (complicated) |
| Heat exchangers | Crystalline vivianite (few other compounds) Fe oxides/hydroxides after THP only (minor) | The solubility of vivianite varies with temperature. Wall temperature are higher than the bulk | Minimize the temperature between the heating/cooling fluid and the sludge. Steam injection for severe cases |

**6**

A common prevention strategy is the use of commercial antiscalant, which is not discussed in this study. It appears that the way sludge streams with different characteristics are admixed (e.g., raw sludge + digested sludge) is an aggravating factor of vivianite scaling. It should be done in units with a high volume/surface ratio like buffer tanks to promote bulk precipitation. Vivianite settling in digesters cannot be classified as a common issue since the case studied involved a unique mixing system that we believe is the cause of the problem.

So far, vivianite scaling did not attract much attention compared to struvite scaling since the importance of vivianite in wastewater treatment was only recently highlighted. Moreover, vivianite scaling is often wrongly mistaken for struvite scaling, while the presence of struvite scaling was never detected in this study. It needs to be noted that struvite scaling is more likely to happen in WWTPs using EBPR (Parsons and Doyle 2002), while vivianite scaling should preferentially happen in WWTPs dosing iron to remove phosphorus. The absence of struvite scaling in the presence of iron can be explained by its higher solubility (5.5 mM for $pK_{sp}$ = 12.6 at pH 7) than the one of vivianite (0.06 mM for $pK_{sp}$= 35.8 at pH 7). Also, vivianite

oxidation leads to the formation of amorphous compounds that are more complicated to identify. Even Mössbauer spectroscopy analysis, the best option for vivianite quantification, presents limitations, especially due to an incomplete database on iron compounds in sludge.

Iron addition may be favorable for energy production via enhanced primary settling. In Chapter 3, a higher iron dosage is favorable for vivianite formation and subsequent magnetic recovery. We foresee that higher iron dosing will be more commonly applied in the near future for different reasons: struvite scaling prevention, sulphide control in biogas, and to meet more stringent legislation requirements for phosphorus removal. Additionally, higher iron dosing increases the share of phosphorus present as vivianite, which can subsequently be recovered via magnetic extraction, providing a new possible phosphorus recovery route (Chapter 2 and 3). Dosing more iron is not incompatible with vivianite scaling prevention since bigger quantities of iron dosed achieve lower soluble phosphorus, more phosphorus chemically fixed, thus less phosphate released from biomass, reducing the phosphorus pool available for vivianite scaling. Vivianite scaling occurrence does not mean that the quantity of iron dosed needs to be adjusted, but rather that it needs to be dosed better. This study raises points of attention and proposes mitigation/prevention solutions that should be evaluated in each specific case by the water utilities.

## 6.4. Conclusion

The main conclusion of this study is that vivianite scaling is occurring more often than the lack of information in the literature suggests. Three preferential scaling places could be identified, each of them presenting a different vivianite formation mechanism. Firstly, the reduction of ferric iron triggered the formation of crystalline vivianite in the sections where undigested sludge met anaerobic conditions (e.g., thickened sludge pipes). Secondly, $CO_2$ stripping occurring during centrifugation of undigested sludge caused a pH increase, responsible for the formation of vivianite that could later oxidize to santabarbaraite. Thirdly, the temperature dependence of the solubility of vivianite can drive the formation of vivianite scaling on the walls of the heat exchangers used for digested sludge heating.

Additionally, scaling prevention solutions were discussed in each case. For example, an anaerobic buffer tank immediately after thickening would promote vivianite formation in the bulk of the sludge, reducing the vivianite scaling issues in the pipes and centrifuges downstream. The choice of the appropriate solution and the related cost analysis should be undertaken in each specific case since costs for maintenance and material vary depending on the WWTP design and location. We believe that this work can be of interest for water authorities for vivianite scaling mitigation, as well as for researchers investigating vivianite recovery from sewage sludge.

# References

Alfa Laval brochure. Last consulted on 17/08/2020 at https://www.alfalaval.com/contentassets/3f718d0f5eeb4d56acc8c7d6eab344a2/alfa_laval_spiral_heat_exchanger_ppi00424en.pdf.

Battistoni, P., Fava, G., Pavan, P., Musacco, A., Cecchi, F. (1997). Phosphate removal in anaerobic liquors by struvite crystallization without addition of chemicals: preliminary results. *Water Research* 1997, 31 (11), 2925–2929. doi:10.1016/S0043-1354(97)00137-1.

Bjorn, A., (2010). Acid Phase Digestion at Derby STW - Context and preliminary optimisation results. Last consulted on 05/11/20 at https://www.atkinsglobal.com/~/media/Files/A/Atkins-Corporate/group/sectors-documents/water/library-docs/technical-papers/acid-phase-digestion-at-derby.pdf.

Buchanan, A., Chan, T. F., Riches, S., Brookes, A., Brown, C. (2014). Starting up a new advanced digestion technology. *19th European Biosolids & Organic Resources Conference.*

Čermáková. Z., Švarcová. S., Hradil. D., Bezdicka. P. (2013). Vivianite: A historic blue pigment and its degradation under scrutiny. *Science and Technology for the Conservation of Cultural Heritage,* 75-78.

Dormann, J. L., Poullen, J. F. (1980). Étude par spectroscopie Mössbauer de vivianites oxydées naturelles. *Bulletin de Minéralogie*, 103 (6), 633-639. doi:https://doi.org/10.3406/bulmi.1980.7431.

Doyle, J., Oldring, K., Churchley, J., Parsons, S. (2002). Struvite formation and the fouling propensity of different materials. *Water Research*, 36(16), 3971–3978. doi:10.1016/s0043-1354(02)00127-6.

Doyle, J. D. and Parsons, S. A. (2002). Struvite Formation, Control and Recovery. *Water Research*, 36 (16), 3925–3940. doi:10.1016/S0043-1354(02)00126-4.

El-Bestawy, E., Hussein, H., Baghdadi, H. H., & El-Saka, M. F. (2005). Comparison between biological and chemical treatment of wastewater containing nitrogen and phosphorus. *Journal of Industrial Microbiology & Biotechnology*, 32(5), 195–203. doi:10.1007/s10295-005-0229-y.

European commission (2017). Ninth Report on the implementation status and the programs for implementation (as required by Article 17) of Council Directive 91/271/EEC concerning urban waste water treatment.

Eshtiaghi, N., Markis, F., Slatter, P. (2012). The laminar/turbulent transition in a sludge pipeline. *Water Science and Technology*, 65 (4), 697–702. doi:10.2166/wst.2012.893.

European Sustainable Phosphorus Platform. (2019). ESPP wastewater phosphorus removal workshop (133). Last consulted on 06/10/2020 at https://phosphorusplatform.eu/images/scope/ScopeNewsletter133_Liege_water_policy_workshop_2019.pdf.

Guo J.C.Y. Theoretical fluid mechanics: turbulent flow velocity profile, Civil engineering, university of Colorado at Denver. Last consulted on 05/11/2020 at https://www.ucdenver.edu/faculty-staff/jguo/Documents/Fluid1/12Turbulent.pdf.

Haldenwang, R., Sutherland, A.P.N., Fester, V.G., Holm, R., Chhabra, R.P. (2012). Sludge pipe flow pressure drop prediction using composite power-law friction factor-Reynolds number correlations based on different non-newtonian Reynolds numbers. *Water Sa*, 38 (4), 615–622. doi:10.4314/wsa.v38i4.17.

Janssen, P.M.J., Meinema, K., van de Roest, H.F. (2002). Biological Phosphorus Removal, Manual for design and operation.

Klencsár, Z. (1997). Mössbauer spectrum analysis by Evolution Algorithm. *Nuclear Instruments and Methods in Physics Research Section B: Beam Interactions with Materials and Atoms*, 129(4), 527–533. doi:10.1016/s0168-583x(97)00314-5.

Kumar, P.S., Korving, L., Van Loosdrecht, M.C.M., Witkamp, G. (2018). Adsorption as a technology to achieve ultra-low concentrations of phosphate: Research gaps and economic analysis. *Water Research X*, 4. doi: 10.1016/j.wroa.2019.100029.

Kumar, P.S., Korving, L., Keesman, K. J., van Loosdrecht, M. C. M., Witkamp, G. J. (2019). Effect of pore size distribution and particle size of porous metal oxides on phosphate adsorption capacity and kinetics. *Chemical Engineering Journal*. 358. doi:10.1016/j.cej.2018.09.202.

Lines, J.R. (1991). Heat Exchangers in municipal wastewater treatment plants. Last consulted on 29/10/2020 at https://www.graham-mfg.com/usr/pdf/TechLibHeatTransfer/13.PDF.

Liu, J., Cheng, X., Qi, X., Li, N., Tian, J., Qiu, B., Qu, D. (2018). Recovery of phosphate from aqueous solutions via vivianite crystallization: Thermodynamics and influence of pH. *Chemical Engineering Journal*, 349, 37–46. doi:10.1016/j.cej.2018.05.064.

Marx, J.J., Wilson, T.E., Schroedel, R.B., Winfield, G., Sokhey, A. (2001). Vivianite: Nutrient's removal hidden problem. *Proceedings of the Water Environment Federation*, 8, 378-388. doi:10.2175/193864701790861721.

McCammon, C. A., and Burns, R. G. (1980). The oxidation mechanism of vivianite as studied by Mossbauer spectroscopy. *American Mineralogist*, 65(3–4), 361–366.

Medina, G., Tabares, J. A., Pérez Alcázar, G. A., Barraza, J. M. (2006). A Methodology to Evaluate Coal Ash Content Using Siderite Mössbauer Spectral Area. *Fuel*, 85 (5-6), 871–873 doi:10.1016/j.fuel.2005.08.034.

Meroney, R. N., and Colorado, P. E. (2009). CFD simulation of mechanical draft tube mixing in anaerobic digester tanks. *Water Research*, 43 (4), 1040–1050. doi:10.1016/j.watres.2008.11.035.

Mersmann, A. (2001). Crystallization technology handbook, Second edition revised and explained.

Panter, K., Holte, H., Walley, P. (2013). Challenges of developing small scale thermal hydrolysis and digestion projects. *18th European Biosolids & Organic Resources Conference & Exhibition*.

Partlan, E., (2018). BlueTech Report on LIFT Water Technology Survey: Wastewater. Last consulted on 29/10/2020 at https://www.waterrf.org/sites/default/files/file/2019-07/LIFT%20Water%20Technology%20Survey%20Report%20-%20Wastewater_0.pdf.

Pathak, B., Al-Omari, A., Smith, S., Passarelli, N., Suzuki, R., Khakar, S., DeBarbadillo, C. (2018). Vivianite occurrence and remediation techniques in biosolids pre-treatment process. *WEF Residuals and Biosolids Conference 2018*.

Pratesi, G., Cipriani, C., Giuli, G., Birch, W. (2003), Santabarbaraite: A new amorphous phosphate mineral. *European Journal of Mineralogy,* 15 (1), 185-192. doi:10.1127/0935-1221/2003/0015-0185.

Priambodo, R., Tan, P. R., Shih, Y.-L., Huang, Y.-J. (2017). Fluidized-bed crystallization of iron phosphate from solution containing phosphorus. *Journal of the Taiwan Institute of Chemical Engineers*, 80, 247–254. doi:10.1016/j.jtice.2017.07.004.

Prot, T., Nguyen, V.H., Wilfert, P., Dugulan, A.I., Goubitz, K., De Ridder, D.J., Korving, L., Rem, P., Bouderbala, A., Witkamp, G.J., Van Loosdrecht, M.C.M (2019). Magnetic separation and characterization of vivianite from digested sewage sludge. *Separation and Purification.* doi:10.1016/j.seppur.2019.05.057.

Prot, T., Wijdeveld, W., Eshun, L. E., Dugulan, A. I., Goubitz, K., Korving, L., Van Loosdrecht, M. C. M. (2020). Full-Scale Increased Iron Dosage to Stimulate the Formation of Vivianite and Its Recovery from Digested Sewage Sludge. *Water Research*, 182. doi:10.1016/j.watres.2020.115911.

Ratkovich, N., Horn, W., Helmus, F. P., Rosenberger, S., Naessens, W., Nopens, I., Bentzen, T. R. (2013). Activated sludge rheology: a critical review on data collection and modeling. *Water Research*, 47 (2), 463–482. doi:10.1016/j.watres.2012.11.021.

Refait, P. H., Abdelmoula, M., Génin J.-M.R. (1998). Mechanisms of formation and structure of green rust one in aqueous corrosion of iron in the presence of chloride ions. *Corrosion Science,* 40 (9), 1547–1560. doi:10.1016/S0010-938X(98)00066-3.

Reusser, S.R. (2009). Proceed with caution in advanced anaerobic digestion system design. *Proceedings of the Water Environment Federation Session,* 41 (50), pp. 3065-3084.

Roldán, R., Barrón, V., Torrent, J. (2002). Experimental alteration of vivianite to lepidocrocite in a calcareous medium. *Clay Miner.* 37 (4), 709–718. doi:10.1180/0009855023740072.

Rothe, M., Kleeberg, A., & Hupfer, M. (2016). The occurrence, identification and environmental relevance of vivianite in waterlogged soils and aquatic sediments. *Earth-Science Reviews*, 158, 51-64. doi:10.1016/j.earscirev.2016.04.008.

Salehin, S., Kulandaivelu, J., Rebosura, M.Jr., Khan, W., Wong, R., Jiang, G., Smith, P., McPhee, P., Howard, C., Sharma, K., Keller, J., Donose, B.C., Yuan, Z., Pikaar, I. (2019). Opportunities for reducing coagulants usage in urban water management: the Oxley Creek sewage collection and treatment system as an example. *Water Research*, 165, 114996–114996. doi: 10.1016/j.watres.2019.114996.

Schwertmann, U. (1991). Solubility and dissolution of iron oxides. *Iron Nutrition and Interactions in Plants,* 3–27. doi:10.1007/978-94-011-3294-7_1.

Seitz, A., Riedner, J., Malhotra, K., Kipp, J. (1973). Iron-Phosphate compound identification in sewage sludge residue. *Environmental Science and Technology*, 7(4), 354-357. doi:10.1021/es60076a005.

Shimada, T., Evers, M., White, J., Kaakaty, C., Sober, J., Kilian R. (2011). Detection and mitigation of vivianite scaling in anaerobic digesters. *Weftec 2011.*

Slatter, P. (2004). The hydraulic transportation of thickened sludges. *Water S.A* 30 (5). doi: 10.4314/wsa.v30i5.5169.

Solon, K., Volcke, E.I.P., Spérandio M., van Loosdrecht, M.C.M. (2019). Resource recovery and wastewater treatment modeling. *Environmental Science: Water Research & Technology,* (4). doi:10.1039/c8ew00765a.

Spiralex brochure. Last consulted on 17/08/2020 at https://www.spiralex.nl/wp-content/uploads/2017/08/Sludge.pdf.

Wang, R., Wilfert, P., Dugulan, I., Goubitz, K., Korving, L., Witkamp, G.-J., van Loosdrecht, M. C. M. (2019). Fe(III) reduction and vivianite formation in activated sludge. *Separation and Purification Technology,* 220, 126–135. doi:10.1016/j.seppur.2019.03.024.

Wilfert, P., Kumar, P. S., Korving, L., Witkamp, G.-J., van Loosdrecht, M. C. M. (2015). The relevance of phosphorus and iron chemistry to the recovery of phosphorus from wastewater: a review. *Environmental Science & Technology*, 49 (16), 9400–9414. doi:10.1021/acs.est.5b00150.

Wilfert, P., Mandalidis, A., Dugulan, A. I., Goubitz, K., Korving, L., Temmink, H., Witkamp, G.J., van Loosdrecht, M. C. M. (2016). Vivianite as an important iron phosphate precipitate in sewage treatment plants. *Water Research*, 104, 449–460. doi:10.1016/j.watres.2016.08.032.

Wilfert, P., Korving, L., Dugulan, I., Goubitz K., Witkamp, G. J., van Loosdrecht M.C.M. (2018). Vivianite as the main phosphate mineral in digested sewage sludge and its role for phosphate recovery. *Water Research*, 144, 312-321. doi:10.1016/j.watres.2018.07.020.

Yousuf, M., & Frawley, P. J. (2018). Experimental evaluation of fluid shear stress impact on secondary nucleation in a solution crystallization of paracetamol. *Crystal Growth & Design*. doi:10.1021/acs.cgd.8b01074.

**6**

## Supplementary information



*Figure S6.1: Location of the WWTPs from which data was collected (The Netherlands: 5, USA: 5, Germany: 1, Finland: 1, United Kingdom: 1, Denmark: 1)*

*Table S6.1: Equilibrium considered for the modelling with Visual Minteq. The equations and equilibrium constants reported are those used in the database of Visual Minteq*

| Equilibrium considered | Log K |
|---|---|
| $3Fe^{2+} + 2\ PO_4^{3+} + 8H_2O = Fe_3(PO_4)_2{*}8H_2O$ | -35.767 |
| $Fe^{3+} + 3\ H_2O - 3\ H^+ = Fe(OH)_3$ | 3.2 |
| $PO_4^{3-} + H^+ = HPO_4^{2-}$ | 12.375 |
| $PO_4^{3-} + 2\ H^+ = H_2PO_4^-$ | 19.573 |
| $PO_4^{3-} + 3\ H^+ = H_3PO_4$ | 21.721 |
| $Fe^{2+} + 2\ H_2O - 2\ H^+ = Fe(OH)_2\ (aq)$ | -20.494 |
| $Fe^{3+} + 2\ H_2O - 2\ H^+ = Fe(OH)_2^+$ | -5.75 |
| $Fe^{2+} + 3\ H_2O - 3\ H^+ = Fe(OH)_3^-$ | -30.991 |
| $Fe^{3+} + 3\ H_2O - 3\ H^+ = Fe(OH)_3\ (aq)$ | -15 |
| $Fe^{3+} + 4\ H_2O - 4\ H^+ = Fe(OH)_4^-$ | -22.7 |
| $Fe^{2+} + H_2O - H^+ = FeOH^+$ | -9.397 |
| $Fe^{3+} + H_2O - H^+ = FeOH^{2+}$ | -2.02 |
| $2\ Fe^{3+} + 2\ H_2O - 2\ H^+ = Fe_2(OH)_2^{4+}$ | -2.894 |
| $3\ Fe^{3+} + 4\ H_2O - 4\ H^+ = Fe_3(OH)_4^{5+}$ | -6.288 |
| $Fe^{2+} + 2\ H^+ + PO_4^{3-} = FeH_2PO_4^+$ | 22.273 |
| $Fe^{3+} + 2\ H^+ + PO_4^{3-} = FeH_2PO_4^{2+}$ | 23.85 |
| $Fe^{2+} + H^+ + PO_4^{3-} = FeHPO_4\ (aq)$ | 15.975 |
| $Fe^{3+} + H^+ + PO_4^{3-} = FeHPO_4^+$ | 22.285 |

## Fluid mechanic evaluation

*Power-law parameters determination*

Three models are typically used to describe the rheology of non-Newtonian fluids like sludge: the Power-law model, the Bingham model, and the Herschel and Bulkley. Ratkovich et al. 2013 reviewed several articles dealing with sludge rheology modeling and concluded that none of these models was better than the others. Moreover, all three models often give a satisfying fitting of the data, which is not surprising since their expressions derive from the other. For this study, the power-law model will be used:

$$\tau = K \left(\frac{dv}{dr}\right)^n$$

Where:

- $\tau$ is the shear stress in $N/m^2$
- $K$ is the fluid consistency coefficient in $N.s^n/m^2$
- $\left(\frac{dv}{dr}\right)$ is the shear rate in $s^{-1}$
- $n$ is the flow behavior index (dimensionless)

The constants $K$ and $n$ vary depending on the solid content, temperature, and state of digestion of the sludge (Cao et al. 2016). They need to be determined by fitting the experimental data. However, no rheological measurements were done in the current study, so the parameters will be estimated from literature data for sludges with similar properties (TSS=3.1%, T=20°C, undigested sludge) and modeled with the power law. From the experimental data of Wei et al. 2018, Honey and Pretorius 2000, Füreder et al. 2018 and Rosenberg et al. 2002, we estimate that the parameters will be in the range 0.2-0.4 for $n$ and 2-100 for $K$ (we excluded some much higher $K$ values found in Rosenberg et al. 2002 since it was in contradiction with the three other sources).

*Flow regime evaluation*

The piping system in Hoensbroek can be visualized below.
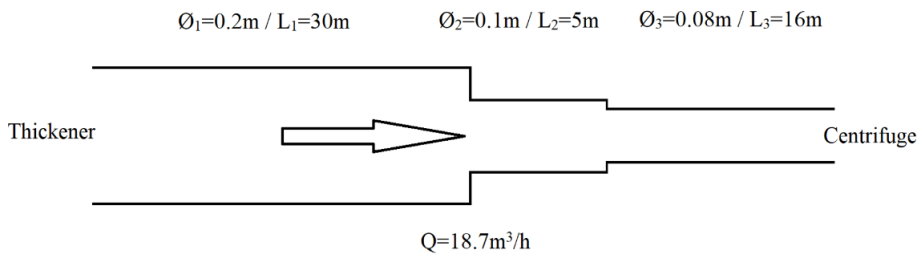


*Figure S6.2: Piping system where vivianite scaling was found in Hoensbroek WWTP.*

To determine the flow regime in the pipes, the Reynolds number derived from power-law modeling needs to be calculated:

$$Re = \frac{\rho V^{2-n} D^n}{K * 8^{n-1}}$$

Where:

- $Re$ is the Reynolds number for the power-law model (dimensionless)
- K is the fluid consistency coefficient in $N.s^n/m^2$
- n is the flow behavior index (dimensionless)
- $\rho$ is the density of the sludge in $kg/m^3$
- D is the diameter of the pipe in m

Unless it has a very high solid content, sludge has a similar density as water, set at 1000 $kg/m^3$ for the following calculation.

Considering the ranges for the n and K factors estimated above, the Reynolds number in pipe 3 ($d_3$=0.08 m / $L_3$=16 m) varies from 13 to 1679, signifying that the flow regime is laminar since Re<2100 (Ratkovich et al. 2013). This is in line with what is usually reported in the literature, where sludge flow in pipes is usually considered laminar (Slatter 2004, Haldenwang et al. 2012). Moreover, the velocity for a laminar/turbulent transition is estimated at 1.5-2.0 m/s (Honey and Pretorius 2000), while the velocity in pipe 3 is 1.0 m/s. Considering that pipe 3 is the smallest of the three pipes, a laminar flow should be observed in the two other pipes as well ($d_1$=0.2 m / $L_1$=30 m and $d_2$=0.1 m / $L_2$=5 m).

*Vivianite scaling formation*

The authors consider that vivianite scaling could form in 2 ways: by collision of the particles with the pipe wall and further agglomeration, or by precipitation from the dissolved species following the iron reduction in a boundary layer. Considering that the flow regime is laminar in the pipe system, the first formation mechanism is unlikely since it would require some transversal vivianite particle movement. From this point on, the second mechanism is studied.

Pipe 3 at Hoensbroek WWTP has been opened after 3.5 years of operation, and a scaling layer of 0.55 cm had formed. Mössbauer spectroscopy indicates that 72% of the scaling is vivianite. Knowing the density of vivianite (d=2.69), it means that 39.6 kg of vivianite scaling formed in the pipe three over 3.5 years (1.29 g/h).

*Velocity profile in the pipes*

From Simpson et al. 2008, the velocity profile in a circular duct for a non-Newtonian fluid following the power law has the following expression:

$$V_r = \frac{3n+1}{n+1}\left[1 - \left(\frac{r}{R}\right)^{\left(\frac{n+1}{n}\right)}\right]V$$

Where:

- n is the flow behavior index (dimensionless) and estimated before ranging from 0.2-0.4
- $V_r$ is the velocity at the radius r
- $r$ is the distance from the centre of the pipe (0<r<R)
- $R$ is the internal radius of the pipe
- $V$ is the average velocity in the pipe

For further calculations, n will be fixed at a value of 0.3.

*Iron reduction rate*

The sludge between the thickener and the centrifuge contains 1070 mg of iron and 560 mg of phosphorus per kg of sludge (TS=3.1%). Under anaerobic conditions, phosphate will be released from the Polyphosphate-Accumulating organisms. However, in chemical sludge (like in Hoensbroek), phosphorus is not only found in PAO's but is also bound to Fe. Wang et al. 2019 observed that vivianite progressively formed during incubation of activated chemical sludge, meaning that some phosphorus was made available for vivianite formation. It is complicated to differentiate the phosphate released from PAO's and iron phosphate minerals. Therefore, estimating the vivianite scaling formed will be done assuming that iron reduction is the limiting factor.

The quantity of iron reduced can be calculated from the retention time in the different layers of the pipe. According to Wang et al. 2019, iron reduction in sludge in anaerobic conditions follows a first-order kinetic with k=0.055 $h^{-1}$. This translates into the reduction of 561 mg of Fe/kg of sludge in the thickener during the residence time of 13.5 h, which will be taken as the initial ($Fe_0$) value for the subsequent iron reduction. We neglect the reduction occurring in pipes 1 and 2 due to the very low retention time compared to the one in the thickener. We obtain the expression:

$$Fe(t) = Fe_0( 1 - \exp(-0.055t))$$

Where:

- Fe(t) represents the quantity of iron reduced into $Fe^{2+}$ after entering the pipe (mg Fe/kg of sludge).
- $Fe_0$ is a constant representing the reducible iron at the beginning of the pipe system, worth 509 of Fe/kg of sludge. (after removing the 561 mg Fe/kg of sludge already reduced in the thickener).
- t is the time elapsed since the sludge enters pipe (h). It also corresponds to the retention time of the sludge in the pipe at a radius r.

Since the retention times in the pipes are relatively small compared to the iron reduction rate, there is almost a linear relationship between the quantity of iron reduced and the retention time. Therefore, the reduced iron is inversely proportional to the velocity of the sludge.
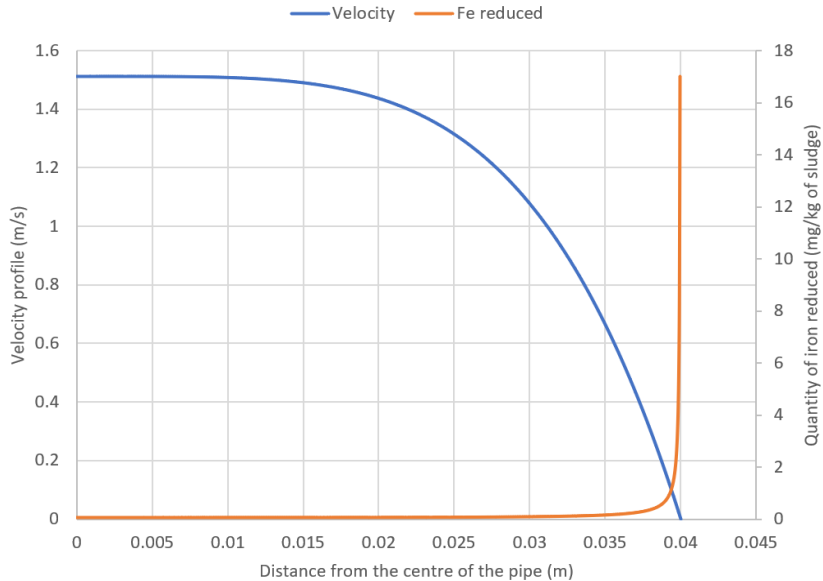
*Figure S6.3: Left axis: Velocity profile of the sludge in the function of its distance from the centre of pipe 3. Right axis: quantity of iron reduced during the stay of the sludge in the pipe in the function of its distance to the centre of the pipe.*

From Figure S6.3, it can be noticed that the velocity profile of the sludge in pipe 3 will create zones near the edge of the pipe where $Fe^{2+}$ concentration will be higher and promote vivianite scaling formation. This iron production, in combination with the phosphorus release from the sludge, will lead to a higher saturation index next to the wall of the pipe than in the bulk (Figure S6.4).
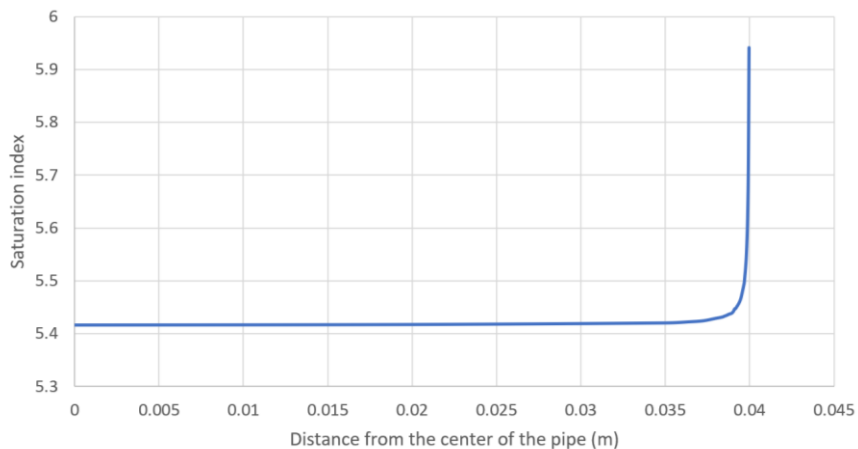


*Figure S6.4: Saturation index in function of its distance from the centre of pipe 3. The calculation has been realized with Visual Minteq. The input values are taken from a series of measurement in the sludge at the end of pipe 3 (P=8.6ppm / $Fe^{2+}$=27.4ppm / $Fe^{3+}$=6.91ppm / pH=6.9 / SI=0.02).*

*Influence of the pipe diameter on vivianite scaling formation*

The evolution of the saturation index (Figure S6.4) suggests that the vivianite scaling formation is a wall mechanism near the edge of the pipe. Therefore, one can assume that bigger pipes would be more favorable than smaller ones since their wall area/volume ratio is lower. To confirm this hypothesis, the iron reduction profile was studied for three pipes of the same length (16 m) and increasing diameter $d_1$=0.2 m, $d_2$=0.1 m, and $d_3$=0.08 m. From Figure S6.5, it can be seen that a pipe with a bigger diameter will logically allow more iron reduction due to an increased sludge retention time.
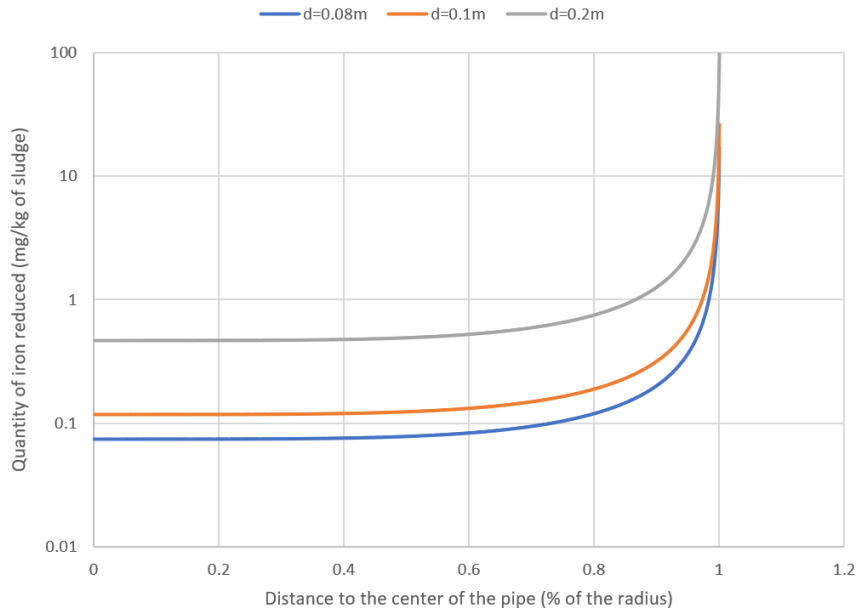


*Figure S6.5: Quantity of iron reduced in the function of the distance to the centre of the pipe for three pipes of different diameters (d=0.08, 0.1, and 0.2 m)*

For further discussion, we arbitrarily assume that vivianite scales in the zones where more than 1 ppm of $Fe^{2+}$ is produced by reduction. From Figure S6.5, we can see that this corresponds to a distance to the wall of 13.5, 1.4, and 0.7 mm for pipe of diameter 0.2, 0.1, 0.08 m, respectively. This is explained by the fact that wider pipes will have lower velocity and longer retention time, allowing more sludge to be reduced. However, if the sludge has a higher retention time, it also means that the flow will be lower, thus creating less vivianite scaling in terms of weight. For example, there is seven times more volume of pipe 1 ($d_1$=0.2 m) that will have Fe>1 ppm compared to pipe 3 ($d_3$=0.08 m). However, 43 times more sludge will effectively be under the condition where Fe>1 ppm if the flow in the different sludge layers is considered (Table S6.2). Similar conclusions can be drawn for limit iron concentration other than 1ppm. From these calculations, and assuming that vivianite scales following a wall mechanism formation, the use of big pipe seems to favor vivianite scaling formation due to the higher retention time, thus higher iron reduction potential. It is also essential to consider

diffusion to verify whether the $Fe^{2+}$ atoms have time to reach the wall in their residence time in the pipe.

Table S6.2: Characteristics of the pipe section where the quantity of iron reduced is higher than 1ppm for three pipes of different diameters. All pipes considered have a length of 16m.

| Pipe diameter | 0.08 m | 0.1 m | 0.2 m |
|---|---|---|---|
| Distance to the pipe wall where iron reduction >1ppm | 0.7 mm | 1.4 mm | 13.5 mm |
| Volume of pipe where iron reduction >1ppm | 3.57% | 5.25% | 25.18% |
| Flow of sludge where iron reduction >1ppm | 0.21% | 0.49% | 9.12% |

## $Fe^{2+}$ diffusion

The time that a $Fe^{2+}$ ion will take to reach the wall of the pipe depending on its position can be approximated with the Einstein law of diffusion (Miller 1924):

$$t = \frac{x^2}{2D}$$

Where:

- t is the time for the particle to cover the distance x (m)
-  x is the distance covered by the particle in the time t (s)
- D is the specific diffusion coefficient for the particle studied in the medium considered (m²/s)

Henry 1994 gives the diffusion coefficient of $Fe^{2+}$ in water at 25C: $7{,}19*10^{-10}$ m².s⁻¹. Zhang et al. 2016 observed that the diffusion coefficient of Iodide in digested sludge was following a logarithmic relationship to the solid content in the sludge. By extrapolating their data for the solid content of the sludge of Hoensbroek, we can estimate that the diffusion coefficient decreased by seven times compared to pure water. We estimate that the evolution of the diffusion coefficient will be the same for $Fe^{2+}$ ions, giving $D{\sim}10^{-10}$ m².s⁻¹. Considering the distance to the pipe wall where the quantity of iron reduced is equal to 1 ppm (Table S6.2), the time required for an atom of $Fe^{2+}$ to diffuse to the wall would be 911250, 9800, and 2450 s for the pipes 1, 2 and 3, respectively. This is much bigger than the retention time of 144 s for the sludge at the location of this pipe. The distance to the pipe wall that would allow $Fe^{2+}$ ions enough time to travel to the pipe wall is 0.28, 0.35, and 0.7 mm for pipes 1, 2, and 3, respectively. It suggests that even though more $Fe^{2+}$ would be produced in bigger pipes due to higher sludge retention time, a big part of the $Fe^{2+}$ produced would not have time to diffuse to the pipe wall to produce scaling.

To summarize, the morphology of the scaling and the laminar flow regime suggest that the scaling found in the pipes before dewatering units follow a growth mechanism rather than an agglomeration mechanism. We hypothesize that the iron reduction due to the anaerobic conditions is the driver of the scaling formation. The lower sludge residence time in bigger

pipes allows more iron to be reduced, potentially creating more scaling. However, both low diffusion velocity and higher iron concentration near the walls imply that a wall-mechanism growth is possible. These observations imply that bigger pipes may be better to use due to their lower wall area/volume ratio.

According to Wang et al. 2019, iron reduction in sludge in anaerobic conditions follows a first-order kinetic with k=0.055 s⁻¹. This translates into the reduction of 561 and 1.5 mg of Fe/kg of sludge in the thickener (residence time of 13.5 h) and in the pipe system (residence time of 3.4 min), respectively. Assuming that all the iron reduced in the pipe scales and that 78% of the iron that scales does it as vivianite (data from Mössbauer spectroscopy), 66.0 g of vivianite could form every hour in the pipe system. This translates into the formation of 5.0 g of vivianite per hour in the small pipe section ($\varnothing_3$=0.08 m / $L_3$=16 m).

When the pipe section before the centrifuge ($d_3$=0.08 m) was opened in Hoensbroek, it revealed that the scaling thickness was 0.55 cm. The pipe was opened in November 2019, 3.5 years after being installed. Mössbauer spectroscopy indicates that 72% of the scaling is vivianite. Hypothesizing a uniform scaling formation on the entire pipe between the thickener and the centrifuge and knowing the density of vivianite (d=2.69), 1.39 g/h of vivianite scaling forms. This represents 28% of the value obtained above, suggesting that a significant fraction of the iron reduced stays in the bulk.

## Iron reduction kinetics

The sludge reaching the dewatering units is anaerobic since it has usually been under anaerobic conditions for a couple of hours (13 h in Hoensbroek, for example). Since the solubility of Fe(II) compounds is higher than the one of Fe(III) compounds, the equilibrium concentration of $Fe^{2+}$ is also higher compared to the one of $Fe^{3+}$ as noticed during on-site measurements ($Fe^{2+}$=27.4 ppm / $Fe^{3+}$=6.91ppm before the centrifuge in Hoensbroek). During centrifugation, the liquid fraction is separated from the sludge and comes in contact with oxygen so that $Fe^{2+}$ can get oxidized to $Fe^{3+}$. The freshly formed $Fe^{3+}$ could immediately precipitate due to the lower solubility of Fe(III) compared to Fe(II) compounds. The following equation rules the oxidation of Fe2+:

$$-\frac{d[Fe^{2+}]}{dt} = k[OH^-]^2[Fe^{2+}]P_{O_2}$$

Where:

$[Fe^{2+}]$ is the concentration of $Fe^{2+}$ in mol/L

$[OH^-]$ is the concentration of OH⁻ in mol/L

$P_{O_2}$ is the partial pressure of $O_2$ worth 0.2 atm in atmospheric conditions. We assume here that the diffusion of the $O_2$ is not limiting due to the important mixing.

k is the kinetic rate of the reaction in L².mol⁻².min⁻¹.atm⁻¹

According to Sung and Morgan 1980, k is worth $2,9.10^{13}$ L².mol⁻².min⁻¹.atm⁻¹ for an ionic strength of 0.02 M. At a pH of 7.22 (measured in the centrate) and a $P_{O_2}$ of 0.2 (air environment in the centrifuge), 4.1 ppm of $Fe^{2+}$ would be reduced in 1min, which in the same order of

magnitude as the retention time in Hoensbroek centrifuge. It seems like this mechanism would not be too significant compared to vivianite formation, which is confirmed by the information collected from the WWTPs: the centrate scaling from Hoensbroek, Blue Plains, and Bosscherveld (containing a high quantity of Fe/P species) require regular cleaning, while the one in Turku (mainly iron oxide/hydroxide) needs to be removed only twice a year.

## Influence of the temperature

We consider here a typical digested sludge from a WWTP using CPR with iron. The characteristics of the soluble phase of this sludge at 37°C are: P=30 ppm, $Fe^{2+}$=15 ppm, pH=7, IS=0.05 M. Soluble phosphorus, pH and IS are average values obtained in Chapter 3 and $Fe^{2+}$ comes from the results from 4 digested sludge studied by Wilfert et al. 2018.

*Table S6.3: Evolution of $pK_{sp}$, SI, P, $Fe^{2+}$, and the vivianite formed at equilibrium for temperature varying from 5 to 90°C.*

| Temperature (°C) | $pK_{sp}$ | SI | P at equilibrium (ppm) | $Fe^{2+}$ at equilibrium (ppm) | Vivianite formed at equilibrium (mg/L) |
|---|---|---|---|---|---|
| 5 | 35.932 | 5.586 | 29.36 | 13.21 | 5.35 |
| 10 | 35.870 | 5.524 | 29.59 | 13.84 | 3.49 |
| 15 | 35.822 | 5.476 | 29.77 | 14.34 | 1.99 |
| 20 | 35.789 | 5.443 | 29.90 | 14.71 | 0.87 |
| 25 | 35.767 | 5.421 | 29.98 | 14.93 | 0.20 |
| 30 | 35.758 | 5.412 | 30.02 | 15.05 | -0.14 |
| 35 | 35.760 | 5.414 | 30.01 | 15.02 | -0.06 |
| 37 | 35.763 | 5.417 | 30.00 | 15.00 | 0.00 |
| 38 | 35.766 | 5.420 | 29.99 | 14.95 | 0.14 |
| 40 | 35.772 | 5.426 | 29.97 | 14.90 | 0.31 |
| 45 | 35.793 | 5.447 | 29.88 | 14.65 | 1.06 |
| 50 | 35.824 | 5.478 | 29.76 | 14.32 | 2.03 |
| 55 | 35.863 | 5.517 | 29.61 | 13.91 | 3.26 |
| 60 | 35.911 | 5.565 | 29.40 | 13.42 | 4.72 |
| 65 | 35.966 | 5.620 | 29.21 | 12.89 | 6.33 |
| 70 | 36.028 | 5.682 | 29.00 | 12.31 | 8.05 |
| 75 | 36.096 | 5.750 | 28.78 | 11.69 | 9.91 |
| 80 | 36.171 | 5.825 | 28.55 | 11.05 | 11.82 |
| 85 | 36.252 | 5.906 | 28.31 | 10.40 | 13.77 |
| 90 | 36.338 | 5.992 | 28.08 | 9.75 | 15.71 |

The software Visual Minteq was used to determine the saturation index and the concentration of the species in the function of the temperature. The value of the pKsp of vivianite was manually modified for each temperature considered following the relation from Al Borno and Tomson 1994: $pKsp = -234.205 + 12{,}242.6/T + 92.510 \log T$. At 37°C, the saturation index for vivianite is 5.417. The conditions at 37°C are considered the equilibrium conditions since it is

the usual temperature of digested sludge. All the equilibrium concentrations showed in Table S6.3 for the different temperatures were calculated to match SI=5.417 as the equilibrium condition.

From the information we collected, the digested sludge is typically brought from 30°C to 38°C, which corresponds to a soluble concentration decrease of 0.03 and 0.1 ppm for phosphorus and $Fe^{2+}$, respectively. It corresponds to the formation of 0.28 mg/L of vivianite.

## Terminal velocity of a particle in a digester

Rheological measurements were not carried out with the sludge of Spokane County, so the value of the apparent viscosity of digested sludge was obtained from the literature review. The digested sludge of Spokane County has an average solid content of 2-2.5%. Literature indicates that the apparent viscosity of digested sludge ranging from 1.8 to 3.6% of solid varies from 0.035 to 0.5 Pa.s (Markis et al. 2016, Eshtiaghi et al. 2012, Goel et al. 2004, Baudez et al. 2011). These values were taken for shear stresses around 100 $s^{-1}$. Since sludge is a shear-thinning fluid, its viscosity decreases with increasing shear rate (Markis et al. 2016, Eshtiaghi et al. 2012). In a digester, the shear rates are not homogeneous and are higher in the zones closer to the stirrer. Baudez et al. 2011, for example, show that the apparent viscosity of a 2.5% solid digested sludge decreases from 0.25 to 0.035 Pa.s for an increasing shear rate from 4 to 90 $s^{-1}$. The shear rate during digestion cannot be too high to preserve the bacteria functioning (Jiang et al. 2016), but high enough to maintain a proper mixing. Therefore, we will consider a case where the shear rate is moderate and assume a viscosity of 0.1 Pa.s.

Newton's law gives the terminal speed of a particle in sludge:

$$v_{tp} = \sqrt{\frac{4g}{3C_d} * \left(\frac{\rho_p - \rho_s}{\rho_s}\right) * d_p}$$

With:

- $v_{tp}$ the terminal velocity of the particle in m/s
- $g$ is the acceleration of the gravity worth 9.81 $m/s^2$
- $C_d$ is the coefficient of drag
- $\rho_p$ and $\rho_s$ the density of the particle worth 2.7 and 1.0 for vivianite and sludge, respectively
- $d_p$ the diameter of the particle in m

The coefficient of drag for a sphere is obtained from the Reynolds number through:

$$C_d = \frac{24}{Re} + \frac{3}{\sqrt{Re}} + 0.34$$

Reynolds number for settling particles is:

$$Re = \frac{v_p d_p \rho_v}{\mu}$$

With:

- - $Re$ the Reynolds number
- - $v_p$ the velocity of the particle in m/s
- - $d_p$ the diameter of the particle in m
- - μ the apparent viscosity in Pa.s

Since the flow regime in the digester is most likely laminar, we first hypothesize a Re of 1, which gives $C_d$=27.34, and a terminal velocity of 19 mm/s. By iteration on Re, $C_d$, and $v_{tp}$, we obtain 0.001, 25000, and 0.63 mm/s, respectively.

For a sludge containing 5% solids, the viscosity would be around 7-8 times higher than for a sludge containing 2.5% of solids according to Goel et al. 2004 and Baudez et al. 2011. Considering a viscosity of 0.8 Pa.s and following the same iteration principle, we obtain Re=$1.5*10^{-5}$, $C_d=1.6*10^6$ and $v_{tp}$=0.078 mm/s.
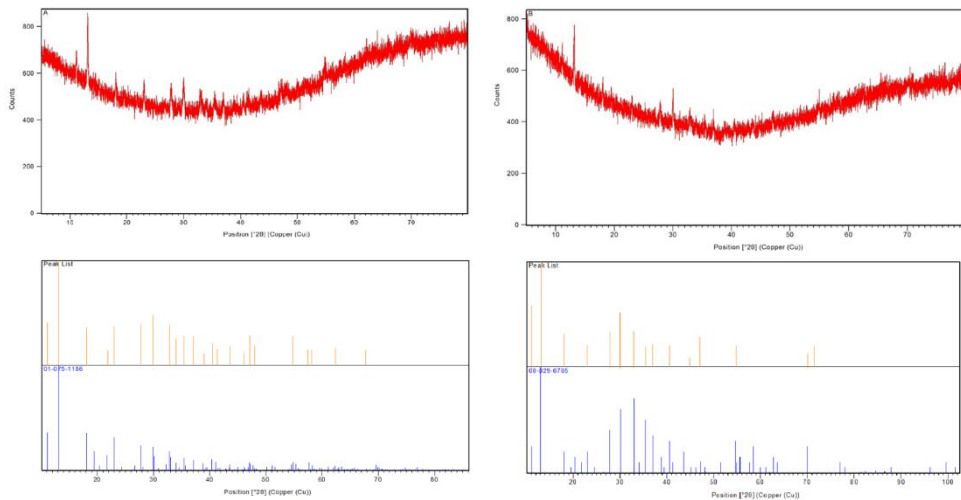


*Figure S6.6: XRD pattern (top) and plot of identified phases (bottom). Left: the samples found in the pipes after the thickener in Hoensbroek WWTP. The pattern only revealed the presence of relatively crystalline vivianite. Right: the sample found in the centrate pipe in Hoensbroek WWTP. The pattern only revealed the presence of amorphous material and impure vivianite.*
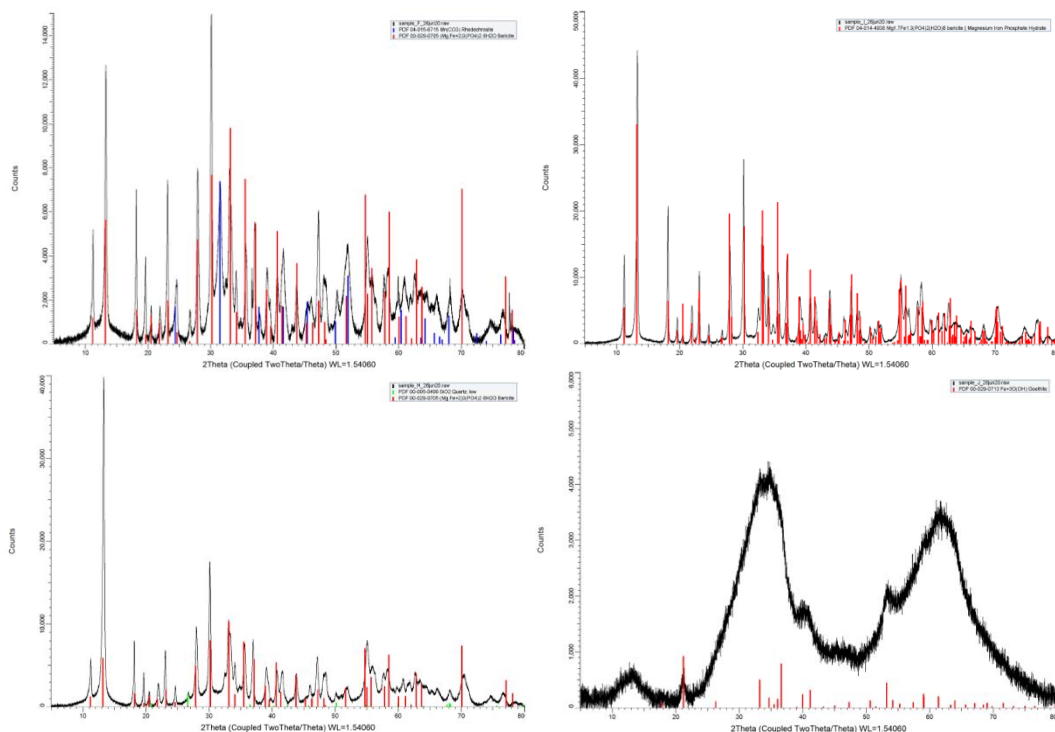
*Figure S6.7: Top-left: XRD pattern the digester withdrawal of Spokane County. The pattern indicates the presence of rhodochrosite (most likely siderite) and baricite (impure vivianite). Top-right: XRD pattern of the scaling found in the heat exchanger of Blue Plains WWTP after THP. The pattern indicates the presence of baricite (impure vivianite) Bottom-left: XRD pattern of the scaling found in the heat exchanger of Amsterdam. The pattern indicates the presence of quartz low and baricite (impure vivianite). Bottom-right: XRD pattern of the scaling found in the centrate of Turku WWTP. The pattern indicates amorphous species, with the possible presence of goethite as a minor phase.*

Table S6.4: Mössbauer spectroscopy parameters for the samples studied. IS=Isomer Shift, QS=Quadrupole Splitting). $Fe^{3+}/Fe^{II}$: $Fe^{3+}$ species other than vivianite and low-spin $Fe^{2+}$ compounds like pyrite. $Fe^{3+}$ (Viv. A+B): total $Fe^{3+}$ vivianite. $Fe^{2+}$ (Viv. A): $Fe^{2+}$ in the site A of vivianite. $Fe^{2+}$ (Viv. B): $Fe^{2+}$ in the site B of vivianite.

| Sample | T (K) | IS (mm·s⁻¹) | QS (mm·s⁻¹) | Phase | Spectral contribution (%) |
|---|---|---|---|---|---|
| Anaerobic pipe Hoensbroek | 300 | 0.35 | 0.81 | $Fe^{3+}/Fe^{II}$ | 22 |
| | | 0.47 | 0.51 | $Fe^{3+}$ (Viv. A+B) | 23 |
| | | 1.21 | 2.39 | $Fe^{2+}$ (Viv. A) | 21 |
| | | 1.22 | 2.94 | $Fe^{2+}$ (Viv. B) | 34 |
| Centrate pipe Hoensbroek | 300 | 0.37 | 0.77 | $Fe^{3+}/Fe^{II}$ | 70 |
| | | 0.47 | 0.51 | $Fe^{3+}$ (Viv. A+B) | 6 |
| | | 1.28 | 2.28 | $Fe^{2+}$ (Viv. A) | 10 |
| | | 1.23 | 2.98 | $Fe^{2+}$ (Viv. B) | 14 |
| Spokane digester withdrawal | 300 | 0.38 | 0.79 | $Fe^{3+}/Fe^{II}$ | 35 |
| | | 0.47 | 0.51 | $Fe^{3+}$ (Viv. A+B) | 15 |
| | | 1.18 | 2.45 | $Fe^{2+}$ (Viv. A) | 12 |
| | | 1.20 | 2.96 | $Fe^{2+}$ (Viv. B) | 21 |
| | | 1.22 | 1.94 | $Fe^{2+}$ (siderite?) | 17 |
| Heat Exchanger Amsterdam | 300 | 0.37 | 0.84 | $Fe^{3+}/Fe^{II}$ | 32 |
| | | 0.47 | 0.51 | $Fe^{3+}$ (Viv. A+B) | 18 |
| | | 1.24 | 2.30 | $Fe^{2+}$ (Viv. A) | 20 |
| | | 1.20 | 2.99 | $Fe^{2+}$ (Viv. B) | 30 |
| Heat Exchanger after THP Blue Plains | 300 | 0.37 | 0.87 | $Fe^{3+}/Fe^{II}$ | 25 |
| | | 0.47 | 0.51 | $Fe^{3+}$ (Viv. A+B) | 25 |
| | | 1.22 | 2.31 | $Fe^{2+}$ (Viv. A) | 21 |
| | | 1.20 | 2.99 | $Fe^{2+}$ (Viv. B) | 29 |
| Centrate Turku | 300 | 0.37 | 0.80 | $Fe^{3+}$ | 100 |
| | 4.2 | 0.43 | -0.16 | $Fe^{3+}$ (Viv. A) | 10 |
| | | 0.52 | -0.18 | $Fe^{3+}$ (Viv. B) | 13 |
| | | 0.38 | 0.02 | Ferrihydrite | 32 |
| | | 0.33 | 0.04 | Ferrihydrite | 45 |
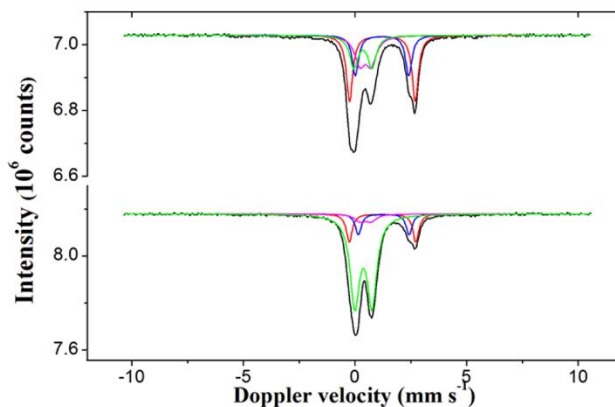
*Figure S6.8: Mössbauer spectra for the scaling found in the pipe after the thickener (top), and in the centrate pipe (bottom) in Hoensbroek WWTP. Black: total spectrum, Green: $Fe^{3+}/Fe^{II}$, Pink: Fe3+ (Viv. A+B), Blue: $Fe^{2+}$ (Viv. A), Red: $Fe^{2+}$ (Viv. B).*
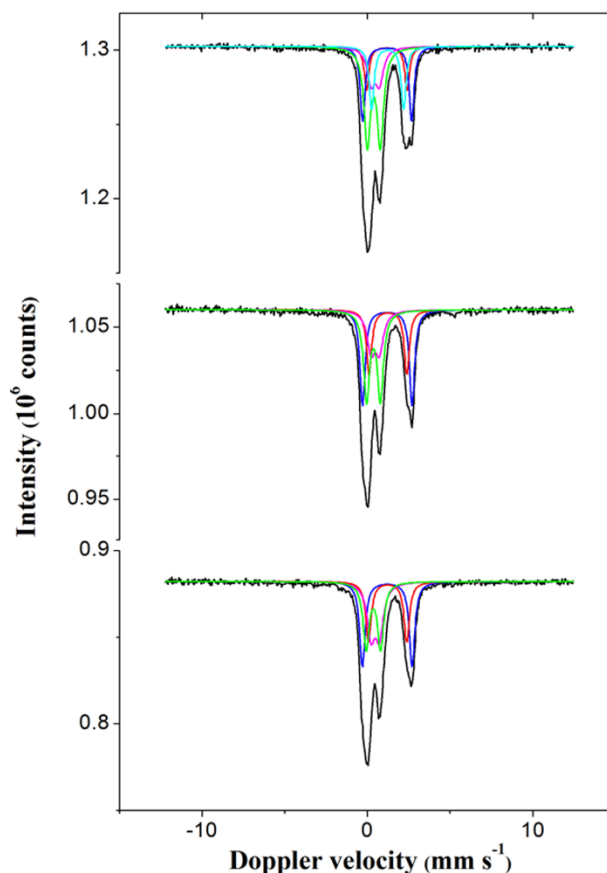


*Figure S6.9: Mössbauer spectra for the digester withdrawal in Spokane County WWTP (top), the scaling found in the heat exchanger in Amsterdam WWTP (middle), and in the heat exchanger after THP in Blue Plains WWTP (bottom). Black: total spectrum, Green: $Fe^{3+}/Fe^{II}$, Pink: Fe3+ (Viv. A+B), Red: $Fe^{2+}$ (Viv. A), Blue: $Fe^{2+}$ (Viv. B), Cyan: $Fe^{2+}$ (siderite?).*

# References used in the supplementary information

Cao, X., Jiang, Z., Cui, W., Wang, Y., Yang, P. (2016). Rheological properties of municipal sewage sludge: dependency on solid concentration and temperature. *Procedia Environmental Sciences*, 31, 113–121 doi: 10.1016/j.proenv.2016.02.016.

Füreder, K., Svardal, K., Krampe, J., Kroiss, H. (2018). Rheology and friction loss of raw and digested sewage sludge with high TSS concentrations: a case study. *Water Science and Technology*, (1), 276–286. doi:10.2166/wst.2018.111.

Goel, R., Komatsu, K., Yasui, H., & Harada, H. (2004). Process performance and change in sludge characteristics during anaerobic digestion of sewage sludge with ozonation. *Water Science and Technology*, 49(10), 105–113. doi:10.2166/wst.2004.0620.

Henry, V. K. (1994). CRC handbook of thermophysical and thermochemical data. *CRC press Inc. Boca Raton*.

Honey, H.C and Pretorius, W.A. (2020). Laminar flow pipe hydraulics of pseudoplastic-thixotropic sewage sludges. *Water Sa,* 26 (1).

Jiang, J., Wu, J., Poncin, S., Li, H. Z. (2016). Effect of hydrodynamic shear on biogas production and granule characteristics in a continuous stirred tank reactor. *Process Biochemistry*, 51(3), 345–351. doi:10.1016/j.procbio.2015.12.014.

Markis, F., Baudez, J.-C., Parthasarathy, R., Slatter, P., and Eshtiaghi, N. (2016). Predicting the apparent viscosity and yield stress of mixtures of primary, secondary and anaerobically digested sewage sludge: simulating anaerobic digesters. *Water Research*, 100, 568–579. doi:10.1016/j.watres.2016.05.045.

Miller, C. C. (1924). The Stokes-Einstein law for diffusion in solution. Proceedings of the Royal Society of London. Series a, Containing Papers of a Mathematical and Physical Character, 106 (740), 724–749.

Prot, T., Korving, L. van Loosdrecht, M.C.M. (2020): Ionic strength of the liquid phase of different sludge streams in a wastewater treatment plant. *ChemRxiv*. Preprint. https://doi.org/10.26434/chemrxiv.13359437.v1.

Rosenberger, R., Kubin, K., Kraume, M. (2002). Rheology of activated sludge in membrane bioreactors. *Engineering in Life Sciences* 2 (9), 269-275. doi:10.1002/1618-2863(20020910)2:9<269::aid-elsc269>3.0.co;2-v.

Simpson, M.M, Janna, W. (2008). Newtonian and non-newtonian fluids: velocity profiles, viscosity data, and laminar flow friction factor equations for flow in a circular duct conference. *ASME 2008 International Mechanical Engineering Congress and Exposition.* doi:10.1115/IMECE2008-67611.

Sung, W. and Morgan, J. J. (1980). Kinetics and product of ferrous iron oxygenation in aqueous systems. *Environmental Science & Technology*, 14(5), 561–568. doi:10.1021/es60165a006.

Wei, P., Tan, Q., Uijttewaal, W. S. J., van Lier, J. B., de Kreuk, M. K. (2018). Experimental and mathematical characterisation of the rheological instability of concentrated waste activated sludge subject to anaerobic digestion. *Chemical Engineering Journal*, 349. doi:10.1016/j.cej.2018.04.108.

Zhang, Y., Li, H., Cheng, Y., Liu, C. (2016). Influence of solids concentration on diffusion behavior in sewage sludge and its digestate. *Chemical Engineering Science*, 152, 674–677. doi:10.1016/j.ces.2016.06.058.

# Chapter 7: Formation of vivianite in iron-amended pig manure and its subsequent magnetic recovery
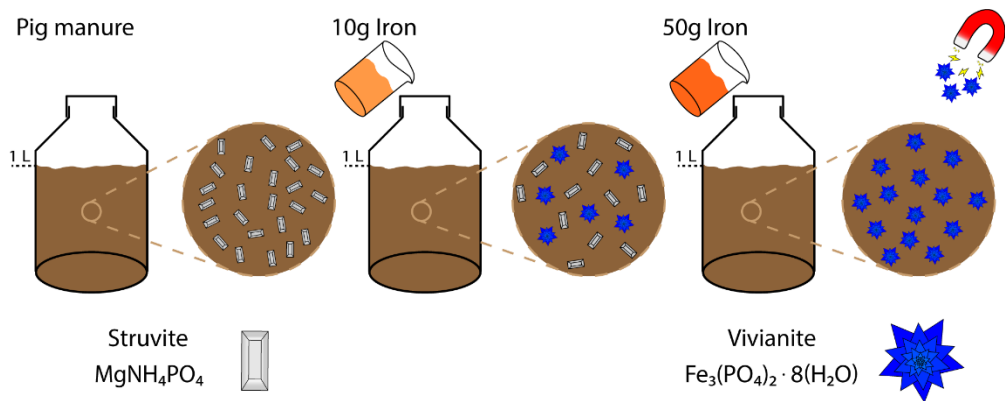


Pig manure  10g Iron  50g Iron

1. L

Struvite
$MgNH_4PO_4$

Vivianite
$Fe_3(PO_4)_2 \cdot 8(H_2O)$

**Highlights**

- Iron addition to pig manure progressively converted struvite to vivianite.

- At a molar Fe/P ratio of 4, 50-80% of the phosphorus was present as vivianite.

- The high Fe/P ratio needed is likely due to the strong iron-organics interactions.

- A lab-scale magnetic separator allowed the recovery of 20-30% of the vivianite.

- A new route for phosphorus recovery from pig manure was proposed in this study.

**Abstract**

Phosphorus is currently obtained via the non-sustainable mining of phosphate rock. Alternative phosphorus sources like animal manure need to be better exploited. Phosphorus recovery from animal manure is especially relevant for countries like the Netherlands or the United Kingdom dealing with phosphorus surpluses from animal wastes. In the present study, the formation of the iron phosphate mineral vivianite is studied as an option for phosphate recovery from manure. At a molar Fe/P ratio around 4, 50-80% of the phosphorus was present as vivianite while struvite progressively dissolved. We foresee that Fe/P ratios of 4-5 would be necessary to maximize the amount of phosphorus present as vivianite in pig manure, which is much higher than 1.5-2 for sewage sludge. This difference is likely due to a large part of the iron preferentially binding to organic matter than phosphorus in pig manure. The understanding of iron-organics interactions deserves more attention to reduce the iron requirement and make the vivianite formation economically feasible. A lab-scale magnetic separator allowed the recovery of 20-30% of the vivianite in the pig manure, which is in line with laboratory experiments with sewage sludge. Recovery of around 80% is expected at a larger scale thanks to industrial equipment and recirculation of the manure based on experience on sewage sludge. This study shows for the first time that vivianite could form upon iron addition to pig manure and could later be magnetically recovered, opening a new phosphorus recovery route from pig manure.

7

## 7.1. Introduction

Phosphorus is an important resource since it is an essential nutrient for every living organism (Westheimer 1987, Kamerlin et al. 2013). It is mainly used as a fertilizer to secure future food production (Blackshaw et al. 2009, Childers et al. 2011), and its demand sharply increased in the last decades due to the growing global population (Scholz et al. 2013). The primary source of phosphorus is phosphate rock, a non-renewable resource, of which Morocco holds 70% of the world resources (Cordell 2015). Additionally, phosphate rock mining releases heavy metals which pollute soil and water (Cordell 2015, El Zrelli et al. 2018). Phosphate rock, as a non-renewable resource, needs to be replaced (Scholz et al. 2013). Therefore, the phosphorus contained in secondary sources like animal manure or wastewater appears to be an attractive alternative source to solve the phosphorus crisis (Barnett 1994, Damalerio et al. 2019).

The recovery of phosphorus from animal manure is especially relevant for areas with intensive farming like the Po Delta in Italy, Chesapeake Bay in the USA, the United Kingdom, and the Netherlands (Greaves et al. 1999). Since the 1970s, the Netherlands is massively exploiting livestock and thus, produces a large amount of manure which is applied on land for nutrients recycling (Henkens et al. 2001). Between the years 2005 and 2009, 70-80 megatons of phosphorus ended up in animal manure, of which 50-60% was applied on land in the Netherlands (Wageningen 2015). Unfortunately, applying manure as excessive fertilizers can lead to a decline in soil fertility, quality of the crops, or surface run-off of minerals due to an oversaturation of nutrients (phosphate, nitrate, and potash) (de Mol et al. 1991). For the latter reason, the UK Ministry of Agriculture Food and Fisheries (MAFF) put in place guidelines encouraging farmers to spread manure in a way that would minimize the run-off to natural water streams (MAFF 1991).

Similarly, the Dutch government applied strict restrictions on manure spreading and limited the number of livestock since 1984 to reduce the nutrient problem because of excessive manure application (Leenstra et al. 2014, de Bont et al. 2003). Consequently, 30-40% of the manure need to be transported to regions with a deficit of nutrient, representing an additional cost and causes emissions (Leenstra et al. 2014, Yyan et al. 2017). For this reason, phosphorus recovery from manure is essential to solve the manure problem in intensive farming areas. With a lower phosphorus concentration in manure, more organic fraction of manure could be reused on the land, while the recovered phosphorus could be recycled as a sustainable fertilizer.

Animal manure contains phosphorus mainly in its solid forms. Pig manure can also contain phytates in its liquid fraction since it is a common phosphorus form in animal feed, which cannot be degraded by non-ruminant (like pigs) digestive system (Abioye et al. 2010, Pagliari and Laboski 2012). Dependent on the manure-specific availability of cations, calcium or magnesium phosphates form and act as phosphorus sink (Ackerman et al. 2016, Pagliari and Laboski 2012). The current processes to recover phosphorus from animal manure either separate phosphorus mechanically based on size separation (90% of the phosphorus of raw pig manure solids are smaller than 100μm according to Masse et al. 2005) or precipitate the soluble species through cation addition (Christensen et al. 2013; Christensen et al. 2020). Before adding cations, an acidification step is possible to allow phosphorus release before its precipitation in the desired phosphorus form (Church et al. 2020, Huang et al. 2014, Vanotti

et al. 2017, Vanotti et al. 2007). For example, Szögi et al. (2015) acidified manure with HCl to a pH between 3 and 5 to solubilize all phosphorus. The acidified liquid fraction entered another unit with $Ca(OH)_2$ injection to induce $Ca_x(PO_4)_y$ precipitation at a pH of 8 to 10. The $Ca_x(PO_4)_y$ entered the third unit with anionic organic polymer to enhance the separation of $Ca_x(PO_4)_y$ particles. Finally, the process recovered up to 90% of the total phosphorus (Szögi et al. 2015). Similar process designs allow to recover phosphorus as struvite ($MgNH_4PO_4*6H_2O$), when instead of calcium, magnesium is added (Burns et al. 2003, Huang et al. 2014, Vanotti et al. 2017). However, the chemical cost to increase the pH of manure is substantial, and struvite recovery from manure is challenging (Shepherd et al. 2009, Zhang et al. 2010, Tao et al. 2016). Current processes focus on magnesium or calcium phosphate recovery, but the extraction of these minerals from manure is arduous (Zhang et al. 2015, Agomoh et al., 2018; Bauer et al., 2007; Szögi et al., 2015).

Vivianite ($Fe(II)_3(PO_4)_2.8H_2O$) is one of the most stable phosphate forms in reductive environments like sediments or digested sewage sludge (Nriagu and Dell 1974). Vivianite forms preferentially over struvite when iron is present in sewage sludge systems (Mamais et al. 1994, Korving et al. 2019) and can bear up to 70-90% of the phosphorus in digested sewage sludge (Wilfert et al. 2018). Different studies already observed a sharp decrease of the soluble phosphorus content following the addition of moderate iron quantities (Fe/P~0.3) for coagulation of pig (Hjorth et al. 2008) and mink manure (Christensen et al. 2020). Since manure is also a reductive environment, it can be expected that vivianite will form over struvite and represent a substantial phosphorus sink upon iron addition. Chemical modelling suggested vivianite formation over calcium phosphate and struvite upon adding iron to mink manure (Christensen et al. 2020). Due to its paramagnetic properties, vivianite could be recovered from digested sludge using magnetic techniques adapted from the mining industry (Chapter 2, Chapter 4). This study aimed to investigate whether it is possible to form vivianite in pig manure by iron addition and then investigate its magnetic recovery.

## 7.2. Materials & Methods

### 7.2.1. Manure sampling and storage

The pig manure was directly collected from the pit of a fattener pig stable containing 4400 animals in Marum, The Netherlands. The manure was immediately sieved with a 200 μm sieve to separate coarse undigested or non-manure related particles. The experiment with a 4 g/L iron dose was performed in November 2019 with pig manure collected the same month, while the experiments with 11 and 52 g/L iron were performed in March 2020 with pig manure collected the same month. Before being used, the pig manure was kept closed at 4°C.

### 7.2.2. Experimental setup

One litre of sieved pig manure was poured into a sealed Duran bottle of 1.5L. The bottle with pig manure received iron in three quantities. The quantities were calculated based on the pig manure composition (Table 7.1) assuming: for the 4g/L dose the total precipitation of FeS and then 50-60% of the phosphorus as vivianite; for the 11g/L, the total precipitation of FeS, then the binding of iron to 25% of the organic carbon and the precipitation of all phosphorus as

vivianite; for the 52g/L dose a significant excess to maximize the quantity of phosphorus present as vivianite. The experiments are later referred to by the amount of iron dosed per liter of pig manure: 4 g/L, 11 g/L, and 52 g/L. The iron was added as $FeCl_2*4H_2O$ solution. The iron solution was carefully added to the manure since acidification by the solution caused the release of gas, forming a floating foam layer. The foam was removed by intense mixing of the reaction liquor before starting the experiments. The bottles were equipped with a valve to avoid overpressure due to gas formation.

Table 7.1: Composition of the raw sieved pig manure used for the three experiments. Note that the manure used is the same for the iron dose 11g/L and 52g/L.

| Iron dose | TS | pH | Total manure (g/kg wet manure) | | | | | Soluble fraction (mg/L) | | | | |
|---|---|---|---|---|---|---|---|---|---|---|---|---|
| | | | P | Fe | Mg | S | Ca | P | Fe | Mg | S | Ca |
| 4g/L | 6.8% | 8.4 | 1.5 | 0.1 | 0.8 | 0.8 | 1.9 | 170 | 1 | 8 | 460 | 220 |
| 11g/L | 5.4% | 8.3 | 1.7 | 0.1 | 1.0 | 1.1 | 2.0 | 240 | 1 | 3 | 600 | 50 |
| 52g/L | 5.4% | 8.3 | 1.7 | 0.1 | 1.0 | 1.1 | 2.0 | 240 | 1 | 3 | 600 | 50 |

The bottles were shaken at 150 rpm on a platform shaker (Heidolph) for one month. The bottles were only opened for sampling after 1, 3, 9, 21, and 36 days (to include the duration of sewage sludge digestion). The sample was taken instantly after intense mixing to ensure the representability of the sample. The taken samples were analyzed immediately.

## 7.2.3.  Analysis

### 7.2.3.1.    Elemental analysis

The analysis was separated into soluble compounds and elements and total elements. For soluble analyses, the samples were filtered with 0.45 µm syringe filters (brand). The filtrate was used to measure anions ($Cl^-$, $SO_4^{2-}$ and $PO_4^{3-}$) by ion chromatography (IC) (Metrohm 761 Compact) and soluble elements (P, Fe, Mg, S, Ca, Na, K) by Inductively Coupled Plasma (Perkin Elmer, type Optima 5300 DV) equipped with an Optical Emission Spectroscopy (ICP-OES). A Perkin Elmer Autosampler, type ESI-SC-4 DX fast, was used, and the software Perkin Elmer WinLab32 was used for data processing. The internal standard was 10 mg/L of Yttrium, and the rinse solution was 2% of $HNO_3$. Total elements were measured by ICP-OES after performing microwave-induced acid digestion with 69% (ultrapure) $HNO_3$ (VWR chemicals) at 200 °C for 15min.

### 7.2.3.2.    Solid characterization

Total solids (TS) were determined by drying 10g of a sample at room temperature to avoid losing temperature-sensitive crystal water like in vivianite. Around 0.5 g of those samples were used for light microscope analysis (Leica MZ95 equipped with a Leica DFC320 camera) and Scanning Electron Microscope coupled with Energy Dispersive X-ray (SEM-EDX, JEOL JSM-6480 LV, and Oxford Instruments x-act SDD) observations. The accelerating voltage was 15 kV at a working distance of 10 mm. The samples were covered with a 10 nm-layer of gold using a JEOL JFC-1200 fine coater to make the surface electrically conductive. The software used was JEOL SEM Control User Interface for the SEM and Oxford Instruments Aztec for the EDX data processing.

For Mössbauer spectroscopy and XRD analysis, 5 mL of wet sample were dried and pulverized in a mortar in an anaerobic chamber to limit the oxidation of vivianite, which complicates the peak assignment. The XRD device was a Bruker D8 Advance diffractometer Bragg-Brentano geometry and Lynxeye position-sensitive detector with Cu-Kα radiation (10-80°2θ, step size 0.008°). The peaks assignment was done with Bruker software DiffracSuite.EVA vs 5.2. For Mössbauer spectroscopy analysis, the powdered samples (manipulated in $O_2$-free conditions) were first introduced in plastic rings sealed with Kapton foil and Epoxy glue and wrapped in aluminum foil. Carbon powder was added to the samples to maintain a maximum iron quantity of 17.5 mg of Fe/cm$^2$. Transmission $^{57}$Fe Mössbauer absorption spectra were collected at 300 K with a conventional constant-acceleration spectrometer using a $^{57}$Co (Rh) source. Velocity calibration was carried out using an α-Fe foil. The program Mosswinn 4.0 was used to fit the Mössbauer spectra (Klencsár 1997).

## 7.2.4. Sequential extractions

The phosphorus speciation of the iron-treated manure was performed using sequential extraction. Firstly, 10mL of manure was added to a 50mL-polycarbonate centrifuge tube and centrifuged at 25,000 g for 30min in a centrifuge from Beckmann Coulter Avanti J-26 XP. The remaining pellet was successively extracted with 30mL of $NaHCO_3$ (0.5M) for 2h, NaOH (0.1M) for 6h, HCl (0.5M) for 2h before being microwave acid-digested. The sequential extraction protocol was adapted from work on sewage sludge and manure (Carliell and Wheatley 1997, Turner and Leytem 2004, Dou et al. 2000). The extraction times were derived from kinetics experiments realized during the current study.

## 7.2.5. Magnetic separation

One month after the iron addition, the manure treated with the "11 g/L Fe dose" and the "52 g/L Fe dose" was processed in a lab-scale magnetic separator to test the possibility of recovering vivianite. Around 100g of wet manure was treated in each case to obtain representative results. The manure treated with "4 g/L Fe dose" was not processed through the separator since no vivianite was detected in this sample. The device was the same as used in Chapter 2 (Figure 7.1). Firstly, the device was submerged in water until the water reaches the magnetized teeth. Then, 2mL of well-homogenized iron-treated manure was slowly poured in-between the teeth, followed by 5 mL of water to detach the non-magnetic particles. Finally, the separator was carefully removed from the water, and a strong stream of water was flushed in-between the teeth to collect the magnetic material, called the magnetic concentrate.
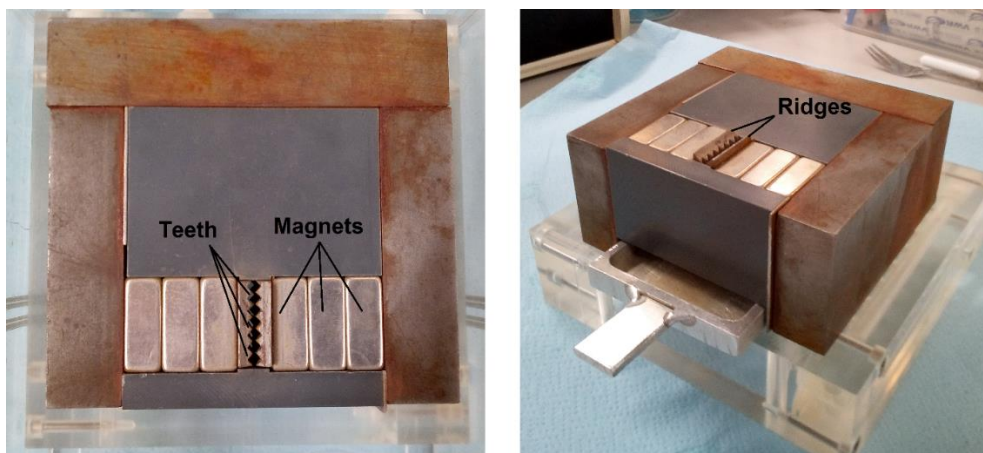
*Figure 7.1: Magnetic separator used to recover the vivianite from the manure treated with 11 and 52 g/L Fe dose (left: top view, right: side view).*

## 7.2.6. Chemical equilibrium modelling

PHREEQC Interactive version 3.5 was used for geochemical modelling (Parkhurst and Appelo 2013). The model simulated ion association based on interactions defined in wateq4f.dat (Appelo and Postma 2004). Wateq4f.dat was extended with humic substance interactions as defined by Tipping and Hurley (Tipping 1998; Tipping and Hurley 1992). Tipping and Hurley described in their WHAM (Windermere Humic Aqueous Model) the ion interactions of Fe, Mg, and Ca, among others, with the negatively charged sites of humate and fulvate. Additionally, humate and fulvate could complex Mg, Ca (Lofts and Tipping 2000), Ni, Cu, Zn, Cd, and Pb. This model did not cover iron surface complexations because experimental data was not available yet and were not simply obtainable.

Volatile fatty acid interactions were not included in wateq4f.dat. The database was extended based on interactions of acetate, propionate, butyrate, and valerate described in minteqv4.dat. The data was initially retrieved from NIST46.4 (National Institute of Standards and Technology (USA)). Furthermore, the precipitates struvite (Ohlinger et al. 1999), brushite, and amorphous calcium phosphate (Daneshgar et al. 2018) were added. All input data were experimentally determined (Table S7.5).

## 7.3. Results & Discussion

The main focus of the present study was to assess whether vivianite $(Fe(II)_3(PO_4^{2-})_2*8H_2O)$ can form in manure after iron addition, similarly to what happens in sewage sludge. The formation of vivianite in manure is discussed in this section, along with the chemical modeling and the sequential extractions. Then, the possibility of recovering the vivianite magnetically was evaluated. Finally, the feasibility of this technology is discussed in light of the lessons learned from vivianite recovery from digested sewage sludge.

### 7.3.1. Vivianite formation in iron-amended pig manure

Before iron addition, it appears that struvite ($MgNH_4PO_4*6H_2O$) was an important phosphorus mineral in raw pig manure since most of the phosphorus clusters revealed by EDX were overlapping with magnesium (Figure 7.2). Based on the elemental composition of the solids in manure, 80-90% of the phosphorus could potentially be bound as struvite (Supplementary information). The presence of struvite is in agreement with chemical modeling predicting its occurrence along with calcium phosphate and sometimes vivianite in pig and mink manure (Christensen et al. 2020, Çelen et al. 2007). Calcium phosphates or struvite were found in pig manure depending on the cations' availability (Pagliari and Laboski 2012). In the present study, struvite was the only phosphate mineral detected in the raw pig manure by XRD and SEM-EDX. Furthermore, the age of manure determined the form of phosphorus. Fresh manure contained more labile-bound phosphorus, and old manure was more comparable to digestate. Over time, labile phosphorus bound with available cations (Corona et al. 2020; Masse et al. 2005). The manure sampled during this study had an unknown retention time in the pit below the stable. However, during winter, animal manure cannot be applied on fields in the Netherlands. Thus, the manure used in this study was likely several months old and partly digested.
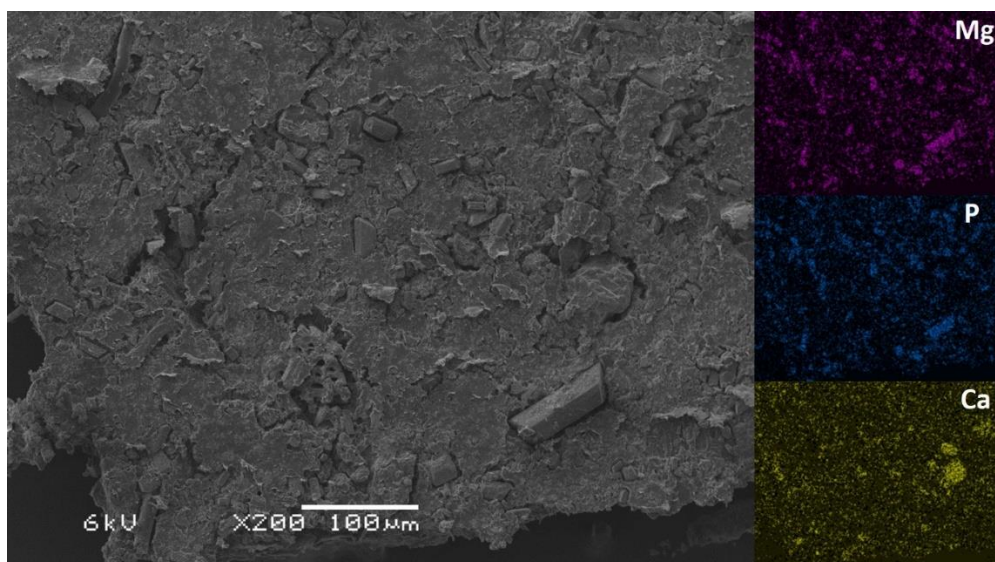


*Figure 7.2: SEM picture of the raw pig manure before the addition of iron. EDX scans of the same frame for the elemental distribution of magnesium, phosphorus, and calcium. A significant quantity of phosphorus overlaps with magnesium-based on the EDX, while no CaP clusters can be observed. It suggests that struvite ($MgNH_4PO_4*6H_2O$) is an important phosphorus fraction, while calcium phosphate is not present.*

Previous work on phosphorus recovery from digested sewage sludge shows that iron will first bind to sulphide before any iron phosphate can form (Chapter 3, Roussel and Carliell-Marquet 2016). Therefore, the dose of iron added to manure in the first batch experiment (4g/L Fe) represented enough iron to bind the totality of the sulphur in manure as FeS (S=0.8g/L), and 55-60% of the phosphorus as vivianite (P=1.5g/L) (Supplementary information). According to

300K-Mössbauer spectroscopy measurements, all the iron present in the sample after the iron addition is either present as Fe(III) or low-spin Fe(II) compounds (possibly pyrite) (Table 7.2). The formation of $FeS_x$ precipitates in manure would not be surprising since it was already observed in anaerobic environments like sewers (Nielsen et al. 2007) and sludge digesters (Yekta et al. 2017).

*Table 7.2: Mössbauer spectroscopy parameters for the samples studied. IS=Isomer Shift, QS=Quadrupole Splitting). $Fe^{3+}/Fe^{II}$: $Fe^{3+}$ species other than vivianite, $Fe^{3+}$ in vivianite, and low-spin $Fe^{2+}$ compounds like pyrite. $Fe^{3+}$: Fe(III) phase, possibly impure ferrihydrite or disordered lepidocrocite. $Fe^{2+}$ (Viv. A): $Fe^{2+}$ in the site A of vivianite. $Fe^{2+}$ (Viv. B): $Fe^{2+}$ in the site B of vivianite.*

| Sample | T (K) | IS (mm·s$^{-1}$) | QS (mm·s$^{-1}$) | Γ (mm·s$^{-1}$) | Phase | Spectral contribution (%) |
|---|---|---|---|---|---|---|
| 4g/L 36 days | 300 | 0.37 | 0.78 | | $Fe^{3+}/Fe^{II}$ | 100 |
| | 4.2 | 0.36 | -0.04 | 0.64 | Ferrihydrite | 19 |
| | | 0.34 | -0.03 | 0.53 | $Fe^{3+}$ | 81 |
| 11g/L 1 day | 300 | 0.36 | 0.81 | 0.49 | $Fe^{3+}/Fe^{II}$ | 63 |
| | | 1.26 | 2.36 | 0.28 | $Fe^{2+}$ (Viv. A) | 9 |
| | | 1.22 | 2.94 | 0.28 | $Fe^{2+}$ (Viv. B) | 12 |
| | | 1.22 | 1.95 | 0.40 | $FeCO_3$ | 16 |
| 11g/L 36 days | 300 | 0.39 | 0.66 | 0.53 | $Fe^{3+}/Fe^{II}$ | 27 |
| | | 1.17 | 2.42 | 0.31 | $Fe^{2+}$ (Viv. A) | 12 |
| | | 1.22 | 2.95 | 0.31 | $Fe^{2+}$ (Viv. B) | 19 |
| | | 1.20 | 1.78 | 0.45 | $FeCO_3$ | 42 |
| 52g/L 36 days | 300 | 0.38 | 0.81 | 0.54 | $Fe^{3+}/Fe^{II}$ | 24 |
| | | 1.29 | 2.46 | 0.41 | $Fe^{2+}$ (Viv. A) | 3 |
| | | 1.20 | 2.92 | 0.41 | $Fe^{2+}$ (Viv. B) | 7 |
| | | 1.23 | 1.86 | 0.38 | $FeCO_3$ | 51 |
| | | 1.20 | 2.42 | 0.38 | $FeCl_2·2H_2O$ | 15 |

Experimental uncertainties: Isomer shift: I.S. ± 0.01 mm s-1; Quadrupole splitting: Q.S. ± 0.01 mm s-1; Hyperfine field: ± 0.1 T; Line width: Γ ± 0.01 mm s-1; Spectral contribution: ± 3%.

In manure systems, iron is sometimes added for coagulation (Fe/P~0.3 in Christensen et al. 2020 and Hjorth et al. 2008) or as nanoparticles for biogas production increase (Abdelwahab et al. 2020, Farghali et al. 2020), but in smaller quantities than in this study. Only one study (Dao et al. 2001) studied the effect of significant iron addition (Fe/P=2) to poultry manure but without evaluating the fate of the iron in the solid phase. In the present study, a decrease of the soluble phosphorus (13% to 2% of the total phosphorus) was observed, which is in accordance with the findings of Christensen et al. 2020 and Dao et al. 2001, who reported more than 80% of removal of the soluble phosphorus, even at low Fe/P ratio (~0.3). However, no vivianite could be detected by microscope or Mössbauer spectroscopy in the manure after one month in the "4g/L Fe dose" experiment.

The precipitation of iron sulphide could not alone explain the absence of vivianite (35-40% of the iron added could theoretically be bound as FeS), suggesting that another compound bound iron. Kleeberg et al. 2013 noticed that before efficient phosphate binding could occur in sediments, the quantity of iron binding as FeS but also associated with organic carbon should be considered. The amount of iron binding to organic matter approximated 20%-25% of the organic carbon, according to Lalonde et al. 2012 and Kleeberg et al. 2013. It was hypothesized that some of the dosed iron was lost to organics, and, therefore, two experiments with higher iron dosage were conducted.

The iron added in the "11 g/L Fe dose" experiment represented enough iron to bind all the sulphur as FeS (S=1.13g/L), bind 25% of the organic carbon in the sample (Volatile Solid=3.4% so Organic Carbon=17g/L according to Hakanson et al. 1983), and all the phosphorus as vivianite (P=1.68g/L). Five times more iron was added for the "52 g/L Fe dose" experiment to completely drive the reaction towards vivianite formation. For both iron doses, the presence of vivianite was confirmed by XRD, Mössbauer spectroscopy, and microscope observations (Figure 7.4). Vivianite crystals with a Fe/P ratio of 1.4-1.6 and presenting the same sheet organization as in digested sewage sludge (Roussel and Carliell-Marquet 2016, Chapter 3) and sediments (Rother et al. 2016) were observed after one day following the iron addition in both experiments (Figure 7.3).
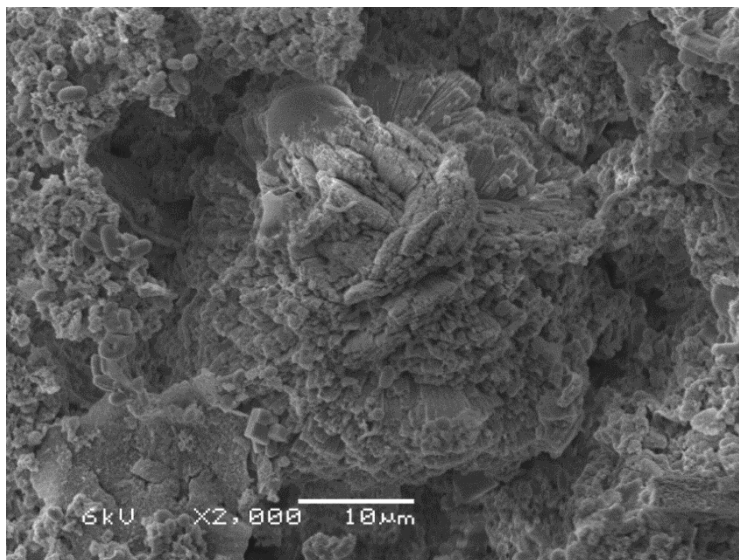


*Figure 7.3: Vivianite crystal present in the manure treated with the "high Fe dose" after one month. The Fe/P of similar particles found in the samples after iron addition was comprised between 1.4 and 1.6, matching the expected ratio of vivianite (1.5).*

Previous studies on vivianite in sewage sludge showed that Mössbauer spectroscopy is the best tool to quantify vivianite, and it was used for the current samples. Vivianite presents two characteristics doublets referred to as Vivianite A (Isomer Shift = 1.2±0.1 mm/s, Quadrupole Splitting = 2.4±0.1 mm/s) and Vivianite B (IS = 1.25±0.1 mm/s, QS = 3.0±0.1 mm/s) that are the pillars of vivianite quantification with Mössbauer spectroscopy (McCammon and Burns 1980, Rouzies and Millet 1993, Nembrini et al. 1983). The fitting of spectra for vivianite

quantification is further detailed in Chapter 3. Mössbauer spectroscopy suggests that in the "11 g/L Fe dose" experiments, around 20% and 30% of the total iron could be present as vivianite after 1 day and 36 days, respectively (Table 7.2). These results indicate that approximately 60% of the phosphorus is bound as vivianite after 1 day and 80% after 36 days (based on the elemental composition of the samples detailed in Supplementary information). These values seem on the high edge considering the numerous crystals of struvite observed by microscope (Figure 7.4). However, the visual observations can be biased since their different density (struvite~1.7, vivianite~2.7) makes that a vivianite particle contains 60% more phosphorus than a particle of struvite of the same size. When the "52 g/L Fe dose" was employed, 10% of the total iron was present as vivianite according to Mössbauer spectroscopy, corresponding to more than 100% of the available phosphorus (after 36 days).
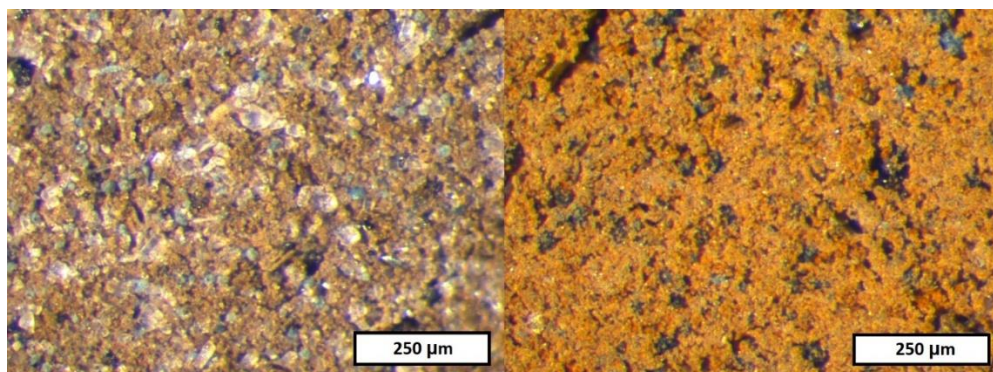


*Figure 7.4: Light microscope picture of the manure treated with the standard (left) and high iron dose after 1 month. The blue particles are vivianite, while most transparent particles are struvite (quartz is also present).*

Several points need to be mentioned concerning the Mössbauer spectroscopy measurements of these samples. Firstly, even though the samples were protected from oxygen as much as possible, it is likely that a part of the vivianite was oxidized based on previous experience (Chapter 2 and 3, Wilfert et al. 2018). The contribution of the $Fe^{3+}$ in vivianite could not be quantified here due to the overlapping with other Fe(III) phases, so a slight underestimation of the vivianite quantity is possible. Secondly, the current lack of knowledge on the iron species in iron-treated manure and the presence of other Fe(II) compounds than solely vivianite (e.g., siderite, Fe(II)Cl$_2$) makes vivianite quantification via Mössbauer spectroscopy more challenging than in sewage sludge. Lastly, the quantity of iron present as vivianite is calculated by summing the contribution of Vivianite Site A and Site B, both bearing uncertainties of 3% (20% of iron as vivianite means 20±6%).

Under these conditions, it is unwise to rely on the Mössbauer results entirely. Considering these uncertainties, we can reasonably assume that nearly all the phosphorus is transformed into vivianite when the "52 g/L Fe dose" was used. Besides, no other phosphorus forms were observed by SEM-EDX nor light microscope with this iron dose. When the "11 g/L Fe dose" is used, it can be said that vivianite formed quickly but did not account for all the phosphorus theoretically available. We propose that 50-80% of the phosphorus is bound to vivianite based

on the Mössbauer spectroscopy data and the microscope observation revealing the co-existence of vivianite and struvite.

Struvite was still present in the manure after treatment with the "11 g/L Fe dose". However, it completely disappeared in the "52 g/L Fe dose" experiment based on the light microscope (Figure 7.4) and SEM-EDX (Figure 7.5) observations. In line with the disappearance of struvite, magnesium was solubilized by the addition of iron, as suggested by chemical modelling (Christensen et al. 2020). While only 1% of the magnesium was soluble in raw manure, the average value on the duration of the experiments increased to $9\% \pm 7\%$ in "4 g/L Fe dose", $19\% \pm 8\%$ in "11 g/L Fe dose", and $84\% \pm 3\%$ in "52 g/L Fe dose" experiments (Supplementary information). Iron addition had more impact on magnesium solubilization at the beginning than at the end of the experiments. On day one, the magnesium solubility was at 16% in the "4 g/L Fe dose" and 33% in the "11 g/L Fe dose". However, on day 30, only 2% in "4 g/L Fe dose" and 8% in "11 g/L Fe dose" of Mg was soluble. The pH drop might also promote the increase of soluble magnesium in all the samples following iron addition: pH=$8.3\pm0.1$ in raw manure, $8.2\pm0.1$ for the "4 g/L Fe dose", $7.5\pm0.2$ for the "11 g/L Fe dose" and $4.9\pm0.3$ for the "52 g/L Fe dose". Christensen et al. 2020 did not observe a significant magnesium release nor pH drop after adding small iron quantities (Fe/P~0.3) to mink manure for coagulation.
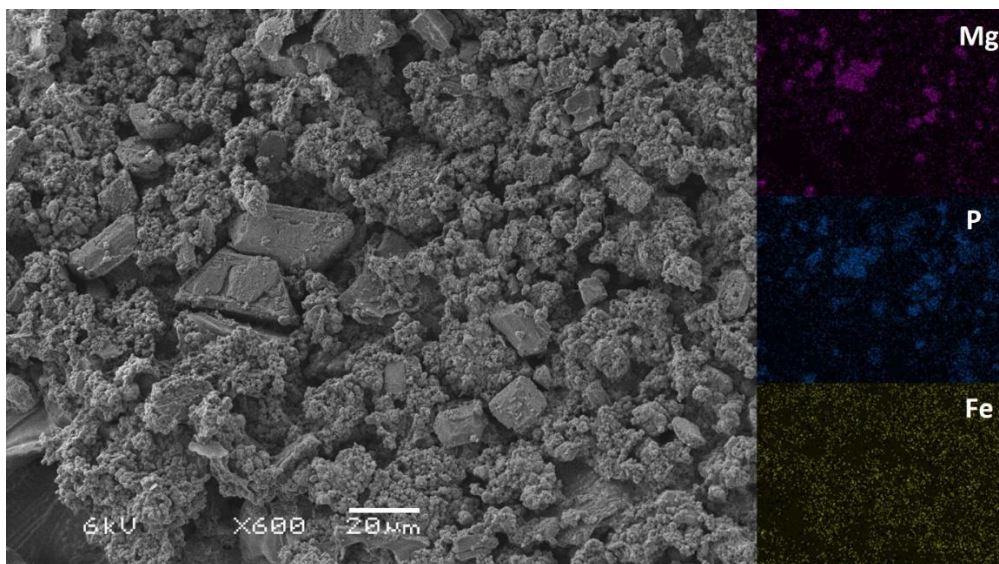


*Figure 7.5: SEM picture of the manure treated with the standard iron dose after 1 month. EDX scans of the same frame for the elemental distribution of magnesium, phosphorus, and iron.*

According to the reductive conditions in manure, the strong Fe-S interactions reported in the literature, and the chemical equilibrium modelling (see below), the presence of $FeS_x$ in the samples is expected. For example, the formation of $FeS_2$ and elemental sulphur in aqueous conditions (Wei and Osseo-Assare 1996), after iron addition to sludge digesters (Park and Novak 2013) and in sewers (Zhang et al. 2010a) was proposed in the literature. The immediate consumption of the soluble sulphur in the manure (75% removal) for all iron doses hinted at

the formation of such $FeS_x$ species (Supplementary information). The $FeS_x$ compounds should be XRD-amorphous since XRD in this study detected no crystalline iron sulphide (Table S7.4). Some works on sewage sludge also reported the absence of crystalline $FeS_x$ (Nielsen et al. 2005, Wilfert et al. 2018, Chapter 3), even though the presence of iron sulphides in a reductive environment like digested sewage sludge is generally accepted.
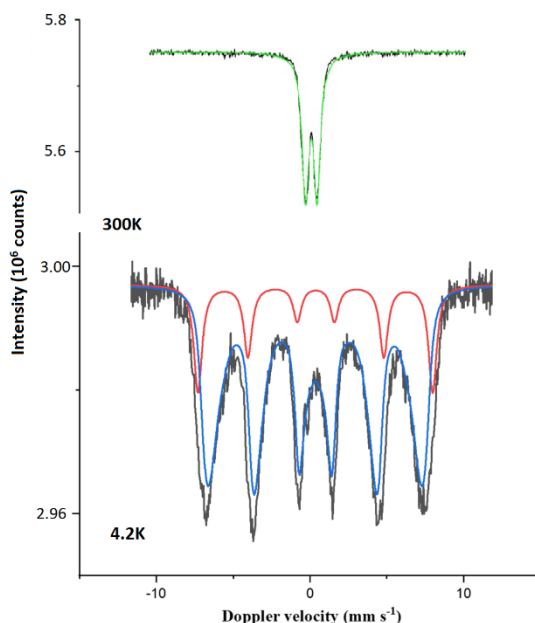


*Figure 7.6: Mössbauer spectra for the manure treated with a "4g/L Fe dose" after 31 days at room temperature (top) and at 4.2K (bottom). The top spectrum only reveals the presence of $Fe^{3+}$ compounds without possible speciation (green curve). The bottom spectrum features ferrihydrite (red curve) and a more disorganized phase (blue curve). This phase could be assigned to ferrihydrite in which iron is partially substituted or lepidocrocite.*

Since iron sulphide was supposed to form at low iron content already due to the strong affinity between iron and sulphide, the sample (4g/L dose) was studied in-depth to uncover the iron sulphide species. The absence of contributions with high isomer shifts (around 1-1.5 mm/s) in the room temperature Mössbauer spectra of the "4g/L Fe dose" excludes the presence of $Fe(II)S_x$ (Figure 7.6). The 4.2K Mössbauer spectroscopy measurements of the same sample indicate that low-spin iron species (like pyrite) cannot be present due to the absence of contribution in the center of the spectra (no magnetic field in the nucleus) (Figure 7.6). Therefore, the Mössbauer results indicate that $FeS_x$ could only be present as an amorphous ferric sulphide in this sample which is very unlikely due to the anaerobic conditions and the instability of ferric sulphide species. Alternatively, FeSx species could quickly oxidize upon oxygen exposure even at low levels (Butler and Rickard 2000) and form iron oxyhydroxides, which could have been caused by oxygen leakages between sample preparation and analysis. It could explain why its presence could not be confirmed in this study and previous works. Further study of iron-sulphur and iron-organic interactions in animal manure is relevant but was out of the scope of this study.

Due to the absence of vivianite in the manure treated with the "4g/L Fe dose", we hypothesized that a large quantity of the iron bound to organic matter. For example, dissolved humic substances, an important organic constituent of pig manure (Huang et al. 2006) have the ability to form complex compounds with iron (Stevenson 1994). The Mössbauer spectroscopy results indicate that the fraction of iron potentially bound to organic matter was present as ferric iron (Table 7.2), possibly ferrihydrite or lepidocrocite. Karlsson and Persson 2012 observed that in natural waters, polymeric Fe(III)-hydr(oxide) phase could form and had a ferryhydrite-like structure. Still, this observation is surprising since the conditions in manure were anaerobic and the samples were dried and prepared in anaerobic conditions. It suggests that oxygen leakages might have occurred between the sample preparation and analysis but such high amount of ferric iron remain strange.

The XRD revealed that besides vivianite, the other iron phases present were siderite and $FeCl_2*4H_2O$ in the manure treated with the "11 g/L Fe dose" and "52 g/L Fe dose", respectively (Table S7.4). Mössbauer spectroscopy suggested that a large share of the iron could be present as siderite in the "52 g/L Fe dose" even though XRD did not detect it (Table 7.2 and Table S7.4). It hinted that another ferrous iron phase was present in this sample but could not be identified. The iron chloride salts detected are suspected to only form during the drying of the sample due to their high solubility. The presence of other iron compounds like iron hydroxides/oxides cannot be ruled out.

Three important conclusions can be drawn from these experiments:

- Vivianite could be formed in animal manure if enough iron is added, opening a possible new route for phosphorus recovery from manure.
- The addition of iron to manure triggered vivianite formation at the expense of struvite, which is in line with the absence of struvite in digesters processing iron-rich sewage sludge (Chapter 2 and 3, Wilfert et al. 2018). In light of the results obtained in this study, we hypothesize that adding 15g of iron per litre of pig manure (with similar composition as in this study) is necessary to convert most phosphorus as vivianite. Digesting the manure to break down the organic matter may be an option to lower this requirement.
- While vivianite immediately formed after iron was added in a 1:1 molar ratio to sulphur in digested sewage sludge systems (Chapter 3), another compound (suspected to be organic matter) binds the iron before vivianite can form in manure. We hypothesize that the order of formation is: $FeS_x$, iron bound to organics (detected as Fe(III) phases with Mössbauer spectroscopy), and then vivianite.

## 7.3.2. Chemical equilibrium modelling

Simulating the addition of iron as $FeCl_2$ indicated that iron precipitates with phosphate, carbonate, and sulphur (Figure 7.7). Iron-containing precipitates formed to a larger extent with increasing iron concentration. The addition of iron caused the ionic strength of the solution to increase, therefore modifying the activity coefficient of the dissolved species, which is a crucial parameter in precipitation equilibria (Stumm and Morgan 2013). Accordingly, the

model simulating and predicting ion interactions was valid on a defined ionic strength range (Appelo and Postma 2005). The maximum ionic strength for the present model to be accurate is 0.5M, considering the Davies model and the WHAM (Tipping and Hurley 1992). The "11g/L Fe dose" resulted in ionic strength of 0.9 M. The accuracy of the model related to ionic strength was tested by removing potassium, sodium, chloride, and organic acids. The variation was within 10%. Therefore, descriptions by the model beyond 11g/L of iron were likely to be inaccurate and will not be discussed in this study. At high ionic strengths, the Pitzer model could present a satisfying accuracy (Pitzer 1973), but Pitzer parameters for compounds in pig manure have barely been established. Therefore, the Pitzer model was not used in this study.
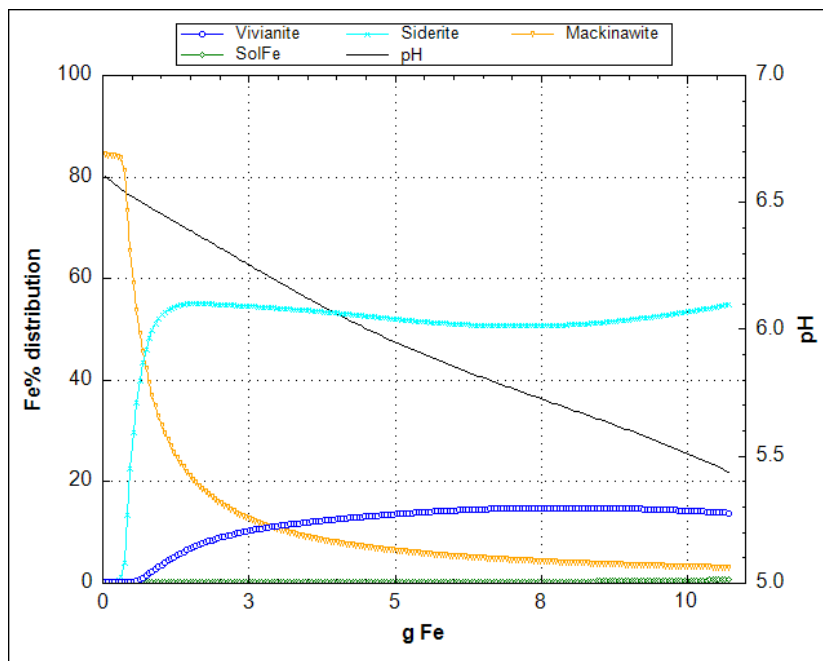


*Figure 7.7: Phreeqc simulation presenting the addition of iron on the x-axis against the iron distribution on the primary y-axis in the minerals Vivianite (blue), Siderite (cyan), Mackinawite (orange), and in solution (SolFe – green) together with the pH (black) development on the secondary y-axis.*

Sulfur and iron have a high affinity for each other and are likely to precipitate together. In the simulation, iron and sulfur formed pyrite ($FeS_2$) immediately with all available sulfur before any other iron precipitate formed. While pyrite is thermodynamically the most stable $FeS_x$ precipitate under anaerobic conditions (Pourbaix 1963), pyritization is a slow process (Nielsen et al. 2005). More realistically, meta-stable amorphous $FeS_x$ would be the dominant iron sulfide species in the time frame of the current experiments and could be a precursor for the slow formation of pyrite (Morse et al. 1987, Dewil et al. 2009). However, pyrite precipitated in the PHREEQC model because the model was based on thermodynamics only and did not include kinetics. Therefore, the precipitation of pyrite was manually blocked in the model, and mackinawite (FeS) was included to represent the formation of the $FeS_x$ species. Even with pyrite formation excluded, the model indicated that sulphide has the highest affinity for iron among carbonate and phosphate in pig manure. No firm evidence of the presence of $FeS_x$ was

found in the experiments. We discussed above that oxygen leakages between the sample preparation and analysis might have occurred, causing the destruction of $FeS_x$.

According to the simulation, iron and carbonate formed siderite ($FeCO_3$) immediately when iron was added to pig manure. The simulation indicated siderite formation after $FeS_x$, but before vivianite formation with the iron affinity ranking $S > CO_3 > PO_4$ (Figure 7.7). Therefore, in the "4 g/L Fe dose" experiment, 40% of the iron supposedly precipitated with sulfur, while the rest would be available for siderite formation and later vivianite. However, siderite and vivianite presence could be excluded by Mössbauer spectroscopy in this experiment. Therefore, the iron considered to form siderite and vivianite in the model probably complexed with dissolved and suspended organic matter instead (Daugherty et al., 2017). In the model, the iron-organic matter interactions were simplified by WHAM to complexations of iron with humate and fulvate (Tipping and Hurley, 1992). In a matrix like pig manure, the variety of organic compounds and possible binding sites for iron is enormous compared to surface water in lakes (which was the original purpose of WHAM). The model should be improved to better take into account iron-organic matter interactions, which appeared to play a dominant role in this study.
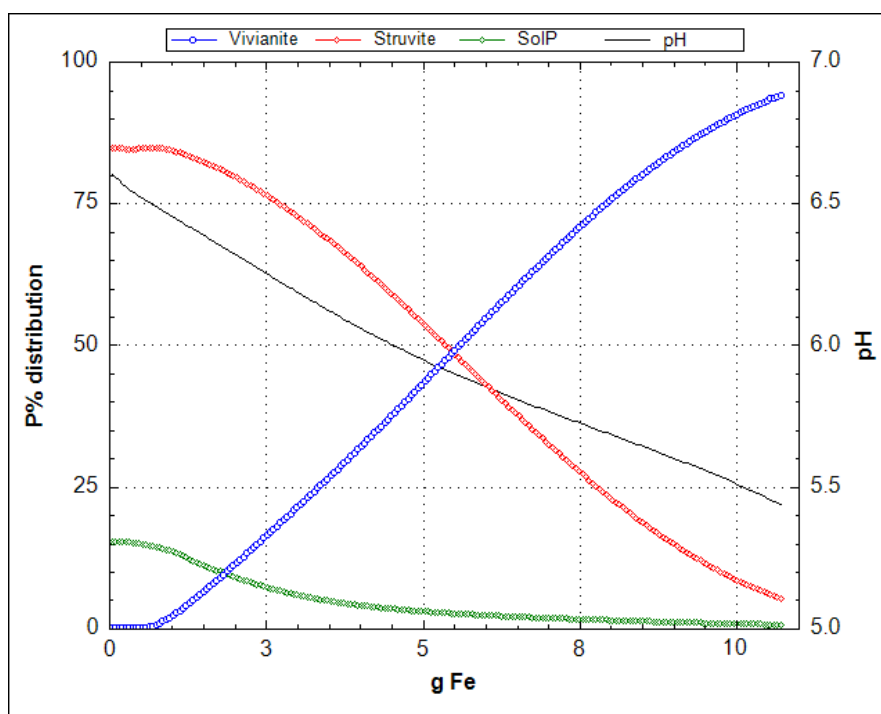


*Figure 7.8: Phreeqc simulation of iron addition on the x-axis against the phosphorus distribution on the primary y-axis in the minerals Vivianite (blue), Struvite (red), and in solution (SolP – green) together with the pH (black) development on the secondary y-axis.*

Phosphorus present as struvite dissolved and transformed to vivianite according to the simulation (Figure 7.8). At 10 g/L iron, the model predicted about 90% phosphorus as vivianite and 10% phosphorus as struvite. Mössbauer spectroscopy suggests that around 80% of the

phosphorus was present as vivianite at 11 g/L iron. It is possible that both the model and Mössbauer spectroscopy overestimated vivianite formation based on microscope observations indicating the presence of significant amount of struvite still at 11 g/L iron (Figure 7.4 and Figure 7.5). This overestimation from the model could be because more iron was bound to organic matter than the model predicted due to its limitation towards ionic strength.

When included in the model, hydroxyapatite ($Ca_{10}(PO_4)_6(OH)_2$) would form based on all available calcium and persist independently of the concentration of iron. Hydroxyapatite has a very low solubility due to its thermodynamic stability but takes time to form (Habraken et al. 2013). In this study, the untreated manure contained mainly struvite and calcium phosphate was not observed. Additionally, the formation of the very stable hydroxyapatite was unlikely in the short experiment of this study (Liu et al. 2016). Amorphous calcium phosphates and precursors of hydroxyapatite were not detected during experiments nor predicted by the model (Figure 7.2). Therefore, hydroxyapatite was manually prevented from forming in the simulation.

The precipitates calcite ($CaCO_3$) and struvite ($MgNH_4PO_4 * 6 H_2O$) increasingly dissolved with the addition of more iron in the simulation and the experiments (Figure 7.8 and Supplementary information). In the simulation, calcite dissolved and siderite formed, indicating the exchange of $CO_3^{2-}$ from calcium to iron. From about 1 g/L to 5 g/L of iron added, calcite further dissolved because more dolomite ($MgCa(CO_3)_2$) precipitated. Beyond 5 g/L of iron, siderite became the only carbonate mineral forming. Dolomite could form because more magnesium became available through the dissolution of struvite (Jun et al. 2017). Dolomite formation could explain the missing soluble magnesium in correlation with struvite dissolution during the lab experiments.

To summarize, the simulation indicated the formation of vivianite through the dissolution of struvite. The results were consistent within 10% variation when testing ionic strength dependency by drastically lowering the salt content to below 0.5 M and, therefore, in the acceptable range of the Davies theory. However, the model was based on thermodynamic stability and did not take kinetics into account. Accordingly, pyrite and hydroxyapatite were blocked from forming in the model because of their absence in the lab experiments and their slow formation rate. The interactions with organic matter were probably underestimated, and the mode could be further improved here. Nevertheless, vivianite formation and struvite dissolution were observed in both the experiments and the model.

### 7.3.3. Limitations of the sequential extraction of phosphorus

The most widely-used method used for phosphorus speciation are sequential extractions with increasingly strong solvents. The results from the sequential extraction revealed that before iron addition, around 30% of the phosphorus is readily bioavailable (soluble phase and bicarbonate extraction) (Figure 7.9). This result disagreed with those of Turner and Leytem 2004 and Dou et al. 2000 where 70-85% of the phosphorus could be extracted with water and bicarbonate. Analyses carried out by 31P NMR (Tiecher et al. 2014) also revealed that most phosphorus in poultry, cow, and swine manure is bioavailable.
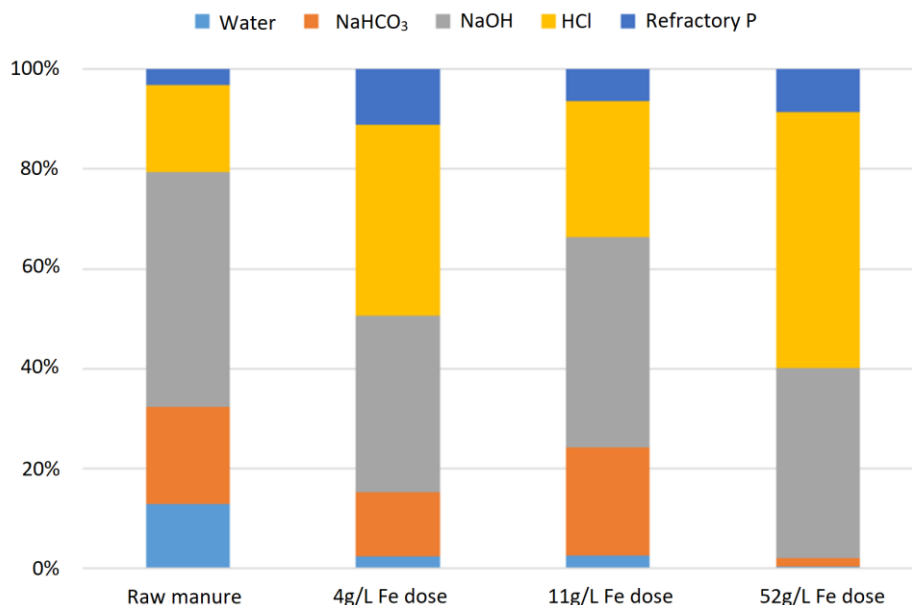
*Figure 7.9: Sequential phosphate extraction of the raw manure and the manure treated with three different iron dosage after 1 month*

The NaOH-extracted fraction, supposedly representing organic and weakly Fe/Al bound phosphorus (Uhlmann et al. 1990), accounted for 47% of the total phosphorus (Figure 7.9). IC-anions analyses show that the phosphorus pool of the extracted fraction is widely dominated by $PO_4^{3-}$, which is in line with literature results (Tiecher et al. 2014, Turner and Leytem 2004, Toor et al. 2005). $PO_4^{3-}$ should be essentially released from inorganic phosphorus species, excluding the presence of important organic phosphorus in the sample. Considering the initial elemental composition of manure, a maximum of 4% and 5% of the phosphorus could be bound to iron and aluminum (assuming P:Fe/Al=1:1). Therefore, it seems impossible that 47% of the total phosphorus would be organic or Fe/Al bound. The sequential extraction of different amounts of untreated manure suggested that not enough solvent was used per gram of solids, leading to the incomplete phosphorus release in every extraction step (Figure 7.10). These experiments, performed after the study, explain the discrepancies observed in the standard addition and show that the results from the sequential extractions need to be treated with precaution.
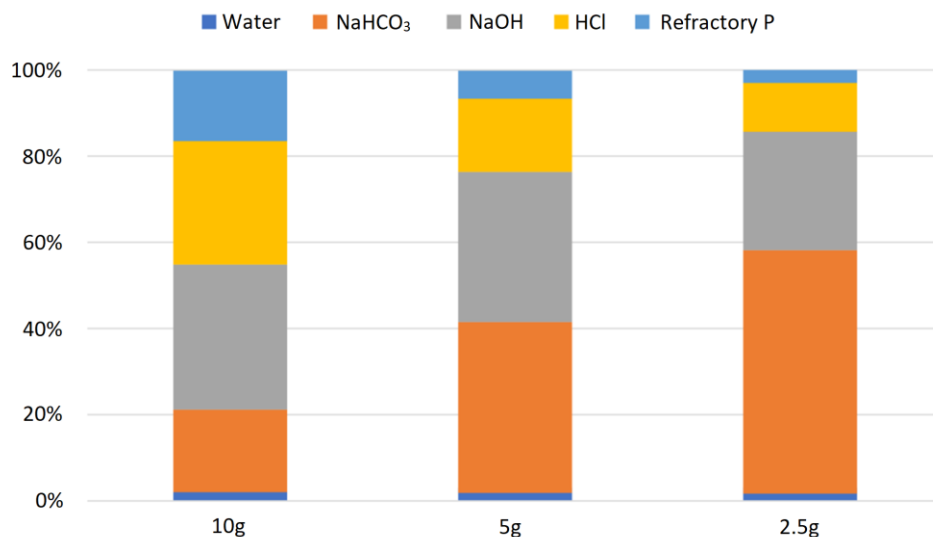
*Figure 7.10: Sequential phosphate extractions for different quantity of raw manure (no iron addition)*

Figure 7.9 suggests a reduction of the bioavailable phosphorus (extracted in water and bicarbonate) after iron addition from 32% in the initial manure down to 2% for the "52g/L Fe dose". This observation is in accordance with the formation of vivianite, which is not readily bioavailable, and the dissolution of struvite, whose phosphorus should partly be recovered in the bicarbonate fraction (Carliell and Weathley 1997). Sequential extraction with purified vivianite extracted from sewage sludge showed that 94% of the phosphorus is released in the NaOH fraction (results not shown). Since vivianite formation was confirmed by XRD, Mössbauer spectroscopy, and microscope observations for the "11g/L Fe dose" and "52g/L Fe dose", the share of phosphorus extracted by NaOH should increase. On the contrary, the share of phosphorus extracted by NaOH stayed at 40%, while it increased from 17% (untreated manure) to 51% ("52g/L Fe dose") for the HCl fraction. The lack of solvent could also explain these illogical results: the formed vivianite is only partly released in the NaOH fraction while the rest is released in the HCl fraction. It could be especially the case for the "52g/L Fe dose" that bears a higher acid buffer. The pH after the NaOH extraction was on average 10.9 ±0.6 for these samples, while it was 12.7±0.1 for the untreated manure.

The quantity of dry manure used per volume of solvent in this study (1g/60mL) is similar to the one used in several other studies (1/60 in Turner and Leytem 2004, 1/50 in Tiecher et al. 2014, 1/100 in Dou et al. 2000). However, these studies worked with a different type of manure (Dou et al. 2000), used different solvents (Tiecher et al. 2014), or used ligands to bind the released ions (Turner and Leytem 2004).

Lastly, the kinetic of the phosphorus release during NaOH extraction of raw manure showed that after being released, the phosphorus concentration decreased, indicating a possible reprecipitation of the phosphorus over time (at least 40% in 24h according to Figure 7.11). Such reprecipitation was not observed by Dou et al. 2000 in their kinetic study for poultry and dairy manure extraction with NaOH. For the current study, the NaOH extraction was stopped

after 6h (since it shows the maximum phosphorus release in Figure 7.11), which minimized the underestimation of the phosphorus released during this step. Still, the use of ligands may further limit the reprecipitation during the NaOH extraction.
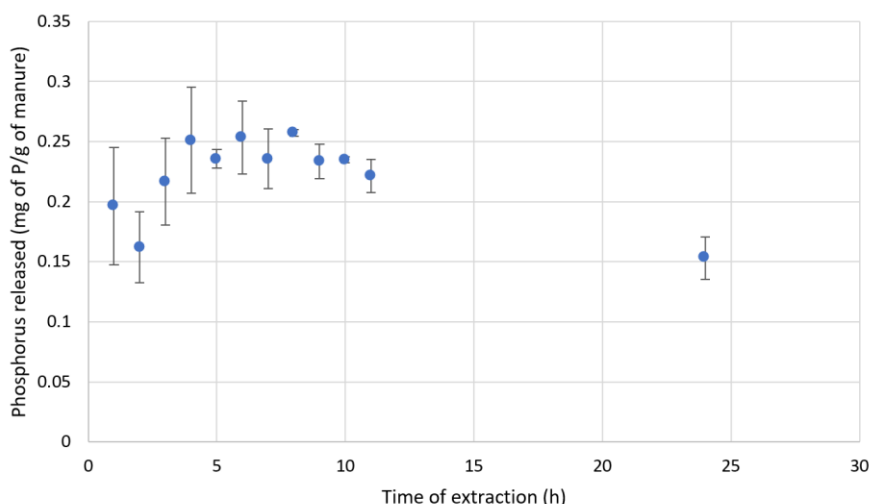


*Figure 7.11: Kinetic of the extraction of phosphorus in raw manure by a 0.1M NaOH solution. This kinetic study was performed on raw manure following the removal of the initial liquid phase and the extraction by NaHCO₃.*

To conclude, the sequential extractions performed in this study were not reliable enough to assess the phosphorus speciation in animal manure. It appears that the ratio of solvent/solids used was too low, which led to the incomplete release of the different phosphorus fractions, which was a significant problem. The use of ligands like EDTA should also be considered since it might reduce the reprecipitation of the released phosphorus. Besides, Carliell & Weathley 1997 showed that the extraction of struvite is not selective since it was parted between the $HCO_3$ and NaOH fraction. The transformation of struvite into vivianite is therefore challenging to assess with sequential extraction.

### 7.3.4. Vivianite can be magnetically recovered from manure

The addition of iron salts to animal manure allowed the formation of the paramagnetic mineral vivianite: $Fe(II)_3(PO_4)_2*8H_2O$. In the scope of phosphorus recovery and to reduce the amount of phosphorus present in animal manure, the feasibility of the magnetic recovery of vivianite was studied. The separation was performed using the same lab-scale separator and similar conditions as Chapter 2. The yield of the separation (percentage of total solid ending up in the magnetic fraction) was 17% for the "11 g/L Fe dose" and 14% for the "52 g/L Fe dose". After processing through the separator, the manure treated with "11 g/L Fe dose" showed that iron was concentrated by a factor of 1.7 while the phosphorus content stayed the same (Table 7.3). Struvite was never found in the magnetic concentrates by microscopic observation (Figure 7.12), even though it was found in the manure (Figure 7.5). It is confirmed by the low concentration factor for magnesium of 0.4. This could explain why the phosphorus is not enriched during magnetic separation: the amount of phosphorus separated as vivianite is

balanced by the amount of phosphorus present as struvite and cannot be magnetically extracted.

*Table 7.3: Composition of the manure fed to the magnetic separator and the concentrate after magnetic separation. The concentration factors and recovery are calculated based on these data. The magnetic extractions were performed once with around 100g of wet manure.*

| mg/g of dried solids | Iron-amended manure | | Magnetic concentrate | | Concentration factors | | Recovery | |
|---|---|---|---|---|---|---|---|---|
| | 11g Fe/L | 52g Fe/L | 11g Fe/L | 52g Fe/L | 11g Fe/L | 52g Fe/L | 11g Fe/L | 52g Fe/L |
| P | 22.8 | 13.5 | 21.9 | 31.7 | 1.0 | 2.3 | 16.0% | 32.9% |
| Fe | 168.4 | 213.1 | 287.3 | 305.6 | 1.7 | 1.4 | 28.3% | 20.1% |
| S | 15.1 | 7.6 | 7.0 | 6.0 | 0.5 | 0.8 | 7.7% | 11.1% |
| Ca | 29.7 | 9.6 | 33.1 | 15.9 | 1.1 | 1.6 | 18.5% | 23.2% |
| Mg | 14.2 | 1.3 | 5.3 | 1.9 | 0.4 | 1.4 | 6.2% | 20.0% |

The concentration factors were significantly higher for phosphorus (2.5) and slightly lower for iron (1.4) after the separation of the manure treated with the "50g/L Fe dose". A higher percentage of phosphorus was converted to vivianite after the high iron dose treatment explaining the higher concentration factor for phosphorus. Even though more vivianite was formed after the "52g/L Fe dose", the percentage of iron present as vivianite was lower according to Mössbauer spectroscopy results (Table 7.2). The lower concentration factor for iron in this experiment compared to the "11g/L Fe dose" suggests that the iron oxy(hydroxides) formed with a high iron dosing are not all magnetic. XRD identified no crystalline magnetic compound in these samples (Table S7.4). At the same time, the phosphorus concentration factor for the "50g/L Fe dose" experiment (2.5) is comparable to the one in Chapter 2 (2.2).

The concentration factor for magnesium was 1.4 for manure treated with "52g/L Fe dose" while it was 0.4 with the "11g/L Fe dose". This difference can be explained by the presence of struvite in the latter case, which was not magnetically extracted. The high concentration factors for calcium (1.6) and magnesium (1.4) for the "52g/L Fe dose" suggests the entanglement of calcium and magnesium compounds particles, most likely in an iron-based magnetic matrix.

Assuming that all the phosphorus in the magnetic concentrate is vivianite, vivianite contents of 18% for the "11 g/L Fe dose" and 26% for the "52 g/L Fe dose" cases can be calculated. Microscope observations revealed a significant quantity of vivianite in both concentrates, agreeing with this calculation (Figure 7.12). These values are lower than in Chapter 2 (50-60%) and Salehin et al. 2020 (35%). Lower vivianite grades could be explained by the entrainment of more foreign particles/fibres in the present study. The fact that the animal manure was not digested (while the experiments in Chapter 2 and Salehin et al. 2020 were with digested sludge) suggests the presence of bigger organic agglomerates, more likely to be retained in the magnetic separator and recovered in the magnetic concentrate.
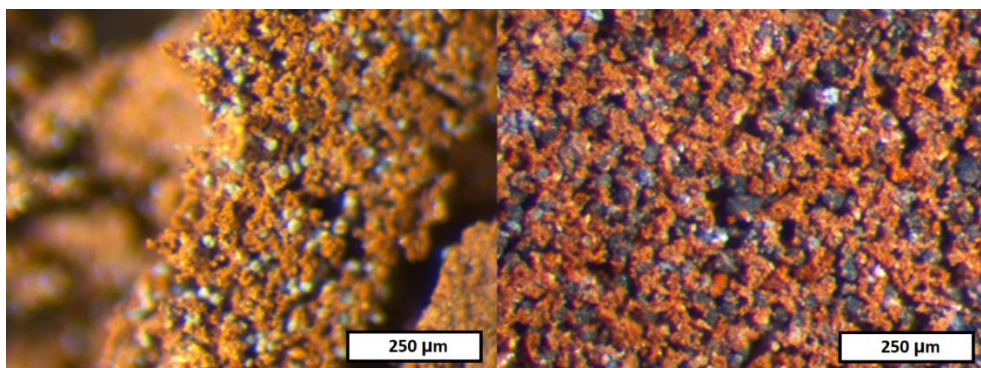
*Figure 7.12: Magnetic fraction after the magnetic separation of the manure treated with the standard (left) and high dose of iron. The blue particles observed are vivianite.*

The phosphorus recovery during these separations was 16% and 33% for the manures treated with 11g/L and 52 g/L of iron, respectively (Table 7.3). These recoveries are lower than Chapter 2 (35-50%) but higher than by Salehin et al. 2020 (5-10%). From the Mössbauer spectroscopy results, it can be assumed that 80% and 100% of the phosphorus was present as vivianite in the manure treated with "11 g/L of Fe dose" and "52 g/L of Fe dose", respectively (Table 7.2 and elemental composition in Supplementary information). It implies that vivianite recoveries were 20% and 33% after the magnetic separation for these two experiments. As discussed above, the percentage of phosphorus present as vivianite in the "11 g/L of Fe dose" experiment was likely overestimated based on the microscopic observations. Therefore, the vivianite magnetic recovery might be higher than 20% for this experiment.

The magnetic separation of vivianite from manure was proven to be possible, reaching a phosphorus concentration factor comparable to the one obtained in Chapter 2 when enough phosphorus was converted to vivianite under high iron dosing conditions. Comparing previous studies based on vivianite extraction from digested sludge revealed similar performances, even though some differences between pig manure and digested sludge make a direct comparison more complicated. For example, the solid content of iron-treated animal manure was higher (5-7%) than the 3-4% of digested sludge. It could have an impact on the mobility of the magnetic particles in the slurry during the separation. Additionally, the vivianite was recovered from sludge after digestion in Chapter 2 and Salehin et al. 2020 while the manure was not digested in our experiments (the batch experiments were carried out at 20°C). Following this proof of principle study, magnetic separation of a higher quantity of iron-treated manure should be undertaken to evaluate its performances better and reduce uncertainty due to the inhomogeneity of manure.

### 7.3.5. Outlook: how applicable is this technology?

So far, iron was added to manure for coagulation purposes (Hjorth et al. 2008, Christensen et al. 2020) or as nanoparticles to promote biogas production (Abdelwahab et al. 2020, Farghali et al. 2020). The interactions between iron and phosphate in animal manure have never been studied. This study showed for the first time that vivianite could be formed in pig manure following the addition of iron and that the vivianite could be subsequently recovered with a

magnetic separator. It provided the proof of principle for a possible new route for phosphorus recovery from animal manure.

Based on the current research, we estimated that a Fe/P molar ratio of 4-5 could be necessary to convert a maximum of phosphorus to vivianite which is much higher than 1.5-2 for digested sludge. While the vivianite recovery in this study was around 20-30%, recent research showed that higher recoveries could be obtained at pilot-scale for two reasons: the use of industrial equipment (pulsation in the slurry, optimized design of the magnetic cassettes) and the recirculation of the non-magnetic stream (Chapter 4). The same study suggested that 80% of the vivianite present in digested sludge could be recovered after two additional recirculations in the magnetic separator. While the performances of the magnetic separation were comparable at lab-scale for manure and digested sludge, differences in the slurry could have an impact on the separation at a larger scale. For example, the solid content in pig manure is higher than in digested sludge, which may decrease the mobility of vivianite particles and the separation efficiency.

After separation from the manure, vivianite amendment on soils can treat iron chlorosis (Eynard et al. 1992, Rosado et al. 2002, Rombolà et al. 2003) or function as a pesticide against snails and slugs as ferric phosphate (EPA, 1998). A downside of the use of iron phosphates as fertilizer is their low bioavailability that is sometimes increased by using chelating agents. These could damage the soil microbiome and threaten soil fertility (Nowack and van Briesen, 2005). Alternatively, an alkaline treatment is an efficient way to separate the iron from the phosphate (Chapter 2 and Salehin et al. 2020). Subsequently, the phosphorus could be upgraded to fertilizer, while the iron could be reused for capturing phosphate in manure. However, the current study showed that vivianite formation comes at the price of high iron dosages, of which more than half would remain in the manure. The high iron content might make the organic matter in pig manure less usable as an organic amendment for functional soils, commonly employed to avoid soil erosion arising in high-intensity agricultural areas (Shi and Schulin, 2018). The potential of manure containing iron as an amendment to fight iron chlorosis should be further studied.

This study provides the first proof of vivianite formation in pig manure and its subsequent magnetic extraction. It opens several research directions that will need to be considered to optimize the process, evaluate the potential of this recovery route, and understand the fundamentals behind vivianite formation in animal manure. The iron quantity necessary to form vivianite needs to be optimized for the process to be economically feasible. For this reason, the study and understanding of the iron-organics interaction in pig manure, which appeared to be different than in sewage sludge, is of paramount importance. Also, meso or thermophilic bioreactors assisted with iron dosing could provide simultaneous recovery of phosphorus and production of biogas. The digestion of manure would lead to the degradation of the organic matter, possibly reducing iron binding to organic matter while freeing the vivianite particle and facilitating their magnetic recovery. Lastly, this study focused on the phosphorus recovery from pig manure only. At the same time, poultry and cow manure also represent important secondary phosphorus sources but contain more fibers, potentially preventing an efficient magnetic separation.

## 7.4. Conclusion

This study showed for the first time that iron addition to pig manure resulted in the formation of vivianite, providing that sufficient iron was added. The Fe/P ratio necessary to maximize vivianite formation was much higher in the current study with pig manure (4-5) compared to sewage sludge (1.5-2) (Wilfert et al. 2018, Chapter 3). We believe that, unlike in sewage sludge, a significant share of iron binds to the organic matter in pig manure before any vivianite can form, substantially increasing the iron requirement. The experimental results suggested that struvite, initially present in manure, was gradually transformed into vivianite, which could bear almost all the phosphorus present in pig manure. Up to 30% of the vivianite could be later recovered by a lab-scale magnetic separator, which was similar to the recovery obtained for vivianite separation from digested sludge at this scale (Chapter 2). This proof-of-concept study proposes a new possibility to recover phosphorus from animal manure, which is essential for countries like Denmark, the United Kingdom, or the Netherlands, dealing with large surpluses of phosphorus in animal wastes

7

# References

Abdelwahab, T. A. M., Mohanty, M. K., Sahoo, P. K., Behera, D. (2020). Impact of iron nanoparticles on biogas production and effluent chemical composition from anaerobic digestion of cattle manure. *Biomass Conversion and Biorefinery*. doi:10.1007/s13399-020-00985-7.

Abioye, S., Ige, D., Akinremi, O., Nyachoti, Flaten, D. (2010). Characterizing Fecal and Manure Phosphorus from Pigs Fed Phytase Supplemented Diets. *Journal of Agricultural Science*, 2 (4).

Ackerman, J.N., Zvomuya, F. and Cicek, N. (2016). Anaerobic Storage of Commercial Pig Manures to Dissolve Phosphorus for Struvite Precipitation. *Applied Engineering in Agriculture* 32(4), 285-292.

Agomoh, I., Zvomuya, F., Akinremi, O.O. and Cicek, N. (2018). Chemically Enhanced Solids and Phosphorus Removal from Liquid Swine Manure. Transactions of the ASABE 61(5), 1705-1712.

Appelo, C.A.J. and Postma, D. (2004). *Geochemistry, Groundwater and Pollution*.

Barnett, G. M. Phosphorus Forms in Animal Manure. Bioresource Technology (1994), 49 (2), 139–147 DOI: 10.1016/0960-8524(94)90077-9.

Bauer, P.J., Szögi, A.A. and Vanotti, M.B. (2007). Agronomic Effectiveness of Calcium Phosphate Recovered from Liquid Swine Manure. *Agronomy Journal* 99(5), 1352-1356.

Blackshaw, R. E., Molnar, L. J. (2009). Phosphorus Fertilizer Application Method Affects Weed Growth and Competition with Wheat. *Weed Science*, *57* (3), 311–318.

de Bont, C. J. A. M., Berkum, S. V., Post, J. H. (2003). Agricultural and rural development and policies in The Netherlands.

Burns, R.T., Moody, L.B., Celen, I. and Buchanan, J.R. (2003). Optimization of phosphorus precipitation from swine manure slurries to enhance recovery. *Water Science and Technology* 48(1), 139-146.

Butler, I. B., Rickard, D. (2000). Framboidal pyrite formation via the oxidation of iron (II) monosulfide by hydrogen sulphide. *Geochimica et Cosmochimica Acta*, 64(15), 2665–2672. doi:10.1016/s0016-7037(00)00387-2.

Burns, R.T., Moody, L.B., Çelen, I. and Buchanan, J.R. (2003). Optimization of phosphorus precipitation from swine manure slurries to enhance recovery. *Water Science and Technology* 48(1), 139-146.

Carliell C.M. and Wheatley A.D., (1997). Metal and phosphate speciation during anaerobic digestion of phosphorus rich sludge, *Water Science and Technology*, Volume 36, Issues 6–7, Pages 191-200, ISSN 0273-1223, https://doi.org/10.1016/S0273-1223(97)00523-4.

Çelen, I., Buchanan, J. R., Burns, R. T., Bruce Robinson, R., & Raj Raman, D. (2007). Using a chemical equilibrium model to predict amendments required to precipitate phosphorus as struvite in liquid swine manure. *Water Research*, 41(8), 1689–1696. doi:10.1016/j.watres.2007.01.018.

Childers, D. L., Corman, J., Edwards, M., Elser, J. J. (2011). Sustainability Challenges of Phosphorus and Food: Solutions from Closing the Human Phosphorus Cycle. *Bioscience*, *61*(2), 117–124 DOI: 10.1525/bio.2011.61.2.6.

Christensen, M.L., Christensen, K.V. and Sommer, S.G. (2013). Solid–Liquid Separation of Animal Slurry.

Christensen, M. L., Keiding, K., Christensen, P. V. (2020). Phosphorus Removal from Manure by Mechanical Separation using Salt and Polymers: Theoretical Simulations and Experimental Data. *Applied Engineering in Agriculture*, 36(2), 175–185. doi:10.13031/aea.13726.

Church, C.D., Fishel, S.K., Reiner, M.R., Kleinman, P.J.A., Hristov, A.N., Bryant, R.B. (2020). Pilot-Scale Investigation of Phosphorus Removal from Swine Manure by the Manure Phosphorus Extraction (MAPHEX) System. *Applied Engineering in Agriculture* 36(4), 525-531.

Cordell, D. (2015). Tracking Phosphorus Security: Indicators of Phosphorus Vulnerability in the Global Food System. *Food Security*, 7 (2), 337–350.

Corona, F., Hidalgo, D., Martín-Marroquín, J.M. and Meers, E. (2020). Study of pig manure digestate pre-treatment for subsequent valorisation by struvite. *Environmental Science and Pollution Research*.

Dai, L., Tan, F., Wu, B., He, M., Wang, W., Tang, X., Hu, Q., Zhang, M. (2015). Immobilization of Phosphorus in Cow Manure during Hydrothermal Carbonization. *Journal of Environmental Management*, 157, 49–53. DOI: 10.1016/j.jenvman.2015.04.009.

**7**

Damalerio, R. G.; Belo, L. P.; Orbecido, A. H.; Pausta, C. M. J.; Promentilla, M. A. B.; Razon, L. F.; Eusebio, R. C. P.; Saroj, D.; Beltran, A. B. (2019). Phosphorus Recovery from Wastewater and Sludge. *Matec Web of Conferences*, 268, 06016–06016. DOI: 10.1051/matecconf/201926806016.

Daneshgar, S., Buttafava, A., Callegari, A. and Capodaglio, A. (2018). Simulations and Laboratory Tests for Assessing Phosphorus Recovery Efficiency from Sewage Sludge. *Resources* 7(3), 54.

Dao, T. H., Sikora, L. J., Hamasaki, A., Chaney, R. L. (2001). Manure Phosphorus Extractability as Affected by Aluminum- and Iron By-Products and Aerobic Composting. *Journal of Environment Quality*, 30(5), 1693. doi:10.2134/jeq2001.3051693x.

Daugherty, E.E., Gilbert, B., Nico, P.S. and Borch, T. (2017). Complexation and Redox Buffering of Iron(II) by Dissolved Organic Matter. *Environmental Science & Technology,* 51(19), 11096-11104.

Dewil, R., Baeyens, J., Roels, J., Van de Steene, B. (2009). Evolution of the Total Sulphur Content in Full-Scale Wastewater Sludge Treatment. *Environmental Engineering Science*, 26(4).

Dou, Z., Toth, J. D., Galligan, D. T., Ramberg, C. F., Ferguson, J. D. (2000). Laboratory Procedures for Characterizing Manure Phosphorus. *Journal of Environment Quality*, 29(2), 508. doi:10.2134/jeq2000.00472425002900020019x.

El Zrelli, R., Rabaoui, L., Daghbouj, N., Abda, H., Castet, S., Josse, C., van Beek, P., Souhaut, M., Michel, S., Bejaoui, N. (2018). Characterization of Phosphate Rock and Phosphogypsum from Gabes Phosphate Fertilizer Factories (se Tunisia): High Mining Potential and Implications for Environmental Protection. *Environmental Science and Pollution Research*, 25 (15), 14690–14702 DOI: 10.1007/s11356-018-1648-4.

EPA, U. (1998) Biopesticides fact sheet iron (ferric) phosphate. Office of Prevention, P.a.T.S. (ed), US government printing office, Washington DC.

Eynard, A., Campillo, M. C., Barròn, V., Torrent, J. (1992). Use of vivianite ($Fe_3(PO_4)_2*8H_2O$) to prevent iron chlorosis in calcareous soils. *Fertilizer Research*, 31(1), 61–67. doi:10.1007/bf01064228.

Greaves, J., Hobbs, P., Chadwick, D., Haygarth, P. (1999). Prospects for the Recovery of Phosphorus from Animal Manures: A Review. *Environmental Technology*, 20(7), 697–708. doi:10.1080/09593332008616864.

Fan, W., Bryant, L., Srisupan, M., Trembly, J. (2018). Clean Technologies and Environmental Policy: Focusing on Technology Research, Innovation, Demonstration, Insights and Policy Issues for Sustainable Technologies, 20 (7), 1467–1478 DOI: 10.1007/s10098-017-1440-z.

Farghali, M., Andriamanohiarisoamanana, F. J., Ahmed, M. M., Kotb, S., Yamamoto, Y., Iwasaki, M., Yamashiro, T., Umetsu, K. (2020). Prospects for biogas production and $H_2S$ control from the anaerobic digestion of cattle manure: The influence of microscale waste iron powder and iron oxide nanoparticles. *Waste Management*, 101, 141–149. doi:10.1016/j.wasman.2019.10.003.

Habraken, W.J.E.M., Tao, J., Brylka, L.J., Friedrich, H., Bertinetti, L., Schenk, A.S., Verch, A., Dmitrovic, V., Bomans, P.H.H., Frederik, P.M., Laven, J., van der Schoot, P., Aichmayer, B., de With, G., DeYoreo, J.J. and Sommerdijk, N.A.J.M. (2013). Ion-association complexes unite classical and non-classical theories for the biomimetic nucleation of calcium phosphate. *Nature Communications*.

Hakanson, L., Janson, M., (1983). Principles of Lake Sedimentology. Springer-Verlag, Berlin, Heidelberg, New York, 283 pp.

Henkens, P. L. C. M., van Keulen, H. (2001). Mineral Policy in the Netherlands and Nitrate Policy Within the European Community. *Njas - Wageningen Journal of Life Sciences*, 49 (2), 117–134 DOI: 10.1016/S1573-5214(01)80002-6.

Hjorth, M., Christensen, M. L., Christensen, P. V. (2008). Flocculation, coagulation, and precipitation of manure affecting three separation techniques. *Bioresource Technology*, 99(18), 8598–8604. doi:10.1016/j.biortech.2008.04.009.

Huang, G. F., Wu, Q. T., Wong, J. W. C., & Nagar, B. B. (2006). Transformation of organic matter during co-composting of pig manure with sawdust. *Bioresource Technology*, 97(15), 1834–1842. doi:10.1016/j.biortech.2005.08.024.

Huang, H.M., Jiang, Y. and Ding, L. (2014). Recovery and removal of ammonia-nitrogen and phosphate from swine wastewater by internal recycling of struvite chlorination product. *Bioresource Technology*, 172, 253-259.

Jun, D., Kim, Y., Hafeznezami, S., Yoo, K., Hoek, E.M.V. and Kim, J. (2017). Biologically induced mineralization in anaerobic membrane bioreactors: Assessment of membrane scaling mechanisms in a long-term pilot study. *Journal of Membrane Science* 543, 342-350.

Kamerlin, S.C., Sharma, P.K, Prasad, R.B., Warshel, A. (2013). Why Nature Really Chose Phosphate. *Quarterly Reviews of Biophysics*, 46 (1), 1–132. DOI:10.1017/S0033583512000157.

Karlsson, T., & Persson, P. (2012). Complexes with aquatic organic matter suppress hydrolysis and precipitation of Fe(III). Chemical Geology, 322-323, 19–27. doi:10.1016/j.chemgeo.2012.06.003.

Kleeberg, A., Herzog, C., Hupfer, M. (2013). Redox sensitivity of iron in phosphorus binding does not impede lake restoration. *Water Research*, 47(3), 1491–1502. doi:10.1016/j.watres.2012.12.014.

Klencsár, Z. (1997). Mössbauer spectrum analysis by Evolution Algorithm. *Nuclear Instruments and Methods in Physics Research Section B: Beam Interactions with Materials and Atoms*, 129(4), 527–533. doi:10.1016/s0168-583x(97)00314-5.

Korving, L., van Loosdrecht, M., Wilfert, P. (2019). Effect of iron on phosphate recovery from sewage sludge. In: Ohtake H., Tsuneda S. (eds) Phosphorus recovery and recycling. Springer, Singapore. https://doi.org/10.1007/978-981-10-8031-9_21.

Lalonde, K., Mucci, A., Quellet, A., Gelinas, Y. (2012). Preservation of organic matter in sediments promoted by iron. *Nature* 483 (7388), 198-200.

Leenstra, F. R., Vellinga, T. V., Neijenhuis, F., de Buisonje, F. E. (2014). Manure: a valuable resource. Wageningen: Wageningen UR Livestock Research.

Liu, X., Xu, Z., Peng, J., Song, Y. and Meng, X. (2016). Phosphate recovery from anaerobic digester effluents using CaMg(OH)4. *Journal of Environmental Sciences* 44, 260-268.

Lofts, S. and Tipping, E. (2000). Solid-solution metal partitioning in the Humber rivers: application of WHAM and SCAMP. *Science of The Total Environment* 251-252, 381-399.

MAFF (1991) Code of good agricultural practice for the protection of water, London HMSO, London, 79pp.

Mamais, D., Pitt, P.A., Cheng, Y.W., Loiacono, J., Jenkins, D. (1994). Determination of ferric chloride dose to control struvite precipitation in anaerobic sludge digesters. *Water Environ Res* 66 (7), 912–918.

Masse, L., I. Massé, D., Beaudette, V. and Muir, M. (2005). Size distribution and composition of particles in raw and anaerobically digested swine manure. *Transactions of the ASAE* 48(5), 1943.

McCammon, C. A., Burns, R. G. (1980). The oxidation mechanism of vivianite as studied by Mossbauer spectroscopy. *American Mineralogist*, 65(3-4), 361-366.

McGowan, G., Prangnell, J. (2005). The significance of vivianite in archaeological settings. *Geoarchaeology*, 21(1), 93–111. doi:10.1002/gea.20090.

Medick, J., Teichmann, I., Kemfert, C. (2018). Hydrothermal Carbonization (htc) of Green Waste: Mitigation Potentials, Costs, and Policy Implications of Htc Coal in the Metropolitan Region of Berlin, Germany. *Energy Policy*, *123*, 503–503 DOI: 10.1016/j.enpol.2018.08.033.

De Mol, R. M., van Beek, P. (1991). An OR Contribution to the Solution of the Environmental Problems in the Netherlands Caused by Manure. *European Journal of Operational Research*, 52 (1), 16–16.

Morse, J., Millero, F., Cornwell, J., Rickard, D. (1987). The Chemistry of the Hydrogen Sulfide and Iron Sulfide Systems in Natural Waters. *Earth-Science Reviews,* 24 (1), 1–42 DOI: 10.1016/0012-8252(87)90046-8.

Nembrini, G.P., Capobianco J.A., Viel, M., Williams A.F. (1983). A Mössbauer and chemical study of the formation of vivianite sediments of Lago Maggiore (Italy). *Geochimica et Cosmochimica Acta*, 47(8), 1459-1464.

Nielsen, A.H., Hvitved-Jacobsen, T., Vollertsen, J., (2007). Effects of iron on chemical sulfide oxidation in wastewater from sewer networks. *J. Environ. Eng.* 133, 655– 658. https://doi.org/10.1061/(ASCE)0733-9372(2007) 133:6(655).

Nielsen, A.H., Lens, P., Vollertsen, J., Hvitved-Jacobsen, T. (2005). Sulphide-iron interactions in domestic wastewater from a gravity sewer. *Water Research*, 39(12), 2747-2755.

Nriagu, J. O., & Dell, C. I. (1974). Diagenetic Formation of lron Phosphates in Recent Lake Sediments. *American Mineralogist*, 59, 934–946.

Nowack, B. and VanBriesen, J.M. (2005) Biogeochemistry of Chelating Agents, pp. 1-18, *American Chemical Society*.

Ohlinger, K.N., P.E., Young, T.M. and Schroeder, E.D. (1999). Kinetics Effects on Preferential Struvite Accumulation in Wastewater. *Journal of Environmental Engineering* 125(8), 730-737.

Pagliari, P.H. and Laboski, C.A.M. (2012). Investigation of the Inorganic and Organic Phosphorus Forms in Animal Manure. *Journal of Environmental Quality* 41(3), 901-910.

Park, C. M. and Novak, J. T. (2013). The effect of direct addition of iron(III) on anaerobic digestion efficiency and odor causing compounds. *Water Science and Technology*, 68(11), 2391–2396. doi:10.2166/wst.2013.507

Parkhurst, D.L. and Appelo, C.A.J. (2013) Description of input and examples for PHREEQC version 3—A computer program for speciation, batch-reaction, one-dimensional transport, and inverse geochemical calculations: U.S. *Geological Survey Techniques and Methods*.

Pitzer, K.S. (1973). Thermodynamics of electrolytes. I. Theoretical basis and general equations. *The Journal of Physical Chemistry* 77(2), 268-277.

Pourbaix, M. (1963) Atlas of Electrochemical Equilibria. Gauthier-Villars, Paris.

Prot, T. J. F., Nguyen, V. H., Wilfert, P. K., Dugulan, A. I., Goubitz, K., de Ridder, D. J., Korving, L., Rem, P. C., Bouderbala, A., Witkamp, G. J., van Loosdrecht, M.C.M. (2019). Magnetic Separation and Characterization of Vivianite from Digested Sewage Sludge. *Separation and Purification Technology*, 224.

Prot, T., Wijdeveld, W., Eshun, L. E., Dugulan, A. I., Goubitz, K., Korving, L., van Loosdrecht, M. C. M. (2020). Full-Scale Increased Iron Dosage to Stimulate the Formation of Vivianite and Its Recovery from Digested Sewage Sludge. *Water Research*. DOI: 10.1016/j.watres.2020.115911.

Rombolà, D., A., Toselli, M., Carpintero, J., Ammari, T., Quartieri, M., Torrent, J., & Marangoni, B. (2003). Prevention of Iron-Deficiency Induced Chlorosis in Kiwifruit (Actinidia deliciosa) Through Soil Application of Synthetic Vivianite in a Calcareous Soil. *Journal of Plant Nutrition*, 26(10-11), 2031–2041. doi:10.1081/pln-120024262.

Rosado, R., del Campillo, M. C., Martínez, M. A., Barrón, V., & Torrent, J. (2002). *Plant and Soil*, 241(1), 139–144. doi:10.1023/a:1016058713291.

Rothe, M., Kleeberg, A., Hupfer, M. (2016). The occurrence, identification and environmental relevance of vivianite in waterlogged soils and aquatic sediments. *Earth-Science Reviews*, 158, 51–64.

Roussel, J. and Carliell-Marquet, C. (2016). Significance of Vivianite Precipitation on the Mobility of Iron in Anaerobically Digested Sludge. *Frontiers in Environmental Science*, 4. doi:10.3389/fenvs.2016.00060.

Rouzies, D. and Millet, J. M. M. (1993). Mössbauer study of synthetic oxidized vivianite at room temperature. *Hyperfine Interactions*, 77(1), 19–28. doi:10.1007/bf02320295.

Saba, A., McGaughy, K., Reza, T. (2019). Techno-Economic Assessment of Co-Hydrothermal Carbonization of a Coal-Miscanthus Blend. *Energies*, 12 (4) DOI: 10.3390/en12040630.

Salehin, S., Rebosura, M., Keller, J., Gernjak, W., Donose, B. C., Yuan, Z., Pikaar, I. (2020). Recovery of in-sewer dosed iron from digested sludge at downstream treatment plants and its reuse potential. *Water Research*, 115627. doi:10.1016/j.watres.2020.115627.

Scholz, R.W., Ulrich, A.E., Eilittä, M., Roy, A. (2013). Sustainable Use of Phosphorus: A Finite Resource. *The Science of the Total Environment*, 461-462, 799–803 DOI: 10.1016/j.scitotenv.2013.05.043.

Seitz, A., Riedner, J., Malhotra, K., Kipp, J. (1973). Iron-Phosphate Compound Identification in Sewage Sludge Residue. *Environmental Science and Technology*, 7(4), 354–357.

Shepherd, T.A., Burns, R.T., Moody, L.B., Raman, D.R., Stalder, K.J. (2009). Investigating conductivity to predict magnesium addition requirements for struvite precipitation in swine manure slurries. *Applied Engineering in Agriculture* 25(1), 103-108.

Shi, P. and Schulin, R. (2018). Erosion-induced losses of carbon, nitrogen, phosphorus and heavy metals from agricultural soils of contrasting organic matter management. *Science of The Total Environment* 618, 210-218.

Song, C., Shan, S., Müller K., Wu, S., Niazi, N. K., Xu, S., Shen, Y., Rinklebe , J., Liu, D., Wang, H. (2018). Characterization of Pig Manure-Derived Hydrochars for Their Potential Application As Fertilizer. *Environmental Science and Pollution Research*, 25 (26), 25772–25779 DOI: 10.1007/s11356-017-0301-y.

Stevenson, F.J., 1994. Humus chemistry: Genesis, composition, reactions, 2nd ed. Wiley, New York.

Stumm, W. and Morgan, J. J. (2013). Aquatic Chemistry: Chemical Equilibria and Rates in *Natural Waters*, 3rd ed.

Szögi, A.A., Vanotti, M.B., Hunt, P.G. (2015). Phosphorus recovery from pig manure solids prior to land application. *Journal of Environmental Management* 157, 1-7.

Tao, W., Fattah, K. P., Huchzermeier, M. P. (2016). Struvite Recovery from Anaerobically Digested Dairy Manure: A Review of Application Potential and Hindrances. *Journal of Environmental Management*, 169, 46–57 DOI: 10.1016/j.jenvman.2015.12.006.

Tiecher, T., Zafar, M., Mallmann, F. J. K., Bortoluzzi, E. C., Bender, M. A., Ciotti, L. H., Santos, D. R. (2014). Animal manure phosphorus characterization by sequential chemical fractionation, release kinetics and 31P-NMR analysis. *Revista Brasileira de Ciência Do Solo*, 38(5), 1506–1514.

Tipping, E. and Hurley, M.A. (1992). A unifying model of cation binding by humic substances. *Geochimica et Cosmochimica Acta* 56(10), 3627-3641.

Tipping, E. (1998). Humic Ion-Binding Model VI: An Improved Description of the Interactions of Protons and MetalIons with Humic Substances. *Aquatic Geochemistry* 4(1), 3-47.

Toor, G. S., Cade-Menun, B. J., Sims, J. T. (2005). Establishing a Linkage between Phosphorus Forms in Dairy Diets, Feces, and Manures. *Journal of Environment Quality*, 34(4), 1380. doi:10.2134/jeq2004.0232.

Turner, B. L., and Leytem, A. B. (2004). Phosphorus Compounds in Sequential Extracts of Animal Manures: Chemical Speciation and a Novel Fractionation Procedure. Environmental Science & Technology, 38(22), 6101–6108. doi:10.1021/es0493042.

Uhlmann, D., Röske, I., Hupfer, M., & Ohms, G. (1990). A simple method to distinguish between polyphosphate and other phosphate fractions of activated sludge. *Water Research*, 24(11), 1355–1360. doi:10.1016/0043-1354(90)90153-w.

Vanotti, M.B., Szogi, A.A., Hunt, P.G., Millner, P.D. and Humenik, F.J. (2007). Development of environmentally superior treatment system to replace anaerobic swine lagoons in the USA. *Bioresource Technology* 98(17), 3184-3194.

Vanotti, M.B., Dube, P.J., Szogi, A.A. and García-González, M.C. (2017). Recovery of ammonia and phosphate minerals from swine wastewater using gas-permeable membranes. W*ater Research* 112, 137-146.

Wageningen UR Livestock Research (2015), "Managing phosphorus cycling in agriculture"

Westheimer, F. H. (1987). Why Nature Chose Phosphates. *Science*, 235 (4793), 1173–1178.

Wei, D. and Osseo-Asare, K. (1996). Particulate pyrite formation by the reaction in aqueous solutions: effects of solution composition. *Colloids and Surfaces A: Physicochemical and Engineering Aspects*, 118(1-2), 51–61. doi:10.1016/0927-7757(96)03568-6

Wijdeveld, W.K., Prot, T., Sudintas, G., Kuntke, P., Korving, L., van Loosdrecht, M.C.M., (2021). Pilot-scale magnetic recovery of vivianite from digested sewage sludge. Manuscript submitted.

Wilfert, P. K., Mandalidis, A., Dugulan, A. I., Goubitz, K., Korving, L., Temmink, H., Witkamp, G. J., van Loosdrecht, M. C. M. (2016). Vivianite As an Important Iron Phosphate Precipitate in Sewage Treatment Plants. *Water Research*, 104.

Wilfert, P., Dugulan, A. I., Goubitz, K., Korving, L., Witkamp, G. J., Van Loosdrecht, M. C. M. (2018). Vivianite As the Main Phosphate Mineral in Digested Sewage Sludge and Its Role for Phosphate Recovery. *Water Research*, 144, 312–321 DOI: 10.1016/j.watres.2018.07.020.

Yyan, J., Buisonjé, F.E., Melse, R.W. (2017). Livestock Manure Treatment Technology of the Netherlands and Situation of China. Report 1048.

Yekta, S.S., Ziels, R.M., Björn, A., Skyllberg, U., Ejlertsson, J., Karlsson, A., Svedlund, M., Willén, M., Svensson, B.H., (2017). Importance of sulfide interaction with iron as regulator of the microbial community in biogas reactors and its effect on methanogenesis, volatile fatty acids turnover, and syntrophic long-chain fatty acids degradation. *J. Biosci. Bioeng*. 123, 597–605. https://doi.org/10.1016/j.jbiosc.2016.12.003.

Zhang, T., Bowers, K. E., Harrison, J. H., Chen, S. (2010). Releasing Phosphorus from Calcium for Struvite Fertilizer Production from Anaerobically Digested Dairy Effluent. *Water Environment Research*, 82 (1), 34–42.

Zhang, L., Keller, J., Yuan, Z. (2010a). Ferrous Salt Demand for Sulfide Control in Rising Main Sewers: Tests on a Laboratory-Scale Sewer System. *Journal of Environmental Engineering*, 136(10), 1180–1187. doi:10.1061/(asce)ee.1943-7870.0000258.

Zhang, H., Lo, V. K., Thompson, J. R., Koch, F. A., Liao, P. H., Lobanov, S., Mavinic, D. S., Atwater, J. W. (2015). Recovery of Phosphorus from Dairy Manure: A Pilot-Scale Study. *Environmental Technology*, *36* (11), 1398–1404 DOI: 10.1080/09593330.2014.991354.wil.

**7**

## Supplementary information

*Table S7.1: Composition of the total manure and its liquid fraction for the experiment with iron dosing of 4g/L.*

| 4 g/L | TS | pH | Total manure (g/kg wet manure) | | | | | Soluble fraction (mg/L) | | | | |
|---|---|---|---|---|---|---|---|---|---|---|---|---|
| | | | P | Fe | Mg | S | Ca | P | Fe | Mg | S | Ca |
| Initial | 6.8% | 8.4 | 1.5 | 0.1 | 0.8 | 0.8 | 1.9 | 170 | 1 | 8 | 460 | 220 |
| 1 days | 6.3% | 8.2 | 1.2 | 3.2 | 0.6 | 0.8 | 1.5 | 15 | 75 | 120 | 180 | 130 |
| 3 days | 5.6% | 8.2 | 1.0 | 3.3 | 0.5 | 0.8 | 1.4 | 25 | 40 | 120 | 130 | 80 |
| 7 days | 6.4% | 8.2 | 1.4 | 3.6 | 0.6 | 0.9 | 1.5 | 25 | 30 | 40 | 130 | 60 |
| 15 days | 6.0% | 8.2 | 1.1 | 3.4 | 0.6 | 1.1 | 1.5 | 40 | 25 | 30 | 130 | 50 |
| 31 days | 7.4% | 8.2 | 1.6 | 4.3 | 1.0 | 1.0 | 2.1 | 50 | 20 | 20 | 120 | 45 |

*Table S7.2: Composition of the total manure and its liquid fraction for the experiment with iron dosing of 11g/L.*

| 11 g/L | TS | pH | Total manure (g/kg wet manure) | | | | | Soluble fraction (mg/L) | | | | |
|---|---|---|---|---|---|---|---|---|---|---|---|---|
| | | | P | Fe | Mg | S | Ca | P | Fe | Mg | S | Ca |
| Initial | 5.4% | 8.3 | 1.7 | 0.1 | 1.0 | 1.1 | 2.0 | 240 | 1 | 3 | 600 | 50 |
| 1 days | 7.1% | 7.3 | 1.0 | 7.9 | 0.7 | 0.9 | 1.3 | 14 | 45 | 250 | 220 | 20 |
| 3 days | 7.7% | 7.4 | 1.9 | 14.6 | 1.1 | 1.1 | 2.4 | 28 | 30 | 200 | 210 | 50 |
| 9 days | 8.3% | 7.4 | 1.3 | 9.3 | 0.8 | 0.8 | 1.6 | 38 | 20 | 210 | 100 | 50 |
| 21 days | 7.9% | 7.6 | 1.5 | 10.4 | 0.9 | 0.8 | 1.7 | 39 | 15 | 180 | 110 | 50 |
| 36 days | 8.1% | 7.9 | 1.3 | 9.5 | 0.9 | 0.9 | 1.7 | 38 | 10 | 85 | 100 | 30 |

*Table S7.3: Composition of the total manure and its liquid fraction for the experiment with iron dosing of 52g/L. The dissolved iron could not be measured accurately and was estimated based on the sequential extraction results. The soluble phosphorus was under the detection limit of the ICP-OES.*

| 52 g/L | TS | pH | Total manure (g/kg wet manure) | | | | | Soluble fraction (mg/L) | | | | |
|---|---|---|---|---|---|---|---|---|---|---|---|---|
| | | | P | Fe | Mg | S | Ca | P | Fe | Mg | S | Ca |
| Initial | 5.4% | 8.3 | 1.7 | 0.1 | 1.0 | 1.1 | 2.0 | 240 | 1 | 3 | 600 | 50 |
| 1 days | 17.4% | 5.3 | 1.2 | 32.0 | 0.7 | 0.8 | 1.5 | 1 | 21000 | 650 | 200 | 160 |
| 3 days | 14.6% | 5.1 | 1.0 | 32.0 | 0.7 | 0.7 | 1.3 | 1 | 21000 | 530 | 180 | 190 |
| 9 days | 14.9% | 4.8 | 0.6 | 34.3 | 0.6 | 0.6 | 0.9 | 1 | 21000 | 630 | 170 | 280 |
| 21 days | 13.9% | 4.9 | 0.6 | 30.7 | 0.5 | 0.6 | 0.8 | 1 | 21000 | 680 | 220 | 390 |
| 36 days | 15.0% | 4.4 | 0.9 | 35.2 | 0.6 | 0.7 | 1.2 | 1 | 21000 | 690 | 200 | 840 |

*Table S7.4: Identified crystalline phases by XRD.*

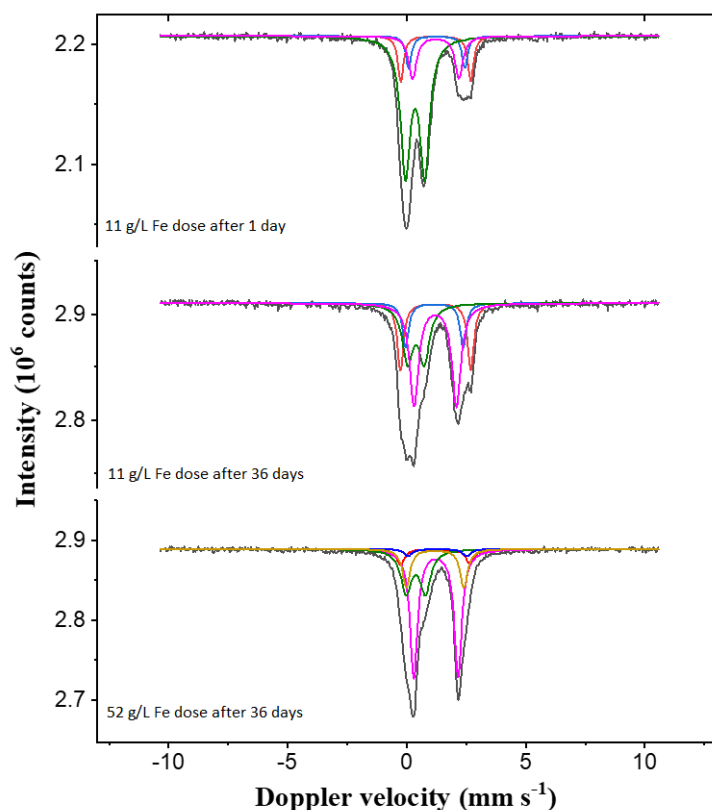| Sample | Compound | |
|---|---|---|
| | Calcite | $CaCO_3$ |
| Raw manure | Sylvite | $KCl$ |
| | Struvite | $(NH_4)Mg(PO_4)*6H_2O$ |
| | Salammoniac | $NH_4Cl$ |
| | Halite | $NaCl$ |
| | Calcite | $CaCO_3$ |
| 11 g/L Fe dose | Siderite | $Fe(CO_3)$ |
| | Potassium Chloride | $KCl$ |
| | Vivianite | $Fe_3(PO_4)_2*8H_2O$ |
| | Struvite (K) | $KMg(PO_4)_2*8H_2O$ |
| | Vivianite | $Fe_3(PO_4)_2*8H_2O$ |
| 52 g/L Fe dose | Iron Chloride Hydrate | $FeCl_2*4H_2O$ |
| | Halite | $NaCl$ |
| | Salammoniac | $NH_4Cl$ |



*Figure S7.1: Mössbauer spectra for the samples measured at 300K. The colors used correspond to, Black: sum of all the contributions, Blue: Vivianite site A, Red: Vivianite site B, Pink: $FeCO_3$, Green: $Fe^{3+}/Fe^{II}$ standing for Fe(III) compounds, and low-spin Fe(II) compounds like pyrite, Yellow: $FeCl_2*2H_2O$.*

*Table S7.5: Input data for the Phreeqc modeling*

| Parameter | Value |
|---|---|
| Temperature | 20°C |
| pH | 8.3 |
| pe | -3.8 |
| density | 1 |
| Alkalinity | 15000 mg/L |
| C | 6000 mg/L |
| Cl | 7500 mg/L |
| K | 7000 mg/L |
| N(-3) (Ammonium) | 5500 mg/L |
| Na | 2000 mg/L |
| P | 600 mg/L |
| S | 600 mg/L |
| Acetate | 2000 mg/L |
| Propionate | 150 mg/L |
| Butyrate | 150 mg/L |
| Valerate | 13000 mg/L |
| Humate | 15000 mg/L |

7
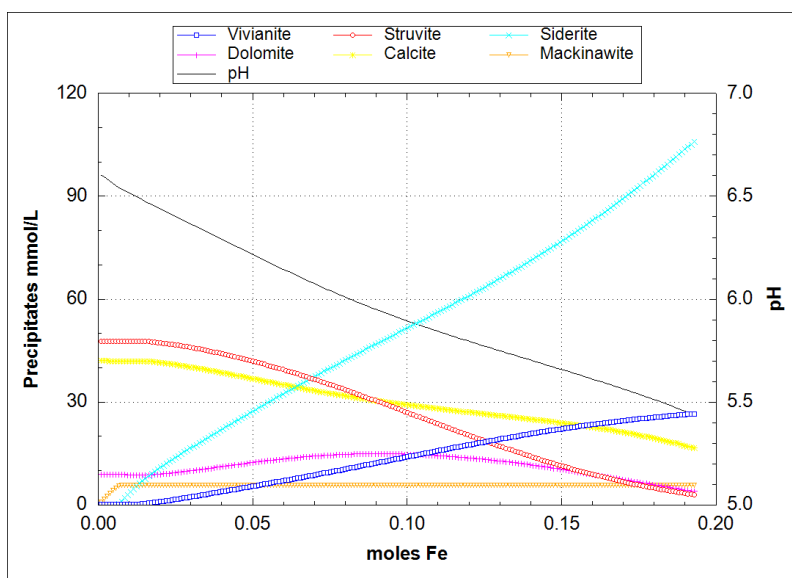
*Figure S7.2: Phreeqc simulation of iron addition on the x-axis against the forming precipitates on the primary y-axis and the pH development on the secondary y-axis.*

**7**
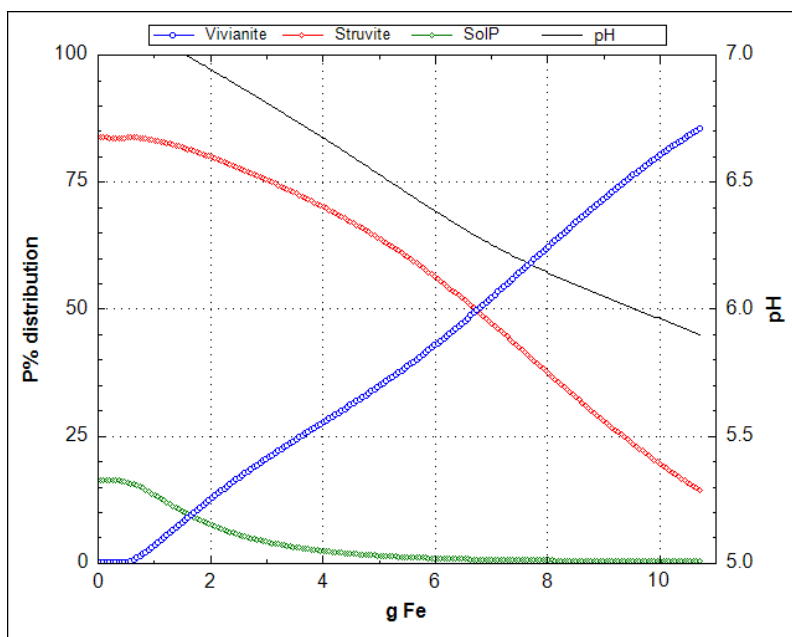


*Figure S7.3: The simulation executed at low ionic strength without potassium, Cl, and low Na balanced with organic acids. At 11 g/L iron, the ionic strength is 0.5 M instead of 0.9 M. Vivianite precipitates less at lower ionic strengths. However, the results did not vary more than 10% from simulation with actual high ionic strength input.*

# Chapter 8: Ionic strength of the liquid phase of different sludge streams in a wastewater treatment plant
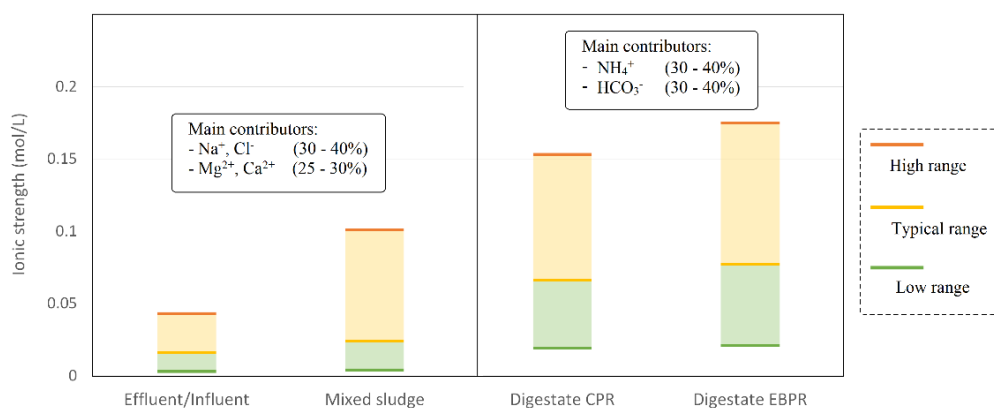
**Highlights**

- The ionic strength for wastewater-based streams ranges from 0.003 to 0.1M.

- $Na^+$, $Cl^-$, $Mg^{2+}$ and $Ca^{2+}$ make 50-70% of the wastewater-based streams' ionic strength.

- The ionic strength for digestates ranges from 0.02 to 0.17M.

- $NH_4^+$ and $HCO_3^-$ account for 65-75% of the ionic strength of digestates.

- Ionic strength is rarely determined and often misused in the literature.

**8**

Keywords: WWTP, digestion, CPR, EBPR, conductivity, wastewater composition

*The following chapter does not directly relate to vivianite and should be seen as an addition, rather than an integral part of the main story. To perform chemical modelling related to the precipitation of vivianite, the ionic strength of different sludge streams was necessary. However, this type of data was complicated to find in the available literature. The same observation was made for the species bearing the highest concentration in those streams. Therefore, concentration ranges were collected from literatureand and used to deduct ionic strength ranges for the liquid fraction of different sludge streams. The obtained ionic strength values were used for chemical modelling in other chapters of this thesis, and were also compared to existing ranges found in the literature.*

## Abstract

In a wastewater treatment plant (WWTP), several sludge streams exist, and their liquid phase composition varies with time and place. For evaluating the potential for the formation of precipitates and equilibria for weak acids/bases, the ionic strength and chemical composition need to be known. This information is often not available in the literature and even neglected in chemical model-based research. Based on a literature review, we proposed three ranges of concentration (low, typical, and high) for the major constituents of the liquid phase of the different streams in a WWTP. The study also discusses the reasons for the concentration evolution and the exceptional cases to allow readers to consider the suitable range depending on their situation. The ionic strength of the different streams and the contribution of their constituents were calculated based on the ionic composition. The major contributors to the ionic strength for the wastewater-based streams (influent, effluent, and mixed sludge) were $Na^+$, $Cl^-$, $Mg^{2+}$ and $Ca^{2+}$ representing 50-70% of the ionic strength. For digestate, $NH_4^+$ and $HCO_3^-$ accounted for 65-75% of the ionic strength. Even though the ionic strength is recognized to impact several essential wastewater treatment processes, its utilization in literature is not always adequate, as discussed in this study.

**8**

Note: the references in this chapter are presented as number for convenience

## 8.1.    Introduction

The last decades saw a significant development in the amount of wastewater treated. In Europe, 95% of the households were connected to a collection system in 2014, representing 517 million people (**22**). China bears the largest municipal wastewater infrastructure in the world, and over 90% of the wastewater of the country was treated in 2018 (**64**). The wastewater composition can vary strongly depending on the location of the wastewater treatment plant (WWTP) and the type of influent streams. For instance, high concentrations of $SO_4^{2-}$, $Na^+$ and $Cl^-$ can be expected in coastal WWTPs, where seawater intrusions can occur (**59**). Even higher salt loads can be found in specific places like Hong Kong, where seawater is directly used for flushing toilets (**46, 88, 90**). It is also common for WWTPs to process some industrial wastewater, which can bear substantial loads of diverse elements, depending on the type of industry.

During municipal wastewater treatment, the pollutant load is oxidized or ending up in the sludge fraction while the treated water is discharged. The composition of the solid fraction of the sludge does not evolve a lot through the different sludge treatment steps, except during digestion, where organic matter is transformed into biogas. However, the liquid fraction of the sludge flows is more dynamic, and its composition varies significantly in the different units. For example, when the sludge encounters anaerobic conditions (typically during thickening and digestion), fermentation occurs, and volatile fatty acids (VFA) are progressively produced (**7, 71**). It creates a pH drop that influences the solubility of several inorganic compounds present in the sludge and thus the composition of the liquid fraction. Digestion is usually the final solid treatment step and provokes a significant increase in bicarbonate and ammonium concentration (**67**) associated with a slight increase in pH. Additionally, WWTPs process designs are numerous, and different succession of units will lead to different soluble phase compositions. For example, a digestate contains higher phosphorus and K concentrations if produced in a WWTP using Enhanced Biological Phosphorus Removal (EBPR) compared to Chemical Phosphorus Removal (CPR) (**34**). Considering that the composition of the wastewater and the sludge soluble phase can vary a lot, evaluating their typical composition is complicated.

Ionic strength can be deducted from the composition of the soluble phase. Ionic strength is an essential parameter in wastewater treatment since it impacts, for example, nitrogen removal (**44, 95**) or the stability of sludge flocs (**55, 96**). Especially all kinds of precipitation reactions will strongly depend on the ionic strength of the solution since the activity coefficients are calculated from ionic strength (**76**). However, ionic strength is often misused in literature by considering vast ranges (**55, 96**) or unrealistic values (**42, 73**). Moreover, the liquid composition of the different sludge streams, and thus their ionic strength, is not widely available in the literature. Ionic strength should preferably be deducted from thorough analyses of the liquid phase composition, but this is not always possible. Therefore, such a study could provide a way to quickly estimate the ionic strength of a sludge stream without the need for complete characterization. We reviewed the literature for data on the main compounds influencing the ionic strength of wastewater and sludge and critically evaluated the data availability. Ionic strength ranges were eventually calculated and used to evaluate the current choices of ionic strength in literature.

## 8.2.   Method

Information from literature was collected to evaluate the composition of the different liquid streams in a WWTP. The study focuses on the dissolved compounds that have the most significant influence on the ionic strength: $SO_4^{2-}$, $Na^+$, $Cl^-$, $PO_4^{3-}$, $Mg^{2+}$, $Ca^{2+}$, $K^+$, VFA, $NH_4^+$, $HCO_3^-$. Values for pH were also collected since it is an important global parameter and it influences, for example, the ionic speciation. Single or multiple concentrations were gathered for all the elements studied, and three ranges (low, typical, high) were determined from the entire dataset. In general, the ranges were built for each parameter on information collected from 10-20 WWTPs (Table 8.7). The ionic strength was later calculated from the composition of the different sludge streams.

For a matter of clarity, the studied streams can be decomposed into three categories depending on their ionic strength:

- Low ionic strength: influent and effluent. The concentration of the soluble species is low compared to the liquid fraction of the sludge. Even though the influent and effluent composition is different, the elements that contribute the most to their ionic strength (e.g., $Na^+$, $Cl^-$) presents similar concentrations.
- Median ionic strength: soluble fraction of sludge before digestion. This category comprises primary sludge, waste activated sludge, and any mix of undigested sludge. For those streams, biological activity has already started (especially after thickening), which increases the concentration of some parameters (P, VFA…). A distinction between primary and secondary sludge was made when possible.
- High ionic strength: soluble fraction of sludge after digestion. Due to the biological activity, anaerobic conditions, and high solid retention time (20-30 days), the composition of the digestate is significantly different from the non-digested streams. Data were gathered from digestate or reject water (after dewatering). Moreover, clear differences were noticed for some compounds, whether the digestate was from a EBPR or CPR plant; therefore, both streams are presented separately.

It was observed that some parameters were constant for the low and typical ionic strength streams. Thus those parameters are presented in a unique range. A similar observation was made for the CPR and EBPR digestates: several compounds present similar concentrations and are therefore presented together.

For each stream, three concentration ranges were given: low, typical, and high. The ranges are wide to cover most of the situations in WWTPs. However, they do not cover extreme cases, but these are discussed when possible. As much as possible, references giving an overview of several installations were prioritized. For some parameters, data are not widely available, but the value given was always based on a minimum of three different sources. It is important to note that different analytical techniques were employed to measure the same parameter depending on the reference, leading to differences in the concentration ranges obtained.

## 8.3. Results & discussion

### 8.3.1 Constant parameters in non-digested streams

In all the streams before digestion, references show that the concentration of sulphate, sodium, and chloride stays relatively constant. A well-documented source of these three elements is the intrusion of seawater or brackish groundwater in the sewer system. The concentration for these elements can be 5-10 times higher than the maximum range given if seawater is used as flushing water like in Hong Kong (**46, 88, 90**). Sulphate and chloride are also commonly added in WWTPs as counter-ion of iron or aluminum (used to flocculate the sludge and remove phosphate) and present in industrial wastewater (**69**).

*Table 8.1: Ranges for the compounds whose concentration is identical in all non-digested streams. The ranges presented are for influent, effluent, and non-digested sludge.*

|                    | Low | Typical | High | Reference                       |
| ------------------ | --- | ------- | ---- | ------------------------------- |
| $SO_4^{2-}$ (mg S/L) | 10  | 30      | 60   | 4, 20, 25, 40, 62, 74, 82, 85, 86 |
| $Na^+$ (mg/L)      | 40  | 100     | 400  | 4, 6, 38, 57, 82, 85, 86        |
| $Cl^-$ (mg/L)      | 30  | 300     | 600  | 4, 28, 30, 80, 82               |

Several sources suggest that these elements go untreated during the wastewater treatment process (besides $H_2S$ oxidation), explaining why their concentration does not vary in non-digested streams (**19, 25, 47, 67, 78, 85**). The dissolved sulphur in the influent is mainly present as $SO_4^{2-}$ (**19, 25**). Almost all sulphur is also present as $SO_4^{2-}$ in secondary sludge. The reduction of sulphate to sulfide gradually happens during gravity-thickening (**19**): for example, 60-80% of the dissolved sulphur is sulphide after thickening of PS and WAS according to (**25**). Then, dissolved sulphide can be eliminated by precipitation as FeS, provided enough iron is present or dosed to prevent $H_2S$ in the biogas.

### 8.3.2 Variable parameters in non-digested streams

The concentration of $PO_4^{3-}$, $Mg^{2+}$, $Ca^{2+}$, $K^+$, VFA, $NH_4^+$, and $HCO_3^-$ are usually lower in influent/effluent than in the mixed sludge; therefore, they are presented separately (Table 8.2 and Table 8.3). Nitrogen and phosphorus species are always low in the effluent since they need to be removed to avoid eutrophication in the water bodies where the water is discharged. 70-80% of the influent nitrogen is ammonia (**38**), while nitrate (**70, 90**) or dissolved organic nitrogen (**60**) are the major nitrogen compounds in the effluent. Typical values for phosphorus in the effluent in Europe are 1mg/L (**21**) and will depend on the local legislation. For example, countries bordering the Baltic Sea, designated as a sensitive area, have to cope with more stringent discharge limits for phosphorus (and nitrogen) to control eutrophication (**23**).

*Table 8.2: Ranges for the compounds whose concentration differs between influent/effluent and non-digested sludge. The ranges presented are for influent and effluent. We believe that these concentrations generally represent the poorly-loaded streams that can be found before digestion.*

|  | Low | Typical | High | Reference |
|---|---|---|---|---|
| pH | 6.5 | 7.5 | 8.5 | 4, 8, 30, 40, 85 |
| P-PO$_4$ (mg P/L) | 0.1 | 5 | 15 | 4, 8, 30, 33, 38, 82, 85 |
| Mg$^{2+}$ (mg/L) | 1 | 15 | 60 | 4, 28, 38, 40, 67, 85 |
| Ca$^{2+}$ (mg/L) | 10 | 60 | 150 | 4, 28, 38, 40, 67, 85 |
| K$^+$ (mg/L) | 10 | 20 | 35 | 4, 6, 38, 67, 82, 85 |
| N-NH$_4^+$ (mg N/L) | 10 | 35 | 75 | 8, 30, 33, 38, 70, 82 |
| Alkalinity (mg/L CaCO$_3$) | 50 | 200 | 550 | 4, 8, 30, 82, 85, |
| HCO$_3^-$ (mg/L) | 20 | 90 | 350 | From Alkalinity and VFA |
| VFA (mg/L HAc) | 10 | 30 | 120 | 8, 13, 30, 67 |

The concentration of magnesium in the influent is greatly influenced by the presence of seawater (up to 350 mg/L according to (**46, 88, 90**) while potassium is mainly influenced by the presence of industrial wastewater (up to 3000 mg/L according to **6**). Similarly to calcium (**67, 85**), magnesium and potassium usually go untreated from the influent to the effluent. A small decrease in their concentration can be sometimes observed (**67, 85**), possibly due to their accumulation by Phosphate Accumulating Organisms (PAO's) as counter ion for the negatively charged poly-phosphates (**34**). We expect this decrease to be more important for WWTPs using EBPR, but no full-scale experimental data were found to confirm it.

NH$_4^+$ is gradually oxidized to NO$_2^-$ and NO$_3^-$, consuming 7.14g of alkalinity per gram of N oxidized under aerobic conditions. In the later anoxic conditions, NO$_3^-$ is reduced to N$_2$O and then release as gaseous N$_2$, producing 3.57g of alkalinity per gram of N reduced (**43**). Alkalinity represents the internal pH buffer of a system and is mainly influenced by HCO$_3^-$, NH$_4^+$, PO$_4^{3-}$ and VFA concentrations in a WWTP (**8**). During the oxidation of the biodegradable organic matter in activated sludge systems, 1.375kg of CO$_2$ is produced per kg of Biological Oxygen Demand (BOD) (**17**). The effect of this large CO$_2$ release on the alkalinity does not appear to be important: desorption predominates in weakly alkaline solution (like wastewater), meaning that CO$_2$ is emitted in the air and does not significantly influence the pH (**45**). As soon as anaerobic conditions are present, fermentation can occur, and significant release of some compounds can be observed, mainly due to biological activity. Volatile Fatty Acids (VFA) concentration can strongly increase, especially during pre-fermentation, due to the decomposition of organic matter (**67**) that mainly takes place during the first two days of fermentation (**71, 91**). The VFA produced, composed of 50-80% of acetate (**7**), explains why the pH of thickened sludge is usually lower than in influent/effluent (**12, 62**).

Total alkalinity increases together with sludge fermentation, and some experimental data are available for this parameter, which is not the case for bicarbonate alkalinity. Since VFA and bicarbonate should be the two main compounds contributing to the total alkalinity, bicarbonate concentration was deducted from VFA concentration and total alkalinity. While a lower pH

**8**

can provoke a dissolution of some precipitates, the biological activity is the main mechanism for releasing $PO_4^{3-}$, $K^+$, and $Mg^{2+}$, following the hydrolysis of polyphosphates by the PAO's. The release of $K^+$ is usually more noticeable than the release of $Ca^{2+}$ and $Mg^{2+}$ since these latter can precipitate in sludge, for example, with phosphate (**67, 85**). The extend of the release of $PO_4^{3-}$, $K^+$, $Ca^{2+}$ and $Mg^{2+}$ are very dependent on the advancement of the fermentation (**8, 51, 62, 85**). This phenomenon should be even more significant for EBPR sludge than for CPR sludge since more $PO_4^{3-}$, $Mg^{2+}$ and $K^+$ were accumulated by PAO's in the first place in EBPR sludges (**12, 34, 67**).

*Table 8.3: Ranges for the compounds whose concentration differs between influent/effluent and non-digested sludge. The ranges presented are for sludge before digestion (primary and secondary). We believe that these concentrations generally represent the highly-loaded streams that can be found before digestion.*

|  | Low | Typical | High | Reference |
| --- | --- | --- | --- | --- |
| pH | 5.5 | 6.5 | 7.5 | 7, 50, 54, 62, 67, 85, 91, 92 |
| P-PO$_4$ (mg P/L) | 0.5 | 20 | 150 | 12, 50, 54, 62, 67, 71, 85, 86, 92 |
| $Mg^{2+}$ (mg/L) | 5 | 20 | 90 | 50, 54, 57, 62, 67, 85, 86 |
| $Ca^{2+}$ (mg/L) | 20 | 80 | 200 | 50, 54, 57, 62, 67, 85, 86 |
| $K^+$ (mg/L) | 10 | 50 | 120 | 50, 57, 67, 85, 86 |
| N-NH$_4^+$ (mg N/L) | 0 | 20/200* | 50/500* | 12, 50, 54, 57, 67, 71, 89, 92 |
| Alkalinity (mg/L CaCO$_3$) | 80 | 500 | 4000 | 7, 12, 89, 91 |
| HCO$_3^-$ (mg/L) | 20 | 200 | 2400 | From Alkalinity and VFA |
| VFA (mg/L HAc) | 50 | 250 | 2500 | 7, 12, 13, 50, 67, 71, 89 |

*Secondary sludge/primary sludge

No apparent differences were noticed in the concentration of $PO_4^{3-}$, $Mg^{2+}$, $Ca^{2+,}$ and $K^+$ between primary sludge and Waste Activated Sludge (WAS). We believe that those concentrations (except $Ca^{2+}$) will depend on the amount of phosphorus stored by PAO's, and therefore, on the WWTP design. On the other hand, the pH seems to be lower in primary sludge than in WAS (**92**), which is in line with the fact that primary sludge starts to ferment immediately into VFA. At the same time, VFA are produced slower in WAS and are then directly converted to $CH_4$. A more evident difference is observed for nitrogen since 5-15 times more soluble Nitrogen was measured in primary sludge than in WAS (**67, 92**). It seems logical considering that ammonia is removed during secondary treatment, producing a sludge poorer in soluble nitrogen. This observation is backed up by the study of (**57**), where the $NH_4^+$ concentration in 7 WAS ranged from 0 to 50, while it reached up to 480 mg/L in thickened primary sludge in some cases (**12**). It can be assumed that most of the soluble nitrogen in the primary sludge is $NH_4^+$ as it is the form under which it arrives at the WWTP (**38**). On the contrary, most of the soluble nitrogen in WAS could nitrate (**70, 90**) or dissolved organic nitrogen (**60**), as in the effluent, but nitrogen will be released from WAS as $NH_4^+$ on sludge hydrolysis.

### 8.3.3   Constant parameters in digested streams

From all the references gathered, the operational pH for digesters treating sludge from EBPR or CPR processes is similar (6.5 to 8), which bears the favorable range for methanogens growth

(6.5-7.2 according to (**5**))(Table 8.4). VFA levels cannot be too high in digester since they can inhibit digestion, from 800mg/L according to (**31**) or from 2000-4000mg/L according to (**5**). Concentration higher than the typical value of 100mg/L can be found for digesters working at short residence time or processing food wastes. The molar ratio VFA/Alkalinity should be <0.25 to maintain good stability of the digestion (**2, 61, 83, 87**) and is commonly around 0.1 in practice (**50, 75**). No clear difference between alkalinity in EBPR or CPR digestates was observed, even though it could decrease in the presence of metal salts due to precipitation with $OH^-$ for example (**52**). During digestion, $HCO_3^-$ is produced to balance the formation of $NH_4^+$, so an equimolar ratio can be assumed for these two ions as suggested by (**79**). This hypothesis is in line with the few cases where both ammonia and bicarbonates concentration were measured (**7, 10, 29, 56**). Therefore, the bicarbonate ranges were calculated from $NH_4^+$ concentration, for which many sources exist.

Chloride and sodium concentrations should not change during digestion since they are not converted during the process (**47, 67, 78, 85**) and not present in large amounts in the waste sludge. Concentrations of 3500-5000 mg/L for sodium and 6000 mg/L for chloride can inhibit digestion and should be avoided (**5**). High concentrations of these two ions can be found in the case of industrial wastewater treatment, intrusion (or use) of seawater, or control of $H_2S$ production by iron chloride salts addition (**14, 27**). Since data on chloride concentration in digesters are rarely reported in the literature (**2**), information was derived from the composition of dewatered sludge from Slibverwerking Noord-Brabant (SNB), which incinerates roughly 25% of all sewage sludge produced in the Netherlands.

*Table 8.4: Ranges for the compounds whose concentration is identical in CPR and EBPR digestates. The values are for the liquid fraction of the sludge for both CPR and EBPR digestates.*

| mg/L | Low | Typical | High | Reference |
|---|---|---|---|---|
| pH | 6.5 | 7 | 8 | 5, 50, 51, 56, 67, 83, 86, 93 |
| Total S (mg S/L) | 5 | 10 | 30 | 2, 14, 20, 25, 85, 86 |
| $Na^+$ (mg/L) | 40 | 100 | 400 | 2, 5, 75, 85, 86 |
| $Cl^-$ (mg/L) | 70 | 300 | 800 | 2 |
| $N-NH_4^+$ (mg N/L) | 200 | 700 | 1450 | 2, 7, 10, 29, 36, 41, 56, 75, 97 |
| Alkalinity ($mg/L\ CaCO_3$) | 1500 | 2500 | 4400 | 2, 7, 36, 50, 51, 56, 67 |
| $HCO_3^-$ (mg/L) | 850 | 3000 | 6300 | Calculated from $NH_4^+$ |
| VFA (mg/L) | 20 | 100 | 500 | 7, 50, 56, 67, 87 |

Sulphate is reduced to sulphide under anaerobic conditions and can then precipitate as $FeS_x$. Iron is sometimes added to digesters to control the $H_2S$ in biogas since $H_2S$ concentrations of 50-200mg/L can inhibit digestion and methanogenesis activity (**5, 32**), and $H_2S$ is detrimental for the biogas use. The concentration of soluble sulphide essentially depends on the quantity of iron present in the digested sludge (**85, 86**) and can be very low (0.1mg/L) if enough iron is present. It has been observed in several cases that 20-50% of the dissolved sulphur can still be sulphate in the digestate (**25, 26, 85**). This result is surprising since the sulphate reduction rate

is short compared to the residence time in an anaerobic digester (**68**). Such observations could be due to errors in the analyses.

Most of the soluble nitrogen (>99%) in the digestate is present as $NH_4^+$ (**49**). Concentrations above 1500 mg/L (reached with co-digestion) are usually avoided since they can inhibit the digestion process. One could expect that $NH_4^+$ concentration would be lower in digesters fed with sludge from EBPR plants due to the formation of struvite, but the pool of $NH_4^+$ is too big compared to $PO_4^{3-}$ and $Mg^{2+}$ to observe a significant difference (**9**).

## 8.3.4 Variable parameters in digested streams

In WWTPs using EBPR, phosphorus, magnesium, and potassium are accumulated by the PAO's in the waterline and later released in the digester (**36, 50, 84**). In digested sludges, phosphorus precipitates preferentially with iron to form vivianite (**85, 86**), then with magnesium to form struvite, and finally with calcium to form calcium phosphate (**66**). In digested sludge from CPR installations, a higher quantity of iron is generally available to bind the phosphate, explaining the higher concentration of soluble calcium and magnesium and the lower phosphate concentration. Concentrations down to 50 mg/L were observed when Mg was dosed in a digester processing EBPR sludge to form struvite (**16**).

*Table 8.5: Ranges for the compounds whose concentration differs between CPR and EBPR digestates. The values are for the liquid fraction of sludge from CPR installations. The data were essentially collected from installations using iron as a coagulant.*

|                    | Low | Typical | High | Reference        |
| ------------------ | --- | ------- | ---- | ---------------- |
| P-PO$_4$ (mg P/L)  | 1   | 30      | 80   | 36, 75, 85, 86   |
| Mg$^{2+}$ (mg/L)   | 5   | 20      | 40   | 2, 36, 75, 85, 86 |
| Ca$^{2+}$ (mg/L)   | 20  | 60      | 200  | 2, 36, 75, 85, 86 |
| K$^+$ (mg/L)       | 60  | 100     | 320  | 2, 36, 75, 85, 86 |

*Table 8.6: Ranges for the compounds whose concentration differs between CPR and EBPR digestates. The values are for the liquid fraction of sludge from EBPR installations.*

|                    | Low | Typical | High | Reference                           |
| ------------------ | --- | ------- | ---- | ----------------------------------- |
| P-PO$_4$ (mg P/L)  | 40  | 200     | 500  | 35, 36, 50, 51, 67, 75, 84, 85, 86  |
| Mg$^{2+}$ (mg/L)   | 1   | 10      | 25   | 16, 35, 50, 51, 67, 75, 84, 85, 86  |
| Ca$^{2+}$ (mg/L)   | 5   | 35      | 70   | 50, 51, 75, 84, 85, 86,             |
| K$^+$ (mg/L)       | 130 | 300     | 600  | 16, 36, 50, 51, 67, 75, 84, 85, 86  |

## 8.3.5 Data availability

To evaluate the relevance of the ranges proposed, it is crucial to evaluate the quality of the data. We believe that information from enough installations was collected in most cases to propose representative ranges of concentration. Additional weight was given to full ranges (opposed to single data points) since they have most likely been obtained by gathering data from multiple sources. Table 8.7 indicates that information from a minimum of 8 different installations (or less if ranges were available) was collected to consider the data satisfying.

*Table 8.7: Number of sources used to propose concentration ranges. On the left of the slash: number of installations from which data have been collected for the parameter. On the right of the slash: number of ranges found in the literature for the parameter. Asterisks indicate that the range could benefit from additional data, which is discussed in the following section.*

| Case/Range | Before digestion | | After digestion | |
|---|---|---|---|---|
| | Influent/Effluent | Mixed sludge | CPR | EBPR |
| $SO_4^{2-}/H_2S$ | 21/1 | | 11/0 | |
| $Na^+$ | 27/0 | | 13/0 | |
| $Cl^-$ | 7/2* | | 1/0* | |
| pH | 8/1 | 9/0 | 10/4 | |
| $P-PO_4^{3-}$ | 9/3 | 17/0 | 7/0 | 10/1 |
| $Mg^{2+}$ | 9/0 | 17/0 | 8/0 | 10/1 |
| $Ca^{2+}$ | 9/0 | 17/0 | 8/0 | 11/0 |
| $K^+$ | 11/1 | 16/0 | 8/0 | 14/0 |
| $N-NH_4^+$ | 6/3 | 19/0 | 26/0 | |
| Alkalinity | 7/2 | 4/0* | 7/2 | |
| $HCO_3^-$ | 0/0 * | 1/0 * | 4/0* | |
| VFA | 13/1* | 20/0 | 4/2 | |

While a satisfying amount of data could be found for most of the parameters, some were more challenging, and the quality of the data is assessed below:

- Chloride concentration is generally not well-measured. While the data were satisfying for influent (2 ranges) and effluent (7 installations), no data were found for mixed sludge. Even though chloride should not be affected by the different treatments, additional information could be interesting since chloride and sodium concentrations in streams before digestion represent 30-40% of the total Ionic strength (Figure 8.1). Only one value was found in the literature for chloride concentration in digestates, so an alternative method was used to propose a concentration range. The composition of 23 dewatered sludge before incineration was obtained from Slibverwerking Noord-Brabant (a company incinerating roughly 25% of the sludge in the Netherlands). Assuming that the chloride present in digested sludge is essentially soluble, a range for soluble chloride could be obtained. Chloride represents only ~5% of the ionic strength of digested streams (Figure 8.1), so the fact that the range proposed is only from installations in the Netherlands seems acceptable.
- While VFA data are available for influent wastewater, no information was found for effluents. Since VFAs are readily biodegradable BOD, they are oxidized in aerated sections and are poorly concentrated in the effluent. Most of the data collected for non-digested sludge were for thickened primary sludges containing very high VFA concentrations. On the contrary, little data was available on VFA production from WAS. Therefore, the range deducted from the literature review (150/500/3500) was lowered to 50/250/2500 to be more representative of both primary sludges and WAS.

- Alkalinity data are generally not widely available in the literature. The range proposed for digestates seems reliable due to existing knowledge for digester stability, but the one given for mixed sludge should be taken with care due to scarce information. In general, the alkalinity should increase with sludge hydrolysis and ammonium release, so the range for mixed sludge should be an intermediate between influent/effluent and digestate.
- The concentration of $HCO_3^-$, or Partial Alkalinity is important since it strongly contributes to the ionic strength, up to 38% for digested streams (Figure 8.1). It is rarely measured (only four references found for digestates); therefore, it was estimated from $NH_4^+$ concentration assuming an equimolar mix as discussed in 8.3.3. $HCO_3^-$ concentration is even more rarely measured in non-digested streams, and therefore, had to be determined indirectly. It was deducted from the alkalinity due to VFA and the total alkalinity since VFA and bicarbonates should represent the major basic compounds in those streams. Even though the ranges proposed are in line with the few experimental data available, it should be taken with care since it was determined indirectly.

Since most of the available data were from installations in Europe and North America, the ranges proposed are regional. Since drinking water is the background of any wastewater, one could adjust the proposed ranges based on the drinking water composition of one's location while considering possible seawater and industrial wastewater contribution.

### 8.3.6 Determination of the ionic strength for the different sludge streams

From the composition of the different sludge liquid fractions, the ionic strength could be calculated. The pH was always considered to be typical for the determination of the ionic strength. The interdependencies of the different concentrations were not considered in order not to complicate the calculations. It means that to calculate the lowest limit of the ionic strength for a stream, all the concentrations from the "low range" of this stream were considered.

The ionic strength of a solution is defined with the Debye-Hückel formula (**76**):

$$IS = 0.5 * \sum_{i=1}^{n} C_i Z_i^2$$

Where:

- $IS$ is the ionic strength in mol/L
- $C_i$ is the concentration of the ion in mol/L
- $Z_i$ is the charge of the ion

Depending on the ionic strength of the ionic solution considered, the relation between activity coefficient and ionic strength will be different, as described in (**76**). For wastewater systems, in which the ionic strength should always be <0.5M, the approximation of Davies is always applicable and is expressed as:

$$Log\ (\gamma_i) = -A * Z_i^2 \left( \frac{\sqrt{IS}}{1 + \sqrt{IS}} - 0.2IS \right)$$

Where:

- $(\gamma_i)$ the activity coefficient of the ion considered
- $A = 1.82*10^6*(\varepsilon*T)$ with $\varepsilon$ being the dielectric constant and T the temperature. A is worth 0.5 in water at 25°C.

Following the information found in the literature and discussed above, $NH_4^+$ and $NO_3^-$ were considered the only soluble nitrogen compounds in the influent/primary sludge and the WAS, respectively. Similarly, $SO_4^{2-}$ was taken as the only sulphur compound in the influent, while $H_2S$ alone was considered in the digester. Lastly, VFA were considered to be acetate and phosphorus to be $HPO_4^{2-}$ (according to the pH).



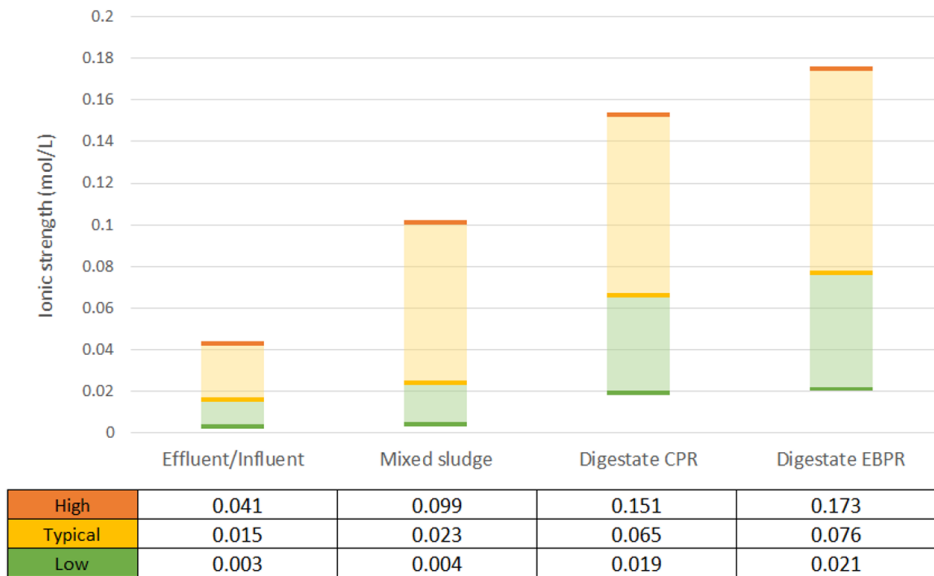| | Effluent/Influent | Mixed sludge | Digestate CPR | Digestate EBPR |
|---|---|---|---|---|
| High | 0.041 | 0.099 | 0.151 | 0.173 |
| Typical | 0.015 | 0.023 | 0.065 | 0.076 |
| Low | 0.003 | 0.004 | 0.019 | 0.021 |

*Figure 8.1: Calculated ionic strength for three ranges (low, typical, and high) for the four different streams of sludge studied. The average value for $NH_4^+$ in primary sludge and waste activated sludge was considered for the mixed sludge.*

Since ionic strength in sludge streams is rarely determined in literature, it is complicated to verify the ranges proposed in this study. In (**10**), the ionic strength of five digestates was calculated and ranged from 0.018 to 0.094M with an average of 0.054M. Overall, their results are consistent with the range proposed in this study. An ionic strength of 0.1M, consistent with our range, was given for an EBPR digestate in (**34**), but not calculation details were given.
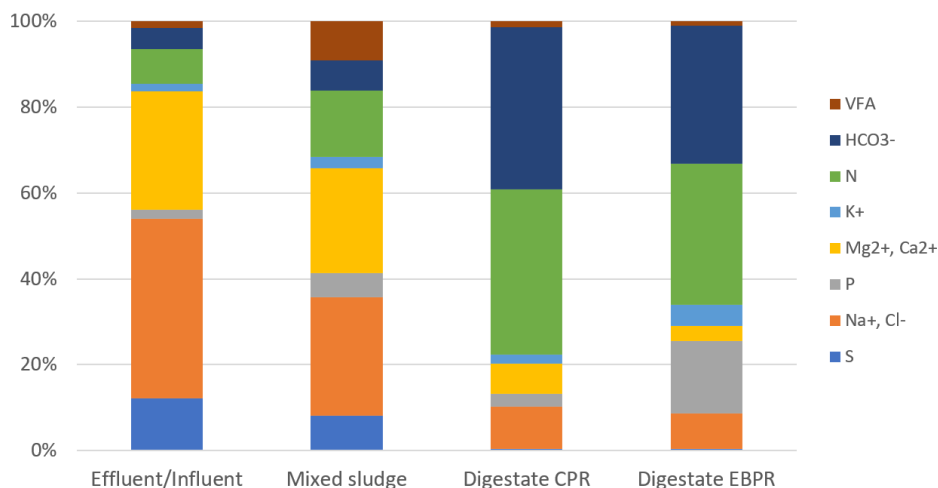
*Figure 8.2: Contribution of the major soluble compounds to the ionic strength of the four sludge streams evaluated. The values determined for the "typical" range were selected to do the calculation.*

The primary conclusion drawn from Figure 8.2 is that the main contributors to the ionic strength vary depending on the sludge stream studied. Salts whose concentration will not be too influenced by the treatment process ($Na^+$, $Cl^-$, $Mg^{2+}$, $Ca^{2+}$) represent up to 50-70% of the ionic strength for the streams before digestion. Their contribution progressively decreases with the increase of the $NH_4^+$ and $HCO_3^-$ concentrations, which will eventually account for around 60-80% of the ionic strength in digestate.

### 8.3.7  Importance of ionic strength in wastewater treatment

Various studies already highlighted the importance of ionic strength and its influence on several processes in wastewater treatment. Chemical precipitation processes are especially impacted by the ionic strength through its influence on the activity coefficients (**63**). The effect can be significant, even at typical ionic strength encountered in WWTP (**53**). It is the case for the crystallization of struvite (**10, 11, 18, 77**) and calcium phosphate (**39, 48, 73**). A higher ionic strength decreases the activity of the ions, thus increasing the solubility of minerals. Not considering ionic strength while studying chemical precipitation has led to discrepancies in the solubility measurements of struvite (**11**). Its consideration is also relevant to predict and remediate unwanted struvite precipitation in WWTP (**58**). Additionally, a study indicates that the purity of recovered struvite from animal manure was influenced by the ionic strength (**11**), which can have considerable importance for its further use.

Additionally, slight variations of ionic strength have a significant effect on the structural properties and, therefore, on sludge flocs' stability. The flocs are first stabilized by an increasing ionic strength (**55**) before being destabilized at IS>0.1M (**96**). High ionic strengths have a negative effect on the dewatering behavior of digested sludge (**15, 65**). Another critical process of wastewater treatment, nitrification/denitrification, is influenced by the salinity via the modification of the microbial community of the WAS (**44, 95**). The effect is positive at first and negative for IS>0.1M (**44**). Such high ionic strength should only be encountered in WAS systems dealing with industrial or very saline wastewater.

While chemical precipitation and enhanced biological removal are the two main routes for phosphorus removal, adsorption on iron oxides is a possible mechanism in some cases. It appears that ionic strength favorably influences this process in the range of (0.001-0.1M) (**1, 3**). The importance of ionic strength may even be higher for membrane-based treatments than for conventional treatment since it was found to impact the membrane fouling in MBR reactors (**81**). Lastly, ionic strength variation and absence of activity correction led to significant differences in predicted process performance evaluated with anaerobic digestion models (**63, 72**).

From the information collected in the literature, it is clear that ionic strength is an essential parameter in wastewater treatment since it is influencing several crucial processes. However, conclusions about the impact on ionic strength are sometimes drawn from only two values of ionic strength tested (**15, 37**). In other cases, the tested range is so wide ($0.00005 < IS < 0.05M$) that not enough information is gathered under conditions of actual sludge systems (**55, 96**). Moreover, the values chosen for ionic strength to study its influence are not always adequate. For example, ionic strength ranges from 0.01 to 0.4M in (**73**) and is fixed at 0.15M in (**42**), while real wastewater would typically have an ionic strength ten times lower (Figure 8.1).

Similarly, values ranging from 0.09 to 0.3M for digester influent were used to model anaerobic digestion (**72**). In comparison, the ionic strength for undigested sludge was evaluated to be 0.1M at the highest (Figure 8.1). Some of these problems could be solved if the studies would be based on actual sludge/wastewater sample measurements, which is not always done (**15, 55, 65, 72, 73**). Alternatively, the ionic strength has been derived from the conductivity in some studies (**24, 77, 96**). However, the linear coefficient linking conductivity and ionic strength greatly depends on the type of stream studied as discussed in (**10**), so extreme care should be taken while using this approximation.

**8**

## 8.4.  Conclusion

The ionic composition of the liquid in the different sludge streams of a WWTP largely depends on the influent wastewater and the WWTP process scheme. Three ranges of concentration were proposed for the main constituents of influent/effluent, undigested sludge, and anaerobically digested chemical or biological phosphate removal sludge from an extensive literature review. From these data, the ionic strength of the different sludge streams was calculated. This study allows the reader to quickly estimate the ionic strength based on the concentration of the compounds influencing it the most. Reviewing numerous studies showed that ionic strength is a crucial parameter since it impacts important wastewater treatment processes. Nevertheless, the range of ionic strength used in the literature studies is rarely motivated and not always adequate, which can weaken the conclusion.

# Reference

1. Ajmal, Z., Muhmood, A., Usman, M., Kizito, S., Lu, J., Dong, R., Wu, S. (2018). Phosphate removal from aqueous solution using iron oxides: Adsorption, desorption and regeneration characteristics. *Journal of Colloid and Interface Science*, 528, 145–155. doi:10.1016/j.jcis.2018.05.084.

2. Akhiar, A. (2017). Characterization of liquid fraction of digestates after solid-liquid separation from anaerobic co-digestion plants. *Chemical and Process Engineering.* Université Montpellier.

3. Antelo, J., Avena, M., Fiol, S., López, R., & Arce, F. (2005). Effects of pH and ionic strength on the adsorption of phosphate and arsenate at the goethite–water interface. *Journal of Colloid and Interface Science*, 285(2), 476–486. doi:10.1016/j.jcis.2004.12.032.

4. Andersen, C. B., Lewis, G. P., Hart, M., Pugh, J. (2014). The impact of wastewater treatment effluent on the biogeochemistry of the Enoree River, South Carolina, during drought conditions. *Water Air and Soil Pollution*, 225 (5), 1–21. doi:10.1007/s11270-014-1955-4.

5. Appels, L., Baeyens, J., Degrève, J., & Dewil, R. (2008). Principles and potential of the anaerobic digestion of waste-activated sludge. *Progress in Energy and Combustion Science*, 34(6), 755–781. doi:10.1016/j.pecs.2008.06.002.

6. Arienzo, M., Christen, E. W., Quayle, W., Kumar, A. (2009). A review of the fate of potassium in the soil-plant system after land application of wastewaters. *Journal of Hazardous Materials,* 164 (2-3), 415–422. doi:10.1016/j.jhazmat.2008.08.095

7. Astals, S., Venegas, C., Peces, M., Jofre, J., Lucena, F., Mata-Alvarez, J. (2012). Balancing hygienization and anaerobic digestion of raw sewage sludge. *Water Research*, 46(19), 6218–6227. doi:10.1016/j.watres.2012.07.035.

8. Barajas, M. G., Escalas, A., Mujeriego, R. (2002). Fermentation of a low VFA wastewater in an activated primary tank. *Water SA*, 28(1), 89. doi:10.4314/wsa.v28i1.4872.

9. Bergmans, B. J. C., Veltman, A. M., van Loosdrecht, M. C. M., van Lier, J. B., Rietveld, L. C. (2013). Struvite formation for enhanced dewaterability of digested wastewater sludge. *Environmental Technology*, 35(5), 549–555. doi:10.1080/09593330.2013.837081.

10. Bhuiyan, M. I. H., Mavinic, D. S., & Beckie, R. D. (2009). Determination of temperature dependence of electrical conductivity and its relationship with ionic strength of anaerobic digester supernatant, for struvite formation. *Journal of Environmental Engineering*, 135(11), 1221–1226. doi:10.1061/(asce)0733-9372(2009)135:11(1221).

11. Bhuiyan, M. I. H., Mavinic, D. S., & Beckie, R. D. (2007). A solubility and thermodynamic study of struvite. *Environmental Technology*, 28(9), 1015–1026. doi:10.1080/09593332808618857.

12. Bouzas, A., Gabaldón, C., Marzal, P., Penya-roja, J. M., Seco, A. (2002). Fermentation of Municipal Primary Sludge: Effect of Srt and Solids Concentration on Volatile Fatty Acid Production. *Environmental Technology*, 23(8), 863–875. doi:10.1080/09593332308618359.

13. Buchauer, K. (1998). A comparison of two simple titration procedures to determine volatile fatty acids in influents to waste-water and sludge treatment processes. *Water SA*, 24, 49-56.

14. Charles, W., Cord-Ruwisch, R., Ho, G., Costa, M., & Spencer, P. (2006). Solutions to a combined problem of excessive hydrogen sulfide in biogas and struvite scaling. *Water Science and Technology*, 53(6), 203–211. doi:10.2166/wst.2006.198.

15. Curvers, D., Usher, S. P., Kilcullen, A. R., Scales, P. J., Saveyn, H., Van der Meeren, P. (2009). The influence of ionic strength and osmotic pressure on the dewatering behaviour of sewage sludge. *Chemical Engineering Science*, 64(10), 2448–2454. doi:10.1016/j.ces.2009.01.043.

16. DeBarbadillo, C. (2016). Evaluation of performance and greenhouse gas emissions for plants achieving low phosphorus effluents. *Werf Research Report Series; IWA Publishing*.

17. Denkert, R., Schulte, P. (2010). Aufstockung der Säurekapazität und Einstellung des KalkKohlensäure-Gleichgewichtes durch Dosierung von alkalischen Additiven in die biologische Stufe einer Kläranlage

18. Desmidt, E., Ghyselbrecht, K., Monballiu, A., Rabaey, K., Verstraete, W., Meesschaert, B. D. (2013). Factors influencing urease driven struvite precipitation. *Separation and Purification Technology*, 110, 150–157. doi:10.1016/j.seppur.2013.03.010.

19. Dewil, R., Baeyens, J., Roels, J., & Steene, B. V. D. (2008). Distribution of sulphur compounds in sewage sludge treatment. *Environmental engineering science*, 25(6), 879–886. doi:10.1089/ees.2007.0143.

20. Du, W., Parker, W. (2013). Characterization of sulfur in raw and anaerobically digested municipal wastewater treatment sludges. *Water Environment Research,* 85 (2), 124–132. doi:10.2175/106143012x13407275694671.

21.European Commission (1991). Council Directive 91/271/EEC of 21 May 1991 concerning urban waste-water treatment.

22. European commission (2017). Ninth Report on the implementation status and the programs for implementation (as required by Article 17) of Council Directive 91/271/EEC concerning urban waste water treatment.

23. European Commission (2020). 10th Technical assessment on the Urban Waste Water Treatment Directive (UWWTD) implementation, European review and national situation.

24. Fattah, K.P. (2012). Assessing Struvite Formation Potential at Wastewater Treatment Plants. *International Journal of Environmental Science and Development,* 3 (6), 548-552. doi:10.7763/IJESD.2012.V3.284.

25. Fisher, R. M., Alvarez-Gaitan, J. P., Stuetz, R. M., Moore, S. J. (2017). Sulfur flows and biosolids processing: Using Material Flux Analysis (MFA) principles at wastewater treatment plants. *Journal of Environmental Management*, 198, 153–162. doi:10.1016/j.jenvman.2017.04.056.

26. Flores-Alsina, X., Solon, K., Kazadi Mbamba, C., Tait, S., Gernaey, K. V., Jeppsson, U., Batstone, D. J. (2016). Modeling phosphorus (P), sulfur (S) and iron (Fe) interactions for dynamic simulations of anaerobic digestion processes. *Water Research*, 95, 370–382. doi:10.1016/j.watres.2016.03.012.

27. Ge, H., Zhang, L., Batstone, D. J., Keller, J., & Yuan, Z. (2013). Impact of iron salt dosage to sewers on downstream anaerobic sludge digesters: sulfide control and methane production. *Journal of Environmental Engineering*, 139(4), 594–601. doi:10.1061/(asce)ee.1943-7870.0000650.

28. Genz, A., Kornmüller, A., Jekel, M. (2004). Advanced phosphorus removal from membrane filtrates by adsorption on activated aluminium oxide and granulated ferric hydroxide. *Water Research*, 38 (16), 3523–3530. doi:10.1016/j.watres.2004.06.006.

29. Hellinga, C., Schellen, A. A. J. C., Mulder, J. W., van Loosdrecht, M. C. M., Heijnen, J. J. (1998). The Sharon process: an innovative method for nitrogen removal from ammonium-rich wastewater. *Water Science and Technology,* 37 (9), 135–142. doi:10.2166/wst.1998.0350.

30. Henze, M., van Loosdrecht, M. C. M., Ekama, G., Brdjanovic, D. (2008). Biological wastewater treatment: principles, modeling and design. doi:10.2166/9781780408613.

31. Hill, D.T., Bolte, J.P. (1987). Using volatile fatty acid relationships to predict anaerobic digester failure. *Transactions of the ASAE*, 30(2), 0502–0508. doi:10.13031/2013.31978.

32. Hulshoff Pol, L. W., Lens, P. N. L., Stams, A. J. M., Lettinga, G. (1998). Anaerobic treatment of sulphate-rich wastewaters. *Biodegradation*, 9(3/4), 213–224. doi:10.1023/a:1008307929134

33. Hvitved-Jacobsen, T., Vollertsen, J., Nielsen, A. H. (2013). Sewer processes: microbial and chemical process engineering of sewer networks, 2nd edition, CRC Press: Boca Raton.

34. Jardin, N., Pöpel, H. J. (1994). Phosphate release of sludges from enhanced biological p-removal during digestion. *Water Science and Technology*, 30(6), 281–292. doi:10.2166/wst.1994.0279.

35. Jeyanayagam, S., Hahn, T., Fergen, R., & Boltz, J. (2012). Nutrient recovery, an emerging component of a sustainable biosolids management program. *Proceedings of the Water Environment Federation*, (2), 1078–1088. doi:10.2175/193864712811693830.

36. Johansson, S., Ruscalleda, M., Saerens, B., & Colprim, J. (2018). Potassium recovery from centrate: taking advantage of autotrophic nitrogen removal for multi-nutrient recovery. *Journal of Chemical Technology & Biotechnology*. doi:10.1002/jctb.5828.

37. Kaseamchochoung, C., Lertsutthiwong, P., Phalakornkule, C. (2006). Influence of chitosan characteristics and environmental conditions on flocculation of anaerobic sludge. *Water Environment Research*, 78(11), 2210–2216. doi:10.2175/106143005x72830.

**8**

38. Kazadi Mbamba, C., Flores-Alsina, X., John Batstone, D., Tait, S. (2016). Validation of a plant-wide phosphorus modeling approach with minerals precipitation in a full-scale WWTP. *Water Research*, 100, 169–183. doi:10.1016/j.watres.2016.05.003.

39. Kezia, K., Lee, J., Zisu, B., Chen, G. Q., Gras, S. L., Kentish, S. E. (2017). Solubility of calcium phosphate in concentrated dairy effluent brines. *Journal of Agricultural and Food Chemistry*, 65(20), 4027–4034. doi:10.1021/acs.jafc.6b05792.

40. Kumar, P. S., Ejerssa, W. W., Wegener, C. C., Korving, L., Dugulan, A. I., Temmink, H., van Loosdrecht, M. C. M., Witkamp, G-J. (2018). Understanding and improving the reusability of phosphate adsorbents for wastewater effluent polishing. *Water Research*, 145, 365–374. doi:10.1016/j.watres.2018.08.040.

41. Lackner, S., Gilbert, E. M., Vlaeminck, S. E., Joss, A., Horn, H., van Loosdrecht, M. C. M. (2014). Full-scale partial nitritation/anammox experiences – An application survey. *Water Research*, 55, 292–303. doi:10.1016/j.watres.2014.02.032.

42. Lei, Y., Song, B., van der Weijden, R. D., Saakes, M., & Buisman, C. J. N. (2017). Electrochemical Induced Calcium Phosphate Precipitation: Importance of Local pH. *Environmental Science & Technology*, 51(19), 11156–11164. doi:10.1021/acs.est.7b03909.

43. Li, B., & Irvin, S. (2007). The comparison of alkalinity and ORP as indicators for nitrification and denitrification in a sequencing batch reactor (SBR). *Biochemical Engineering Journal*, 34(3), 248–255. doi:10.1016/j.bej.2006.12.020.

44. Li, X., Yuan, Y., Yuan, Y., Bi, Z., Liu, X., Huang, Y., … Xu, S. (2018). Effects of salinity on the denitrification efficiency and community structure of a combined partial nitration- anaerobic ammonium oxidation process. *Bioresource Technology*, 249, 550–556. doi:10.1016/j.biortech.2017.10.037.

45. Lijklema, L. (1971). Factors affecting pH change in alkaline wastewater treatment: II, Carbon dioxide production. *Water Research*, 5, 123-142.

46. Liu, X., Dai, J., Ng, T.-L., Chen, G. (2019). Evaluation of potential environmental benefits from seawater toilet flushing. *Water Research,* 162, 505–515. doi:10.1016/j.watres.2019.07.016.

47. Madison metropolitan sewer district. (2015). Chloride compliance study, Nine springs WWTP, Final report.

48. Mañas, A., Pocquet, M., Biscans, B., & Sperandio, M. (2012). Parameters influencing calcium phosphate precipitation in granular sludge sequencing batch reactor. *Chemical Engineering Science*, 77, 165–175. doi:10.1016/j.ces.2012.01.009.

49. Mantovani, M., Marazzi, F., Fornaroli, R., Bellucci, M., Ficara, E., Mezzanotte, V. (2020) Outdoor pilot-scale raceway as a microalgae-bacteria sidestream treatment in a WWTP. *Science of the Total Environment*, 710.

50. Marti, N., Bouzas, A., Seco, A., & Ferrer, J. (2008). Struvite precipitation assessment in anaerobic digestion processes. *Chemical Engineering Journal*, 141(1-3), 67–74. doi:10.1016/j.cej.2007.10.023.

51. Martí, N., Pastor, L., Bouzas, A., Ferrer, J., Seco, A. (2010). Phosphorus recovery by struvite crystallization in WWTPs: Influence of the sludge treatment line operation. *Water Research*, 44(7), 2371–2379. doi:10.1016/j.watres.2009.12.043.

52. Maurer, M., Boller, M. (1999). Modeling of phosphorus precipitation in wastewater treatment plants with enhanced biological phosphorus removal. *Water Science and Technology*, 39(1), 147–163. doi:10.2166/wst.1999.0033.

53. Millero, F. J., Schreiber, D. R. (1982). Use of the ion pairing model to estimate activity coefficients of the ionic components of natural waters. *American Journal of Science*, 282(9), 1508–1540. doi:10.2475/ajs.282.9.1508.

54. Mitani, Y., Sakai, Y., Mishina, F., & Ishiduka, S. (2003). Struvite recovery from wastewater having low phosphate concentration. *Journal of Water and Environment Technology*, 1(1), 13–18. doi:10.2965/jwet.2003.13.

55. Moghadam, M. A., Soheili, M., Esfahani, M. M. (2005). Effect of ionic strength on settling of activated sludge. *Iranian Journal of Environmental Health Science & Engineering*, 2, 1-5.

56. Moretto, G., Ardolino, F., Piasentin, A., Girotto, L., Cecchi, F. (2019). Integrated anaerobic codigestion system for the organic fraction of municipal solid waste and sewage sludge treatment: an Italian case study. *Journal of Chemical Technology & Biotechnology*. doi:10.1002/jctb.5993.

57. Novak, J. T., Park C. (2004). Chemical conditioning of sludge. Water Science and Technology: A Journal of the International Association on Water Pollution Research, 49 (10), 73–80.

**8**

58. Ohlinger, K. N., Young, T. M., Schroeder, E. D. (1998). Predicting struvite formation in digestion. *Water Research*, 32(12), 3607–3614. doi:10.1016/s0043-1354(98)00123-7.

59. Osman, O., Aina, O. D., & Ahmad, F. (2017). Chemical fingerprinting of saline water intrusion into sewage lines. *Water Science and Technology*, 76(8), 2044–2050. doi:10.2166/wst.2017.374.

60. Pagilla, K. R., Urgun-Demirtas, M., Czerwionka, K., & Makinia, J. (2008). Nitrogen speciation in wastewater treatment plant influents and effluents—the US and Polish case studies. *Water Science and Technology*, 57(10), 1511–1517. doi:10.2166/wst.2008.213.

61. Palacios-Ruiz, B., Méndez-Acosta, H. O., Alcaraz-González, V., González-Álvarez, V., & Pelayo-Ortiz, C. (2008). Regulation of volatile fatty acids and total alkalinity in anaerobic digesters. *IFAC Proceedings Volumes*, 41(2), 13611–13616. doi:10.3182/20080706-5-kr-1001.02305.

62. Pathak, B., Al-Omari, A., Smith, S., Passarelli, N., Suzuki, R., Khakar, S., DeBarbadillo, C. (2018). Vivianite occurrence and remediation techniques in biosolids pre-treatment process. *WEF Residuals and Biosolids Conference 2018*.

63. Patón, M., González-Cabaleiro, R., & Rodríguez, J. (2018). Activity corrections are required for accurate anaerobic digestion modeling. *Water Science and Technology*, 77(8), 2057–2067. doi:10.2166/wst.2018.119.

64. Qu, J., Wang, H., Wang, K., Yu, G., Ke, B., Yu, H.-Q., Ren, H., Zheng, X., Li, J., Li, W., Gao, S., Gong, H. (2019). Municipal wastewater treatment in China: Development history and future perspectives. *Frontiers of Environmental Science & Engineering*, 13(6). doi:10.1007/s11783-019-1172-x.

65. Rasmussen, H., Bruus, J. H., Keiding, K., Nielsen, P. H. (1994). Observations on dewaterability and physical, chemical and microbiological changes in anaerobically stored activated sludge from a nutrient removal plant. *Water Research*, 28(2), 417–425. doi:10.1016/0043-1354(94)90279-8.

66. van Rensburg, P., Musvoto, E., Wentzel, M., Ekama, G.(2003). Modeling multiple mineral precipitation in anaerobic digester liquor. *Water Research*, 37(13), 3087–3097. doi:10.1016/s0043-1354(03)00173-8.

67. Roldán, M., Bouzas, A., Seco, A., Mena, E., Mayor, Á., Barat, R. (2020). An integral approach to sludge handling in a WWTP operated for EBPR aiming phosphorus recovery: Simulation of alternatives, LCA and LCC analyses. *Water Research*, 115647. doi:10.1016/j.watres.2020.115647

68. Rubio-Rincón, F., Lopez-Vazquez, C., Welles, L., van den Brand, T., Abbas, B., van Loosdrecht, M., & Brdjanovic, D. (2017). Effects of electron acceptors on sulphate reduction activity in activated sludge processes. *Applied Microbiology and Biotechnology*, 101(15), 6229–6240. doi:10.1007/s00253-017-8340-3.

69. Rubio Rincon, F. J. (2017). Effect of sulphide on enhanced biological phosphorus removal. CRC Press / Balkema.

70. Sattayatewa, C., Pagilla, K., Sharp, R., Pitt, P. (2010). Fate of organic nitrogen in four biological nutrient removal wastewater treatment plants. *Water Environment Research*, 82(12), 2306–2315. doi:10.2175/106143010x12609736966324.

71. Soares, A., Kampas, P., Maillard, S., Wood, E., Brigg, J., Tillotson, M., Parsons, S., Cartmell, E. (2010). Comparison between disintegrated and fermented sewage sludge for production of a carbon source suitable for biological nutrient removal. *Journal of Hazardous Materials*, 175(1-3), 733–739. doi:10.1016/j.jhazmat.2009.10.070.

72. Solon, K., Flores-Alsina, X., Mbamba, C. K., Volcke, E. I. P., Tait, S., Batstone, D., Gernaey K.V., Jeppsson, U. (2015). Effects of ionic strength and ion pairing on (plant-wide) modeling of anaerobic digestion. *Water Research*, 70, 235–245. doi:10.1016/j.watres.2014.11.035.

73. Song, Y., Hahn, H. H., Hoffmann, E. (2002). Effects of solution conditions on the precipitation of phosphate for recovery. *Chemosphere*, 48(10), 1029–1034. doi:10.1016/s0045-6535(02)00183-2.

74. STOWA (2011). Zwafel in de RWZI Autotrofe denitrificatie en zwavelterugwinning als zuiveringstechniek voor RZWI's - een haalbaarheidsstudy.

75. STOWA (2016). De Invloed van kationen en beluchting op slibontwatering.

76. Stumm, W., Morgan, J. J. (2013). Aquatic Chemistry: Chemical Equilibria and Rates in Natural Waters, 3rd ed.

77. Tao, W., Fattah, K. P., Huchzermeier, M. P. (2016). Struvite recovery from anaerobically digested dairy manure: A review of application potential and hindrances. *Journal of Environmental Management*, 169, 46–57. doi:10.1016/j.jenvman.2015.12.006.

78. United States Environmental Protection Agency (EPA). (1975). Determination of incinerator operating conditions necessary for safe disposal of pesticides.

**8**

79. Volcke, E. I. P., Van Hulle, S. W. H., Donckels, B. M. R., van Loosdrecht, M. C. M., Vanrolleghem, P. A. (2005). Coupling the SHARON process with Anammox: Model-based scenario analysis with focus on operating costs. *Water Science and Technology*, 52(4), 107–115. doi:10.2166/wst.2005.0093.

80. de Vries, A., Veraart, J. A., de Vries, I., Oude Essink, G. H. P., Zwolsman, G. J., Creusen, R., & Buijtenhek, H. S. (2009). Vraag en aanbod van zoetwater in de Zuidwestelijke Delta: een verkenning. Samenvatting. *Utrecht: Kennis voor Klimaat, Programmabureau Kennis voor Klimaat*.

81. Wang, F., Zhang, M., Peng, W., He, Y., Lin, H., Chen, J., Honh, H., Wang, A., Yu, H. (2014). Effects of ionic strength on membrane fouling in a membrane bioreactor. *Bioresource Technology*, 156, 35–41. doi:10.1016/j.biortech.2014.01.014.

82. Wastewater characteristics and effluent quality parameters. Consulted last on 06/11/2020 at http://www.fao.org/3/t0551e/t0551e03.htm.

83. Water pollution control federation (1987). Anaerobic sludge digestion, Manual of Practice No. 16 (2nd edition), Techna Type, Inc., Alexandria, VA.

84. Wild, D., Kisliakova, A., Siegrist, H. (1997). Prediction of recycle phosphorus loads from anaerobic digestion. *Water Research*, 31(9), 2300–2308. doi:10.1016/s0043-1354(97)00059-6.

85. Wilfert, P. K., Mandalidis, A., Dugulan, A. I., Goubitz, K., Korving, L., Temmink, H., Witkamp, G J., van Loosdrecht, M. C. M. (2016). Vivianite as an important iron phosphate precipitate in sewage treatment plants. *Water Research*, 104, 449–460. doi:10.1016/j.watres.2016.08.032.

86. Wilfert, P., Korving, L., Dugulan, I., Goubitz K., Witkamp, G. J., van Loosdrecht M. C. M. (2018). Vivianite as the main phosphate mineral in digested sewage sludge and its role for phosphate recovery. *Water Research*, 144, 312-321. doi:10.1016/j.watres.2018.07.020.

87. Wisconsin department of natural resources bureau of science services. (1992) *Advanced Anaerobic Digestion Study Guide*.

88. Wright, J., Colling, A. (1995). Salinity in the oceans; seawater: its composition, properties and behaviour (second edition), 29-38.

89. Xu, J., Li, X., Gan, L., & Li, X. (2018). Fermentation liquor of $CaO_2$ treated chemically enhanced primary sedimentation (CEPS) sludge for bioplastic biosynthesis. *Science of The Total Environment*, 644, 547–555. doi:10.1016/j.scitotenv.2018.06.392.

90. Yu, S. M., Leung, W. Y., Ho, K. M., Greenfield, P. F., Eckenfelder, W. W. (2002). The impact of sea water flushing on biological nitrification-denitrification activated sludge sewage treatment process. *Water Science and Technology*, 46 (11-12), 209–216. doi:10.2166/wst.2002.0740.

91. Yuan, Q., Sparling, R., & Oleszkiewicz, J. A. (2011). VFA generation from waste activated sludge: Effect of temperature and mixing. *Chemosphere*, 82(4), 603–607. doi:10.1016/j.chemosphere.2010.10.084 .

92. Yuan, Q., Baranowski, M., & Oleszkiewicz, J. A. (2010). Effect of sludge type on the fermentation products. *Chemosphere*, 80(4), 445–449. doi:10.1016/j.chemosphere.2010.04.026.

93. Zhang, C., Su, H., Baeyens, J., & Tan, T. (2014). Reviewing the anaerobic digestion of food waste for biogas production. *Renewable and Sustainable Energy Reviews*, 38, 383–392. doi:10.1016/j.rser.2014.05.038.

94. Zhao, H. (2004). Analysis of the performance of an anaerobic digestion system at the Regina wastewater treatment plant. *Bioresource Technology*, 95(3), 301–307. doi:10.1016/j.biortech.2004.02.023.

95. Zhu, I. X., Liu, J. R. (2017). Introductory chapter: effects of salinity on biological nitrate removal from industrial wastewater. Nitrification and denitrification. doi:10.5772/intechopen.69438.

96. Zita, A. and Hermansson, M. (1994). Effects of ionic strength on bacterial adhesion and stability of flocs in a wastewater activated sludge system. *Applied and Environmental Microbiology*, 60 (9), 3041-3048.

97. Zuliani, L., Frison, N., Jelic, A., Fatone, F., Bolzonella, D., Ballottari, M. (2016). Microalgae cultivation on anaerobic digestate of municipal wastewater, sewage sludge and agro-waste. *International Journal of Molecular Sciences*, 17(10), 1692. doi:10.3390/ijms17101692.

**8**

# Chapter 9: Discussion and outlook
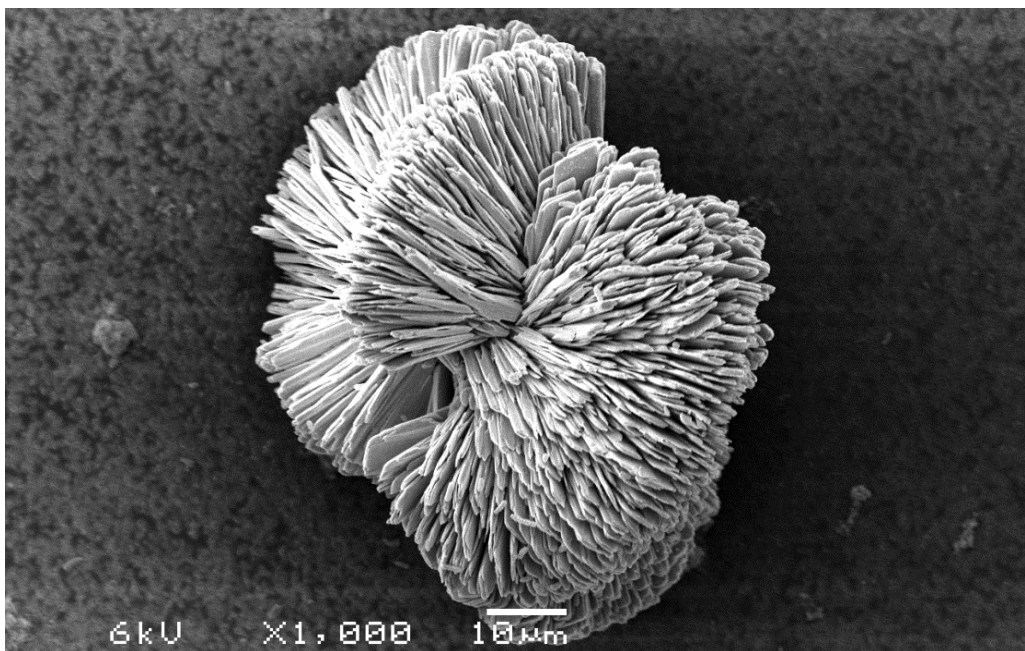
## 9.1.    Conclusion

### 9.1.1.   Main conclusion of this thesis

The main objective of this thesis was to assess the role of vivianite in WWTPs, and see if the knowledge gathered in this field could be applied in other domains. Vivianite recovery from sewage sludge consists of two major steps: the maximization of the quantity of phosphorus present as vivianite (and thus becoming recoverable) and the separation of the vivianite.

The information discussed in Chapter 3 showed that increasing the iron dosing in a WWTP was an efficient way to increase the quantity of phosphorus present as vivianite. Comparing the results of this study to previous results from our group revealed that before any vivianite could form in digested sludge, one mole of iron was "lost" per mole of sulphur. It signifies that iron needs to be dosed more than stoichiometrically to convert a maximum of phosphorus as vivianite. Interestingly, the iron binding to sulphur is not truly lost since it would most likely be dosed anyway to the sludge digester to control the $H_2S$ content of the biogas. Once the sulphide has been consumed, iron seems to be used preferentially to form vivianite without forming other Fe-compounds. A WWTP digester can efficiently be converted into a vivianite formation unit by applying a molar Fe/P ratio of around 1.5.

The second chapter of this thesis was dedicated to the proof of principle of the magnetic separation of vivianite using a technology borrowed from the mining industry. It was shown to be feasible with a lab-scale model that was not optimized. Follow-up testing at bench-scale and especially pilot-scale (Chapter 4) indicated that the separation was scalable and performed better at a larger scale due to the pulsating of the slurry and the use of rods matrices, giving hopes for further scaling-up of the technology. Around 80% of the vivianite could be recovered at pilot-scale after two additional recirculations of the digested sludge through the separator, corresponding to the recovery of more than 60% of the phosphorus present in the influent of the WWTP. For a full-scale application, the use of three magnetic separators in series could be imagined but would result in higher capital investment. One key message to take home from this thesis is that a multidisciplinary approach (wastewater treatment + mineral processing) can bring unforeseen solutions.

However, the importance of vivianite in WWTP is not limited to the digested sludge. Crystals of vivianite have already been noticed in surplus sludge or after the anaerobic storage of waste activated sludge. We discussed in Chapter 5 that 2-4 days of residence under anaerobic conditions for an undigested sludge would be enough to form a significant quantity of vivianite. It appeared that the iron reduction was strongly correlated to vivianite formation. As soon as the iron reduction was completed (2-4 days), almost all the Fe(II) present in the sludge was vivianite. Like in digested sludge, not all the iron was present as vivianite, potentially explained by the preferential formation of $FeS_x$. This chapter showed that an anaerobic sludge digester might not be necessary to recover phosphorus as vivianite, increasing the market potential for this technology. For example, 25% of the sludge in the Netherlands was not digested in 2018 (Unie van Waterschappen 2018).

Not everything about vivianite is positive. The ability of vivianite to form a hard scale on the surfaces of different units in a WWTP was investigated in Chapter 6. This research revealed

that vivianite scaling could be very problematic and involve expensive maintenance. Besides, it appears that vivianite scaling can be mistakenly attributed to the widely reported struvite scaling and that it is occurring more often than the lack of reported cases in the literature suggested. Investigating the different units where vivianite scaling could form, and their associated formation mechanisms allowed us to propose prevention strategies and helped develop our knowledge of vivianite occurrence in WWPT. While some operators/plant managers may be afraid of dosing extra iron in their plant due to the formation of vivianite scaling, it should not be the case. The most important message of this study was that vivianite scaling does not come from an excess of iron in the system but rather that the way/place of dosing needs to be optimized.

As discussed repeatedly in this thesis, the current way phosphorus is obtained is not optimal and secondary sources of phosphorus need to be exploited. While sewage sludge was the primary source studied in this thesis, animal manure represents an important phosphorus reservoir (four times more phosphorus in manure than in sewage in the Netherlands). In addition, local phosphorus surpluses are a big problem in regions with intensive farming like the Po Delta in Italy, the United Kingdom, and the Netherlands. The possibility of forming vivianite in pig manure and later recovering it magnetically was investigated in Chapter 7. This study showed that while formation and recovery were possible, the quantity of iron necessary to form vivianite was twice higher than in digested sewage sludge. It seems that the iron behaves differently in these two matrices, and we suggest that the interactions between organic matter and iron played an important role. More research will be carried out in a new Ph.D. position.

### 9.1.2. Quantification of vivianite

To get a good understanding of vivianite formation in digested sludge and evaluate its separation efficiency, reliable analytical methods to quantify its presence are necessary. Mössbauer spectroscopy, a technique able to quantify iron compounds, was used by Philipp Wilfert to quantify vivianite in sludge during his Ph.D. This technique was the best available but necessitated further developments (discussed below) to be more reliable. The rarity of this technique and its high price also called for developing an alternative quantification strategy. Four methods were proposed to quantify vivianite during my project and are discussed below with their pros and cons.

#### *9.1.2.1. Thermo-gravimetry*

At the start of my research, it was noticed that vivianite loses around 30% of its weight when heated up, as seen in Figure 9.1. Using Thermo-Gravimetry (TG), Differential Calorimetry Scanning (DSC) equipped with a Mass Spectrometer (MS) revealed that most of the weight losses were due to water evaporation. The 30% of weight losses correspond to the evaporation of the eight crystal water molecules present in vivianite. Other measurements showed that vivianite could lose crystal water already at 40-50°C. Therefore, all the samples were dried at ambient temperature in this thesis to avoid the deformation of the vivianite structure.
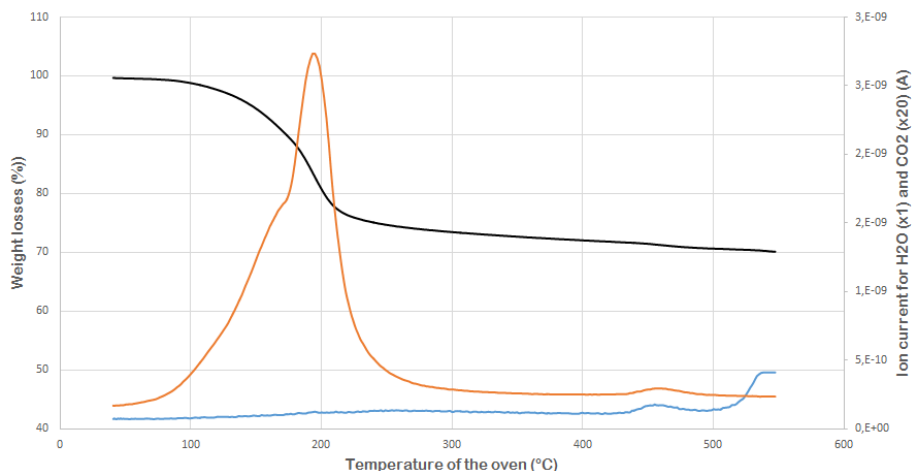
*Figure 9.1: TG-DSC-MS curve for a sample of scaling harvested in Venlo in 2017, and mainly composed of vivianite. Primary axis: the black curve corresponds to the weight losses. Secondary axis: the orange and blue curves correspond to the release of $H_2O$ and $CO_2$, respectively.*

A quantification method of vivianite was sought to be developed based on the weight losses of crystal water in vivianite. Figure 9.1 showed that vivianite loses the majority of its crystal water molecules before 200°C. Therefore, heating a sludge sample containing vivianite would lead to a weight drop in the same temperature range, partly due to the evaporation of the crystal water molecules of vivianite. The vivianite content could theoretically be calculated based on the intensity of the drop. However, some setbacks were encountered in the development of this quantification approach.

Since the sludge samples containing vivianite had to be dried at ambient temperature, it was very likely that some interstitial water, not part of the vivianite structure, remained in the samples. This water would evaporate upon drying of the samples in the same range as the crystal water of vivianite. Besides, some organic compounds present in sludge could also disintegrate in the same temperature range as the crystal water of vivianite. Some preliminary tests on a standard addition method based on TG-DSC-MS were carried out, but this quantification strategy needs to be further investigated.

Separate lesson: One thing to remember from these experiments is that the determination of Volatile Solid and Total Solids can be biased if the sludge contains a high amount of vivianite. Indeed, a part of the crystal water will evaporate in the range used to determine TS (<105°C), leading to underestimating the solid content of the sludge. Similarly, some crystal water will evaporate in the range used for VS measurement (105-550°C) and will cause an overestimation of the organic content of the sample. This point needs to be taken into account when dealing with sludge bearing high iron content.

### 9.1.2.2. XRD

X-Ray Diffraction (XRD) coupled with the standard addition of vivianite has been used in Wilfert et al. 2018 and Salehin et al. 2020 to quantify vivianite in different sewage sludges. In the first study, the results from XRD were compared with Mössbauer spectroscopy results

and revealed that XRD seemed to underestimate vivianite in undigested sludges and overestimate it in digested sludges. This different behavior could be explained by the fact that vivianite formed before and during digestion may differ. The vivianite present before digestion may not be fully crystallized yet or be present as smaller particles, which would affect the measurements. Also, the vivianite used for the standard addition must be similar to the one found in sludge. The presence of some overlapping peaks of vivianite with quartz (commonly found in sludge) can also be problematic. Another point of attention is that vivianite can easily be oxidized upon oxygen and light exposure (Čermáková et al. 2013, McCammon and Burns 1980). During oxidation, some ferrous ions in the structure are transformed into ferric iron, while a proton is removed from the structure to balance the charge. It causes a destabilization of the structure, progressively transforming vivianite into metavivianite and the more XRD-amorphous santabarbaraite. Since XRD only detects crystalline phases, the presence of oxidized vivianite may be detrimental to the quantification using this strategy.

### 9.1.2.3. Sequential extraction

A common strategy for phosphorus speciation in soil, sediments, and sludge is the sequential extraction with solvents of increasing strengths. This strategy offers a lot of flexibility compared to the others methods mentioned in this section and can be used on-site. It was not used on sewage sludge during this research but was previously used in the literature. Wilfert et al. 2016 discussed that the quantification of iron phosphates by extraction with water, pyrophosphate, sulphide, and ammonium oxalate was less accurate than with Mössbauer spectroscopy and XRD. Roussel and Carliell-Marquet 2016 claimed that vivianite could be quantified with sequential extraction targeting iron rather than phosphorus compounds. Sequential extractions targeting phosphorus species were employed in this research to follow vivianite formation in animal manure. The results of the extractions were not satisfying, and several points will need to be taken into account if a use with sludge is sought. Firstly, the quantity of solvent used needs to be in significant excess compared to the compounds to extract. With pig manure, a big part of the phosphorus present in bioavailable fraction (extracted with $HCO_3^-$) was reported to the following solvent, $OH^-$, due to a low solvent/manure ratio (Figure 9.2). This also caused an important underestimation of the vivianite content in the pig manure samples that were amended with iron.

During the extraction of with NaOH, it was also noticed that phosphorus was released at first until 6h and later reprecipitated (the species was not identified). This underlines that ligands (like EDTA) are essential to bind the released ions and prevent them from interacting with each other (Turner and Leytem 2004). While this method would be the fastest and the cheapest alternative, it may be the one that requires the most development to be effective. The proper substrate/solvent ratio and the use of ligands should be kept in mind for further development of this strategy for vivianite quantification. In addition, the parallel iron speciation (with sequential extraction) and cross-checking of the results with Mössbauer spectroscopy seem essential.
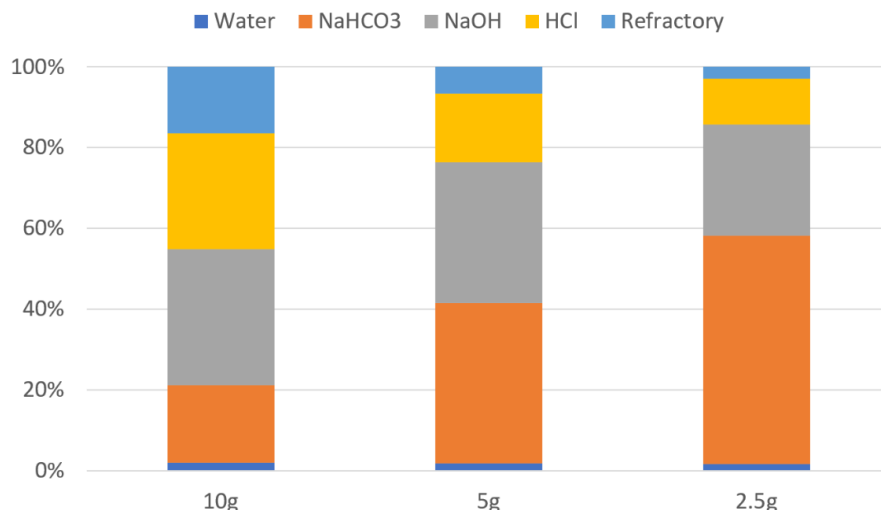
*Figure 9.2: Sequential extraction of pig manure for 30mL of each solvent. The phosphorus distribution in the different solvents should be identical no matter the quantity of pig manure used if the extraction worked properly. However, it can be seen that the distribution changed with the pig manure/solvent ratio.*

### 9.1.2.4. Mössbauer spectroscopy

Since 2015 and the first research on vivianite in sewage sludge, Mössbauer spectroscopy was the best technique to quantify vivianite. The biggest advantage of Mössbauer spectroscopy is that it targets iron-based compounds only, which significantly reduces the number of possible species that can interfere. Also, this technique can easily differentiate species based on their oxidation state and analyze both crystalline and amorphous compounds. However, this technique is rare (only one installation in the Netherlands), and the interest in vivianite is relatively new. Therefore, the Mössbauer database on iron compounds and vivianite in sludge (and manure) is limited. Consequently, best practices to quantify vivianite in these systems had to be developed in this project.

A crystal unit of vivianite bears three locations for iron: one octahedral site called site A and two equivalent octahedral sites called B. The Mössbauer spectroscopy spectrum of vivianite is characterized by two doublets for these two sites. The doublet B presents a spectral contribution twice bigger than the doublet A since it represents the signal for two iron atoms. The parameters for these two doublets are easy to identify, and the iron present in those sites can then be quantified with accuracy (Isomer Shift (IS) = 1.2±0.1 mm/s, Quadrupole Splitting (QS) = 2.4±0.1 mm/s) and Site B (IS = 1.25±0.1 mm/s, QS = 3.0±0.1 mm/s) (McCammon and Burns 1980, Rouzies and Millet 1993, Nembrini et al. 1983). However, whenever vivianite oxidizes, some of the $Fe^{2+}$ present in those sites will oxidize to $Fe^{3+}$, characterized by a doublet with a lower IS. Unfortunately, this new doublet will overlap with the contribution from several iron hydroxides/oxides and FeS species that can be present in sludge, making the quantification of the oxidized fraction of vivianite challenging. The study of the samples at a lower temperature (down to 4.2K) allows the different contributions of vivianite to split, potentially making the characterization easier. Unfortunately, the complexity

of the spectra obtained (several series of doublets and sextuplets) makes it even more challenging to work at a lower temperature. Based on this information, the strategy to quantify vivianite with Mössbauer spectroscopy in sludge was improved three times over the four years of my Ph.D.

The first approach (used in Chapter 2) was to protect the samples as much as possible from oxygen to minimize the share of oxidized iron and assume that most of the vivianite is unoxidized. This approach presents two problems. Firstly, the sample preparation was very tenuous, and practical mistakes are common; the drying and the encapsulation of the samples in the anaerobic chamber are difficult. If one sample presents an oxygen leakage, which happened several times during this project, the sample would be compromised. However, it is almost impossible to notice if such leakage occurs, bringing uncertainty to the results. Secondly, it is possible that some vivianite already formed in the waterline in the local anaerobic zones, persisted through the treatment, and oxidized in the aerobic zones. It would mean that no matter how well the samples were protected from oxygen, the vivianite content could still be underestimated due to the presence of early-formed and partly oxidized vivianite.

The second approach (used in Chapter 3) aimed at quantifying the oxidized fraction of vivianite to avoid underestimating the vivianite content. This strategy allows a more flexible preparation of the samples while diminishing the impact of oxygen contamination. From the spectra of synthetic oxidized vivianite, the contribution for ferric iron in vivianite was defined with the following doublet: (IS=0.46 mm/s and QS=0.63 mm/s) (Figure 9.3). This strategy offers the advantage of taking the oxidized iron into account but becomes complicated to apply when a high concentration of iron is present. For example, this approach did not work in animal manure since other $Fe(III)$ species were present, overlapping with the signal proposed for oxidized vivianite.
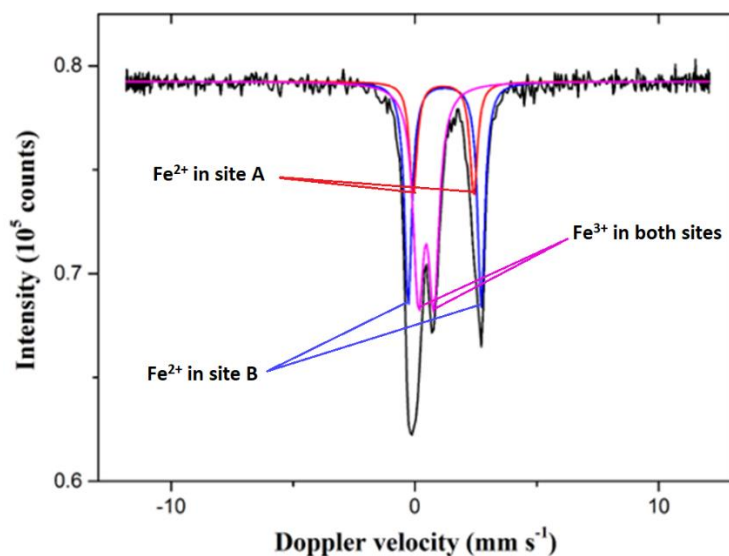


*Figure 9.3: Mössbauer spectra of oxidized synthetic vivianite showing the three main contributions of the mineral once partially oxidized.*

The third and most recent approach was more empirical and consisted of exposing the samples to oxygen for a few days to reach a (meta)stable oxidation stage. During my Ph. D., several measurements realized on synthetic vivianite and vivianite extracted from sludge suggested that vivianite oxidation reaches an equilibrium at 30% of total iron oxidized after a couple of days exposed to air. This finding was in accordance with results from Dormann and Poullen 1980 on natural vivianite and Rouzies and Millet 1993 on synthetic vivianite. Therefore, a more practical approach was followed where the quantity of Fe(II) (Site A + Site B) in vivianite was measured by Mössbauer spectroscopy: it was assumed that 30% of the total iron present in the sample as vivianite was oxidized. The big advantage of this approach is that the vivianite presents a similar oxidation degree in all the samples. With the previous strategies, accidental (and impossible to detect) oxygen leakages would partly oxidize vivianite to an unknown level. Considering that the oxidized fraction of vivianite is hard to measure in sludge/manure samples, the uncontrolled oxidation of vivianite is a real disadvantage. Additionally, the fact that the samples do not need to be prepared in oxygen-free conditions is a real advantage since it is often impossible to do on-site.

Even though this was a recurrent point of attention during my four-year working on this project and some improvements have been made, more work will be necessary. Mössbauer spectroscopy is the most accurate method so far to quantify vivianite in sludge. However, some method development will likely be necessary when further work will be realized on different matrices than sewage sludge (manure or sediments). Besides, Mössbauer spectroscopy is expensive (500-1000€ per sample), not widely available (one installation in the Netherlands), and the fitting of the spectra requires a good knowledge of the possible iron compounds present. The ideal scenario would be using a cheaper and widely available method like chemical extraction or thermo-gravimetry, with the support of Mössbauer spectroscopy for the method development. Developing a lab-scale method to extract all the vivianite in a sample magnetically could also be an interesting approach.

### 9.1.3. Iron measurements

The concentration and speciation of soluble iron in sludge streams are essential information to understand the processes linked to iron precipitation in sewage sludge. However, its determination is not always easy since oxidation of ferrous iron happens quickly, filtration can be complex, and centrifugation of the samples is not always possible. There are two widely used measurement methods for iron speciation in solution: with phenanthroline or with ferrozine. Both methods rely on the complexation of $Fe^{2+}$ by the colored agent that will give a pink or orange tint to the solution. The absorbance of the solution is then measured to obtain the concentration of soluble $Fe^{2+}$. A reductive agent is then added to the sample to reduce all the $Fe^{3+}$ to $Fe^{2+}$ and complex all the iron. The measurement of the absorbance gives the total concentration of the soluble iron in the sample. However, it seems that both of these quantification methods present limitations. Not all the iron in the liquid phase is present as truly soluble iron but can also form colloids with organic matter. While this point is rarely addressed in wastewater treatment, it is extensively studied in the natural water field (Hyacinthe and van Cappellen 2004, Herzog et al. 2020, Tipping and Ohnstad 1984, Jackson

et al. 2012). During the complexation of $Fe^{2+}$ by either phenanthroline or ferrozine, a part of the $Fe^{2+}$ bound to organic colloids may not be complexed by the colored reagent. The subsequent reduction step may release this organic-bound $Fe^{2+}$ that would then be misattributed to $Fe^{3+}$. Also, the organically bound iron could not be released during reduction and not be measured at all (Wilfert et al. 2016, Viollier et al. 2000).

Besides some deviations in the analysis itself, the sample preparation can significantly influence the final concentration of iron measured. There is no consensus in the wastewater treatment field to prepare the sample best, which is often not discussed. The samples are not always filtered with the same pore size and are not always centrifuged with the same centrifugal intensity (Table 9.1). Similar inconsistencies exist for the pore size of the filter used even though 0.45 µm is more widely employed since it is the one recommended by the official guidelines. The sample preparation would not significantly influence the iron concentration measurements if the organically-bound or solid iron could easily be separated with 0.45µm-filtration. However, based on the information reported in the natural water field, a significant fraction of the iron going through these filters is not truly soluble.

*Table 9.1: Sludge samples pre-treatment in some studies.*

| Source | Centrifugation | Filtration | Comments |
|---|---|---|---|
| Wilfert et al. 2018 | yes | 0.45 µm | Transported on ice |
| Chapter 3 | no | 0.45 µm | Samples fixed on-site with HCl |
| Mamais et al. 1994 | no | 0.45 µm | |
| Rasmussen et al. 1994 | yes | 0.22 µm | |
| Azam and Finneran 2014 | no | 0.2 µm | |
| Roussel and Carliell-Marquet 2016 | yes | 0.45 µm | |
| Hao et al. 2017 | yes | 0.22 µm | Acidification before filtration |

In natural waters, iron is mainly present as organic matter complexes and oxy(hydroxides) (Herzog et al. 2020). The colloidal oxy(hydroxides) are mainly amorphous ferric oxides, nano-hematite, or ferrihydrite (Hyacinthe and van Cappellen 2004). The studies generally agree that the iron colloids are in the hundreds of nanometers range. Tipping and Ohnstad 1984 propose that the iron oxides in freshwater lakes are in the range of 0.05-0.5µm. Herzog et al. 2020 observed that bare iron oxides, iron-organic complexes, and iron oxy(hydroxides bound to chromophoric molecules would dominate the fraction <0.1 µm, 0.1-0.2 µm and >0.2 µm, respectively. A considerable fraction of those solids iron species would get through the pores of a 0.45 µm filter. While filtration can settle a part of these compounds, not all of them will be removed (Hyacinthe and van Cappellen 2004, Herzog et al. 2020). Tipping and Ohnstad 1984 suggest that 0.01 µm would be necessary to remove all the particles.

The standard guidelines for wastewater and sludge analysis recommend the use of a 0.45µm filter without centrifugation. If we assume that the iron colloids and iron interactions are similar to natural waters, it will lead to an overestimation of the soluble iron. It could be one reason why the saturation index for vivianite precipitation in digested sludge was around 4 in

this thesis, while a value closer to 0 could be expected. Besides, the conditions related to the presence or absence of oxygen affect the interactions between iron and organic matter and influence the size of the iron complexes (Gaffney et al. 2008, Jackson et al. 2012). For this reason, the type of sludge studied will influence the quantity of iron passing through the pore and its settleability. Jackson et al. 2012 suggest that more iron is bound to the organic matter under oxic conditions due to the mechanism: oxidation of the iron, binding to organic matter, and thermal reduction of the bound iron.

The conclusion is that the iron passing through the pores of a 0.45µm filter should not systematically be considered soluble. Preliminary experiments were carried out to evaluate the fraction of iron misattributed to the soluble fraction. Thickened sludge from the WWTP Limmel (using CPR) was centrifuged at different centrifugal intensities (up to 1h at 3500 rpm) before being 0.45µm-filtered. It revealed that about one-third of the iron measured in the supernatant of this sludge could be removed by centrifugation, indicating that it was not all soluble. All of the iron removed was measured as $Fe^{3+}$, suggesting the presence of Fe(III) oxy(hydroxides). Similar studies of the influence of centrifugation and filtration were realized for digested sludge, but the quick oxidation of the samples during the filtration made the results unusable.

Overall, more care should be taken when measuring the "soluble iron" and our field could get inspired by the work done in the natural water domain. The ideal sample preparation to measure the soluble iron can be complicated: centrifugation at high speed (10 000 rpm for digested sludge most likely), 0.2µm-filtration, possibly working under anaerobic conditions. Still, more efforts should be put into the sample preparation to minimize the share of non-soluble iron wrongly attributed to soluble iron. The uncertainties due to the sample preparation should also be discussed and the error estimated.

### 9.1.4. Crystallization of vivianite

When my Ph.D. started, all the vivianite particles reported in sewage sludge were small (20-200µm) and seemed to be trapped in an organic matrix (which is not necessarily true according to our most recent results), supposedly complicating their separation. One of the main objectives of my Ph.D. was to understand how vivianite formed in sewage sludge, the factors influencing its crystallization, and eventually find a way to grow bigger crystals. The installations to recover struvite can produce crystals in the millimeter range. Can similar crystal be reached for vivianite? A significant part of my Ph.D. was invested in trying to grow bigger vivianite crystals but no important breakthrough could be achieved. The following section describes the theoretical basis necessary to understand the crystallization of vivianite and presents the main experimental outcomes of my Ph.D on this specific topic.

#### 9.1.4.1. Crystallization theory

This section is based on Mullin 2001. Any crystallization process is based on the saturation index (SI) of the species studied. The SI is defined as the ratio of the ionic activity product (IAP) and the solubility constant of the compound considered. Sometimes, the SI is defined as the log of this ratio (it is the case in this thesis) to avoid huge numbers. The IAP and the SI are then defined as followed for vivianite:

$$SI = \log\left(\frac{IAP}{K_S}\right) \qquad \text{with} \qquad IAP = \left(\gamma_{Fe^{2+}} * \frac{C_{Fe^{2+}}}{C_0}\right)^3 \left(\gamma_{PO_4^{3-}} * \frac{C_{PO_4^{3-}}}{C_0}\right)^2$$

With:

- $K_s$ the solubility product of vivianite at 25°C worth $10^{-35.76}$ (Al Borno et al. 1994)
- $\gamma$ is the activity coefficient of the ion in solution and is unitless
- $C_0$ is unit molality always worth 1 mol/L
- $C_x$ the concentration of the ion X in solution in mol/L

Based on this definition, vivianite can form when its SI is >0, and the solution is defined as supersaturated towards vivianite. When SI=0, the solution is saturated and is in equilibrium: no vivianite will form or dissolve. When SI<0, the solution is unsaturated, and vivianite will not form but even dissolve if solid vivianite is present in this solution. During this thesis, the SI in digested sludge was mainly between 2 and 5, suggesting that it is the equilibrium zone. The SI may have been overestimated due to an overestimation of the soluble iron concentration, as explained in section 9.1.3.
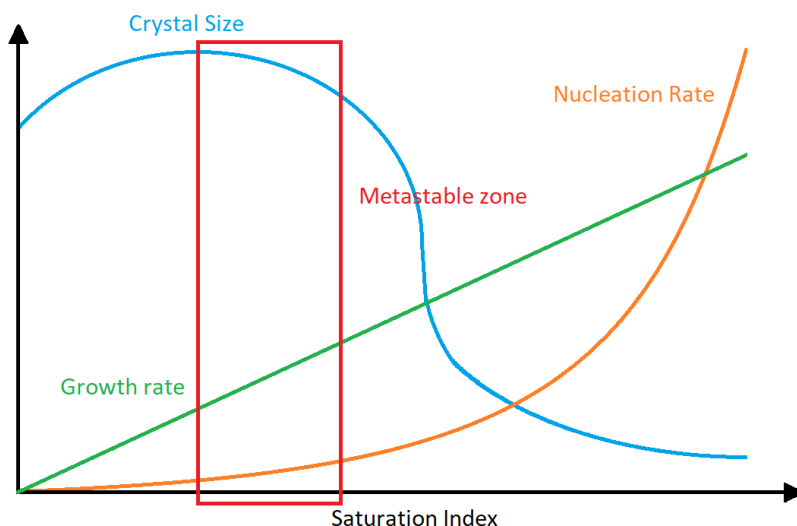


*Figure 9.4: Scheme depicting the evolution of the growth rate, crystal size, and nucleation rate in function of the saturation index. The red zone represents the metastable zone. Adapted from https://www.crystallizationsystems.com/applications/MSZW.*

The first step of any crystallization process is nucleation, forming a stable nucleus that will act as a center of crystallization. Theoretically, nucleation can happen as soon as the SI of a compound is higher than 0. Three types of nucleation can occur: primary homogeneous, primary heterogeneous, and secondary. Primary homogeneous nucleation happens when molecules constituting the compound coagulate without redissolving. A stable nucleus can contain up to several thousands of molecules, showing that primary homogeneous nucleation is relatively hard to achieve and will require a high SI. True homogeneous nucleation is very rare and is often related to heterogeneous nucleation. This mechanism relies on impurities in the system that provide a surface on which the crystal can start growing. It lowers the energy

and SI necessary to the nucleation compared to homogeneous nucleation. The SI necessary can be even smaller if the foreign particles present a similar crystalline structure to the crystal studied. For example, quartz can be used as a seed for the crystallization of vivianite since it presents a similar crystalline structure (Priambodo et al. 2017). When crystals of the solutes are already present in the medium, the SI can be even smaller, and nucleation under these conditions is called secondary nucleation.

Once stable nuclei are present in the solution, some solute can bind to them and start crystal growth. This process is the one that allows the presence of big crystals and was the one we wanted to study in this thesis. However, crystal growth does not happen under all conditions but essentially in the metastable zone. This zone is shown in Figure 9.4 and is characterized by a small nucleation rate, a big crystal size, and a relatively slow growth rate. The saturation index needs to be adjusted to be within the metastable zone to study the crystallization of vivianite and the parameters influencing it. If the SI is too low, the growth rate would be too slow to create any crystal. If the SI is too high, then the primary mechanism would be precipitation driven by nucleation and provoking the formation of plenty of tiny crystals.

### 9.1.4.2. Experimental findings

The first objective of the crystallization study performed during this study was to find the SI corresponding to the metastable zone. In the case of vivianite, the SI is defined by the concentration of soluble $Fe^{2+}$ and $PO_4^{3-}$, which depends on the pH. During my Ph.D., several mixtures of iron and phosphate at different pH were prepared to create different SI conditions. One series was seeded with quartz, while the other one was left unseeded. The metastable zone should be characterized by conditions at which no homogeneous nucleation happens (no formation of vivianite in the unseeded experiments) and vivianite forms on the seeds (Figure 9.5). Unfortunately, the right conditions to grow vivianite seeds were never found; precipitation by forming new nuclei was always preferred.
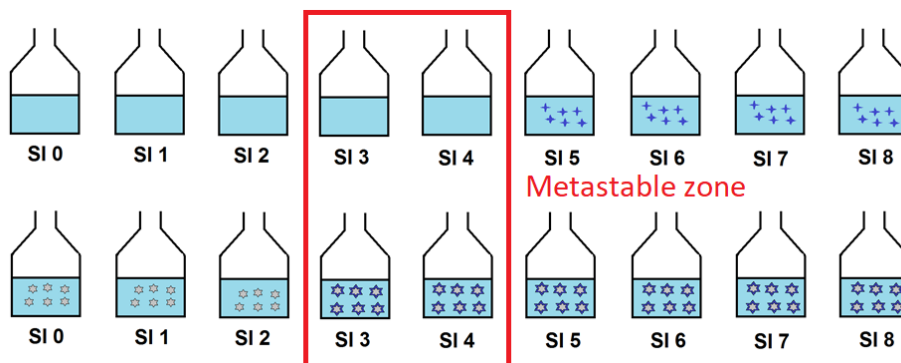


*Figure 9.5: Experimental plan to find the metastable zone. Blue particles represent the crystals of vivianite, while grey particles represent the vivianite seeds.*

Theoretical calculations were undertaken to compare the width of the metastable zone of vivianite to the one of struvite to understand why the empirical determination of the metastable zone failed. The following assumptions were made to perform these calculations:

- The ionic strength was fixed as 0.07 mol/L as it is a typical value for digestates, according to Chapter 8. Digestates (or reject water) are where the crystallization of vivianite and struvite are commonly studied.
- The concentration of $NH_4^+$ was fixed at 700 mg/L, which is typical in digestates according to Chapter 8.
- For struvite, the concentration of $Mg^{2+}$ was taken equal to total dissolved phosphate and was the variable.
- For vivianite, the concentration of $Fe^{2+}$ was taken equal to total dissolved phosphate and was the variable.
- It was assumed that the pH was 7, according to Chapter 8.
- It was assumed that the width of the metastable zone is defined as $\log(1) < SI$ metastable $< \log(1.5)$.

Under these assumptions, the metastable zone for struvite can be found between concentrations of phosphate of 74 to 93 ppm of P. In contrast, for vivianite, the concentrations were 0.96 to 1.04 ppm of P. The metastable zone as defined here is 250 times wider for struvite than for vivianite in terms of phosphate concentrations. This is mainly due to the dependence of the IAP of vivianite to the power 5 of the concentration of the solutes against the power 3 for struvite. It means that slight variations of concentrations will have a significant impact on the saturation index. From the width of the metastable zone defined here, it is easy to understand that it is much easier to be in the metastable conditions for struvite than for vivianite crystallization, and consequently easier to grow big crystals of struvite.

### 9.1.4.3. Lessons learned

From the calculations presented above and the numerous experimental failed attempts, it can be said that the study of vivianite crystallization at the typical pH of a digester (around 7) is complicated. The narrow metastable zone makes it very hard to feed the iron and phosphorus accordingly. Besides, the addition of chemicals creates local supersaturation in the case of vivianite due to the considerable dependence on its SI on the concentration of the solutes. A modification of the pH instead of the concentration of iron and phosphorus could provide an interesting alternative to avoid local supersaturation. Working at a lower pH seems to be the only way to control the conditions inside of the metastable zone. With the assumptions described in the previous section, the width of the metastable zone would be 50 ppm in terms of total phosphorus at a pH 4. It would greatly ease the growth study but at the expense of using a non-realistic pH for sludge digester. Alternatively, Priambodo et al. 2017 showed that the precipitation of vivianite and its agglomeration on quartz seed in a fluidized-bed reactor was possible. These experiments were duplicated during my research and will be further scaled up by Wokke Wijdeveld in the European project Water Mining. His research aims to recover phosphorus (~5ppm) from a WWTP effluent by vivianite granulation in a similar fluidized-bed reactor.

**9**

## 9.2. Outlook

### 9.2.1. Vivianite recovery from sewage sludge

Will the magnetic recovery of vivianite be the next big development in the resource recovery field? It is possible. During the last 2-3 years, the scientific interest in vivianite in wastewater treatment significantly grew. Several research groups are now interested in vivianite research, and related Ph.D. positions started to appear in several countries. In the meantime, the technology was developed from idea to pilot-scale in the scope of the EIT project Vivimag. The first point to consider in developing this technology was the maximization of the amount of phosphorus present as vivianite. It is discussed in detail in Chapter 3 that describes the results of the full-scale increased iron dosing. It turns out that vivianite can efficiently be produced in the sludge digester as soon as the iron dose increases. Considering that iron preferentially binds to sulphide, it can be estimated that a Fe/P molar ratio around 1.5-1.8 should be enough to find more than 80% of the phosphorus in vivianite in digested sludge. The second step was to prove that the magnetic separation of vivianite from digested sludge could be performed at a larger scale. It was proven possible at pilot-scale using a device treating the equivalent sludge production of 20,000 p.e. at the WWTP Nieuwveer with a vivianite recovery of 80% (after three passes of the sludge). Considering that 90% of the influent phosphorus ends up in the sludge, more than 60% of the phosphorus present in the influent wastewater could be recovered with this technology, which is in line with the most stringent legislation in Europe (>50% recovery in Germany).

*Table 9.2: Elemental composition after microwave digestion and ICP-MS. The digested sludge is from the WWTP Nieuwveer, where the pilot described in Chapter 4 was operated. The purified magnetic concentrate was the product of the pilot-scale separation after purification with dissolved air flotation and hydrocyclone. This sample was treated with a KOH solution (2.9M), and the composition of the solid fraction is indicated below.*

| Element content (mg/kg dry solid) | Digested sludge | Purified magnetic concentrate | Solid fraction after alkaline splitting |
|---|---|---|---|
| Fe | 38000 | 290000 | 490000 |
| P | 49000 | 115000 | 8000 |
| As | 10 | 2 | 1 |
| Cd | 1 | 0.2 | 0.2 |
| Cr | 51 | 16 | 40 |
| Cu | 470 | 41 | 72 |
| Ni | 16 | 9 | 16 |
| Pb | 62 | 12 | 21 |
| Zn | 970 | 160 | 250 |

In the coming years, the technology should be further developed at pilot scale to optimize the separation. For example, different steel matrices (made of magnetic rods that the sludge goes through during separation) should be used to reduce possible blockage and associated maintenance costs. The proof that the pilot can be operated continuously over several days is also required before further scaling-up. It is important to remember that the device used so far

was not designed for this application but ore processing. It is then possible that after adequate engineering, the separation efficiency further increases. One other point is crucial for the technology to be successful: the valorization of the vivianite. High-value applications like lithium-ion batteries, flame retardants, and use as a pigment could represent exciting niche markets but necessitate more development. More realistically, phosphorus and iron can be recovered from the vivianite to be reused separately. An efficient way to separate iron and phosphorus from vivianite is via an alkaline treatment, as discussed in Chapter 2. The iron hydr(oxides) could then be recycled by addition to sludge digesters to produce more vivianite, while the phosphorus-rich solution could be included in processes forming PK fertilizers. It was already discussed in this thesis that the heavy metals concentrations in the recycled phosphorus solution are following the legislation and would not cause a problem (Chapter 2). The remaining heavy metals (besides Arsenic) accumulate in the iron fraction (Table 9.2), mainly as hydroxides, but not at concentrations problematic for iron recycling (confidential information from Kemira cannot be shared here). The residual phosphorus and organic matter might be a bigger issue and will be assessed in the future. The concentration of micropollutants in the magnetic concentrate produced with the pilot installation was very similar to those observed in struvite produced at four WWTPs (STOWA 2015) (Table 9.3). These concentrations are significantly lower than the dutch limits for phosphorus fertilizer, indicating that no problem should be expected on this aspect. The pathogens still need to be quantified.

*Table 9.3: Micropollutants content in the vivianite fraction recovered during the pilot-scale operation at the WWTP Nieuwveer (Chapter 4). Grade C stands for the magnetic concentrate after separation, while grade C is the purified grade C after DAF and hydrocyclone. The results are compared to 4 struvite obtained from digested sludge or reject water and the UBM (Uitvoeringsbesluit Meststoffenwet), the dutch fertilizer act implementation decree (STOWA 2015). CH*

| mg/kg $P_2O_5$ | Grade A | Grade C | Struvite | UBM limits |
|---|---|---|---|---|
| Chlorinated hydrocarbons | 0.04-0.25 | 0.04-0.25 | 0.00-0.29 | 1.2-310* |
| Sum PCDD/PCDF | 0.0012 | 0.0012 | 0.001-0.004 | 0.019 |
| Mineral hydrocarbons | 900 | 4300 | 200-3300 | 935000 |
| Sum polycyclic aromatic hydrocarbons (PAK) | 4.0 | 12.9 | 0.1-41 | 11500 |
| Sum Polychlorinated Biphenyls (PCB) | 0.04-0.24 | 0.04-0.27 | 0.00-0.21 | 375 |

*The limits vary from 1.2 to 310 mg/kg $P_2O_5$ depending on the pollutant.

Directly using vivianite as a phosphate fertilizer presents low interest due to its low bioavailability and the high concentration of iron it bears. However, the option of reusing the vivianite as an iron fertilizer exists and is more promising. Several studies showed that vivianite amendments are an efficient remedy to treat iron chlorosis (Eynard et al. 1992, Rombolà et al. 2007, Rosado et al. 2002). Iron chlorosis is a common plant disease characterized by the yellowing of the leaves (indicating a lack of chlorophyll), leading to lower plant growth, fruit production yield, and possibly death. Some pot studies are currently carried out at various locations with vivianite recovered during the Vivimag project.

After its recovery from sewage sludge, it is unlikely that vivianite can be immediately considered as a valuable product. Therefore, other parameters need to be taken into account to make this technology economically viable. The biggest economic driver for this technology is the sludge disposal costs. Let us consider a WWTP producing 10,000 tons of dry solids per year after digestion and a sludge composition of P:2%, S:1%, and Fe:7%. If 10% of the iron comes from the influent wastewater and the rest needs to be dosed, 630 tons of iron need to be used per year, corresponding to 500,000€ (1ton of iron~800€). Around 25% of the iron in this digested sludge would be lost to sulphide (molar Fe:S ratio = 1), but the rest would contribute to vivianite formation. The "S-corrected Fe/P molar ratio" is then 1.45, and it can be assumed that around 85% of the phosphorus will be present as vivianite (Wilfert et al. 2018). According to the pilot-scale study, it represents the annual production of 1,400 tons of vivianite, of which 80% can be recovered magnetically.

Considering the sludge disposal costs in the Netherlands (385€/tons of dry solids), the annual savings would be around 540,000€. It is important to note that WWTPs already dosing a significant quantity of iron are already budgeting the iron salts dosage. For example, many northern Europe WWTPs are already dosing sufficient iron (Fe/P> 1.5 are typical) to optimize vivianite production. The magnetic separator treating 10,000 tons of solids per year would cost approximately 1-2 M€ (CAPEX), while the OPEX is comparable to a belt-press system. These rough calculations are incomplete but consider the three major costs involved in vivianite recovery from sludge: iron dosing, sludge disposal costs, and cost of the separator. It shows that the Vivimag approach is economically viable and with a short return on investment time (2-4 years in this example), especially for installations already dosing a significant amount of iron. The iron present in the influent wastewater also contributes to vivianite formation, which lowers the necessary dosage for plants treating industrial iron-containing wastewater. In addition, the quantity of iron dosed for phosphorus removal is already significant in countries with strict effluent criteria (e.g., Baltic countries), making WWTPs in these areas directly suitable for vivianite recovery. It is important to emphasize that in countries where the sludge disposal costs are lower, for example where the sludge can be spread on land (e.g. Australia), the return on investment time will be longer. A similar conclusion can be drawn in coutries where alum used is more economical than iron. In the current situation, it seems unwise for a WWTP mainly relying on EBPR or dosing a limited quantity of iron to dose more iron for vivianite recovery alone. Chapter 5 also shows that vivianite can be formed in excess sludge after 2-4 days of anaerobic storage time. This approach would require constructing a buffer tank to hold the sludge for the designated amount of time. According to Chapter 6, it would minimize scaling build-up in the dewatering units downstream and save maintenance costs, representing an interesting economic driver. To conclude, it can be said that the Vivimag approach is an interesting phosphorus recovery technology but that many parameters will influence its economic and technological feasibility (size of the WWTP, CPR/EBPR strategy, regional sludge disposal and iron salts costs…).

### 9.2.2. Challenges and research opportunities

With the thesis of my predecessor Philipp Wilfert, my thesis, and the Vivimag project, a significant quantity of information has been gathered about the recovery of vivianite from sludge. The valorization of the extracted vivianite may be the biggest remaining challenge

from a practical point of view (an outlet needs to be found for the technology to be viable), but also from a research point of view. As discussed above, vivianite as an iron fertilizer to prevent iron chlorosis (Eynard et al. 1992, Rombolà et al. 2007, Rosado et al. 2002) seems to be the most promising option in the short term since it may not need a significant upgrading of the vivianite. The alkaline splitting of vivianite works at lab-scale (Chapter 2), and the strategies to reuse the iron and the phosphorus will be further investigated in a future Ph.D. project. Other valorization options like its use as pigment or in the composition of flame retardants represent attractive niche markets but could not entirely cover

While iron phosphates in sewage sludge were studied in-depth in this thesis (and in the one of Philipp Wilfert), aluminum is also dosed in wastewater to remove phosphorus since it is cheaper in some countries like Italy (from a discussion with an Italian waterboard). The recovery of aluminum phosphate may be an interesting new axis research. However, aluminum phosphate is not magnetic, so a different approach should be undertaken for its recovery. So far, this topic does not seem to have attracted much interest. It may be due to the powerful bond between aluminum phosphate, making their separation difficult.

Besides its role in wastewater treatment, vivianite may be of interest for phosphorus recovery from manure. As discussed in the introduction, animal manure contains a greater potential for phosphorus recovery in countries with many livestock, like the Netherlands. Chapter 7 showed that the formation of vivianite and its recovery were possible in iron-amended pig manure. One of the significant findings of this study was that a Fe/P molar ratio of around 4 was necessary to maximize content, while a ratio of 2 was necessary for sewage sludge. This difference cannot only be explained by the preferential precipitation of iron sulphide. In fact, no proof of the presence of iron sulphide was found in pig manure during our study. The iron sulphide interaction in pig manure (but also in sewage sludge) should not be forgotten in the upcoming project. The central hypothesis to explain the higher iron dose necessary in pig manure was iron binding to organic matter. This hypothesis will need to be carefully challenged using the knowledge of iron-organic interactions from the natural water field. On the one hand, iron was not added to animal manure for phosphorus recovery before, so there are plenty of opportunities for innovative research in this area. On the other hand, the lack of previous research can make the project challenging, and the information from other fields of research will need to be reviewed and transposed.

One of the other axes of research of the phosphate recovery theme of Wetsus is the removal and recovery of phosphorus from poorly concentrated waters, typically lakes. The presence of phosphate in natural waters can cause eutrophication, which harms biodiversity and decreases water quality. For this reason, particulate and soluble phosphate needs to be removed. However, lake sediments hold some phosphate themselves, which can be released over time and strongly contribute to the algae bloom (Kagalou et al. 2008). The removal of phosphate in the soluble water phase of lakes is then not sufficient since the sediments will cyclically release phosphorus. One of the ideas studied with Wageningen university was to add iron to lake sediments to fix the phosphates more strongly. Due to the anaerobic conditions present in lake sediments, vivianite was already found there and can represent an important phosphorus sink (Manning et al. 1991, Nriagu et al. 1974). The addition of iron to lake

**9**

sediment may eventually form vivianite, which should not redissolve due to its low solubility and be an ideal burial medium for phosphorus. We can imagine that the sediments could eventually be processed magnetically to recover the vivianite after a few years. Vivianite recovery could, for example, be combined with sediment dredging, a common lake remediation strategy (van der Does et al. 1992). The recovery of phosphorus from iron-amended manure and the use of vivianite for lake remediation are two exciting new Ph.D. topics that will be investigated in the phosphate recovery theme in the coming four years.

### 9.2.3. The future of phosphorus recovery

Nowadays, only 60% and 50% of the wastewater is collected and treated worldwide, respectively (Jones et al. 2021). Treating the totality of the wastewater remains the most prominent and more urgent challenge of the wastewater treatment field. The Urban Waste Water Treatment (UWWT) Directive 91/271/EC of 1991 obliged the European cities of more than 2000 inhabitants to collect and treat their wastewater. It led to an increase of 50% of the sludge produced between 1992 and 2005 in Europe (Kelessidis and Stasinakis 2012). A similar result can be expected worldwide when a more significant fraction of the wastewater will be treated. At first, the sewage sludge will most likely be used as a soil amendment as it is still the case in most European countries (Kabbe et al. 2019). With the rising concerns about emerging contaminants, we can assume that this use will eventually be forbidden. The sludge production increase means that the quantity of phosphorus available in sewage sludge will significantly increase, and viable technologies should be available to minimize the phosphorus wasted.

The technologies currently available on the market focus on phosphorus recovery from sludge ash (incineration) and reject water after digestion (struvite). However, phosphorus recovery after incineration is only an option when sludge is the only substrate burned in mono-incinerators. Incineration of sludge in co-incineration plants decreases phosphorus content in the ashes, making its leaching for phosphorus recovery less economical. Phosphorus recovery from mono-incineration plants is a technology that shows great potential. It allows the recovery of more than 80% of the phosphorus from the ashes, which is the requirement set by Germany for future phosphorus recovery installations. Struvite recovery has been developed during the last 20 years. However, the phosphorus recovery stays low and varies from 10 to 30% of the phosphorus present in the influent of the WWTP (Wilfert et al. 2016). The biggest limitation of this strategy is that phosphorus needs to be soluble in the reject water or digestate. Phosphorus will preferentially bind to metal salts like aluminum or iron that can be present in the influent wastewater and will not be available for recovery via struvite. For on-site phosphorus recovery approaches, the German legislation set that the phosphorus content needs to be below 20mg/g of dry solids for sludge to be co-incinerated with a phosphorus recovery from the sludge higher than 50%. It is unlikely that these requirements will be matched by struvite in the future without using an expensive chemical approach to release the phosphorus from sludge before precipitation. It can be expected that other countries will progressively apply similar regulations as Germany and Switzerland in the future. Recovery of the phosphorus via post-precipitation (Ravita process, Rossi et al. 2018) or iron-coagulated sludge (Vivimag) appear to be two promising approaches regarding the foreseen legislation. However, their feasibility needs to be proven at full scale. One advantage of the Vivimag

approach worth mentioning is that no important modification needs to be brought to the existing installations to implement it: the iron dosing can be increased if necessary, and the magnetic separator only needs to be connected to the digested sludge output.
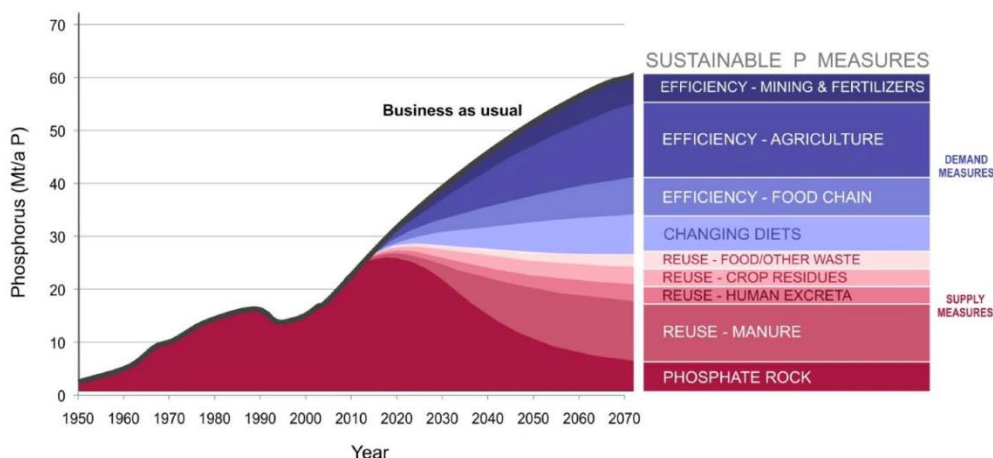


*Figure 9. 6: Sustainable phosphorus supply and demand measures for meeting long-term future global food demand. (from Cordell and White 2013)*

Phosphorus recovery from wastewater or animal manure is essential to close the phosphorus loop and make our food production more viable (Figure 9. 6). In Europe, 1.4Mt of phosphorus is present in animal manure (European Commission 2014), while wastewater bears 0.4Mt of phosphorus per year (Van Dijk, 2016). Considering that Europe imports 1.6Mt of phosphorus per year, the recovery from those sources could cover a significant fraction of the European phosphorus needs. The recovery of phosphorus from animal manure is particularly impactful since it represents the biggest secondary phosphorus sink. While pig and poultry manure can easily be collected, it is not always the case for dairy manure, which represent more than 75% of the manure produced in Europe (Köninger et al. 2021). Therefore, not all the phosphorus present in animal manure is centralized and possible to recover, unlike most of the phosphorus present in wastewater. Besides its recovery, the way that phosphorus is currently used also needs to be improved (Figure 9. 6). For example, it is possible to reduce by 20-25% the quantity of phosphorus in the animal feed without consequences on the health of the animal (Schoumans et al. 2015). Also, it is estimated that a maximum of 10-20% of the phosphorus put on crops is used by the plants (Schoumans et al. 2015). The way fertilizers are currently produced needs to be improved. The fertilizer of the future needs to be specially engineered for the crop it is used for in terms of composition and release rate (Kratz et al. 2019). Poor utilization of the fertilizer also leads to an increased run-off from the fields that will provoke more eutrophication in the natural waters. However, not all the phosphorus that is not absorbed by the crop is released in the aquifers of water streams. Around 0.9Mt of phosphorus per year could be accumulated in agricultural soils in Europe (Schoumans et al. 2015), creating a new secondary source of phosphorus. Overall, a wiser utilization of fertilizers combined with an efficient phosphorus recovery from secondary sources (manure and wastewater) are keys to a circular utilization of phosphorus.

# References

Azam, H. M., & Finneran, K. T. (2014). Fe(III) reduction-mediated phosphate removal as vivianite (Fe3(PO4)2·8H2O) in septic system wastewater. *Chemosphere*, 97, 1–9. doi:10.1016/j.chemosphere.2013.09.032.

Čermáková. Z., Švarcová. S., Hradil. D., Bezdicka. P. (2013). Vivianite: A historic blue pigment and its degradation under scrutiny. *Science and Technology for the Conservation of Cultural Heritage,* 75-78.

Cordell, D., & White, S. (2013). Sustainable Phosphorus Measures: Strategies and Technologies for Achieving Phosphorus Security. *Agronomy*, 3(1), 86–116. doi:10.3390/agronomy3010086

van der Does, J., Verstraelen, P., Boers, P., Van Roestel, J., Roijackers, R., & Moser, G. (1992). Lake restoration with and without dredging of phosphorus-enriched upper sediment layers. *Hydrobiologia*, 233(1-3), 197–210. doi:10.1007/bf00016108

Dormann, J-L., Poullen, J-F. (1980). Étude par spectroscopie Mössbauer de vivianites oxydées naturelles. *Bulletin de Minéralogie*, 103, 6, 633-639. https://doi.org/10.3406/bulmi.1980.7431.

European Commission (2014). Collection and analysis of data for the control of emissions for the spreading of manure. Available at: https://ec.europa.eu/environment/air/pdf/Final%20Report.pdf.

Eynard, A., Campillo, M.C., Barrón, V., Torrent, J., (1992). Use of vivianite (Fe3(PO4)2.8H2O) to prevent iron chlorosis in calcareous soils. *Fertil. Res*. 31, 61–67. https://doi.org/10.1007/BF01064228.

Jones, E. R., van Vliet, M. T. H., Qadir, M., Bierkens, M. F. P.(2021). Country-level and gridded estimates of wastewater production, collection, treatment and reuse, *Earth Syst. Sci. Data*, 13, 237–254, https://doi.org/10.5194/essd-13-237-2021, 2021.

Kabbe, C. (2019). Global compendium on phosphorus recovery from sewage/sludge/ash.

Kelessidis, Alexandros & Stasinakis, Athanasios. (2012). Comparative Study of the Methods Used for Treatment and Final Disposal of Sewage Sludge in European Countries. Waste management (New York, N.Y.). 32. 1186-95. 10.1016/j.wasman.2012.01.012.

Kagalou, I., Papastergiadou, E. and Leonardos, I. (2008). Long-term changes in the eutrophication process in a shallow Mediterranean lake ecosystem of W. Greece: response after the reduction of external load. *Journal of environmental management* 87(3), pp. 497–506.

Köninger, J., Lugato, E., Panagos, P., Kochupillai, M., Orgiazzi, A., & Briones, M. J. I. (2021). Manure management and soil biodiversity: Towards more sustainable food systems in the EU. *Agricultural Systems,* 194, 103251. doi:10.1016/j.agsy.2021.103251

Kratz, S., Vogel, C. & Adam, C. (2019) Agronomic performance of P recycling fertilizers and methods to predict it: a review. *Nutr Cycl Agroecosyst* 115, 1–39. https://doi.org/10.1007/s10705-019-10010-7.

Hao, X., Wei, J., van Loosdrecht, M. C. M., & Cao, D. (2017). Analysing the mechanisms of sludge digestion enhanced by iron. *Water Research*, 117, 58–67. doi:10.1016/j.watres.2017.03.048.

Herzog, S. D., Gentile, L., Olsson, U., Persson, P., & Kritzberg, E. S. (2020). Characterization of Iron and Organic Carbon Colloids in Boreal Rivers and Their Fate at High Salinity. *Journal of Geophysical Research: Biogeosciences*, 125(4). doi:10.1029/2019jg005517.

Hyacinthe, C., & Van Cappellen, P. (2004). An authigenic iron phosphate phase in estuarine sediments: composition, formation and chemical reactivity. *Marine Chemistry*, 91(1-4), 227–251. doi:10.1016/j.marchem.2004.04.006.

Jackson, A., Gaffney, J. W., & Boult, S. (2012). Subsurface Interactions of Fe(II) with Humic Acid or Landfill Leachate Do Not Control Subsequent Iron(III) (Hydr)oxide Production at the Surface. *Environmental Science & Technology*, 46(14), 7543–7550. doi:10.1021/es301084c.

Mamais, D., Pitt, P. A., Cheng, Y. W., Loiacono, J., & Jenkins, D. (1994). Determination of ferric chloride dose to control struvite precipitation in anaerobic sludge digesters. *Water Environment Research*, 66(7), 912–918. doi:10.2175/wer.66.7.8

Manning, P. G., Murphy, T. P., & Prepas, E. E. (1991). Intensive formation of vivianite in the bottom sediments of mesotrophic Narrow Lake, Alberta. *Canadian Mineralogist*, 29, 77–85.

McCammon, C. A., & Burns, R. G. (1980). The oxidation mechanism of vivianite as studied by Mossbauer spectroscopy. *American Mineralogist*, *65*(3–4), 361–366.

Mullin, J.W. (2001). Crystallization, Fourth Edition.

Nembrini, G.P., Capobianco J.A., Viel, M., Williams A.F. (1983). A Mössbauer and chemical study of the formation of vivianite sediments of Lago Maggiore (Italy). *Geochimica et Cosmochimica Acta*, 47(8), 1459-1464.

Nriagu, J. O., & Dell, C. I. (1974). Diagenetic Formation of lron Phosphates in Recent Lake Sediments. *American Mineralogist*, 59, 934–946.

Priambodo, R., Tan, P. R., Shih, Y.-L., Huang, Y.-J. (2017). Fluidized-bed crystallization of iron phosphate from solution containing phosphorus. *Journal of the Taiwan Institute of Chemical Engineers*, 80, 247–254. doi:10.1016/j.jtice.2017.07.004.

Prot, T., Nguyen, V.H., Wilfert, P., Dugulan, A.I., Goubitz, K., De Ridder, D.J., Korving, L., Rem, P., Bouderbala, A., Witkamp, G.J., Van Loosdrecht, M.C.M (2019). Magnetic separation and characterization of vivianite from digested sewage sludge. *Separation and Purification* (224)

Rasmussen, H., Bruus, J. H., Keiding, K., & Nielsen, P. H. (1994). Observations on dewaterability and physical, chemical and microbiological changes in anaerobically stored activated sludge from a nutrient removal plant. *Water Research*, 28(2), 417–425. doi:10.1016/0043-1354(94)90279-8.

Rombolà, A. D., Toselli, M., Carpintero, J., Quartieri, M., Torrent, J., Marangoni, B. (2007). Prevention of Iron - Deficiency Induced Chlorosis in Kiwifruit (Actinidia deliciosa) Through Soil Application of Synthetic Vivianite in a Calcareous Soil, *Journal of plant nutrition*, 26(10-11), 2031-2041.

Rosado, R., del Campillo, M. C., Martínez, M. A., Barrón, V., Torrent, J. (2002). Long-term effectiveness of vivianite in reducing iron chlorosis in olive trees. *Plant and Soil*, 241(1), 139–144. doi:10.1023/a:1016058713291

Rossi, L., Reuna, S., Fred, T., & Heinonen, M. (2018). RAVITA Technology – new innovation for combined phosphorus and nitrogen recovery. *Water Science and Technology*, 78(12), 2511–2517. doi:10.2166/wst.2019.011.

Roussel, J., & Carliell-Marquet, C. (2016). Significance of Vivianite Precipitation on the Mobility of Iron in Anaerobically Digested Sludge. *Frontiers in Environmental Science*, 4. doi:10.3389/fenvs.2016.00060.

Rouzies, D., & Millet, J. M. M. (1993). Mossbauer Study of Synthetic Oxidized Vivianite at Room-Temperature. *Hyperfine Interaction,* 77(1-2), 19-28.

Salehin, S., Rebosura, M., Keller, J., Gernjak, W., Donose, B. C., Yuan, Z., & Pikaar, I. (2020). Recovery of in-sewer dosed iron from digested sludge at downstream treatment plants and its reuse potential. *Water Research*, 115627. doi:10.1016/j.watres.2020.115627.

Schoumans, O. F., Bouraoui, F., Kabbe, C., Oenema, O., & van Dijk, K. C. (2015). Phosphorus management in Europe in a changing world. *AMBIO*, 44(S2), 180–192. doi:10.1007/s13280-014-0613-9

Standard Methods for the Examination of Water and Wastewater (2017) 3500-Fe IRON DOI: 10.2105/SMWW.2882.055.

STOWA (2015). Verkenning van de kwaliteit van struvite uit de communale afvalwaterketen. Consulted last on 10/05/2021 at: https://www.stowa.nl/sites/default/files/assets/PUBLICATIES/Publicaties%202015/STOWA%202015-34.pdf.

Tipping, E. and Ohnstad, M. (1984). Colloid stability of iron oxide particles from a freshwater lake. *Nature*, 308(5956), 266–268. doi:10.1038/308266a0.

Turner, B. L., & Leytem, A. B. (2004). Phosphorus Compounds in Sequential Extracts of Animal Manures: Chemical Speciation and a Novel Fractionation Procedure. Environmental *Science & Technology*, 38(22), 6101–6108. doi:10.1021/es0493042.

Unie van Waterschappen (UvW), 2018. Last consulted on the 20/04/2021 at https://www.waterschapsspiegel.nl/wp-content/uploads/2019/09/Bedrijfsvergelijking-Zuiveringsbeheer-2018.pdf

Viollier, E., Inglett, P.W., Hunter, K., Roychoudhury, A.N., van Cappellen, P. (2000). The ferrozine method revisited: Fe(II)/Fe(III) determination in natural waters. *Appl. Geochem.* 15 (6), 785-790.

Wilfert, P., Kumar, P. S., Korving, L., Witkamp G.J., Van Loosdrecht, M. C. M. (2015). The relevance of Phosphorus and iron chemistry to the recovery of  phosphorus from wastewater. *Environmental Science and Technology,* 49(16)

Wilfert, P., Mandalidis, A., Dugulan, A. I., Goubitz, K., Korving, L., Temmink, H., Witkamp G.J., Van Loosdrecht, M. C. M. (2016). Vivianite as an important iron phosphate precipitate in sewage treatment plants. *Water Research*, 104, 449–460

**9**

Wilfert, P., Korving, L., Dugulan, I., Goubitz K., Witkamp, G. J., Van Loosdrecht M.C.M. (2018). Vivianite as the main phosphate mineral in digested sewage sludge and its role for phosphate recovery. *Water Research,* 144, 312-321
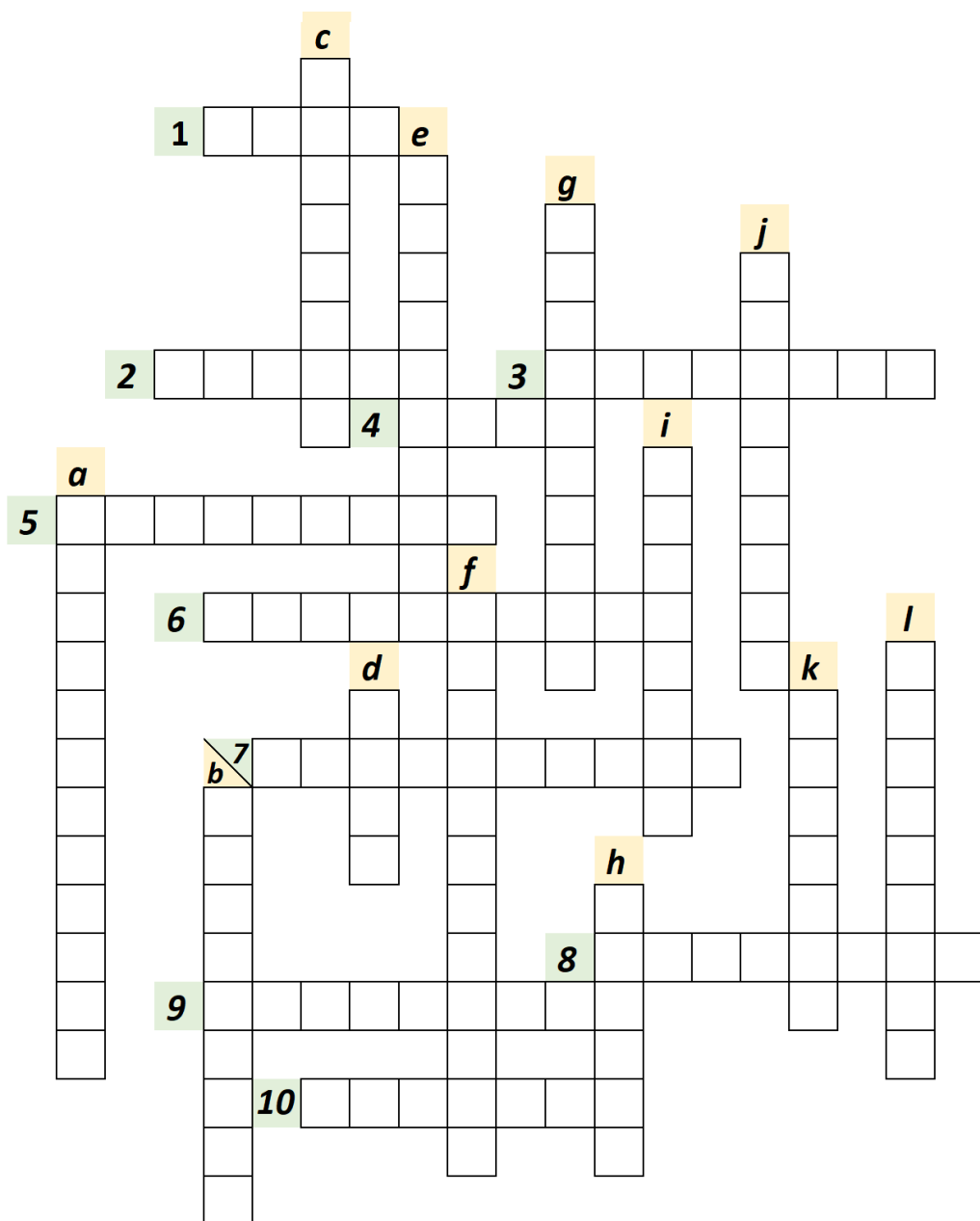
**9**

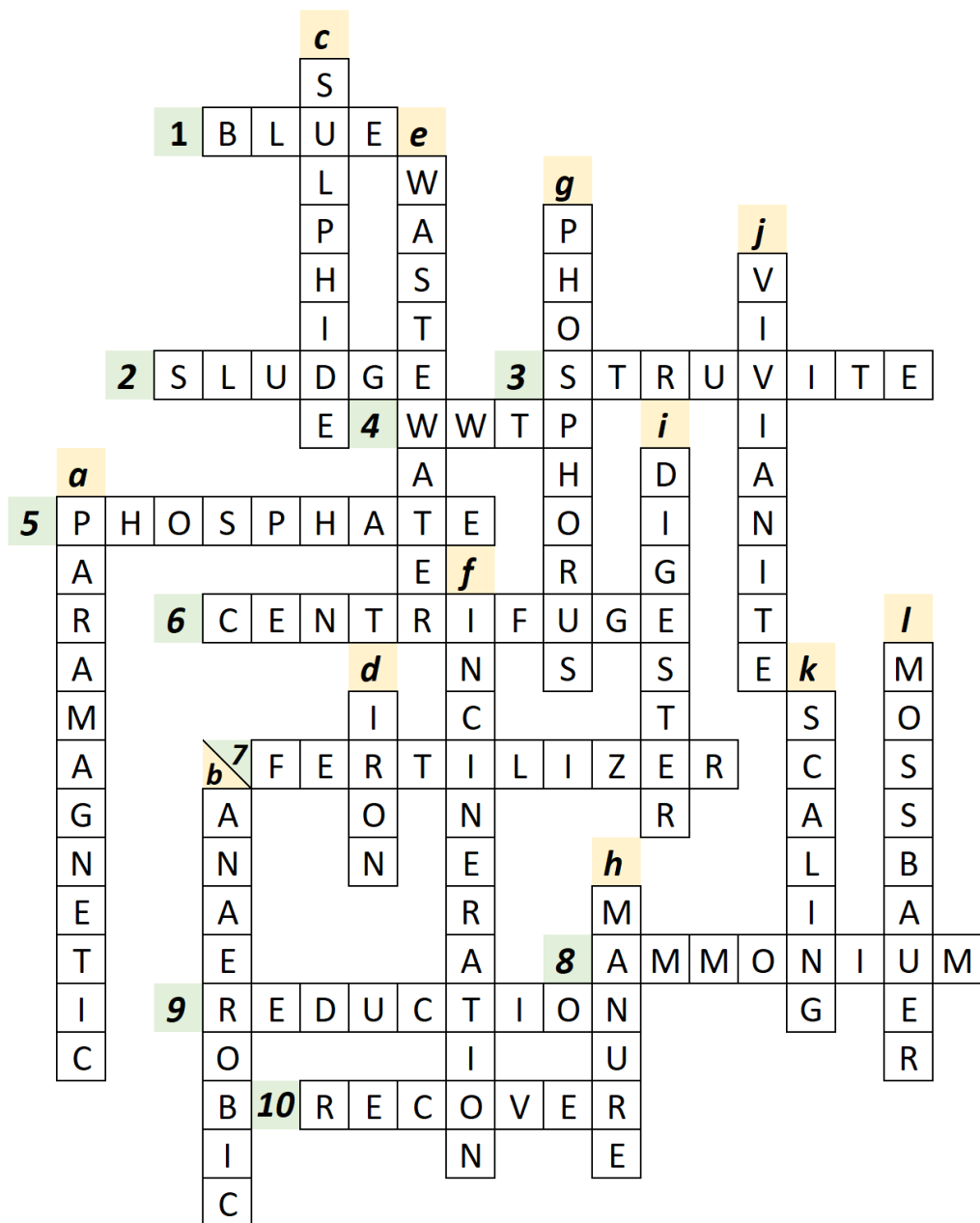# Let's see what you can remember...

## Horizontally

| | |
|---|---|
| 1 | Colour of "j" when oxidized. |
| 2 | Slurry where the pollutants removed from "e" end up. |
| 3 | Other mineral involved in the "10" of "g". |
| 4 | Acronym for the place where "e" is treated. |
| 5 | Name of the molecule which is the most common form of "g". |
| 6 | Common unit to dewater "2", can heavily suffer from "k" build-up. |
| 7 | Most common use for "5" and "8". |
| 8 | Main form of nitrogen in "e". |
| 9 | Chemical or biological mechanism involving the transformation of Fe(III) to Fe(II) |
| 10 | Synonym of recycle; what we want to do with the "j". |

## Vertically

| | |
|---|---|
| a | Characteristic of "j" that make its extraction from "2" possible. |
| b | Condition in "i" associated with the absence of oxygen |
| c | Molecule that binds to "d" before "j" can form. |
| d | Element commonly added to "e" to remove "g". |
| e | Name of the influent that is treated at "4". |
| f | Common strategy to dispose of "2" by burning it. |
| g | Element that can be removed chemically or biologically from "c". |
| h | The major secondary source of "g", essentially from cow, pig or poultry. |
| i | Installation used to stabilize "2", produce biogas and place where "j" forms. |
| j | Star of the show, mineral composed of "d" and "5". |
| k | Unwanted mineral deposit in "4" that can be made of "3" or "j". |
| l | Best technique to quantify "j" so far. |

*All the answers are mentioned in the popular summary of the thesis (p.6-8)*

# Crossword Puzzle

**Across:**
1. BLUE
2. SLUDGE
3. STRUVITE
4. WWTP
5. PHOSPHATE
6. CENTRIFUGE
7. FERTILIZER
8. AMMONIUM
9. REDUCTION
10. RECOVER

**Down (lettered):**
- a. PARAMAGNETIC
- b. ANAEROBIC
- c. SULPHIDE
- d. IRON
- e. WASTE
- f. INCINERATION
- g. PHOSPHORUS
- h. MANURE
- i. DIGESTER
- j. VIVIANITE
- k. SCALING
- l. MOSSBAUER

# Thank you

A Ph.D. can be a tough experience that puts people under pressure and prevents them from having a good time. It was not the case for me, and it is mainly due to all the persons that contributed to making my Ph.D. (and life) a pleasant moment. I find it essential to acknowledge the persons that made it possible, and my only fear is to forget some of you.

First of all, I would like to thank Leon Korving, my direct supervisor during my Ph.D. I learned so much from you, not only on applied science but also on people and project management. As coordinator of the P-team, you created a positive environment for the PhDs to interact with the different partners and learn from them. I am convinced that you are the reason why the Phosphate-team has so much success. I do not doubt that it will keep going as long as you are the captain of the ship. I am even more grateful for the time you invested in helping me, pushing me, or simply being always available when I needed you. I was never scared to fail during my Ph.D. since I knew you would be here to support me.

Mark van Loosdrcht was my promotor during my Ph.D., and I fl vry lucky to hav orkd ith him. Mark, I alays apprciatd to discuss ith you sinc it as focusd on the big pictur, hich I somtims forgot during my Ph.D. I spcially njoyd th tim spnt togthr at confrncs. vn though many popl antd to talk to you, you alays took th tim to chit chat ith m and introduc m to othr prsons. I am also glad that you got a new laptop with a working keyboard 😊.

Besides Leon and Mark, Philipp Wilfert, my co-promotor, was the other person that I discussed the most scientific content with. As my vivianite predecessor, you did a great job setting the foundations of my project. Since we have very different approaches to a problem, I usually disliked your suggestion (like reading more articles), even though I ended up doing it. Even though it was decided late to make you my official co-promotor, I feel that it was the right decision, not only for your scientific input but also for your support throughout the years.

Many other persons were part of the phosphate team and contributed to my work. Prashanth, my beloved first supervisor, you are the one who made me want to do a Ph.D., even though it was absolutely not my plan before working with you. Wokke, we did not manage to make a nice goodie from vivianite, but we still have two years to do this! Carlo, I thank you a bit later, so you have to be patient. Nouran, your enthusiasm, and joy make me want to talk to you when I am a bit down. Ha, I know that you will be embarrassed when reading these lines, but do not worry, you will be a great Ph.D., even though you still doubt it now. Jessica, glad to have a new metal gig partner around! Sophie, you did not start your adventure with us yet, but you will soon see how great it is to work in this team.

Several companies were part of the P-team and were very important to my project: Kemira, Waterschap Brabantse Delta, Waterschapsbedrijf Limburg, Vandcenter Syd, Aquacare, Aquaminerals and ICL Fertilizers. You were always very curious about our work and made us feel like what we were doing mattered. Your "industrial" perspective was valuable to keep in mind that the research should serve society in the end. Having partners so strongly involved gave us many opportunities to go beyond our project. I especially want to thank Bengt Hansen, Outi Grönfors, Saskia Hanneman, Wout Pannekoek, Leonie Hartog, Per Hendrik Nielsen and Nina Almind-Jørgensen for the help you all gave me at some point of my project.

Without Wetsus, this Ph.D. would not have been possible. For this reason, I want to thank Cees, Johannes, and Beert. My favorite value is joy (by far), and I think you should choose it as the value of the month more often.

festivals/concerts whenever I can. Jojo and Lolo have been my best partners for this activity. Our yearly expedition to the metallic land of the Graspop was always a blast, even in the mud. Carlo, Advait, Angel, Dada, Giulia, Hector Gautier, and Aubin are also in the loop, and we hope to all meet for a fiery 2022 edition!

Related to this topic, I would like to thank the numerous metal/rock bands that I have been listening to non-stop during my four years of Ph.D. For the roughly 4000+ hours of music (if you ever read this thesis), thank you: Scorpions, Iron Maiden, Queensryche, Powerwolf, In Flames, Kiss, As Lions, Parkway Drive, Faith no More, Nightwish, Alter Bridge, Tool, SOAD, Metallica, Ozzy, Mötley Crüe, Ghost, Sabaton, Avatar, Volbeat, Journey, Dream Theater, Rammstein, Slipknot, Judas Priest, The Hu, Soen, Steel Panther, Beast in Black…it goes on forever.

Wetsus is a nice place to do research, but an even better one to meet new friends. Karinette, we had countless dinners, parties, movie nights (when you were not watching ☺), and other activities together #almostflatmates. Angelito, we spent countless hours watching sports together, and you were always available to teach me about PHA and be my internet provider. Advait, we shared the same passion for football even though Man U games were terribly boring. I still hope to come to Leuven before you finish. Maarten van de Swagg, I loved to have a competitive board game partner, and now I get more time to kick your ass. Rita, even though you are always busy, we found time to chitchat and do some activities together. Paulina and Hector, thank you so much for the amazing (and exhausting) trip to Mexico; we will surely go back with Rebeca! Raquel, I liked talking to you every time we met, even though it was only for 10 min. Airbag, you made it on time; congratulations. More seriously, we got to spend some time together, and I ask for more now! Other colleagues from Wetsus also need to be mentioned since they contributed positively to my Wetsus experience: Olga, Kestral, Laura, Jaap, Ettore, Rose, Emad, João, Diego, Qingdian, Olivier (Alsace power), Jannie, Gerrit, Nynke, Manduli, GJ, Paraschos, Laurens, Lisette, Mieke, Marianne, John, Patricia, and Jolanda.

Even though we were far from each other, we always stayed in touch with le "groupe des copains" from ENSCMu. Spending time together during the gathering weekend, New Year's Eve, or just online playing Among Us always reminded me that you don't need to see your good friends every day to stay close. We have ridiculous nicknames, but that's alright: Jojo (not sure you deserve to be acknowledged), Elochai, Lolo, Dada, Sysy, Damien, Cloclo, Kiki, Cycy, Xaviern, Bibou. In addition to this group, there are two other French friends that I need to mention. Elodie, we always arranged our schedule to see each other when we were coming back home. Corail, only a year together in the same building, was enough to become great friends. By video chat or face to face when possible, we managed to exchange the latest news of our life during all those years.

Now it is time to praise my two paranymphs; otherwise, they will not help me prepare for my defense. Carlo, gropd, you were my first new P-PhD colleague ever. I was supposed to show you around at first. Since we have plenty of common interests, sport, music, food, and phosphate, we got to spend much time together and became friends. Thank you for welcoming me to Padova, for the scientific and non-scientific discussions, attempts to speak french, and in general, for all the good times we spend together. Griz, besides Rebeca, you were the most present person in my Wetsus adventure, even before my Ph.D. started. It is hard to mention

all the things we did together since we have seen each other almost every day since 2016. Living together for more than three years may have something to do with it. Thank you for taking care of me when I was injured, keeping me busy when I was sad, and saving our asses when we missed planes or trains. We share many memories, and I know we will create some more in the coming years. As a token of our friendship, I will not teach you the TFM ways to keep it interesting and will keep the mysterious Kebab event for myself.

I would also like to take a moment to thank all the teachers that made me like studies, triggered my curiosity, and taught me all kinds of things. If I ended up following (long) studies, it is mainly thanks to you all, who have made me love learning.

Voici le moment d'écrire un peu en français. Être loin de ma famille ne m'a jamais posé de problèmes. Dès l'âge de 18 ans, j'ai quitté la maison pour aller vivre à Mulhouse, pour revenir tous les week-ends au début, et de moins en moins par la suite. Maintenant que je vis à l'étranger, je reviens encore moins souvent mais ma vraie maison est à Steige, nulle part ailleurs. Je suis sûr que c'est la même chose pour mes frères, Simon, Aubin et Gautier avec qui nous essayons de revenir à la maison au même moment pour passer du temps ensemble. Pour nous avoir élevés, éduqués, soutenus quels que soient nos projets et fait de nous les personnes que nous sommes aujourd'hui, Papa, Maman, merci beaucoup. A côté de ça, nous avons une super famille qui était présente depuis notre enfance et que nous sommes toujours heureux de voir. Fan, Lu, Mi, Gégé, mamie, Jean-Louis et tous les autres, je sais que vous avez fortement contribué aux bons souvenirs que nous avons et à la bonne entente dans notre famille, merci.

A Olga, Javi y Cristina, muchas gracias por acogerme tan calurosamente en mi nueva familia española. Espero que pronto pueda haceros descubrir Francia, y especialmente mi pueblo.

To finish, I would like to thank Rebeca, mapoule, for everything. We met in early 2015 during our time as students as Wetsus, and we have been together since then. I love the relationship we have since we share everything but are still two independent persons. You are my best travel companion, best support during my harder times, and best enfermera when (often) needed. It felt natural when we decided to spend our life side by side, right? We started to live together right before Covid time, and after this experience, I want to start our life for real because I know it is the one I want. Te quiero mi pouletita.

# Curriculum Vitae

After preparing for two years for the national examination to enter French engineering schools, he integrated the "Ecole Nationale Supérieure de Chimie de Mulhouse" (France) in 2012. There, he studied various domains of chemical engineering with a specialization in sustainable chemistry. During a gap year, he worked for six months in Chicoutimi (Canada) in the laboratory LASEVE focusing on extracting and isolating valuable products from the boreal forest plants. The second half of his gap year took place in Wetsus, European centre of excellence for sustainable water technology in Leeuwarden (The Netherlands), where he worked on phosphorus adsorption with Prashanth Suresh Kumar. After completing his last year of studies in Mulhouse, he returned to Wetsus for his Master thesis, again within the "Phosphate Recovery" theme. From 2017, Thomas started the Ph.D. project "Phosphorus recovery from iron-coagulated sewage sludge", which was initiated by TU Delft and Wetsus. The results produced with this 4-year project are documented in this work.

# List of publications

Prot, T., Nguyen, V. H., Wilfert, P., Dugulan, A. I., Goubitz, K., De Ridder, D. J., Korving, L., Rem, P., Bouderbala, A., Witkamp, G.J., van Loosdrecht, M. C. M. (2019). Magnetic separation and characterization of vivianite from digested sewage sludge. *Separation and Purification Technology*, 224, 564-579. doi:10.1016/j.seppur.2019.05.057.

Prot, T., Wijdeveld, W., Eshun, L. E., Dugulan, A. I., Goubitz, K., Korving, L., van Loosdrecht, M. C. M. (2020). Full-scale increased iron dosage to stimulate the formation of vivianite and its recovery from digested sewage sludge. *Water Research*, 182. https://doi.org/10.1016/j.watres.2020.115911.

Prot, T., Korving, L., Dugulan, A.I., Goubitz, K., van Loosdrecht, M.C.M. (2021). Vivianite scaling in Wastewater Treatment Plants: occurrence, formation mechanisms and mitigation solutions, *Water Research*, 197, 117045.https://doi.org/10.1016/j.watres.2021.117045.

Wijdeveld, W.K., Prot, T., Sudintas, G., Kuntke, P., Korving, L., van Loosdrecht, M. C. M. Pilot-scale magnetic recovery of vivianite from digested sewage sludge, submitted to Water Research.

Prot, T., Pannekoek, W., Belloni, C., Hendrikx, R., Dugulan, A. I., Korving, L., van Loosdrecht, M. C. M. Formation of vivianite in excess waste activated sludge and its correlation with Fe(III) reduction, submitted to Water Research.

Prot, T. and Schott, C., Fleury, E., Dugulan, A.I., Hendrikx, R., van der Weijden, R.D., Cunha, J.R., Korving, L., Buisman, C., van Loosdrecht, M.C.M. Formation of vivianite in iron-amended pig manure and its subsequent magnetic recovery, submitted to Water Research.

Prot, T., Korving, L., van Loosdrecht, M. C. M. Ionic strength of the liquid phase of different sludge streams in a wastewater treatment plant, available as preprint under DOI: 10.26434/chemrxiv.13359437, submitted to Environmental Science and Technology.